

# For Reference

NOT TO BE TAKEN FROM THIS ROOM

Ex LIBRIS  
UNIVERSITATIS  
ALBERTAENSIS







Digitized by the Internet Archive  
in 2019 with funding from  
University of Alberta Libraries

<https://archive.org/details/Slight1974>











T H E   U N I V E R S I T Y   O F   A L B E R T A

RELEASE FORM

NAME OF AUTHOR       .....BRUCE..WILLIAM..SLIGHT.....  
TITLE OF THESIS       ....DYNAMIC...ANALYSIS...OF.....  
                              ....REINFORCED..CONCRETE...SHEAR.....  
                              ....WALL...BUILDINGS.....  
DEGREE FOR WHICH THESIS WAS PRESENTED   Doctor.of.Philosophy..  
YEAR THIS DEGREE GRANTED       .....1974.....

Permission is hereby granted to THE UNIVERSITY OF  
ALBERTA LIBRARY to reproduce single copies of this  
thesis and to lend or sell such copies for private,  
scholarly or scientific research purposes only.

The author reserves other publication rights, and  
neither the thesis nor extensive extracts from it may  
be printed or otherwise reproduced without the author's  
written permission.





THE UNIVERSITY OF ALBERTA

DYNAMIC ANALYSIS OF REINFORCED CONCRETE

SHEAR WALL BUILDINGS

by



BRUCE WILLIAM SLIGHT

A THESIS

SUBMITTED TO THE FACULTY OF GRADUATE STUDIES AND RESEARCH  
IN PARTIAL FULFILMENT OF THE REQUIREMENTS FOR THE DEGREE  
OF DOCTOR OF PHILOSOPHY

DEPARTMENT OF CIVIL ENGINEERING

EDMONTON, ALBERTA

FALL, 1974



THE UNIVERSITY OF ALBERTA  
FACULTY OF GRADUATE STUDIES AND RESEARCH

The undersigned certify that they have read, and recommend to the Faculty of Graduate Studies and Research, for acceptance, a thesis entitled "DYNAMIC ANALYSIS OF REINFORCED CONCRETE SHEAR WALL BUILDINGS" submitted by BRUCE WILLIAM SLIGHT in partial fulfilment of the requirements for the degree of Doctor of Philosophy.



## ABSTRACT

This dissertation presents a method of predicting the load-deformation response of a reinforced concrete member under repeated reversing cyclic load. Deformations due to flexure, shear and axial load are accounted for at all times using separate hysteresis loops for flexure and shear.

A method of predicting the response of a reinforced concrete frame subjected to an earthquake loading is presented. The method accounts for deformations in addition to elastic flexural deformations by introducing an equivalent rotational spring at each member end. By defining the properties of the spring properly, the response of the model can closely simulate that of the actual member.

Standard slope deflection equations are modified to accommodate elastic members with rotational springs at their ends. When these equations are used to construct the frame stiffness matrix, computations in the inelastic range can be done in the same manner as those in the elastic range. The stiffness matrix is thus updated to be compatible with the deteriorated structure at each instant of the motion. The equations of motion are solved using a linear acceleration method.

A behavioral study is presented based on the analyses of seven twenty story shear wall structures. Variables within the behavioral study were horizontal force factor  $K$ , shear





stiffness and taper. The results of the behavioral study are discussed and compared and conclusions drawn.



## ACKNOWLEDGEMENTS

Dr. J.G. MacGregor supervised this study. The author acknowledges this supervision and would like to thank Dr. MacGregor for the help which he willingly gave during the course of this study.

The study was supported by National Research Council Grant No. A1673.

The author would like to acknowledge the help given him by Dr. Masaaki Suko.

The author would also like to acknowledge the understanding and forbearing of his wife, Marlene, during this time of stress.



# TABLE OF CONTENTS

	Page
Library Release Form	i
Title Page	ii
Approval Sheet	iii
Abstract	iv
Acknowledgements	vi
Table of Contents	vii
List of Tables	xi
List of Figures	xii
List of Symbols	xv
Chapter 1 INTRODUCTION	1
1-1 Observed Performance of Reinforced Concrete Buildings under Earthquake Loading	1
1-2 Present Philosophy for Earthquake Resistant Reinforced Concrete Structures	2
1-3 Purpose of Investigation	4
Chapter 2 PREVIOUS RESEARCH	5
2-1 Review of Previous Studies	5
2-2 Member Response to Repeated Reversed Cyclic Load	5
2-3 Member Response	14
2-3-1 Member Response due to Flexure	14
2-3-2 Member Response due to Shear	19
2-4 Reported Frame Behavior	21





		Page
Chapter 3	MEMBER RESPONSE DURING STRUCTURAL VIBRATION	31
3-1	Introduction	31
3-2	Moment-Axial Load-Curvature Relationship	32
3-3	Applied Shear - Shear Strain Relationship for Members with Diagonal Cracks	34
3-4	Participation of Flexural and Shear Deformations in Member Total Deformations	36
3-5	Hysteresis Loop	39
3-6	Comparison with Experiment	40
Chapter 4	EARTHQUAKE ANALYSIS	54
4-1	Introduction	54
4-2	Analytical Model	55
4-3	Equivalent Rotational Springs	57
4-4	Stiffness Matrix for Frame	61
4-4-1	Slope Deflection Equations for Members with Rotational Springs and Rigid Stubs	61
4-4-2	Stiffness Matrix for the Frame	66
4-5	Equations of Motion	68
4-5-1	Formulation of Equations of Motion	68
4-5-2	Numerical Integration	71
4-5-3	Natural Periods of Vibration	73
Chapter 5	BEHAVIORAL STUDY	83



		Page
5-1	Introduction	83
5-2	Building Frame Considered	83
5-3	Building Parameters Studied	84
5-3-1	Range of Building Parameters Studied	86
5-4	Dynamic Response Spectrum for Elastic Systems	88
5-5	Observed Structural Response	91
5-5-1	Presence of Various Modes in Observed Structural Responses	92
5-5-2	Effect of Horizontal Force Factor K	92
5-5-3	Tapered Structures versus Prismatic Structures	93
5-5-4	Effect of Changing Shear Stiffness	94
5-6	Performance of Structures	96
Chapter 6	CONCLUSIONS AND RECOMMENDATIONS	135
6-1	Conclusions	135
6-2	Recommendations for Future Research	136
	REFERENCES	137
Appendix A	MOMENT-AXIAL LOAD-CURVATURE PROGRAM	142
A-1	Description of the Program	142
A-2	Input Data	142
A-3	Description of Subprograms and Flowcharts	143
A-4	Listing of Program	150



		Page
Appendix B	DILGER SHEAR-GAMMA RELATIONSHIP	156
B-1	Introduction	156
B-2	Input Data	156
B-3	Description of Program	157
B-4	Listing of Program	159
Appendix C	DERIVATION OF MODIFIED SLOPE DEFLECTION EQUATIONS	162
Appendix D	MAIN COMPUTER PROGRAM	168
D-1	Description of Program	168
D-2	Input Data	168
D-3	Presentation of Results	175
D-4	Description of Subprograms and Flow Charts	177
D-5	Listing of Program	205
Appendix E	$M_s - \delta\theta_s$ Program	236
E-1	Introduction	236
E-2	Input Data	236
E-3	Description of Program	237
E-4	Listing of Program	242





## LIST OF TABLES

TABLE		Page
3-1	Specimen Properties	42
3-2	Ratio of Flexural to Shear Deformations	43
5-1	Horizontal Force Factor "K" for Buildings or Other Structures	99
5-2	Properties of Shear Walls	100
5-3	Properties of Frame TR2.17	101
5-4	Properties of Frame TR1.33	102
5-5	Properties of Frame TR0.67	103
5-6	Properties of Frame PR0.67	104
5-7	Properties of Frame TI0.67	105
5-8	Properties of Frame PI0.67(12)	106
5-9	Properties of Frame PI0.67(6)	107
5-10	Natural Periods of Frames	108
5-11	Modal Analysis	109
5-12	Maximum Responses of Frame TR2.17	110
5-13	Maximum Responses of Frame TR1.33	111
5-14	Maximum Responses of Frame TR0.67	112
5-15	Maximum Responses of Frame PR0.67	113
5-16	Maximum Responses of Frame TI0.67	114
5-17	Maximum Responses of Frame PI0.67(12)	115
5-18	Maximum Responses of Frame PI0.67(6)	116



## LIST OF FIGURES

FIGURE		Page
2-1	Load-Deflection Response of a Typical Reinforced Concrete Beam	27
2-2	Load-Deflection Response of Reinforced Concrete Beam with No Degradation of Load Carrying Capacity	28
2-3	Load-Deflection Response of Reinforced Concrete Beam with Degradation of Load Carrying Capacity	29
2-4	Moment-Curvature Idealizations	30
3-1	Steel Stress-Strain Curve	44
3-2	Moment-Curvature Response of a Shear Wall	45
3-3	Dilger Shear Deformation Model	46
3-4	Williot Diagram for Dilger Shear Deformation Model	47
3-5	Typical $V-\gamma$ Relationship	48
3-6	Ultimate Rotation versus Shear Stress	49
3-7	Typical Load-Deformation Hysteresis Loop	50
3-8	Load-Deformation Response of Beam 35	51
3-9	Load-Deformation Response of Beam 43	52
3-10	Load-Deformation Response of Beam 46	53
4-1	Analytical Model	74
4-2	Numbering Convention	75
4-3	Column with Axial Load	76
4-4	Restrained Column	77
4-5	Typical $M_s - \delta \theta_s$ Relationship for Reversing Cyclic Load	78



FIGURE		Page
4-6	Typical Member	79
4-7	Equilibrium of Forces in Motion	80
4-8	Chart for Numerical Integration	81
5-1	Shear Wall Frame	117
5-2	Response Spectra for Elastic Systems, 1940 El Centro Earthquake	118
5-3	Maximum Displacements	119
5-4	Maximum Displacements	120
5-5	Maximum Interfloor Displacements	121
5-6	Maximum Interfloor Displacements	122
5-7	Maximum Column Rotations	123
5-8	Maximum Column Rotations	124
5-9	Maximum Shear Wall Rotations	125
5-10	Maximum Shear Wall Rotations	126
5-11	Maximum Displacements	127
5-12	Maximum Displacements	128
5-13	Maximum Interfloor Displacements	129
5-14	Maximum Interfloor Displacements	130
5-15	Maximum Column Rotations	131
5-16	Maximum Column Rotations	132
5-17	Maximum Shear Wall Rotations	133
5-18	Maximum Shear Wall Rotations	134
A-1	Flow Chart for M-P- $\phi$ Program	147
A-2	Discretized Reinforced Concrete Cross Section	148



FIGURE		Page
A-3	Stress-Strain Diagrams	149
B-1	Flow Chart for V- $\gamma$ Program	158
C-1	Equilibrium of Forces	167
D-1	Main Program	193
D-2	$M_s - \delta\theta_s$ Relationship in General Situation	194
D-3	Subroutine STIFF	195
D-4	Subroutine JISHIN	196
D-5	Subroutine SAIBUN	197
D-6	Subroutine SUCHI	198
D-7	Subroutine KYOTO	199
D-8	Subroutine NARA	200
E-1	Flow Chart for $M_s - \delta\theta_s$ Program	238
E-2	Input V- $\gamma$ Relationship	240
E-3	Input M-P- $\phi$ Relationship	241





## LIST OF SYMBOLS

### SYMBOL

$A$	Cross-sectional area
$A_i, A'_i$	Coefficients used to describe the modified slope deflection equations
$A_{cv}$	Area of inclined concrete strut
$A_s$	Area of tension steel in beam cross-section
$A_s'$	Area of compression steel in beam cross-section
$A_{sv}$	Area of stirrups crossing inclined section
$A_{sv}'$	Area of stirrup (all legs)
$b$	Thickness of rectangular beam cross-section
$\{B\}$	Known vector (right hand side vector) in equilibrium equations
$c_i$	Damping coefficient of the $i$ -th story
$C_v$	Compression force in web
$C$	Compression force in beam cross-section
$CMA$	Sum of the mass times the acceleration (relative to the ground) above the $i$ -th floor excluding the $i$ -th floor
$CSM$	Sum of the masses above the $i$ -th floor (including the $i$ -th floor) as defined in Eq. 3-35
$d$	depth from top fibre of beam to tension reinforcement
$d'$	depth from top fibre of beam to compression reinforcement
$E_c$	Modulus of Elasticity of concrete



## SYMBOL

$E_s$	Modulus of Elasticity of steel
$EI$	Modulus of Elasticity of cross-section times Moment of Inertia of cross-section
$f'_c$	28 day concrete strength
$f_y$	yield stress of steel
$f_{max}$	ultimate stress of steel
$[G]$	Frame stiffness matrix
$G$	Modulus of Rigidity
$h_i$	constant used to determine the damping constant at the i-th story
$I$	Moment of Inertia
$jd$	distance between tension and compression force centroids in working stress design
$K$	Horizontal Force Factor
$L$	Length of an equivalent cantilever column or the member length
$m_i$	mass concentrated at the i-th story
$M$	Bending moment at a cross-section
$M_s$	Moment in an equivalent rotational spring
$N_s$	Number of stories
$N_b$	Number of bays
$P$	Axial Load on a member
$p_v$	percentage of web reinforcing steel in a reinforced concrete beam



## SYMBOL

$p'$	Percentage of compression steel in a reinforced concrete cross-section
$p$	Percentage of tension steel in a reinforced concrete cross-section
$p_b$	Balanced steel ratio in a reinforced concrete cross-section
$\{Q\}$	story shears due to frame action
$[R]$	coefficient matrix in equilibrium equations
$s$	spacing of stirrups in a reinforced concrete beam
$S_A$	Spectral acceleration
$S_V$	Spectral velocity
$S_i(t)$	One of the terms in the equations of motion defined by Eq. 3-33.
$t$	time in seconds
$T$	Tension force in reinforced concrete cross-section
$U$	Required strength to resist design loads or their related internal moments and forces
$V$	Shear at a beam division point
$V_B$	Shear at the base of a building determined using code specified static earthquake loads
$V_c$	Maximum shear force at which a reinforced concrete beam does not develop inclined cracking
$v$	shear stress
$v_{cr}$	shear stress corresponding to $V_c$
$v_{ult}$	shear stress at which a reinforced concrete member fails
$w$	uniformly distributed load
$W$	Weight of a building



# SYMBOL

$\{x\}$	displacement relative to the ground
$\{\dot{x}\}$	velocity relative to the ground
$\{\ddot{x}\}$	acceleration relative to the ground
$Z$	Seismic zone factor
$\lambda_1$	Ratio of length of rigid stub at the left end of a beam to the entire member length
$\lambda_2$	Ratio of length of rigid stub at the right end of a beam to the entire member length
$\lambda_3$	$1-\lambda_1-\lambda_2$
$\alpha_o$	inclination of stirrups
$\alpha_1, \alpha_2$	Coefficients used to describe the $M_s-\delta\theta_s$ relationship of an equivalent rotational spring
$\beta_o$	inclination of cracks in reinforced concrete beam
$\beta_1, \beta_2$	Coefficients used to describe the $M_s-\delta\theta_s$ relationship of an equivalent rotational spring
$\epsilon_{sv}$	steel strain in stirrups
$\epsilon_{cv}$	Concrete strain in compression struts
$\gamma$	Shear strain
$\theta$	joint rotation
$\theta_u$	ultimate joint rotation
$\{\theta\}$	unknown vector in equilibrium equations
$\phi$	curvature
$\phi_{cap}$	capacity reduction factor
$\rho$	sway rotation





## SYMBOL

$\Delta t$	Increment in time when equations of motion are solved numerically
$\{n_i\}$	i-th column of a stiffness matrix
$\{\xi\}$	constant vector expressing index deflections
$\{\xi_0\}$	Initial deflections due to vertical loads only
$\omega_i$	Circular frequency in the i-th natural mode of vibration
$\Delta_{top}$	Deflection at top of cantilever columns
$\Delta_{v_i}$	Deflection at column division point due to shear deformation
$\Delta_{F_i}$	Deflection at column division point due to flexural deformation
$\Delta$	Total deflection at top of cantilever column
$\Delta M$	Change in moment at column division point due to axial load effects
$\delta\theta_s$	Relaxation angle produced by an equivalent rotational spring.
$K$	Stiffness of a one degree-of-freedom system



## Chapter 1

### INTRODUCTION

#### 1-1 Observed Performance of Reinforced Concrete Buildings under Earthquake Loading

A study of the literature <sup>1,2,3,4,7</sup> on the structural damage incurred by buildings subjected to major earthquakes reveals that those buildings most severely damaged were those possessing design faults with respect to earthquake resistance. Next were those buildings having structural frames or elements with limited ductility. Buildings which by design had adequate ductility, although possibly severely deformed, still possessed their integrity.

Because ductile moment-resisting frames have performed well under earthquakes, they have become the standard for earthquake resistant design. However, recent earthquakes have shown that ductile beam-column frames may be too flexible. Although this type of frame assures limited structural distress, high story to story deflections may occur causing heavy damage to the non-structural elements of the building (finishes, partitions, glass, mechanical and electrical equipment) which together can comprise up to 80% of the cost of a building.

Structures possessing greater rigidity such as those with shear walls are presently being thought desirable due to their ability to limit non-structural damage. Shear wall-



frame structures possessing necessary damage control backed up by a moment-resisting frame as a second line of defense seem to offer considerable advantages over moment-resisting beam-column frames.<sup>4</sup>

# 1 - 2 Present Philosophy for Earthquake Resistant Reinforced Concrete Structures<sup>5</sup>

The performance criteria of most earthquake code 8,9,10,11 provisions require that a structure be able to:

- (1) resist minor earthquakes without damage
- (2) resist moderate earthquakes with minor structural and some non-structural damage
- (3) resist major catastrophic earthquakes without collapse

Collapse is defined as that state when occupants cannot escape from a building because of failure of the structure.

The above performance criteria allow only for the effects of a typical earthquake ground shaking. The effects of slides, subsidence or active faulting in the immediate vicinity of a structure, which may accompany an earthquake are not considered.

Code guidelines for the day-to-day design of earthquake resistant structures must compromise exactitude and realism for speed and simplicity of application. The result of this is a partly rational, partly empirical prescription of equivalent static forces to simulate earthquake induced inertial forces. Such a loading is assumed to be resisted





by the structure within its elastic working range of stresses.

The code specified equivalent forces are considerably smaller than those which would be developed in a structure responding elastically to an earthquake with an intensity such as the 1940 El Centro, California earthquake. Buildings designed under present codes would be expected to undergo lateral displacements approximately 5 times those resulting from code specified equivalent static forces when subjected to an El Centro type base motion. These large deformations would indicate yielding in many members of the structure, and this is the intent of the codes. The acceptance of the fact that it is not economical to design most multistory buildings to resist major earthquakes elastically and the recognition of the capacity of structures possessing adequate strength and ductility to withstand major earthquakes by responding inelastically, lies behind the relatively low forces specified by the codes coupled with the requirements for ductility in the structure, particularly at member joints. Analytical studies<sup>6</sup> have shown that 20 story reinforced concrete building frames designed to resist code-specified lateral forces elastically, would in fact respond inelastically under an El Centro type earthquake. The calculated ductility ratios, defined as the ratio of maximum to yield deformation, ranged from 4 to 6.

The capacity of a structure to deform in a ductile





manner, that is, to deform beyond the yield limit without significant loss of strength, allows such a structure to absorb and/or dissipate a significant portion of the energy from an earthquake without serious damage.

### 1-3 Purpose of Investigation

Accepting present code philosophy and acknowledging the apparent desirability of shear wall buildings in resisting earthquake induced loadings, the first objective of this dissertation is to develop a reasonably realistic analysis procedure to model the behavior of a shear wall under major earthquake induced loadings so that strength and deformation requirements can be examined.

The second objective of this dissertation is to present the results of a behavioral study performed using the analytical procedure. Seven twenty story shear walls were analyzed. The structure analyzed was a typical high-rise apartment building wherein all lateral and axial forces are carried by shear walls.

The following factors were considered in the behavioral study:

1. Ratio of ultimate moment of shear wall to design seismic moment.
2. Cross-sectional shape of shear wall.
3. Taper of shear wall.



## Chapter 2

### PREVIOUS RESEARCH

#### 2-1 Review of Previous Studies

This chapter represents an attempt to review the present state of knowledge concerning reinforced concrete members and frames under repeated reversed cyclic loading. Observed experimental member response will first be discussed. Methods of predicting member responses will be considered next. Observations determined from frame analyses using various member response expressions are then studied.

#### 2-2 Member Response to Repeated Reversed Cyclic Load

The load-deflection response of a typical under-reinforced concrete beam under monotonically increasing load is shown in Fig. 2-1. The response of such a beam consists essentially of three sloping lines, the end coordinates of which represent the deformation and load corresponding to flexural cracking, yield of tensile steel, and the ultimate strength of the beam. The slope of the line at any point represents the stiffness of the beam. Members having this type of load-deflection response are considered desirable in all load situations because:

1. they maintain their ability to hold load at deformations greater than yield thus allowing redistribution of load from section to section within the structure.



2. the large amount of deformation after the yield load indicates a ductile failure giving adequate warning of overload in static load situations.

3. the large amount of deformation after the yield load allows the cross-section to absorb energy in seismic load situations or other conditions requiring energy absorption.

It is the intention of most building codes that this type of behavior should be preserved in all members in all loading situations. Any action which an engineer can take to extend the ability of a member to sustain load and deformation to required levels is considered desirable. These actions, usually involved with delaying the occurrence of tensile steel fractures, concrete crushing, compression steel buckling, and shear failures have been the subject of a large number of research papers involving reinforced concrete. Only a few of these concerned with reinforced concrete members under repeated reversed cyclic loading will be mentioned here however.

The load-tip deflection response of a doubly-reinforced concrete member,<sup>12</sup> containing more stirrups than required by conventional design, subjected to repeated reversed moment and shear is shown in Fig. 2-2. The following observations can be made from this figure:

1. The load-deformation response is similar in both directions of loading.

2. There is no significant drop in load capacity for





succeeding large deformation cycles.

3. Two kinds of hysteresis loops can be distinguished. Before large deformation cycles the loops are stable and spindle shaped. During large deformation cycles the loops take on a pinched shape.

4. The member is subject to stiffness degradation, ie. the slope of the line describing the relationship between load and deformation below yield level decreases..

The noticeable degradation of unloading stiffness was described by Burns and Siess.<sup>13,14</sup> They found they could relate the unloading stiffness to the magnitude of the "damage ratio" expressed as the ratio of the present plastic deformation to the total plastic deformation at failure. Material considerations corresponding to this were not considered.

In describing the pinched shaped load-deformation hysteresis loops, Park, Kent and Sampson<sup>15</sup> concluded that over a large portion of the response for beams, the moment is carried by a steel couple alone. This phenomenon is due to the yielding of steel in tension causing cracks in the tension zone which, because of the plastic elongation of the steel, do not close when the moment is returned to zero. When the direction of moment is changed, that steel is put into compression and must carry all of the compressive force because cracks now exist in the compression zone. The steel must yield in compression before these cracks close and enable some of the compressive force to be carried by the





concrete.

It is evident that the flexural stiffness of the section is reduced when the moment is being carried by a steel couple alone but increases when the concrete begins to carry compression. The increase in stiffness due to closing of the cracks in the compression zone is more sudden in theoretical curves than in test curves. This is probably because in practice some compression can be carried across cracks before they close. Particles of concrete which flake off during cracking and small relative shear displacements along the cracks cause compression to be transferred across the cracks gradually as high spots come into contact rather than suddenly as implied by theory. Nevertheless, it is evident that the presence of open cracks in the compression zone which eventually close causes a marked pinching in of the moment-curvature response.

A second load-tip deflection response<sup>16</sup> is shown in Fig. 2-3. This beam displayed similar characteristics to those shown in Fig. 2-2 except that its load carrying ability degrades and its stiffness degradation is more substantial.

The improvement in response of Fig. 2-2 over Fig. 2-3 has principally evolved through the inclusion of compression, confining and shear reinforcing steel within the body of the reinforced concrete member. It has even been suggested that the members of an earthquake resistant structure should have stirrups for the total shear corresponding to the maximum



moment the cross-section can reach at any strain rate.<sup>19</sup> The main reason for this is to counteract the following mechanisms described by Popov, Bertero and Krawinkler<sup>12</sup> in their discussion of the deterioration of shear resistance:

1. Deterioration of Shear Resisting Capacity of Stirrups under Load Reversals

The presence of web reinforcement impedes the growth of diagonal tension cracks and reduces their penetration into the compression zone, leaving more uncracked concrete at the head of the crack to resist the combined action of shear and compression. Prior to yielding of the stirrups they limit crack widths allowing aggregate interlock and dowel action to develop. Closed stirrups confine the concrete core and permit larger concrete strains to be attained than in unconfined concrete. Stirrups also provide support for longitudinal reinforcement so that buckling of the compression reinforcement is delayed.

Load reversals reduce the effectiveness of the stirrups in performing these functions. After diagonal tension cracks occur, the portions of the web reinforcement where these cracks cross the stirrups undergo cycles of unidirectional straining that may lead to a gradual reduction of the bond between stirrups and concrete. Further deterioration can occur from motion of the concrete along diagonal cracks leading to a reduction in aggregate interlock and stirrup bond.



A secondary effect which may be related to the lessening of stirrup effectiveness in controlling cracking is that if flexural and diagonal tension cracks are present in both directions from preceding load reversals, the compression zone at the tip of the diagonal tension crack may be fractured by flexural cracks. Then the shear resistance of the compression zone has to depend mainly on dowel action in the compression steel and on aggregate interlocking resistance. This together with the deterioration in the web reinforcement bond is believed to be the main reason for the deterioration of the shear resistance of beams with diagonal cracks across the whole beam subject to repeated reversing load. This deterioration is evidenced simultaneously by a drop in resistance and large displacements across the main diagonal cracks.

## 2. Dowel Action and Loss of Bond in Longitudinal Steel Bars

Bond stresses in the longitudinal bars tend to build up close to the flexural cracks and can lead to deterioration of bond under cyclic loading. The prying action of the dowel shear accelerates the deterioration of bond between the longitudinal steel and the concrete. As a consequence, the composite action of steel and concrete deteriorates and the beam stiffness decreases.

## 3. Abrasion of Cracked Surfaces and Aggregate Interlocking Resistance.





The nature of aggregate interlocking shear resistance under monotonic loading was investigated among others by Fenwick and Paulay<sup>17</sup> who formulated a semi-empirical equation for its analysis. Aggregate interlocking shear is related to the width of the diagonal tension cracks, shear displacements across the cracks and concrete strength. This kind of resistance is weakened under load reversals by abrasion of the two contacting surfaces at the cracks. Surface granules wear off, crack widths may increase, and interlocking resistance may deteriorate substantially.

The effects described by Popov, Bertero and Krawinkler for members with inclined cracks are substantiated by Brown and Jirsa<sup>16</sup> in their discussion of the mechanism of shear resistance and its deterioration for the more serious case of a member which has been flexurally cracked throughout perpendicular to its longitudinal axis during the course of its repeated reversed cyclic loading. Brown and Jirsa thought that before a design method could be developed which would predict the shear capacity of flexurally cracked beams under load reversals, research would be needed which related the shear transfer capacity across cracked sections to the number and intensity of cycles of load reversal. They felt that the shear friction technique used in the design of brackets and corbels might be adaptable to this problem. Using such a technique, a coefficient of friction, dependent upon the intensity of the load or deformation and





number of load cycles, might be developed and used to determine the shear transfer capacity of the concrete. To date, Brown and Jirsa have not published any information concerning their suggestions.

Wight and Sozen<sup>18</sup> emphasized the need to consider the possible reduction in shear strength of reinforced concrete members loaded to deflections which correspond to strains in the concrete compression zone leading to splitting cracks. A comparison of their specimens with and without axial load indicated the following for specimens with the same transverse reinforcement ratio:

- (1) During cycles with the same ratio of maximum deflection to yield deflection, the specimens without an axial load suffered a more rapid decrease in strength with each complete cycle of load reversal.

- (2) The strain hardening slope in the shear-deflection curves beyond yield was steeper for the specimens without an axial load.

- (3) The specimens with axial loads had higher yield and ultimate shear capacities.

Axial load hindered the opening of inclined cracks and closed flexure shear cracks opened in the previous half cycle. In the specimens with no axial load, the flexure shear cracks usually opened wider and the cracks formed in the previous half cycle did not always close when the load was reversed, resulting in the formation of nearly vertical



cracks which were continuous throughout the total depth of the specimens. This phenomenon tended to increase the length of the range of low stiffness in the load-deflection relationships.

Test results quoted by Bertero<sup>19</sup> at high axial load levels show that the reduction in strength, deformational energy absorption and energy dissipation capacities increases with the number of cycles of repeated reversed loadings. However, for columns with shear span ratios larger than 2, by increasing the amount of web reinforcement, especially by decreasing the spacing of hoops, the reduction is limited and it is possible to have very ductile column behavior even under high axial loads and large numbers of repeated alternating bending moment cycles.

Very short columns in which shear forces predominate become brittle. Studies carried out by Yamada<sup>20</sup> on very short columns (shear span ratio = 1.2) subjected to constant high axial forces and repeated alternating transverse loads show that when the web reinforcement ratio is less than 0.44%, the columns show an explosive brittle failure immediately after diagonal cracking. On the other hand, columns with web reinforcement ratios equal to or larger than 0.88% showed ductility after diagonal cracking. Yamada concluded that the web reinforcement ratios necessary to prevent a shear explosion failure and to give sufficient ductility under the effect of severe ground motion are shown by tests -



to be larger than 1%. This requires very closely spaced hoops.

## 2-3 Member Response

Load-deformation responses have traditionally been calculated by integrating beam curvatures thus considering only the flexural component of deformation. Shear deformations are usually considered insignificant. This has led to excellent results especially for steel members. The deflections of concrete beams under monotonic loading are generally calculated in the same manner. One must however consider both flexural and shear deformations in reinforced concrete members under repeated reversing cyclic load subject to flexural and shear stiffness degradation, as each form a significant part of the total member deformation:

### 2-3-1 Member Response due to Flexure

Earliest attempts to predict the load-deformation response of members under repeated reversed cyclic load assumed that shear deformations were insignificant and thus only required appropriate moment-curvature diagrams. Analytical models of the moment-curvature diagrams for this case have undergone a steady process of evolution.

Sinha, Gerstle and Tulin<sup>21</sup> proposed moment-curvature curves derived using a trilinear stress-strain curve for reinforcing steel and a concrete stress-strain curve derived from tests of plain concrete under compressive cyclic load.





In these tests the envelope concrete stress-strain curve was very close to the virgin stress-strain curve for the same concrete. The unloading and reloading stress-strain curves did not parallel the first loading stress-strain curve, however. They obtained reasonable correlation with moment-curvature curves from reinforced concrete beams cycled unidirectionally.

Aoyama<sup>22</sup> developed moment-curvature curves for concrete beams under repeated reversed cyclic loading using an elastoplastic stress-strain relationship for concrete neglecting any stress in tension. When the outcome of the analysis was compared with test results, it was found that the agreement was almost perfect for initial loading and for the first reversal which was made slightly after the yielding in the initial loading. The only disagreement found was that the stiffness at moments close to yield was overestimated. The agreement was not very good for reversals after the first reversal from a point considerably beyond yielding, however. One reason for this was that the Baushinger effect was not considered in the stress-strain assumptions.

Agrawal, Tulin and Gerstle<sup>23</sup> agreed with Aoyama and concluded that the response to repeated loading may be elastic-plastic for engineering purposes, but the behavior under alternating plasticity is highly nonlinear and can be predicted only by considering the Baushinger effect in the steel.

Brown and Jirsa<sup>16</sup> developed moment-curvature relationships to predict the response of their test specimens





during the third half-cycle of load reversal. Their analysis was formed using stress-strain curves for confined concrete by Yamashiro<sup>35</sup> and for unconfined concrete by Karsan.<sup>36</sup> The stress-strain curves were shifted on the strain axis by a strain equal to 40% of the maximum tensile strain at the surface of the concrete in the previous direction.

Steel stress-strain curves used in the analysis were those developed by Singh, Gerstle and Tulin<sup>38</sup>, which consider the Baushinger effect within the stress-strain response. Strain hardening of the steel was also considered. They found their computation procedure to be generally satisfactory. The main discrepancy between their computed and measured load-deflection curves was a pinching of the measured curves toward the origin which they attributed to shear deformations.

Park, Kent and Sampson<sup>15</sup> have recently developed moment-curvature curves for reinforced concrete beams under repeated reversed cyclic load. Their steel stress-strain curve accounted for Baushinger effect and strain hardening. Kent and Park<sup>37</sup> developed the stress-strain curve for confined concrete used in the analysis. They found they could reasonably trace the moment-curvature and load-deflection response of their test beams and those of Aoyama for initial loading and first and second load reversals.

Due to the intricate shape of moment-curvature curves developed in this way, much effort is required to



trace the load-deflection response of a beam under repeated reversed cyclic load. Park, Kent and Sampson required approximately 3 hours of IBM 360/44 computer time to trace the load-deflection response of one beam during three half-cycles of load. Because of this and at the same time to adjust for discrepancies within their predicted load-deformation responses, several authors have idealized the appropriate moment-curvature diagrams using series of straight lines in defined patterns. Some authors have presented this material in terms of moment-curvature loops, some in terms of load-deformation loops. For members having predominant flexural deformations the two methods of presentation will be assumed to be analogous.

The idealizations proposed by five different authors are shown in Fig. 2-4.

The moment-curvature relationships shown in Fig. 2-4(a) have been presented by Clough<sup>6</sup>, by Monnier<sup>24</sup> and by Takeda<sup>25</sup>. All three relationships are defined by the same set of rules; the principal difference between the various relationships lies in the slope taken for the unloading path.

The bilinear moment-curvature relationships shown in Fig. 2-4(b) have also been used to predict load-deformation behavior<sup>26,34</sup>. The bilinear loop is a stable parallelogram shape in which loading and unloading always follow the initial elastic slope. The degrading bilinear loop loads and unloads on a slope which degrades according to the previous maximum curvature.



Imbeault<sup>26</sup> compared actual load-deformation responses of flexural members tested on the University of Illinois shaking table to those predicted using linear elastic, bilinear, Clough, Takeda and degrading bilinear load-deflection responses. He found that linear elastic responses have little resemblance with measured dynamic responses. The large magnitude of energy absorbed through inelastic deformation and the discontinuity of yielding throughout the duration of the response invalidated the computation of a transient or random response using a linear elastic system having a constant equivalent viscous damping coefficient.

Imbeault found that the bilinear system satisfactorily predicts the maximum acceleration responses of yielding systems. Because the bilinear system does not account for the degradation of stiffness, however, the time history acceleration response, the maximum displacement and the time history displacement responses were not well predicted by this moment curvature relationship.

Clough's and Takeda's hysteretic models predicted the maximum and the time-history responses of the reinforced concrete specimens within an accuracy of the order of 20 percent of the maximum. Imbeault found no other source of energy absorption (other than hysteretic energy) was necessary to satisfactorily predict the responses.

The degrading bilinear response required an additional viscous damping of 5 percent of critical to account for the





energy absorbed through the "true" hysteresis loop at low levels of excitation. This model calculated the maximum and time history dynamic responses with the same degree of accuracy as the more complex Clough's or Takeda's systems.

Park et al.<sup>15</sup> also traced load-deflection responses using the degrading stiffness straight line moment-curvature relationship proposed by Clough and found it to be a reasonable idealization. They warned however that Clough's model did not simulate well the pinching effect developed in moment curvature curves of an axially loaded member.

### 2-3-2 Member Response due to Shear

Static load-deflection models have been proposed for members subjected mainly to shear. These models are assumed to apply to shear walls in low rise buildings which are subjected to high shear force and small moment.

Yamada, Kawamura and Katagihara<sup>27,28</sup> tested low rise reinforced concrete shear walls with boundary beams and columns and with and without openings. They formulated a theory for strength and deformation based on equilibrium of forces and compatibility of strains resulting from flexure of the beams and columns with the shear wall under diagonal compression. They found they could reduce their model to the boundary frame with an equivalent diagonal compression strut. Tests carried out by Barda<sup>29</sup> at the Portland Cement Association seem to substantiate their assumptions for low rise walls.





Zimmerli<sup>30</sup> has proposed a model for the ultimate strength of shear walls under high shear with axial forces. The model consists of concrete diagonals, horizontal steel stirrups and vertical steel stringers. Assuming all elements are plastified and using equilibrium, a relationship is found between load and deformation at ultimate. Three different deformation modes were considered, corresponding to separate yielding of all the stirrups, the concrete diagonals or the vertical stringers.

Two authors<sup>31,39</sup> have developed shear-deflection analyses based on the assumption that the shear acting on a cracked reinforced concrete member is carried by a truss mechanism. Each analysis integrates the strains in the concrete diagonals and tension steel stirrups to find component deformations which are then superimposed using a Williot diagram to give the total deflection due to shear.

O'Leary<sup>47</sup> tested reinforced concrete beams under increasing moment, shear and axial tension. He studied the crack patterns of his beams and assumed that there were three paths to carry shear between the base of his specimen and the point of shear application. He proportioned the total shear so that the deformation of each load path was equal. He found however that without knowledge of stirrup anchorage slip-load relationships, it was impossible to predict shear deflections adequately from analysis of the analogous truss.

Dilger<sup>31</sup> has formulated a model for the shear component



of the total deformation of T-beams under monotonic loading. This model will be illustrated in Chapter 3 as shear deformations are included in developed moment-rotation characteristics.

The importance of a shear deformation term in analytical load-deformation responses for members under repeated reversed cyclic load has been illustrated in tests performed by Brown and Jirsa.<sup>16</sup> Their cantilever beams were cycled between deformation limits. As the number of cycles increased, flexural deformations as given by rotation meters decreased and shear deformations increased.

#### 2-4 Reported Frame Behavior

Clough and Benuska<sup>6</sup> reported on the behavior of twenty story three bay pure frame structures having fundamental periods of 1.6, 2.2 and 2.8 seconds. The structures were subjected to the ground acceleration history recorded in the El Centro earthquake of May 18, 1940 (N-S component). Bilinear moment-rotation properties were developed for each member and a stable elastic-plastic bilinear hysteresis loop was assumed. Columns were designed to have yield moments six times those required by elastic analysis; beam yield moments were two times greater. Clough and Benuska concluded:

1. Displacements and member forces caused in a typical multistory frame by code lateral loads are smaller than would be generated in the structure by a moderate earthquake,



if the structure were to respond elastically.

2. Lateral displacements developed in the nonlinear earthquake response of a tall building appear to be similar in magnitude to the elastic displacement response.

3. In a typical building design, the nonlinear member deformations tend to be concentrated in the girders, while the columns remain elastic, (except in the top few stories). Girder ductility factors developed during a relatively severe earthquake may be of the order of 4 to 6 in a typical design.

4. For the tall buildings considered, the period of vibration and height of the structure do not appear to be important factors in determining the amount and distribution of ductile deformations which will result from an earthquake excitation.

5. Ductile deformations tend to avoid strong members and to concentrate in weak members; thus the girders will tend to yield if the columns are made stronger, or vice versa. On this basis, it is evident that the frame design should not include weak zones which may attract a major part of the ductile deformations.

By studying cantilever beam models of tall structures, Giberson<sup>32</sup> hoped to gain a fuller understanding of why the displacements, interfloor displacements, shear forces and total accelerations have differing dependencies upon the various modes as well as upon the position in the structure.





Two linear elastic continuous cantilever beams which represented limiting cases of tall structures were studied. In one, the stiffness and mass distribution were uniform, while in the other these distributions taper to a point at the top.

Giberson subjected the beam models to an ensemble of earthquakes and then examined their responses for general trends.

Giberson stated that a mass particle at the top of a severely tapered structure could be expected to feel very high acceleration. He also stated that structural damage would be increased in a tapered structure because interfloor displacements appeared to be dependent upon higher modes, which are emphasized in a tapered structure.

Giberson concluded that in order to minimize structural damage and accelerations in a structure, particularly in the upper portions, it is best to have the stiffness and mass distributions as uniform as possible.

Husid<sup>33</sup> reported on the effect of gravity on the earthquake response of one degree of freedom yielding structures subjected to earthquake-like excitation. His results show that the effect of gravity is to increase significantly the development of permanent set over that occurring when gravity is ignored. Because the gravity effect increases as the deflections grow, the permanent set increases rapidly just prior to failure.

Otani<sup>34</sup> predicted the response of his model three





story one bay reinforced concrete frames tested using the University of Illinois Earthquake Simulator. In analyzing the overall response of these frames, the portion of the beam or column between the varying point of contraflexure and the joint was considered as a basic unit. The stiffness characteristics of the basic unit were determined by the primary force deflection and rotation relations of a cantilever and Takeda's hysteresis rule. Rotation due to bond slip of the tensile reinforcement was simulated by placing, at the ends of the frame members, bilinear rotation springs with a simplified hysteresis based on Takeda. Deformations due to axial loads acting through member displacements were not considered. Member forces were calculated at the end of each load increment. If a member force exceeded a limiting value, the member stiffness was modified for the next load increment.

Comparisons of calculated response waveforms with those measured are summarized as follows:

(1) The analytical model was stiffer than the test specimen, especially at low-amplitude oscillations.

(2) Large oscillations were favorably simulated by the analytical model, if the intensity of base motion was relatively high, and if the damage in the test specimen was small prior to the test run.

(3) The analytical model with viscous damping proportional to stiffness (a first mode damping factor of 2 percent of critical at the initial uncracked stage was preferable to



the model without viscous damping in the prediction of higher frequency components in the calculated acceleration waveforms.

(4) The analytical model predicted closely the maximum accelerations and displacements at the third level, and the maximum base shears and base moments.

Imbeault<sup>26</sup> analyzed four moment-resisting frames, 6 to 30 stories in height with periods varying from 0.63 to 2.8 seconds, to determine their response to five different earthquakes. He analyzed each frame assuming bilinear elastic-plastic and degrading bilinear member responses.

He found that in the bottom section of a frame, the average bilinear girder ductility factors of the frames analyzed could be averaged within plus or minus one ductility factor. Associated with the different earthquakes, the average girder ductility factors were:

Jennings A-1	4.5
Jennings B-1	3.5
El Centro NS 1940	2.5
Olympia S80W 1949	1.5
Taft N21E 1952	1.0

Imbeault found ductility demands to be 0.5 to 2.0 ductility factors higher in the top section of the frames which he attributed to higher mode effects.

Imbeault noted that the location of yielding is a property of the structural system and is independent of



earthquake characteristics.

In comparing responses obtained using bilinear and degrading bilinear member responses, Imbeault found that the reduction in energy absorption capacity of the degrading bilinear system led to significant increases in ductility requirements.

Depending upon the earthquake characteristics the maximum increases in the magnitude of the ductility of the degrading bilinear responses compared to the bilinear responses were:

Jennings A-1	90%
Jennings B-1	50%
El Centro NS 1940	30%
Olympia S80W 1949	20%
Taff N21E 1952	10%

Other significant differences, if any, between the observed bilinear and degrading bilinear response were not discussed.





FIG. 2-1 LOAD-DEFLECTION RESPONSE OF A TYPICAL  
REINFORCED CONCRETE BEAM





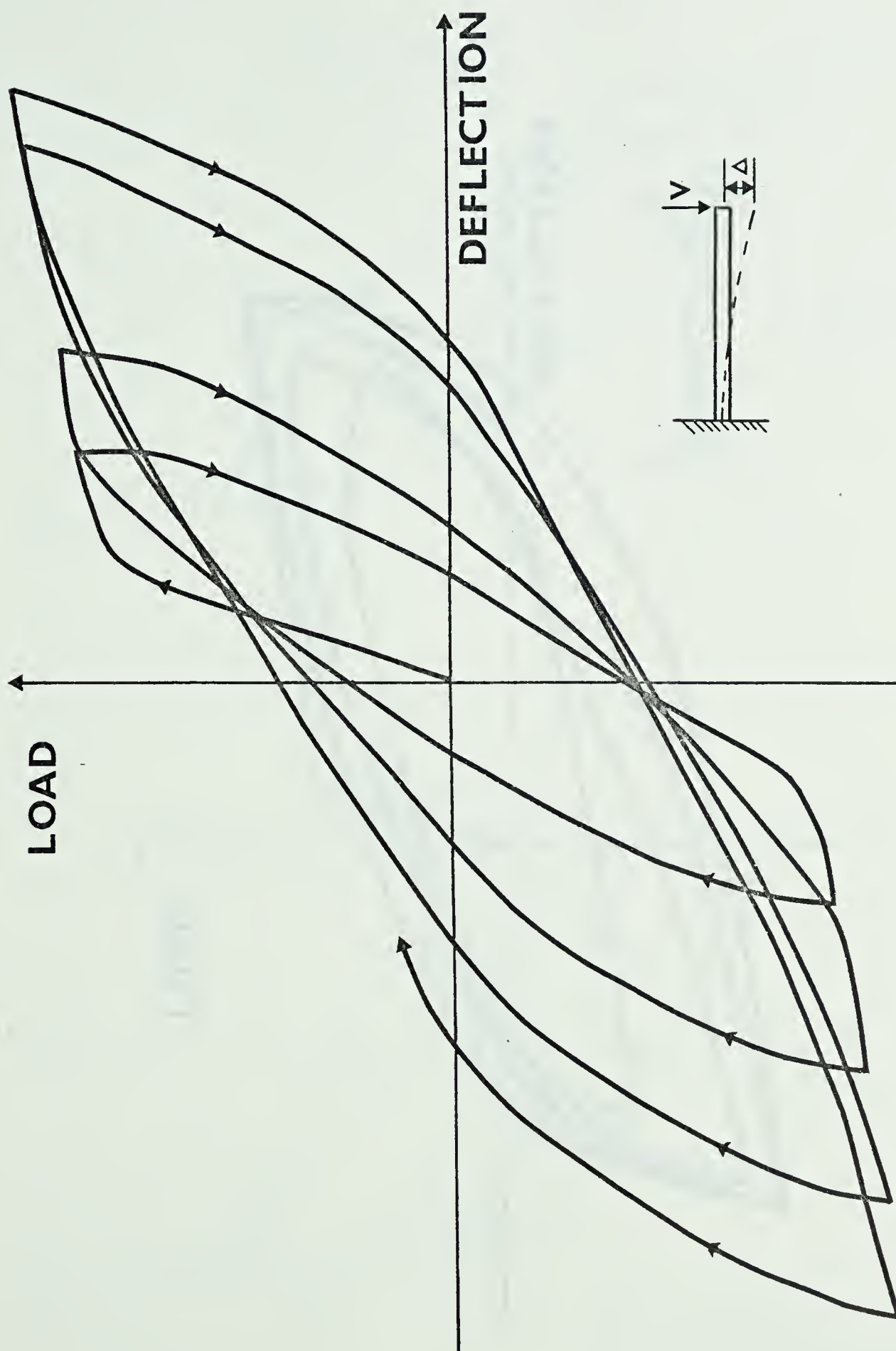


FIG. 2-2 LOAD-DEFLECTION RESPONSE OF REINFORCED CONCRETE BEAM  
WITH NO DEGRADATION OF LOAD CARRYING CAPACITY



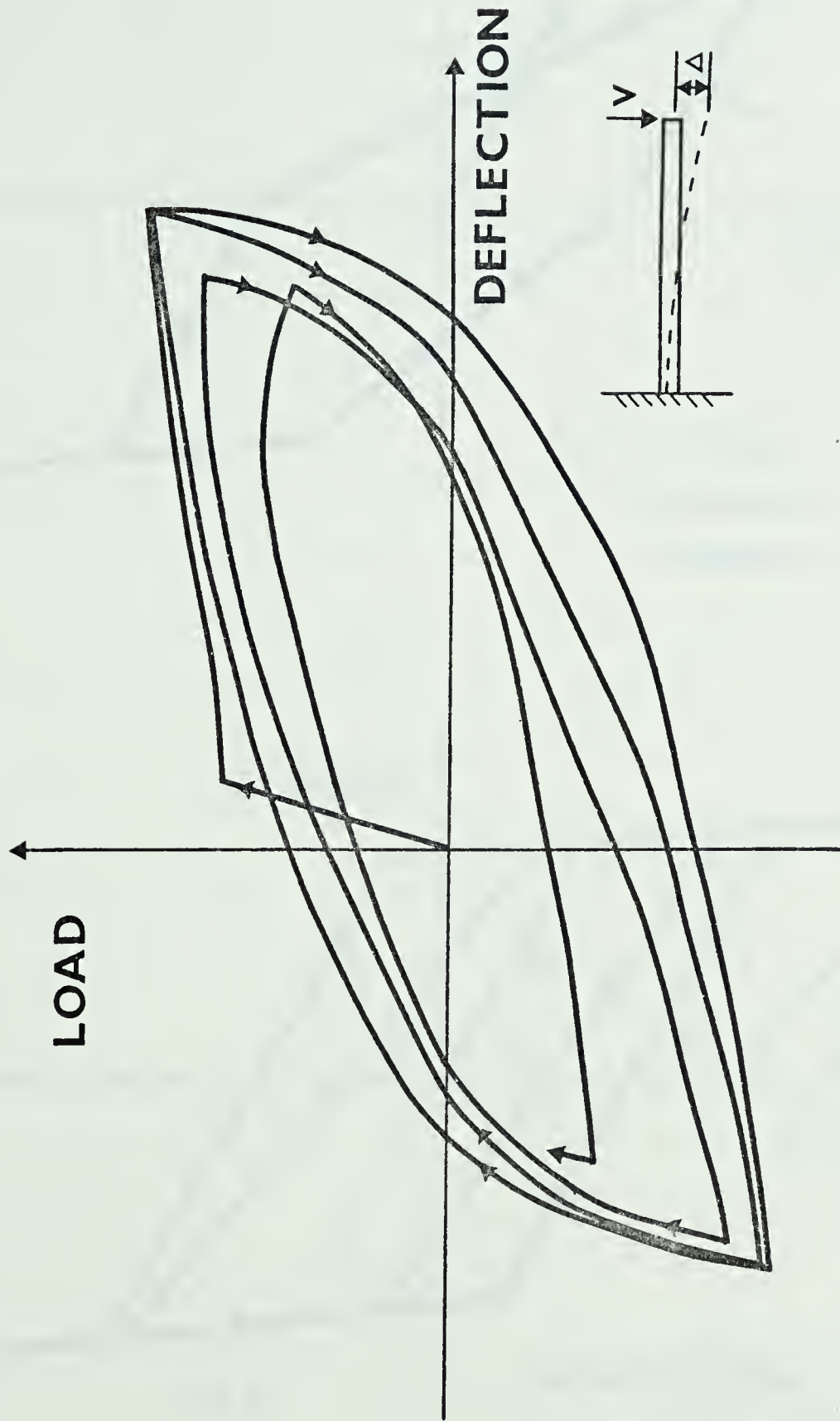


FIG. 2-3 LOAD-DEFLECTION RESPONSE OF REINFORCED CONCRETE BEAM  
WITH DEGRADATION OF LOAD CARRYING CAPACITY



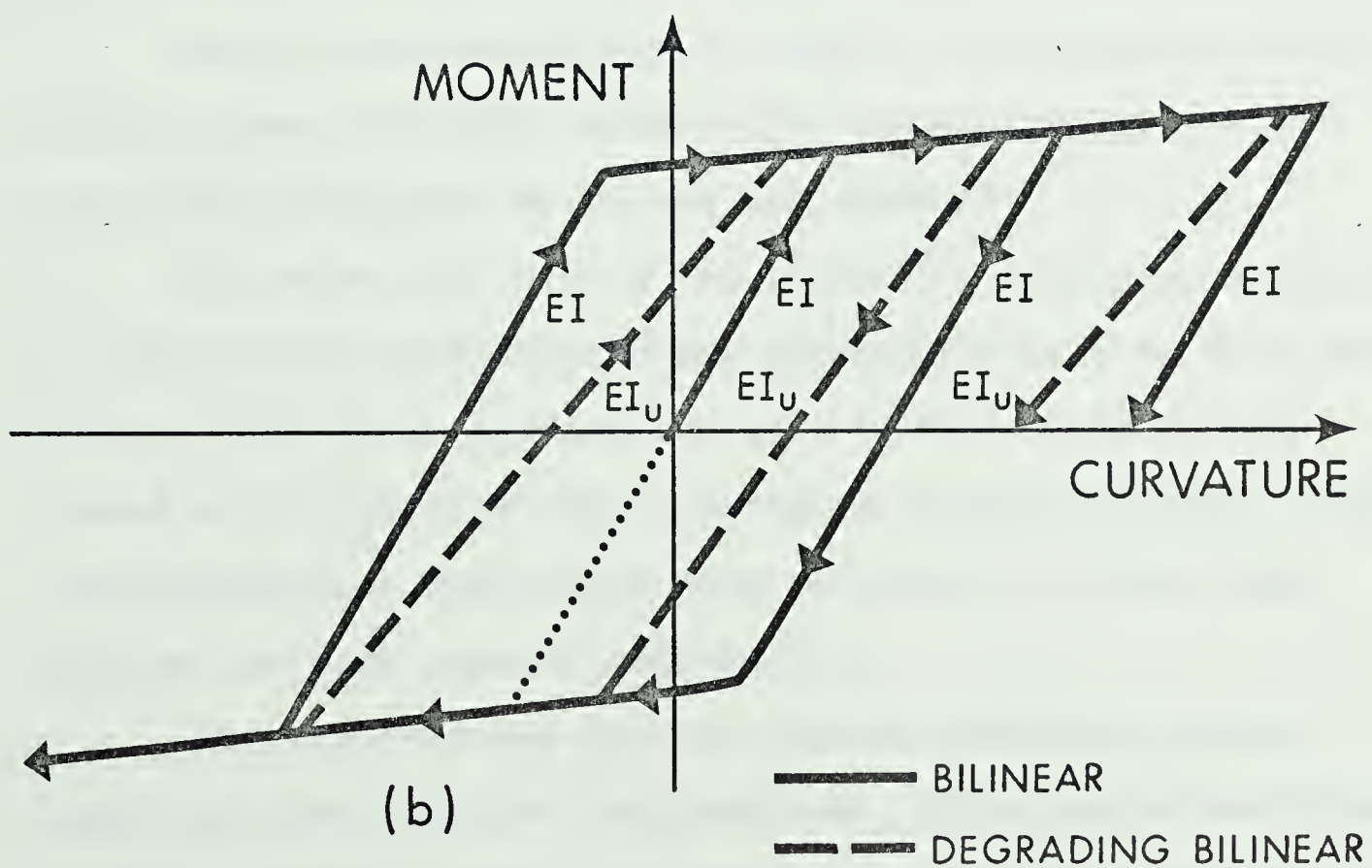
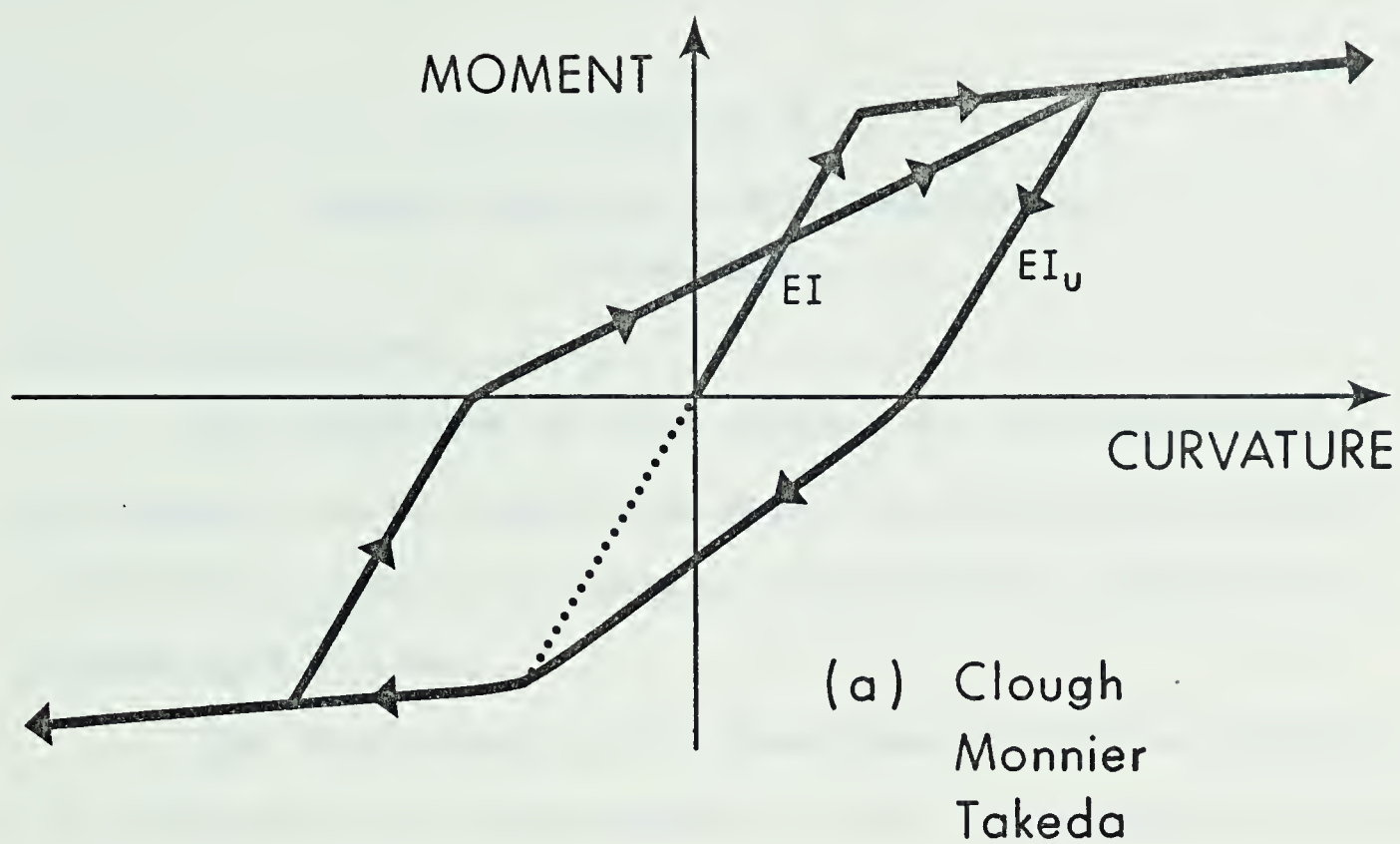


FIG. 2-4 MOMENT-CURVATURE IDEALIZATIONS





## Chapter 3

### MEMBER RESPONSE DURING STRUCTURAL VIBRATION

#### 3-1 Introduction

The objective of this chapter is to present the development of an analytical model to predict the elastic-inelastic response of a member subjected to repeated reversed cyclic load.

The first step in the development involved combining the stress-strain relationships of the constituent materials within the reinforced concrete cross-section into a moment-axial load-curvature ( $M-P-\phi$ ) relationship.

Next it was necessary to find a relationship between applied shear and shear strain ( $V-\gamma$  relationship). A relationship developed by Dilger was adopted.

The next step within the procedure involved choosing an appropriate load-deformation hysteresis rule so that the flexural and shear deformation of a member could be predicted at any point within a member's loading history. The load-deformation hysteresis loop proposed by Clough was adopted for each type of deformation.

The deformations due to flexure, shear and axial load were then computed and combined. This was accomplished within a computer program in which the curvatures were integrated and shear strains multiplied by appropriate lengths



and the resultant deformations added.

Analytic load-deformation responses predicted using Clough's hysteresis loop were then compared with experimental values for beams under repeated reversing cyclic load.

### 3-2 Moment - Axial Load - Curvature Relationship

The first step in developing the moment-axial load-curvature relationship of the cross-section was to select appropriate stress-strain curves for the constituent materials within the cross-section.

The trilinear stress-strain relationship depicted in Fig.3-1 was chosen for the 60 ksi steel assumed within each cross-section. This relationship was arbitrarily picked to represent the average of a number of published stress-strain curves for 60 ksi reinforcing steel. Hognestad's compressive stress-strain curve along with a tensile stress-strain curve proposed by MacGregor<sup>42</sup> made up the stress-strain curve accepted for concrete.

Rate of loading affects were ignored for conservatism. Since nominal  $f'_c$  and  $f_y$  values were used, it did not seem statistically reasonable to adjust these values for rate of loading effects. In addition, tests carried out in air on reinforcing steels and concrete cylinders were felt to be not entirely representative of the real case.

It was assumed that the concrete could take a reasonable amount of tensile stress. The stress-strain relation-



ship for concrete under tension was taken from Ref. 42. Ref. 43, which also used this same tensile stress-strain relationship, states that tensile stress in the concrete affects the initial part of the moment-curvature curve prior to cracking but has no significant effect on the ultimate capacity of sections. It also states that the effect of the tensile stress diminishes as the axial load and/or steel percentage increases.

The developed M-P- $\phi$  program assumes  $\phi$  and iterates the position of the cross-section neutral axis until equilibrium of the internal forces and the external axial force is achieved. The moment occurring in conjunction with the axial force and curvatures is then calculated.

The cross-section is sliced into elements which may vary in thickness if desired. Up to 80 elements are used to describe the cross-section; more elements generally result in better accuracy however computer costs are likely to rise disproportionately.

The position of the neutral axis of the cross-section is independent of the way in which the cross-section is sliced up, "discretized" into elements. Thus the neutral axis may lie within an element of the discretized cross-section. Stresses are calculated at the centroids of the elements of the discretized cross-section. The computer program is listed and more fully explained in Appendix A.





A typical M-P- $\phi$  response for a shear wall is shown in Fig. 3-2 and a typical diagram for a beam has been presented in Fig. 2-1.

The moment-axial load-curvature relationship for a typical reinforced concrete beam is usually adequately described using three straight lines as shown in Fig. 2-3. For shear wall shapes containing distributed reinforcing, however, six straight lines were considered necessary as shown in Fig. 3-2.

### 3-3 Applied Shear-Shear Strain Relationship for Members with Diagonal Cracks

The shear deformation model presented by Dilger is developed through a sectioning and analysis of the cracked reinforced concrete beam shown in Fig. 3-3(a).

Analyzing the section inclined at  $\beta_o$  shown in Fig. 3-3 (b) for forces and strains we obtain:

$$T_v = V / \sin \alpha_o$$

$$A_{sv} = \frac{A_{sv}' j d (\cot \alpha_o + \cot \beta_o)}{s}$$

$$\epsilon_{sv} = \frac{T_v}{E_s A_{sv}}$$

putting  $P_v = \frac{A_{sv}'}{s \sin \alpha_o} b$

we get  $\epsilon_{sv} = \frac{V}{p_v E_s \sin^2 \alpha_o b' j d (\cot \alpha_o + \cot \beta_o)}$





Analyzing the section inclined at angle  $\alpha_0$  shown in Fig. 3-3(c) for forces and strains we obtain:

$$C_v = -V/\sin\beta_0$$

$$A_{cv} = (\cot\alpha_0 + \cot\beta_0)\sin\beta_0 bjd$$

$$\epsilon_{cv} = \frac{C_v}{A_{cv}E_c}$$

or

$$\epsilon_{cv} = \frac{-V}{E_c bjd \sin^2\beta_0 (\cot\alpha_0 + \cot\beta_0)}$$

Combining the strains using the Williot Diagram depicted in Fig. 3-4 we obtain

$$\gamma = \frac{V}{bjd(\cot\alpha_0 + \cot\beta_0)^2} \left( \frac{1}{P_v E_s \sin^4\alpha_0} + \frac{1}{E_c \sin^4\beta_0} \right)$$

This equation may be modified for decreased strains due to part of the shear being carried by the concrete alone, however Dilger obtained better comparisons with experimental results when the shear carried by the concrete,  $V_c$ , was assumed equal to zero or the ratio  $\frac{V-V_c}{V}$  was very close to one.

When using this model to predict shear deformations for beams under repeated reversing cyclic load,  $\beta_0$  was assumed to be  $45^\circ$  for all beams and the  $V_c$  term was set



equal to zero for all cycles if it was expected that  $V_c$  would be exceeded in any cycle. The  $V-\gamma$  relationship was assumed to be linear up to 0.95 of the shear corresponding to flexural yield of the cross-section. The  $V-\gamma$  relationship was then empirically adjusted to the form shown in Fig. 3-5 to obtain a reasonable comparison with the experimental load-deformation response of Beam 35 tested by Popov, Bertero and Krawinkler. Comparisons with experimental load-deformation responses are presented in Section 3-5.

The computer program to predict the  $V-\gamma$  relationship of a reinforced concrete cross-section is presented in Appendix B.

#### 3-4 Participation of Flexural and Shear Deformations in Member Total Deformations

The prediction of a member's total deformation using flexural and shear deformation models independent of the  $M/V_d$  ratio of a member is a somewhat crude procedure.

It is easily shown that the ability of a member to deflect and the amount of flexural or shearing deformation involved in the total member deformation changes with the ratio of  $M/V_d$ .

H. Bachmann<sup>44</sup> has presented the diagram given in Fig. 3-6 showing the generalized dependency of the ultimate rotation  $\theta_u$  on the shear stress  $v$ . If  $v$  is less than  $v_{cr}$ , only flexural cracks occur. If  $v$  is greater than  $v_{cr}$



flexure-shear cracks are developed. Bachmann explained that corresponding to these crack patterns a flexural crack hinge or a shear crack hinge develops. In a flexural crack hinge the plastic deformations are concentrated into a smaller zone as  $v$  increases since the increased moment gradient restricts the zone of yielding to a zone immediately adjacent to the point of maximum moment. The value of the ultimate rotation  $\theta_u$  accordingly decreases as shown in Fig. 3.6. Assuming that a rupture of the steel occurs, the reduction of  $\theta_u$  is very high. In the case of a concrete fracture a reduction is also confirmed. If the shear stress is enough to produce flexure-shear cracks, the rotation  $\theta_u$  considerably increases since plastic deformations occur on a much wider zone. With increasing shear stress  $v$ , the rotation  $\theta_u$  decreases again. If sufficient shear reinforcement exists, however, a drastic reduction occurs only when  $v$  approaches  $v_{ult}$  through crushing of the concrete in the web due to shearing deformations and inclined compression forces.

In addition to the effects described by Bachmann, if  $v$  is less than  $v_{cr}$  and the tensile steel yields within the flexural crack hinge and the flexural crack opens, shear is resisted only by the concrete at the head of the crack and the dowel shear of the yielded reinforcing. In this instance slip may occur parallel to the crack and thus the flexural action of the beam has affected its shear resistance. This





is particularly true if cyclic loads alternately cause yielding of the top and bottom steel in the beam.

It is believed however that the deformation models developed herein may be applied throughout a fairly broad range of  $M/V_d$  values without serious error.

The shear deformation model developed herein has been developed for a midrange value of  $M/V_d$  of about 3.0. As such it is believed that changes in the value of  $M/V_d$  would change the cracking angle of the shear deformation model but that this effect would not be serious for values of  $M/V_d$  from approximately 2 to 5.

At  $M/V_d$  values above 5 shear deformations are not significant as shear stress are lower at higher  $M/V_d$  values. In this range deformations found using M-P- $\phi$  curves have been found to be realistic.

$M/V_d$  values below 2 are considered to be outside the range of the deformation models developed herein. Deformation models such as those of Zimmerli<sup>30</sup> or Yamada<sup>27,28</sup> et al. are more likely to suit this case.

It is known that the  $M/V_d$  ratio of a member in a structure may change as the earthquake progresses and the various modes of the structure interact. However it is thought that once a member's crack pattern has been established according to its original  $M/V_d$  ratio, it is not likely to change significantly. Thus even though the  $M/V_d$



ratio of a member may in future take on a value outside the range of apparent applicability, it is felt that the deformation models postulated will still adequately predict the member's deformations.

### 3-5 Hysteresis Loop

To predict the deformations of a member throughout its loading history, one must have a method of predicting what curvatures and shear strains exist at various sections of the member length at all times. These curvatures and shear strains are then integrated to give the member's deformation profile at any desired time.

As previously explained in Sec. 2-3, the intricate curves describing the relationship between moment and curvature are usually approximated by series of straight lines in defined patterns. In this thesis, the set of rules defining the pattern of the moment-curvature hysteresis loop is also used to define the pattern of the shear-shear strain hysteresis loop. The set of rules defining this pattern was originally presented by Clough.<sup>6</sup>

The series of rules establishing the moment-curvature loop is listed here:

1. the moment-curvature relationship for monotonic loading is defined with a bilinear curve; the point of stiffness change corresponding to the yield moment and curvature.



2. If the moment on the member does not rise above yield at any time no hysteresis loop is generated.

3. The slope of the unloading branch is equal to that of the initial elastic response,  $EI$ .

4. If the moment has exceeded the yield moment in one direction only, loading in the opposite direction follows the line passing through the points defined by the residual curvature at zero moment and the opposite yield moment and curvature.

5. If the moment has exceeded the yield moment in both directions, loading in an opposite direction follows the line passing through the points defined by the residual curvature at zero moment and the highest curvature and moment reached in the opposite direction.

6. Loading beyond any previously reached moment and curvature follows the monotonic bilinear moment-curvature relationship.

Fig. 3-7 depicts the hysteresis loop defined by the rules stated above. The method of combining the deformations predicted using the strains defined by this hysteresis loop is explained in Section 4-3 and in Appendix E of this thesis.

### 3-6 Comparison with Experiments

The load-deformation plots of three beams tested by Popov, Bertero and Krawinkler are shown in Fig. 3-8, Fig. 3-9 and Fig. 3-10 respectively. Analytically predicted





responses including both shear and flexural effects are also shown within each figure. The properties of these three beams are summarized in Table 3-1.

The comparison between experiment and analysis is quite reasonable. In general the unloading stiffness of the analytical model is a little greater than that measured and any pinching of the experimental curve toward the origin such as that in Fig. 3-8 is not predicted too well.

The ratio of the analytically predicted flexural and shear deformations of these three beams is presented in Table 3-2. The beams were designated as Beam 35, Beam 43 and Beam 46. The first number of the identification represented the size of the stirrup reinforcing bar, the second number the spacing of the stirrups. Two things are noteworthy in Table 3-2. One is the fact that the analytically predicted shear deformations are just as significant and often times more significant than the predicted flexural deformation. The second is the fact that as the stirrup spacing is decreased and/or the size of stirrup reinforcing bar is increased the model correctly follows the expected trend that the shear stiffness will increase.





TABLE 3-1 SPECIMEN PROPERTIES

PARAMETERS		BEAM 35*	BEAM 46	Beam 43
L (in)		78.0	78.0	78.0
t (in)		29.0	29.0	29.0
b (in)		15.0	15.0	19.0
d (in)		25.25	25.25	25.25
d' (in)		3.75	3.75	3.75
$A_s$ (in <sup>2</sup> )		6.00	6.00	6.00
$A'_s$ (in <sup>2</sup> )		6.00	6.00	6.00
p		0.0158	0.0158	0.0158
p'		0.0158	0.0158	0.0158
$p_b$	(compression reinforcement is neglected)	0.0235	0.0242	0.0336
$f_y$	for main reinf. (ksi)	67.0	67.0	60.0
$f_{max}$	for main reinf. (ksi)	103.0	103.0	97.0
$f_y$	for stirrup ties(ksi)	53.0	60.0	60.0
$f_{max}$	for stirrup-ties(ksi)	90.0	96.0	96.0
$f'_c$	(ksi)	3.86	3.99	5.03
design criteria		ACI-63 Code	ACI-63 Code, except $V_u$ taken by stirrups only	ACI-71 Code, $V_u$ taken by stirrups only
stirrup-ties size		# 3	# 4	# 4
stirrup-ties spacing (in)		4.5	6.0	3.0

\*The stirrup-tie spacing used was 4.5 in., but for simplicity the specimen was called Beam 35 and not Beam 34.5



TABLE 3-2 RATIO OF FLEXURAL TO SHEAR  
DEFORMATIONS

	Elastic	Yield	Inelastic
Beam 35	1:1	1:2	1:3
Beam 46	1:1	1:1	1:2
Beam 43	4:3	2:1	4:3





FIG. 3-1 STEEL STRESS-STRAIN CURVE





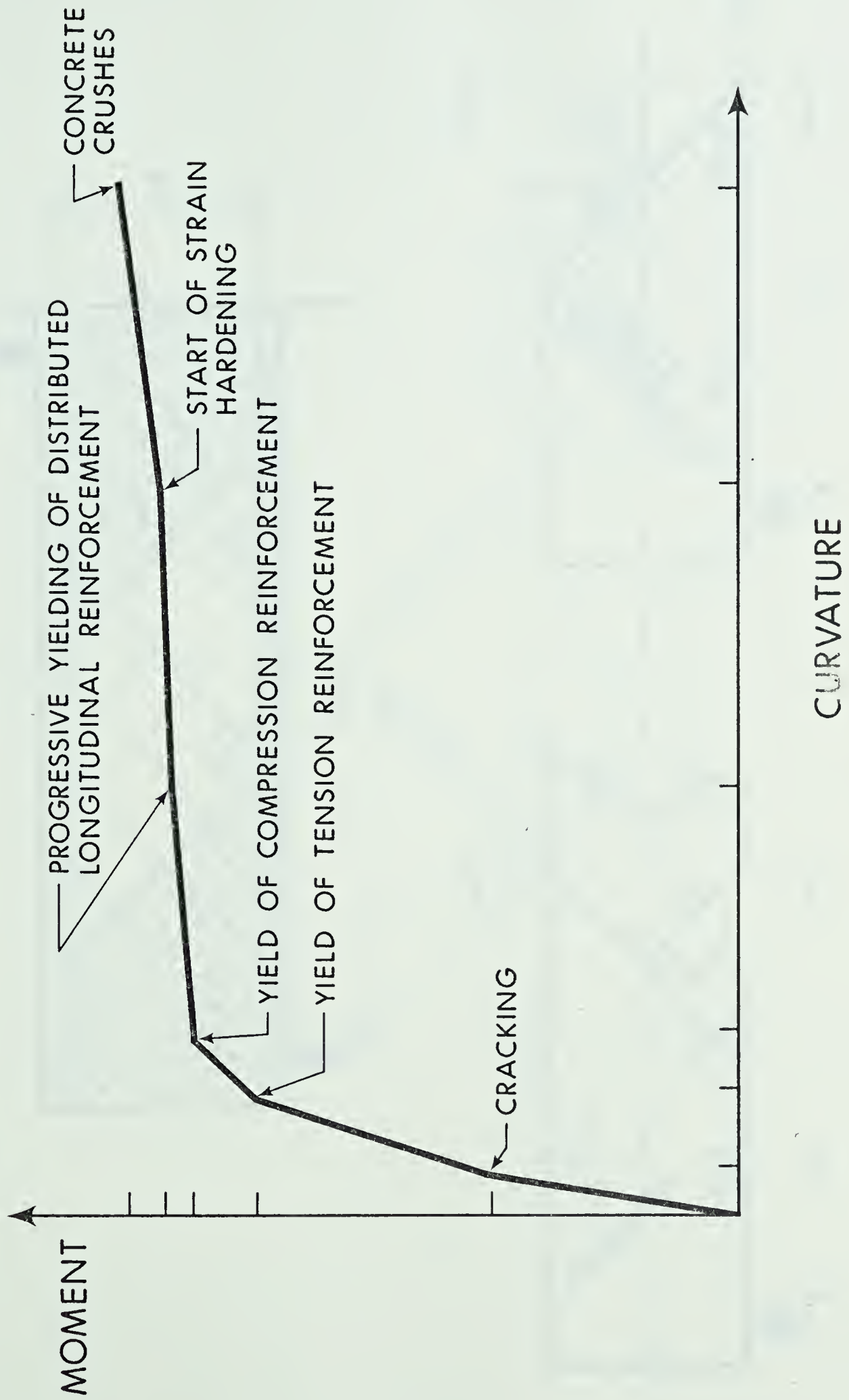


FIG. 3-2 MOMENT-CURVATURE RESPONSE OF A SHEAR WALL



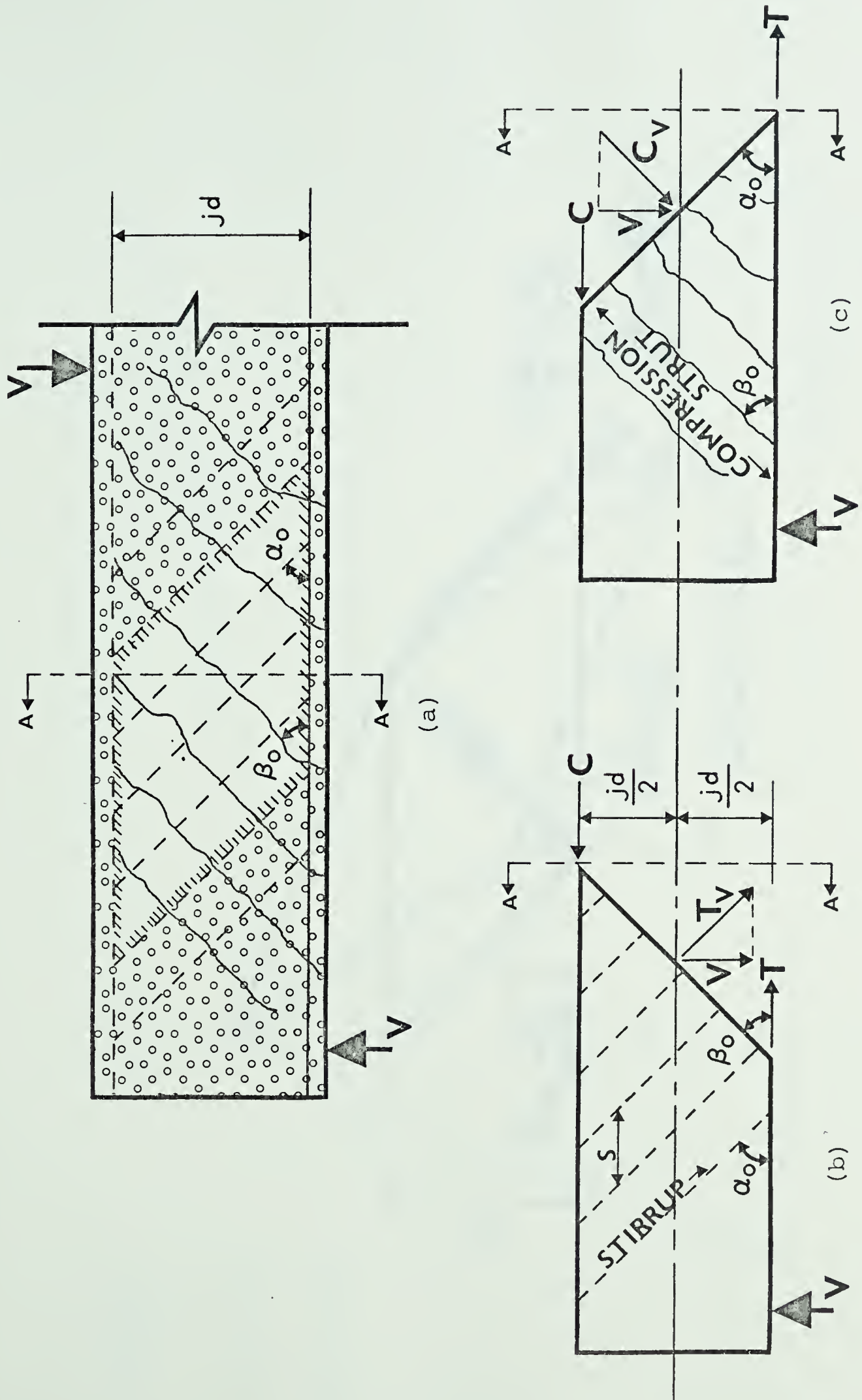


FIG. 3-3 DILGER SHEAR DEFORMATION MODEL



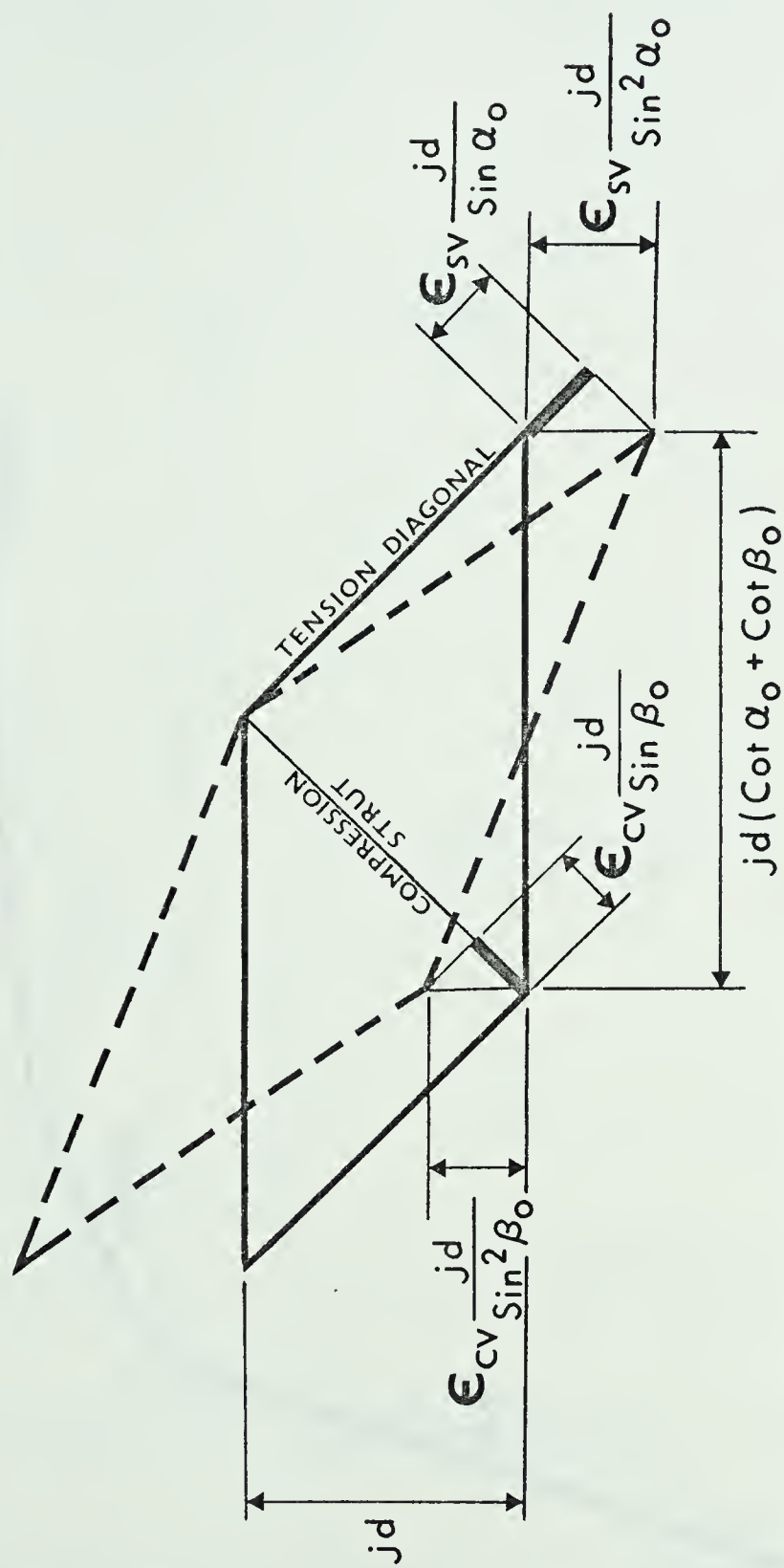


FIG. 3-4 WILLIOT DIAGRAM FOR DILGER SHEAR DEFORMATION MODEL



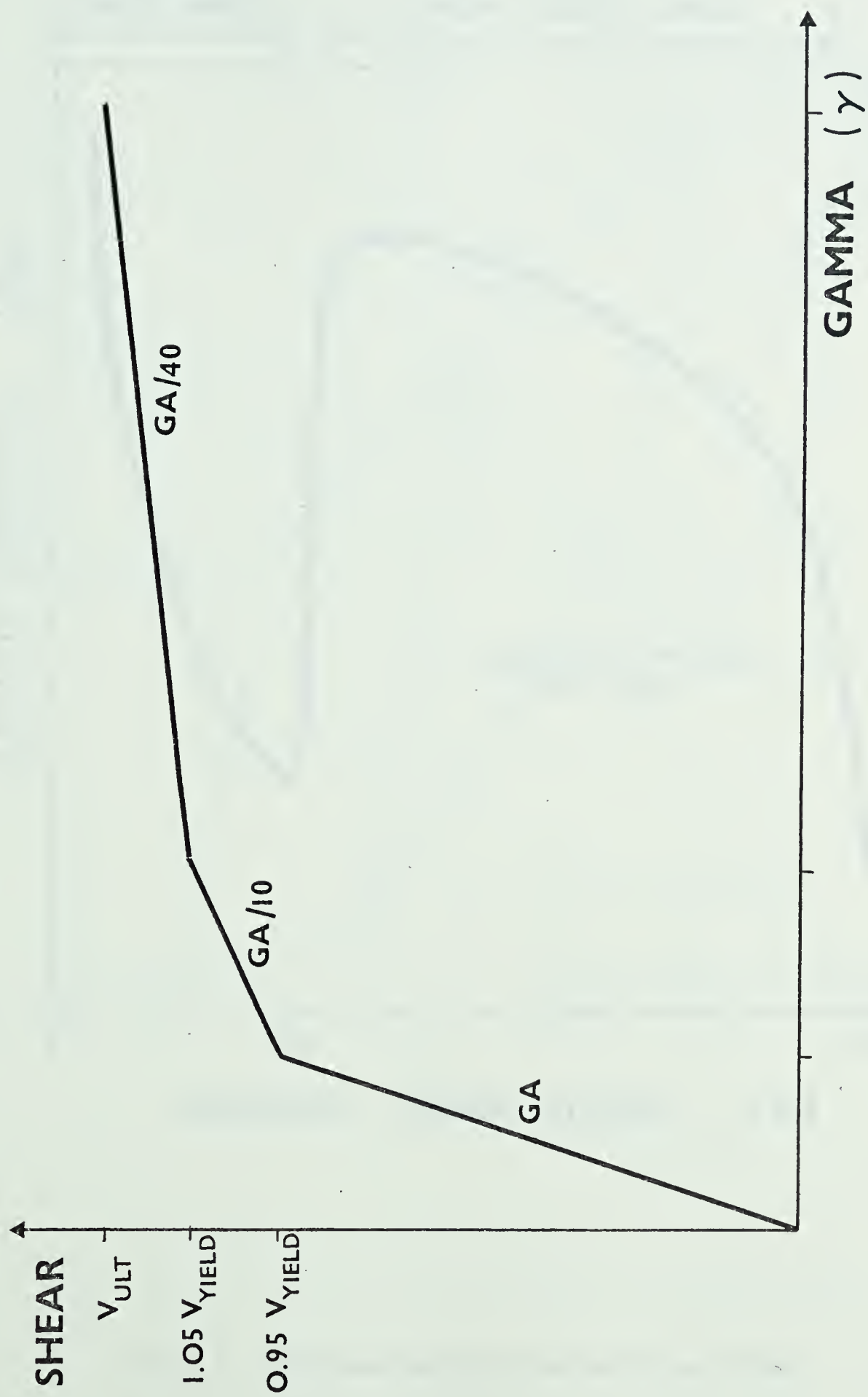


FIG. 3-5 Typical V- $\gamma$  Relationship





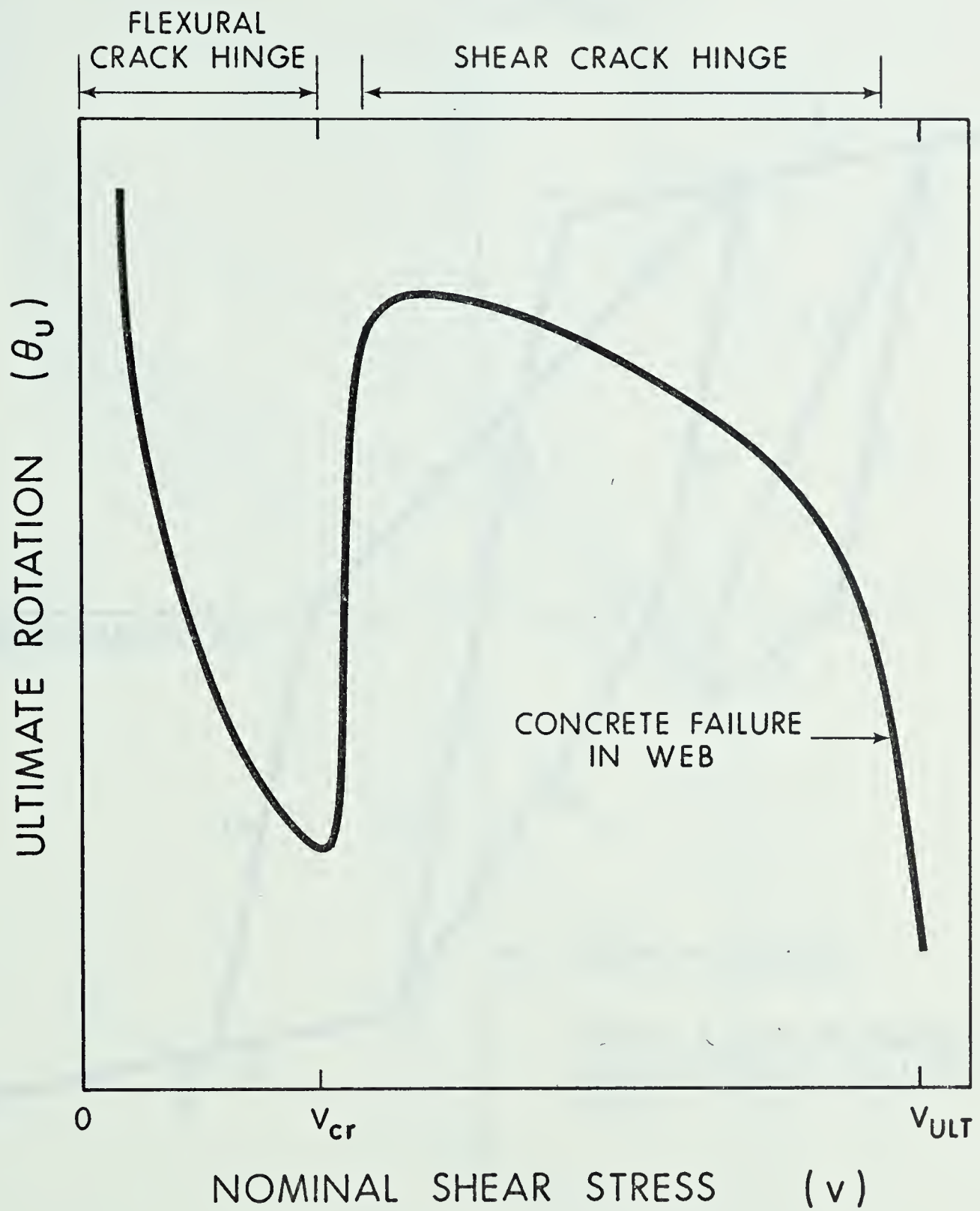


FIG. 3-6 Ultimate Rotation Versus Shear Stress



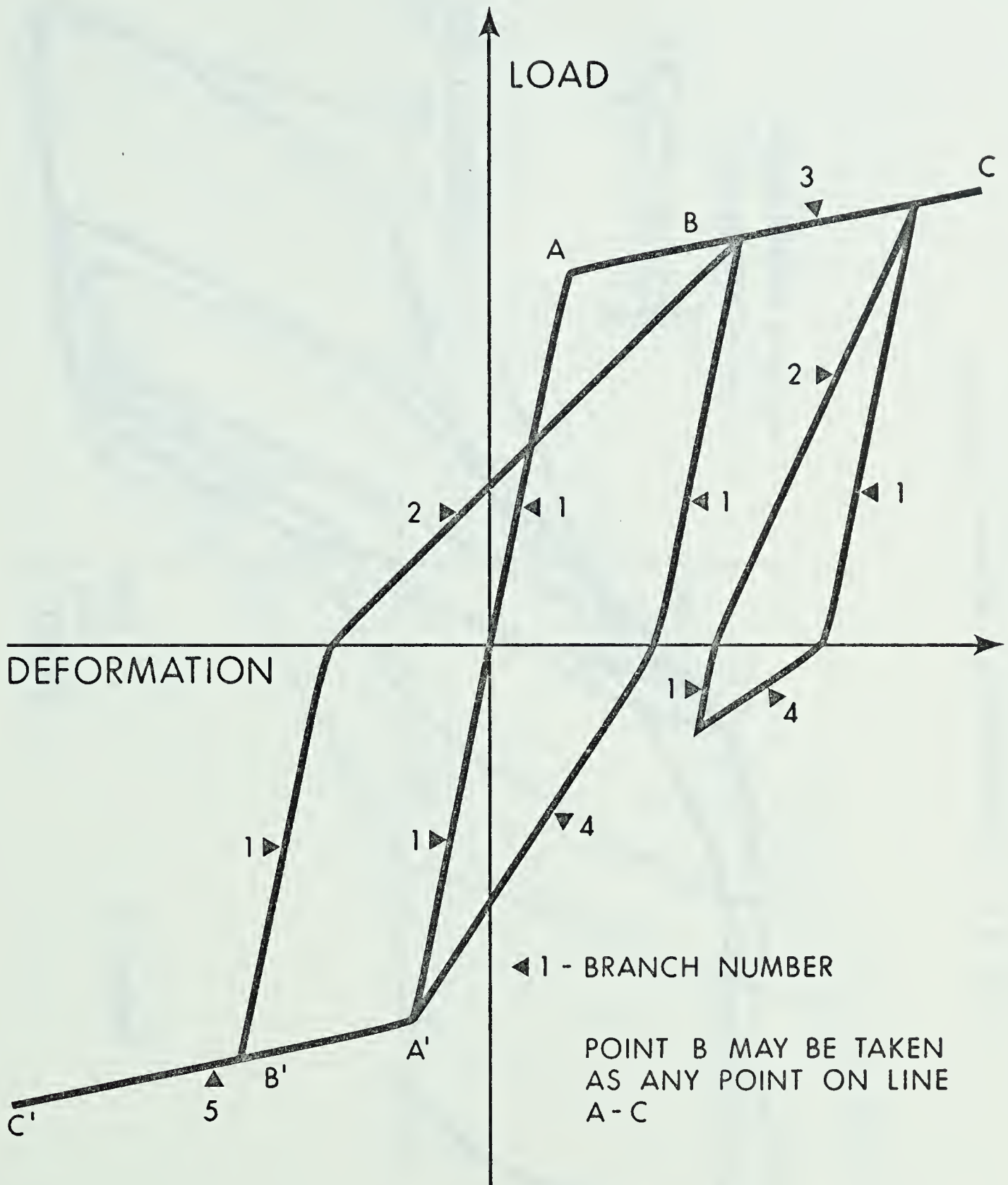


FIG. 3-7 TYPICAL LOAD-DEFORMATION HYSTERESIS LOOP



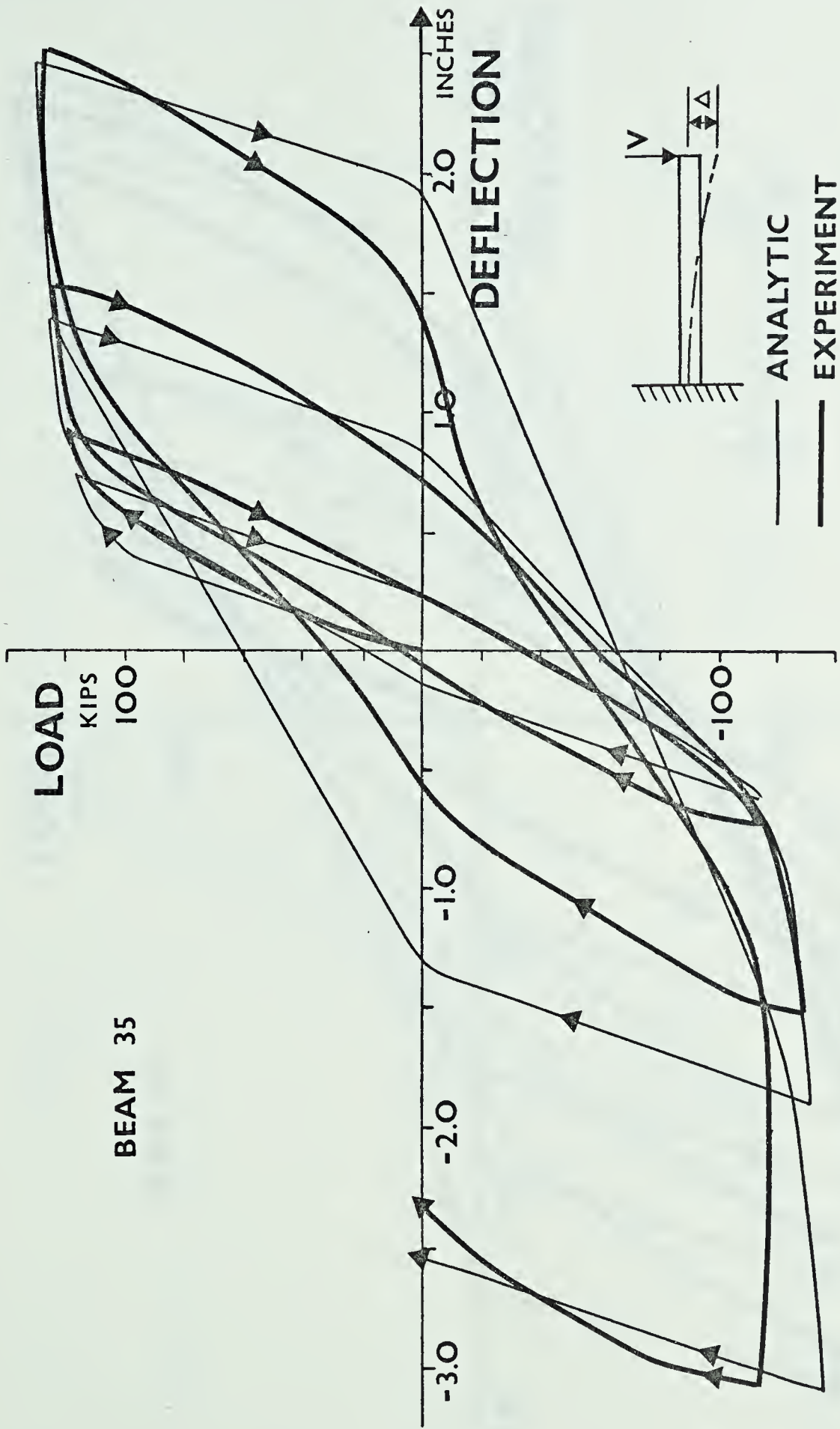


FIG. 3-8 Load-Deformation Response of Beam 35





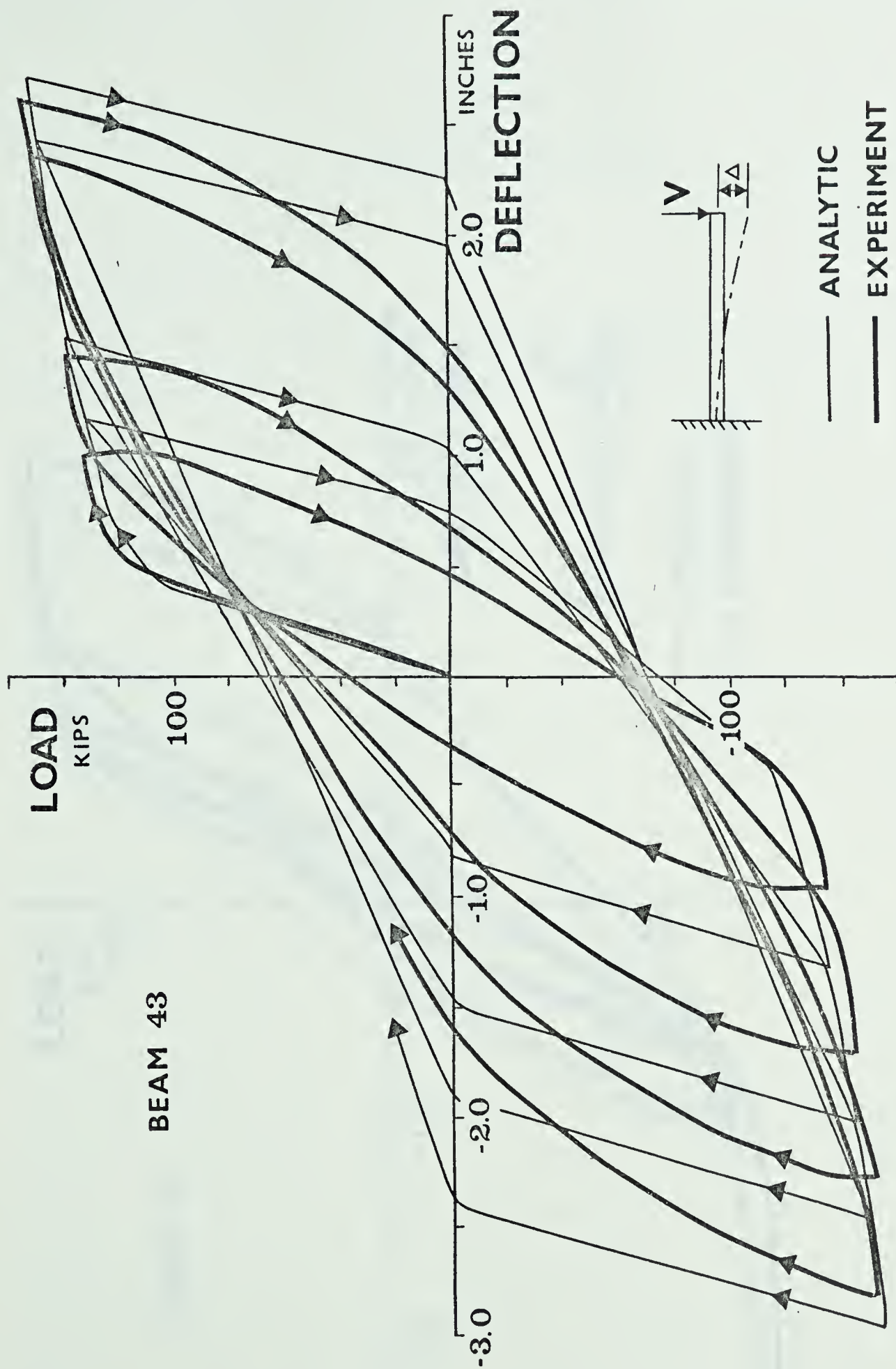


FIG. 3-9 Load-Deformation Response of Beam 43



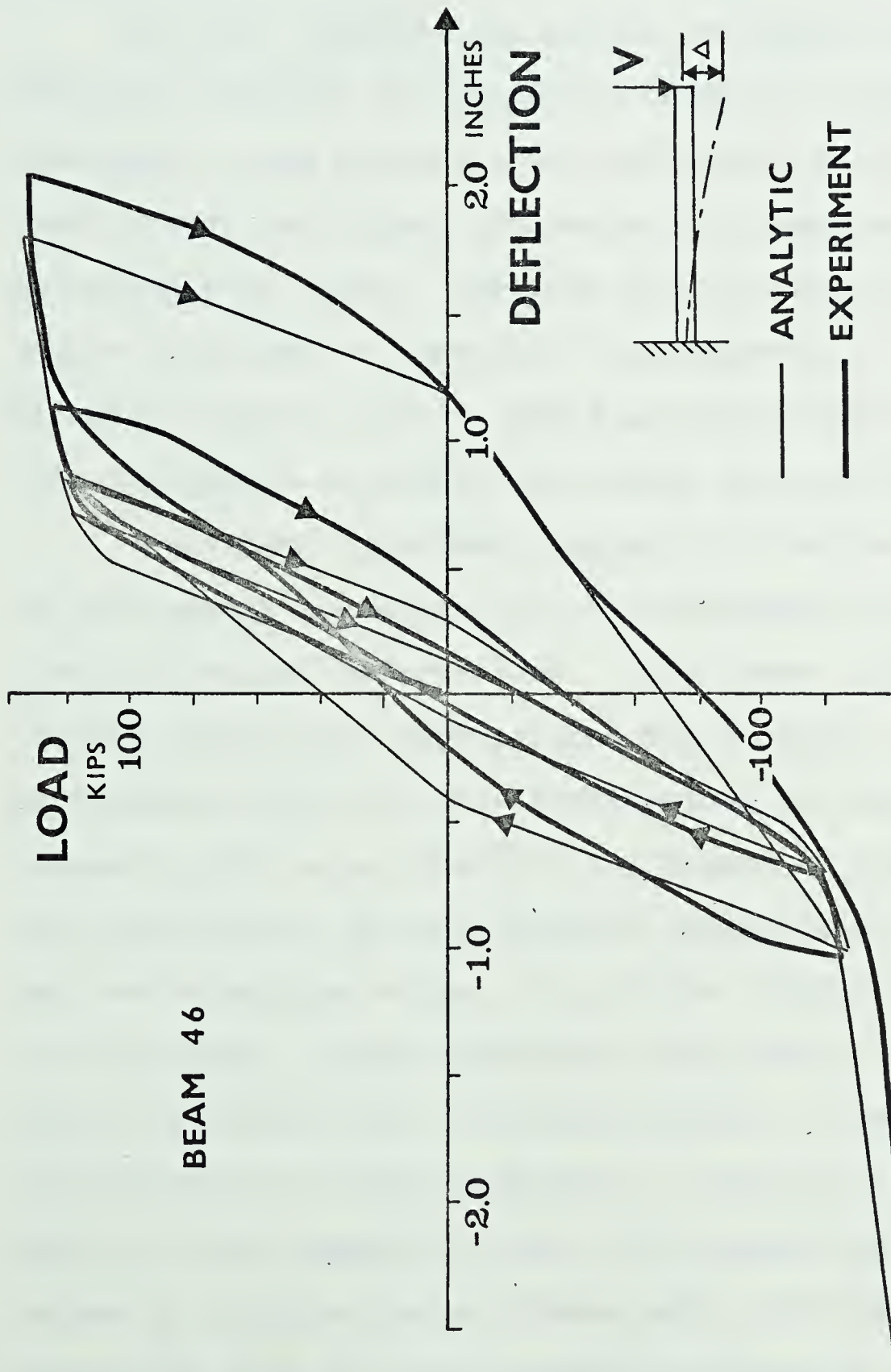


FIG. 3-10 Load-Deformation Response of Beam 46



## Chapter 4

### EARTHQUAKE ANALYSIS

#### 4-1 Introduction

In this chapter, the method of analysis used to study the behavior of reinforced concrete frames will be developed. This procedure was originally developed for steel frames and formed the basis of a computer program developed by M. Suko. Sections 4.2, 4.4 and 4.5 of this chapter and much of Appendix C and Appendix D are taken directly from Dr. Suko's thesis and are presented rather than referenced to assist the reader of this thesis.

Equivalent rotational springs are used at the ends of each member to account for all deformations other than elastic flexural deformations. Thus these rotational springs account for deformations due to axial load, shear deformations and inelastic deformations for each member. Estimating the axial load and the moment to shear ratio for each member, the relationship between the moment,  $M_s$ , and the relaxation angle,  $\delta\theta_s$  of the rotational spring is calculated. Slope deflection equations are modified for members attached with rotational springs. The  $M_s - \delta\theta_s$  relationships are then combined to construct a stiffness matrix for the complete frame. The dynamic equations are solved by changing the stiffness matrix so that it is compatible with the deteriorated structure at every instant





of the motion.

To apply this analysis to reinforced concrete frames it was necessary to redefine the manner in which the  $M_s-\delta\theta_s$  relationship was computed to include both shear and flexural terms and to include the degrading stiffness loop.

#### 4-2 Analytical Model

The frame to be analyzed is modeled as shown in Fig. 4-1. The number of stories,  $N_s$ , and the number of bays,  $N_b$ , as well as the story height for each story and the bay width for each bay in the model correspond to those of the original frame. The frame must be at least one bay wide thus a fictitious beam and column must be added to analyze a building with only a shear wall to resist lateral and axial loads.

The stiffness of a member in the modeled frame is taken to be equal to the elastic stiffness of the corresponding member in the actual frame and is assumed to be unchanged throughout the response regardless of the stress level. A rotational spring is placed between each member and the corresponding joint (or a rigid stub) as shown in the figure, to account for the inelastic action of the member and the secondary effects. The procedures used to determine the properties of this spring will be discussed in the following section. If a shear wall is present, it is simulated by a column which has a bending stiffness and





strength equivalent to those of the original shear wall and is attached to the adjacent beams through rigid stubs. The stub length simulates the wall width effect. This column is then treated in the usual manner.

The bottom story columns may be attached to the foundation by elastic rotational springs to account for the flexibility of the foundation. The secondary effects produced by axial shortening or elongation of the columns are ignored. Uniformly distributed loads may be applied to the beams although the possibility of forming a plastic zone within the span length of a member is not checked.

The masses are assumed to be concentrated at each floor level and to translate in a horizontal direction only as shown graphically in Fig. 4-1. A mass concentrated at a floor level is denoted by  $m_i$ , in which the subscript  $i$  identifies the floor level.

Damping forces are assumed to be developed by the relative motion of adjacent floors. Thus the damping force at the  $i$ -th story is expressed as  $c_i(\dot{x}_i - \dot{x}_{i+1})$ , in which  $c_i$  represents the damping coefficient which is constant throughout the motion within a story; and  $\dot{x}_i$  and  $\dot{x}_{i+1}$  represent the velocities relative to the ground of the  $i$ -th story and the story below.

Each nodal point and member are numbered as shown in Fig. 4-2. Floors and stories are numbered from the top. Bays and columns are numbered from the left. The joint of



the  $i$ -th floor (from the top) and the  $j$ -th column row (from the left) is called the  $\{(N_b+1) (i-1) + j\}$ -th joint. The beam of the  $i$ -th floor and the  $j$ -th bay is called the  $\{(2N_b+1) (i-1) + j\}$ -th member and the column of the  $i$ -th story and the  $j$ -th column row is similarly called the  $\{(2N_b+1) i - (N_b+1) + j\}$ -th member. Thus a  $N_b$ -bay,  $N_s$ -story frame consists of  $(N_b+1)N_s$  joints and  $(2N_b+1)N_s$  members.

#### 4-3 Equivalent Rotational Springs

Properties of equivalent rotational springs are determined in the following steps. The cantilever column shown in Fig. 4-3 simulates the portion of a member between its point of inflection and corresponding joint. This column under monotonically increasing load is subject to elastic and inelastic flexural deformations, shear deformations, and additional flexural deformations caused by the axial load acting through the flexural and shear deformations of the member.

The column shown in Fig. 4-3 is then replaced by the column shown in Fig. 4-4. The lateral load  $V$  is now assumed to produce only elastic flexural deformations. All other deformations are accounted for through a rotation of the equivalent rotational spring at the base of the column. For any moment,  $M_s$ , produced by lateral load,  $V$ , the relationship between  $M_s$  and the rotation of the spring,  $\delta\theta_s$  is:



$$M_s = -VL \quad (4-1)$$

$$\delta\theta_s = (\Delta - \Delta_{\text{elastic}})/L \quad (4-2)$$

The relationship between  $M_s$  and  $\delta\theta_s$  is found from zero load to failure. The procedure followed leading to a complete  $M_s$ - $\delta\theta_s$  diagram for each member is listed below:

1. The cantilever column length is divided into as many segments as desired. Commonly the column length is divided into 20 segments.
2. A concentrated lateral shear force,  $V_1$ , is applied at the top of the member.
3. The input  $V$ - $\gamma$  relationship is searched to find  $\gamma_1$ , for  $V_1$ . The deformations due to shear,  $\Delta_{v_i}$ , are found at each column height division point by multiplying  $\gamma_1$  by the distance that the division point is from the base of the column.
4. The moment at every division point  $M_i$  corresponding to shear  $V_1$  is found.
5. The input  $M$ - $P$ - $\phi$  diagram is searched to find the curvature  $\phi_i$  corresponding to each moment  $M_i$ .
6. Moment-Area principles are applied to find the flexural deformation at each column height division point,  $\Delta_{F_i}$ .
7. The deformation profile of the column is found by adding the flexural and shearing deformations,  $\Delta_i =$







$$\Delta_{V_i} + \Delta_{F_i}.$$

8. If axial load is present on the column, additional moment is added to each division point equal to  $\Delta M = P (\Delta_{top} - \Delta_i)$ .

9. The procedure cycles through steps 5 to 8 until a stable deformation pattern is reached ie. the bending moment diagram of the column does not change significantly between two cycles.

10.  $M_s$  and  $\delta\theta_s$  are recorded where  $M_s$  and  $\delta\theta_s$  are defined by Eqns. 4-1 and 4-2 respectively.

11. The column shear is incremented and the procedure starts again at step 3.

12. The procedure is stopped when the moment at a column division point requires a curvature equal to or in excess of the largest curvature defined by the member's input M-P- $\phi$  relationship.

The procedure as listed herein may be followed for members under reversing cyclic load as long as hysteresis loops are defined for the members V- $\gamma$  relationship and M-P- $\phi$  relationship. This was done when tracing the load-deformation responses of Beam 35, Beam 43 and Beam 46 described in section 3-6.

The computer program which performs the operations listed above is listed in Appendix E.

The  $M_s$ - $\delta\theta_s$  relationship of the monotonically loaded



cantilever column is approximated as a bilinear relationship. The point at which the  $M_s - \delta\theta_s$  relationship changes slope corresponds to the point at which the slope of the  $M-P-\phi$  diagram first becomes very small. This point is indicated in Fig. 3-2 as the point at which the compression reinforcement yields.

Once the column has been analyzed and the monotonic  $M_s - \delta\theta_s$  relationship recorded it is assumed that a member of length  $L_o$  loaded so as to have the same  $M/V_d$  ratio as the column analyzed will have deformations equal to its elastic flexural deformations plus  $\delta\theta_s$  times its length  $L_o$ . The stiffness matrix of any member is then found readily.

The frame members of the building studied within this thesis were analyzed using cantilever column lengths corresponding to the  $M/V_d$  ratios imposed on them by code specified static earthquake loads. This assumption was made by the author because:

1. No other  $M/V_d$  values were available.
2. A realistic  $M_s - \delta\theta_s$  relationship was required for every member. This  $M_s - \delta\theta_s$  relationship would be invariant throughout the dynamic analysis. The dynamic analysis program as written could not generate  $M_s - \delta\theta_s$  relationships corresponding to the various values of  $M/V_d$  that a member was found to have as the earthquake progressed.



The decision to accept the code values of  $M/V_d$  was tempered by the fact that code force distributions are based on response spectrum analyses of elastic structures. It was assumed that until the earthquake accelerations were high enough to cause inelastic action within any member, the members would indeed be subjected to the code values of  $M/V_d$ . Crack patterns would thus be established according to these initial  $M/V_d$  values and thus even though the  $M/V_d$  value of a member might change, the deformations of the member would be close to those defined by the initial  $M/V_d$  ratio. Arguments have also been presented in Section 3.4 describing why the deformations of these members may be assumed to be more or less insensitive to changes of  $M/V_d$ .

The dynamic analysis program developed by M. Suko was modified to follow a Clough type hysteresis load-deformation response following the rules presented in Section 3-5. The resulting  $M_s - \delta\theta_s$  relationship is shown in Fig. 4-5.

#### 4-4 Stiffness Matrix for Frame

##### 4-4-1 Slope Deflection Equations for Members with Rotational Springs and Rigid Stubs





The actual structure has been modeled according to the procedure described in the previous sections (Sec. 4-2 to 4-3). In order to calculate the response of the frame, it is first necessary to modify the standard slope deflection equations to accommodate the presence of rotational springs at the member ends and, if required, the presence of rigid stubs which simulate the wall width effect.

The member, a-c-d-b, shown in Fig. 4-6 is considered a general example. The entire member length is denoted by  $L$  and the rigid stubs placed at the left and right ends have lengths of  $\lambda_1 L$  and  $\lambda_2 L$ , respectively. Thus the length of the elastic portion of the member is  $\lambda_3 L$ , where

$$\lambda_1 + \lambda_2 + \lambda_3 = 1$$

and

$$\lambda_1 \geq 0; \quad \lambda_2 \geq 0; \quad \lambda_3 \geq 0.$$

A sway rotation,  $\rho$  (between the end a and the end b), is permitted for a column but not for a beam. A uniformly distributed load,  $w$ , may be applied to a beam over its entire length. Equivalent rotational springs are located at the ends of the rigid stubs at points c and d. The portion c-d is assumed to remain elastic regardless of the deflected shape of the member.





The  $M_s - \delta\theta_s$  relationship for the rotational spring for each member end has been determined by the method described in Sec. 4-3.

The additonal angle change at point c,  $-\delta\theta_c$ , and the end moment,  $M_{cd}$ , are related by:

$$M_{cd} = \alpha_1(-\delta\theta_c) + \beta_1 \quad (4-3)$$

and similarly at point d:

$$M_{dc} = \alpha_2(-\delta\theta_d) + \beta_2 \quad (4-4)$$

with appropriate values of  $\alpha_1$ ,  $\beta_1$ ,  $\alpha_2$  and  $\beta_2$  depending upon which branch of the moment-relaxation angle relationship is describing the present condition.

The end moments,  $M_{ab}$  and  $M_{ba}$ , are calculated as:

$$M_{ab} = \frac{\frac{2EI}{\lambda_3 L} (A_1 \theta_a + A_2 \theta_b + A_3 \rho + A_4 \frac{\beta_1}{\alpha_1} + A_5 \frac{\beta_2}{\alpha_2}) + A_6 C_{cd}}{A_7} + A_8 D_{ab} \quad (4-5)$$

$$M_{ba} = \frac{\frac{2EI}{\lambda_3 L} (A_2 \theta_a + A_1' \theta_b + A_3' \rho + A_5' \frac{\beta_1}{\alpha_1} + A_4' \frac{\beta_2}{\alpha_2}) + A_6' C_{dc}}{A_7} + A_8' D_{ba} \quad (4-6)$$

in which

$$C_{cd} = - \frac{1}{12} w (\lambda_3 L)^2 \quad (4-7)$$

$$C_{dc} = \frac{1}{12} w (\lambda_3 L)^2 \quad (4-8)$$



$$A_8^D{}_{ab} = -\frac{1}{2}w \lambda_1 (1-\lambda_2) L^2 \quad (4-9)$$

$$A_8^D{}_{ba} = \frac{1}{2}w \lambda_2 (1-\lambda_1) L^2 \quad (4-10)$$

and

$$A_1 = 2 + 6\frac{\lambda_1}{\lambda_3} + 6\left(\frac{\lambda_1}{\lambda_3}\right)^2 + 6\frac{EI}{L}\left(\frac{1}{\alpha_2 \lambda_3} + \frac{2\lambda_1}{\alpha_2 \lambda_3^2} + \frac{\lambda_1^2}{\alpha_1 \lambda_3^3} + \frac{\lambda_1^2}{\alpha_2 \lambda_3^3}\right) \quad (4-11)$$

$$A_1' = 2 + 6\frac{\lambda_2}{\lambda_3} + 6\left(\frac{\lambda_2}{\lambda_3}\right)^2 + 6\frac{EI}{L}\left(\frac{1}{\alpha_1 \lambda_3} + \frac{2\lambda_2}{\alpha_1 \lambda_3^2} + \frac{\lambda_2^2}{\alpha_1 \lambda_3^3} + \frac{\lambda_2^2}{\alpha_2 \lambda_3^3}\right) \quad (4-12)$$

$$A_2 = 1 + 3\frac{\lambda_1}{\lambda_3} + 3\frac{\lambda_2}{\lambda_3} + 6\frac{\lambda_1 \lambda_2}{\lambda_3^2} + 6\frac{EI}{L}\left\{\frac{\lambda_1}{\alpha_1 \lambda_3^2} + \frac{\lambda_2}{\alpha_2 \lambda_3^2} + \left(\frac{1}{\alpha_1} + \frac{1}{\alpha_2}\right)\frac{\lambda_1 \lambda_2}{\lambda_3^3}\right\} \quad (4-13)$$

$$A_3 = -(A_1 + A_2) \quad (4-14)$$

$$A_3' = -(A_1' + A_2') \quad (4-15)$$



$$A_4 = 2 + 3\frac{\lambda_1}{\lambda_3} + 6\frac{EI}{L}\left(\frac{1}{\alpha_2\lambda_3} + \frac{\lambda_1}{\alpha_2\lambda_3^2}\right) \quad (4-16)$$

$$A'_4 = 2 + 3\frac{\lambda_2}{\lambda_3} + 6\frac{EI}{L}\left(\frac{1}{\alpha_1\lambda_3} + \frac{\lambda_2}{\alpha_1\lambda_3^2}\right) \quad (4-17)$$

$$A_5 = 1 + 3\frac{\lambda_1}{\lambda_3} + 6\frac{\lambda_1 EI}{\alpha_1\lambda_3^2 L} \quad (4-18)$$

$$A'_5 = 1 + 3\frac{\lambda_2}{\lambda_3} + 6\frac{\lambda_2 EI}{\alpha_2\lambda_3^2 L} \quad (4-19)$$

$$A_6 = 1 + 6\frac{EI}{L}\left(\frac{1}{\alpha_2\lambda_3} - \frac{\lambda_1}{\alpha_1\lambda_3^2} + \frac{\lambda_1}{\alpha_2\lambda_3^2}\right) \quad (4-20)$$

$$A'_6 = 1 + 6\frac{EI}{L}\left(\frac{1}{\alpha_1\lambda_3} + \frac{\lambda_2}{\alpha_1\lambda_3^2} - \frac{\lambda_2}{\alpha_2\lambda_3^2}\right) \quad (4-21)$$

$$A_7 = 1 + 4\frac{EI}{L}\left\{\frac{1}{\lambda_3}\left(\frac{1}{\alpha_1} + \frac{1}{\alpha_2}\right) + \frac{3}{\alpha_1\alpha_2\lambda_3^2}\frac{EI}{L}\right\} \quad (4-22)$$

If the sway rotation,  $\rho$ , is set equal to zero in the preceding equations, the behavior of a beam is simulated.

If

$$w = 0$$

and

$$\lambda_1 = \lambda_2 = 0; \quad \lambda_3 = 1$$

are substituted, the equations simulate the action of a column. The derivation of Eqs. 4-5 and 4-6 is detailed in Appendix C.

It is noted that the inelastic behavior (in this case, the  $M_s - \delta\theta_s$  relationships for the rotational springs deviate





from the initial linear branch passing through the origin) is expressed by the same equations, by changing the coefficients  $\alpha_1$  and  $\beta_1$  or  $\alpha_2$  and  $\beta_2$  in Eqs. 4-3 and 4-4, and in Eqs. 4-5 and 4-6.

#### 4-4-2 Stiffness Matrix for the Frame

When the end moments for each member have been expressed by Eqs. 4-5 and 4-6, it is possible to formulate the moment equilibrium condition at each nodal point and the shear equilibrium equation for each story. In these equations, the joint rotations and story shears are written in terms of the horizontal deflections at each floor level.

Using the notation defined in Sec. 4-2, the number of unknowns is equal to the sum of the number of stories,  $N_s$ , and the number of joints,  $N_s(N_b+1)$ ; ie., a total of  $N_s(N_b+2)$ . The coefficient matrix,  $[R]$ , is therefore  $N_s(N_b+2) \times N_s(N_b+2)$  in size. Letting the vector  $\{\theta\}$  denote the unknowns (consisting of joint rotations and story shears), the equilibrium equations are expressed as:

$$[R] \{\theta\} = \{B\} \quad (4-23)$$

where the vector  $\{B\}$  consists of fixed end moment terms and the sway rotation terms. By arranging the equilibrium equations in an appropriate order, the coefficient matrix  $[R]$  becomes a band matrix with a width of  $2N_b+3$  and will have the diagonal elements dominant in most cases.



The horizontal loads (or story shears) compatible with the assumed deflection shape used to obtain the vector  $\{B\}$  are determined by extracting the story shear terms from the solution  $\{\theta\}$ . If the vector  $\{B\}$  is computed by assuming the sway rotations are zero at every story, the story shears (the sum of the horizontal loads applied at floor levels above a particular story) required to restrain the frame in this position are calculated. This vector is denoted by  $\{\eta_0\}$ , which is a zero vector unless the uniformly distributed loads on the beams produce lateral sways. If the vector  $\{B\}$  is calculated by permitting a unit displacement only at the  $i$ -th floor level (from the top), the story shears required to maintain the other floor levels in the undeflected position can be calculated as  $\{\eta_i^!\}$ . Then, the  $i$ -th column of frame stiffness matrix,  $[G]$ , is given by  $\{\eta_i\}$ , which is:

$$\{\eta_i\} = \{\eta_i^!\} - \{\eta_0\} \quad (4-24)$$

Repeating the computation of  $\{\eta_i\}$  for  $i = 1$  to  $N_s$ , the elements of the complete frame stiffness matrix are obtained. Thus the story shears  $\{Q\}$ , and the corresponding deflections at each floor level,  $\{x\}$ , are related by:

$$\{Q\} = [G] (\{x\} - \{\xi_0\}) \quad (4-25)$$

where the vector  $\{\xi_0\}$  is the initial deflection at each floor level produced by vertical loads alone applied to the beams, and is obtained by:

$$\{\xi_0\} = -[G]^{-1}\{\eta_0\} \quad (4-26)$$



Eq. 4-25 is valid if the  $M_s - \delta\theta_s$  relationship for every rotational spring in the frame remains elastic. If any of the rotational springs are forced into the inelastic branches of the  $M_s - \delta\theta_s$  relationships, the stiffness matrix must be adjusted. Let the vector  $\{\xi\}$  be the deflections at each floor level and let the vector  $\{\eta\}$  be the story shears at the instant that changes are required in the stiffness matrix. Equilibrium equations, similar to Eq. 4-23, are constructed using new branches of the  $M_s - \delta\theta_s$  relationships (substituting a new set of  $\alpha_1$  and  $\beta_1$  or a new set of  $\alpha_2$  and  $\beta_2$  in the modified slope deflection equations) at the pertinent member ends. The new stiffness matrix,  $[G]$ , is calculated in exactly the same manner as before. The deflection at the floor levels,  $\{x\}$ , and the story shears,  $\{Q\}$ , are now related by:

$$\{Q\} = [G] (\{x\} - \{\xi\}) + \{\eta\} \quad (4-27)$$

The preceding procedure is repeated as required to obtain the updated stiffness matrix and the corresponding relationship between the story shears and deflections.

## 4-5 Equations of Motion

### 4-5-1 Formulation of Equations of Motion

If the masses,  $m_i$ , are assumed to be concentrated at each floor level and damping is assumed to be developed by the relative motion of adjacent floors as stated in Sec. 4-2 or as shown in Fig. 4-1, the equations of motion are formulated





as outlined below.

Let  $x_i$ ,  $\dot{x}_i$ , and  $\ddot{x}_i$  be the deflection, velocity and acceleration, respectively, at the  $i$ -th floor relative to the ground and let vectors  $\{x\}$ ,  $\{\dot{x}\}$ , and  $\{\ddot{x}\}$  represent sets of such values from the top floor to the bottom floor at any instant during the motion.

The restoring shear at the  $i$ -th story,  $Q_i$ , is the  $i$ -th element of the vector  $\{Q\}$ , which is a function of  $\{x\}$  and is expressed in general by Eq. 4-27; i.e.,

$$\{Q\} = [G] (\{x\} - \{\xi\}) + \{\eta\}$$

where the stiffness matrix,  $[G]$ , and the vectors,  $\{\xi\}$  and  $\{\eta\}$  depend upon the behavioral history of the frame from the initiation of motion to the instant under consideration.

If the acceleration of the ground motion is given by  $\ddot{y}_0(t)$ , the acceleration at the  $i$ -th floor with respect to the absolute axis is  $\ddot{x}_i + \ddot{y}_0$ , and thus the inertia force due to D'Alembert's principle is  $-m_i(\ddot{x}_i + \ddot{y}_0)$ .

The evaluation of the damping effect is complex. However, it is simply assumed here that the damping force is proportional to the relative velocity of adjacent floors and is given by  $c_i(\dot{x}_i - \dot{x}_{i+1})$ , where the damping coefficient,  $c_i$ , is taken as:

$$c_i = \frac{2h_i G_{ii}}{\omega_1} \quad (4-28)$$

in which  $G_{ii}$  is the  $i$ -th diagonal element of the initial





stiffness matrix  $[G]$  (which is expressed in terms of story shears), and  $\omega_1$  is the circular frequency in the first natural mode of the undamped frame;  $h_1$  is an arbitrary constant serving the same purpose as does the percentage of critical damping in the analysis of single degree-of-freedom systems.

Since the applied loads (inertia forces) must be in equilibrium with the frame restoring forces and the forces developed by damping as shown in Fig. 4-7, the following conditions must be satisfied.

At the first story:

$$-m_1 (\ddot{x}_1 + \ddot{y}_0) = Q_1 (\{x\}) + c_1 (\dot{x}_1 - \dot{x}_2) \quad \dots (4-29)$$

At the  $i$ -th story ( $i = 2, 3, \dots, N_s - 1$ ):

$$\sum_{j=1}^i \{-m_j (\ddot{x}_j + \ddot{y}_0)\} = Q_i (\{x\}) + c_i (\dot{x}_i - \dot{x}_{i+1}) \quad \dots (4-30)$$

At the bottom story (the  $N_s$ -th story):

$$\sum_{j=1}^{N_s} \{-m_j (\ddot{x}_j + \ddot{y}_0)\} = Q_{N_s} (\{x\}) + c_{N_s} \dot{x}_{N_s} \quad (4-31)$$

Or in a concise form:

$$\ddot{x}_i = - \frac{1}{m_i} \{c_i \dot{x}_i + Q_i (\{x\}) + S_i(t)\} \quad (4-32)$$

for  $i = 1, 2, \dots, N_s$ . These equations are termed the equations of motion. Where:



$$S_i(t) = CMA_i + \dot{Y}_0(t) \cdot CSM_i - c_i \dot{x}_{i+1} \quad (4-33)$$

and the last term,  $c_i \dot{x}_{i+1}$ , is zero for  $i = N_s$ .  $CMA_i$  and  $CSM_i$  are given by:

$$\text{for } i = 1 : CMA_i = 0 ; CSM_i = m_1$$

$$\text{for } i = 2 \text{ to } N_s - 1 : CMA_i = \sum_{j=1}^{i-1} m_j \dot{x}_j ;$$

$$CSM_i = \sum_{j=1}^i m_j \quad (4-34)$$

$$\text{for } i = N_s : CMA_i = \sum_{j=1}^{N_s-1} m_j \dot{x}_j ; CSM_i = \sum_{j=1}^{N_s} m_j$$

#### 4-5-2 Numerical Integration

To solve the coupled second order differential equations such as Eq. 4-32, a numerical integration method is employed. The linear acceleration method is used in this study.

The acceleration at any floor is assumed to change linearly within the time interval,  $\Delta t$ ; i.e., if the acceleration at a time  $n\Delta t$  (from the initiation of vibration;  $n$  is an integer) at the  $i$ -th floor is  $\dot{x}_i^*(n)$  and the acceleration at time  $\Delta t$  later at that floor is  $\dot{x}_i^*(n+1)$ , then the derivative at time  $n\Delta t$ ,  $\dot{x}_i^*(n)$ , is assumed to be:



$$\ddot{x}_i(n) = \frac{\dot{x}_i(n+1) - \dot{x}_i(n)}{\Delta t}, \quad (4-35)$$

and the fourth (and higher degree) derivative of  $x_i$  vanishes. Therefore, assuming that  $x_i(t)$  is differentiable for at least three times between  $n\Delta t$  and  $(n+1)\Delta t$ , Taylor's expansion is written as:

$$x_i(n+1) = x_i(n) + \frac{\dot{x}_i(n)}{1!}\Delta t + \frac{\ddot{x}_i(n)}{2!}\Delta t^2 + \frac{\ddot{\ddot{x}}_i(n)}{3!}\Delta t^3 \dots \quad (4-36)$$

and by differentiating:

$$\dot{x}_i(n+1) = \dot{x}_i(n) + \frac{\ddot{x}_i(n)}{1!}\Delta t + \frac{\ddot{\ddot{x}}_i(n)}{2!}\Delta t^2 \quad (4-37)$$

Substituting Eq. 4-35 into Eqs. 4-36 and 4-37,  $x_i(n+1)$  and  $\dot{x}_i(n+1)$  are, respectively, expressed as:

$$x_i(n+1) = x_i(n) + \dot{x}_i(n)\Delta t + \frac{1}{3}\ddot{x}_i(n)\Delta t^2 + \frac{1}{6}\ddot{\ddot{x}}_i(n+1)\Delta t^2 \dots \quad (4-38)$$

and

$$\dot{x}_i(n+1) = \dot{x}_i(n) + \frac{1}{2}\ddot{x}_i(n)\Delta t + \frac{1}{2}\ddot{\ddot{x}}_i(n+1)\Delta t. \quad (4-39)$$

Eqs. 4-38 and 4-39 together with Eq. 4-32 determine the deflection, velocity and acceleration at each floor at every instant of the motion. For determination of these values, however, an iterative procedure is required. The chart shown in Fig. 4-8 describes this procedure.





The computer program which is used to perform the dynamic analysis of a frame shown in Fig. 4-1, using the above method of numerical technique, is listed in Appendix D.

#### 4-5-3 Natural Periods of Vibration

It is sometimes necessary to know the smallest natural period of a frame to select a proper time interval for the numerical integration process. When the linear acceleration method is used to solve Eq. 4-32, the time step,  $\Delta t$ , in Eqs. 4-38 and 4-39 must be less than approximately one-tenth of the smallest natural period in order to obtain convergence.

The natural periods are also used as reliable parameters to classify the overall stiffness of frames. For this purpose, however, only the first two or three modes would be sufficient.

In the computer program listed in Appendix D, the minimum natural period and the first three natural periods and their corresponding natural modes are calculated prior to the response calculation. The smallest and the largest natural periods are computed using Stodola's method (power iteration method). Knowing the first eigenvalue (largest natural period) and the corresponding eigenvector (mode), the second and the third eigenvalues and the corresponding eigenvectors are obtained successively using Wielandt's deflation method.



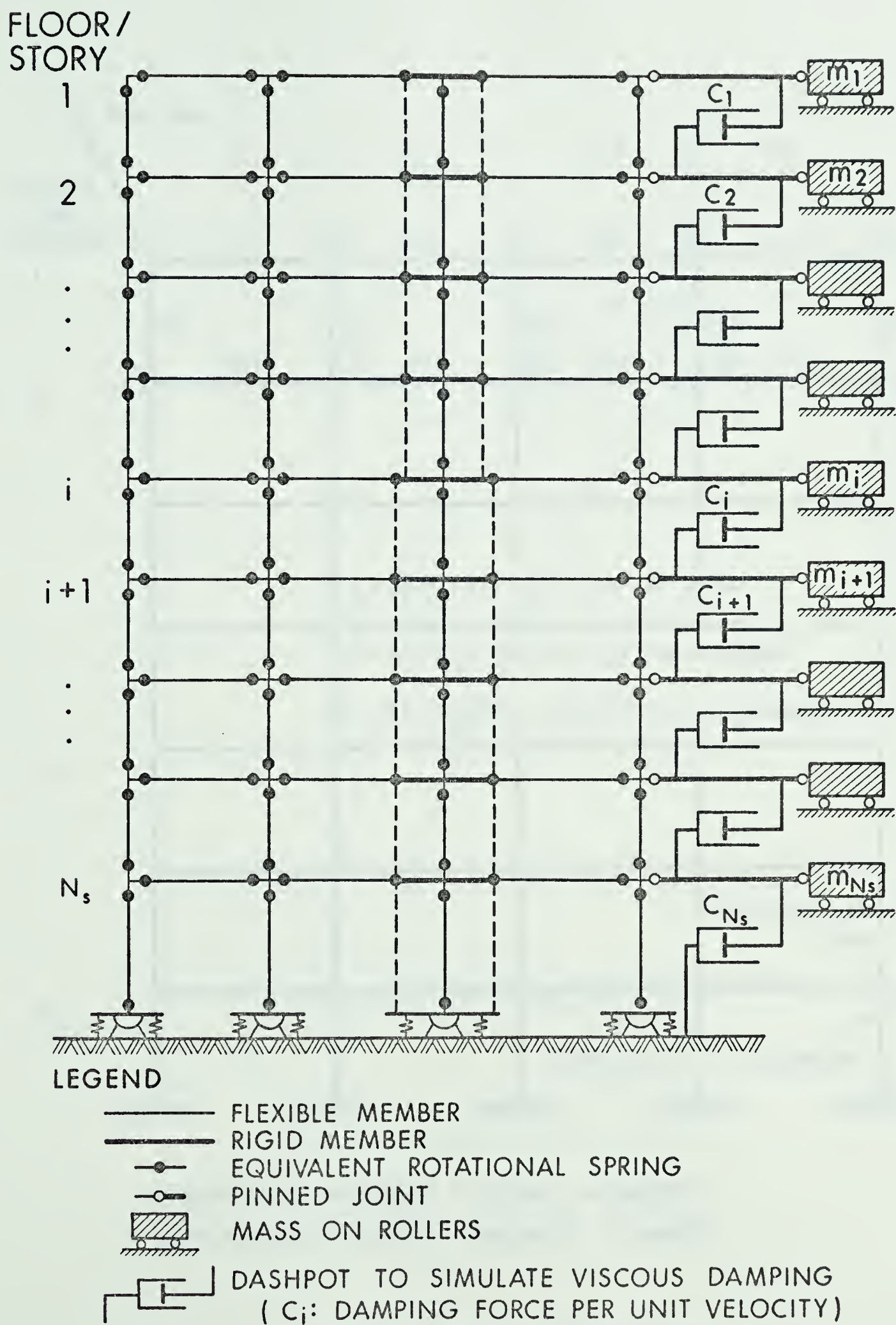
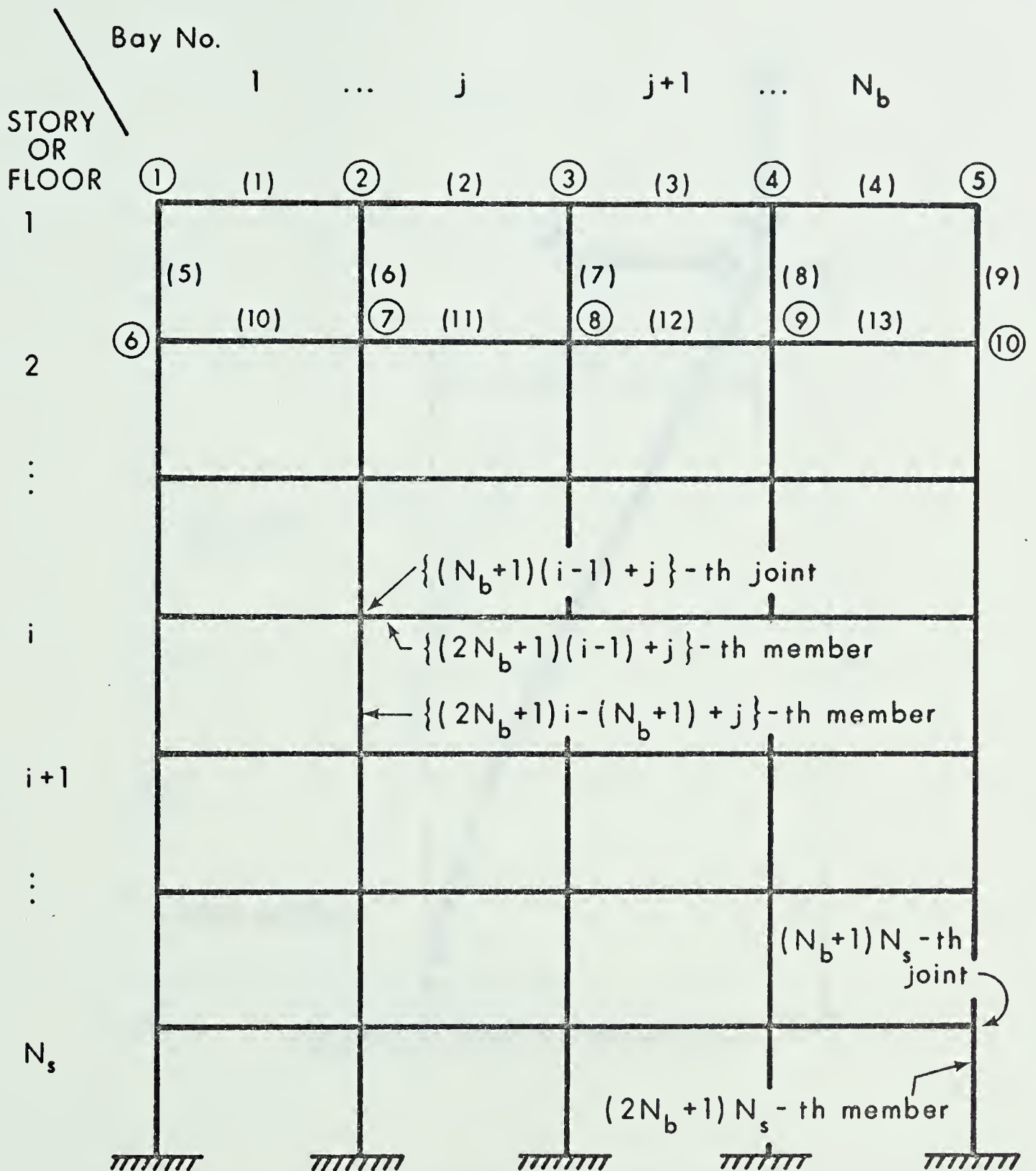


FIG. 4-1 ANALYTICAL MODEL







ENCIRCLED NUMBER : JOINT NUMBER  
BRACKETED NUMBER : MEMBER NUMBER

FIG. 4-2 NUMBERING CONVENTION



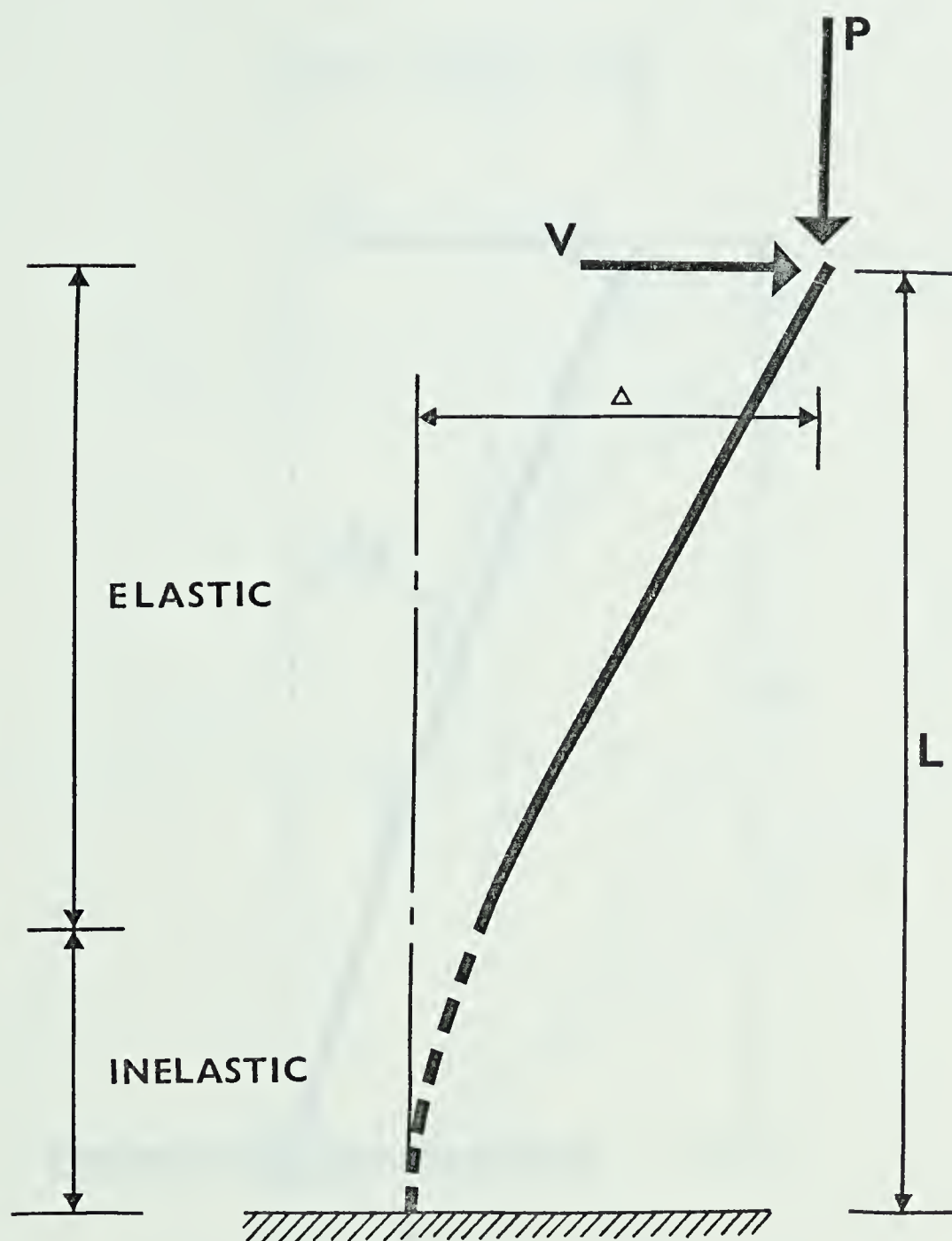


FIG. 4-3 COLUMN WITH AXIAL LOAD





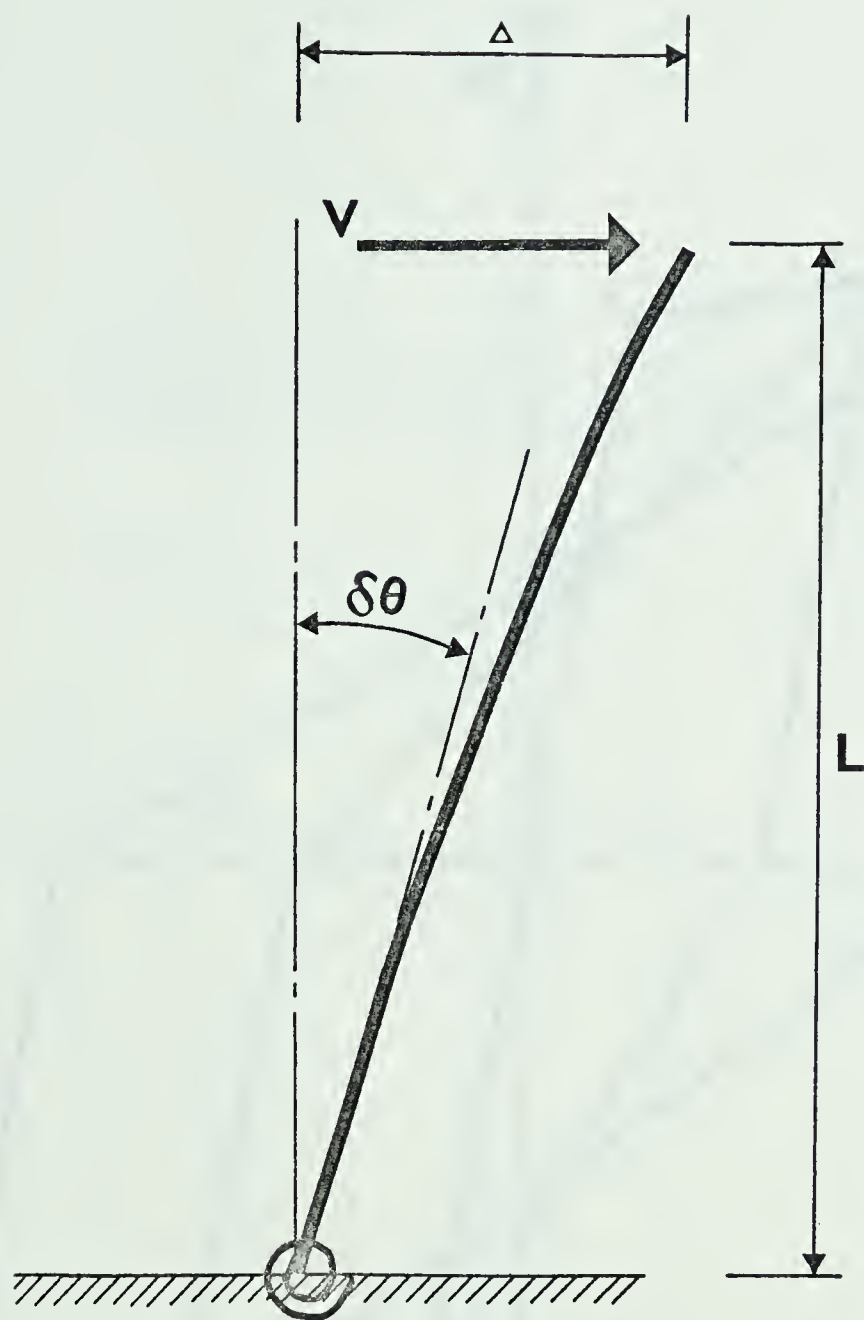


FIG. 4-4 RESTRAINED COLUMN



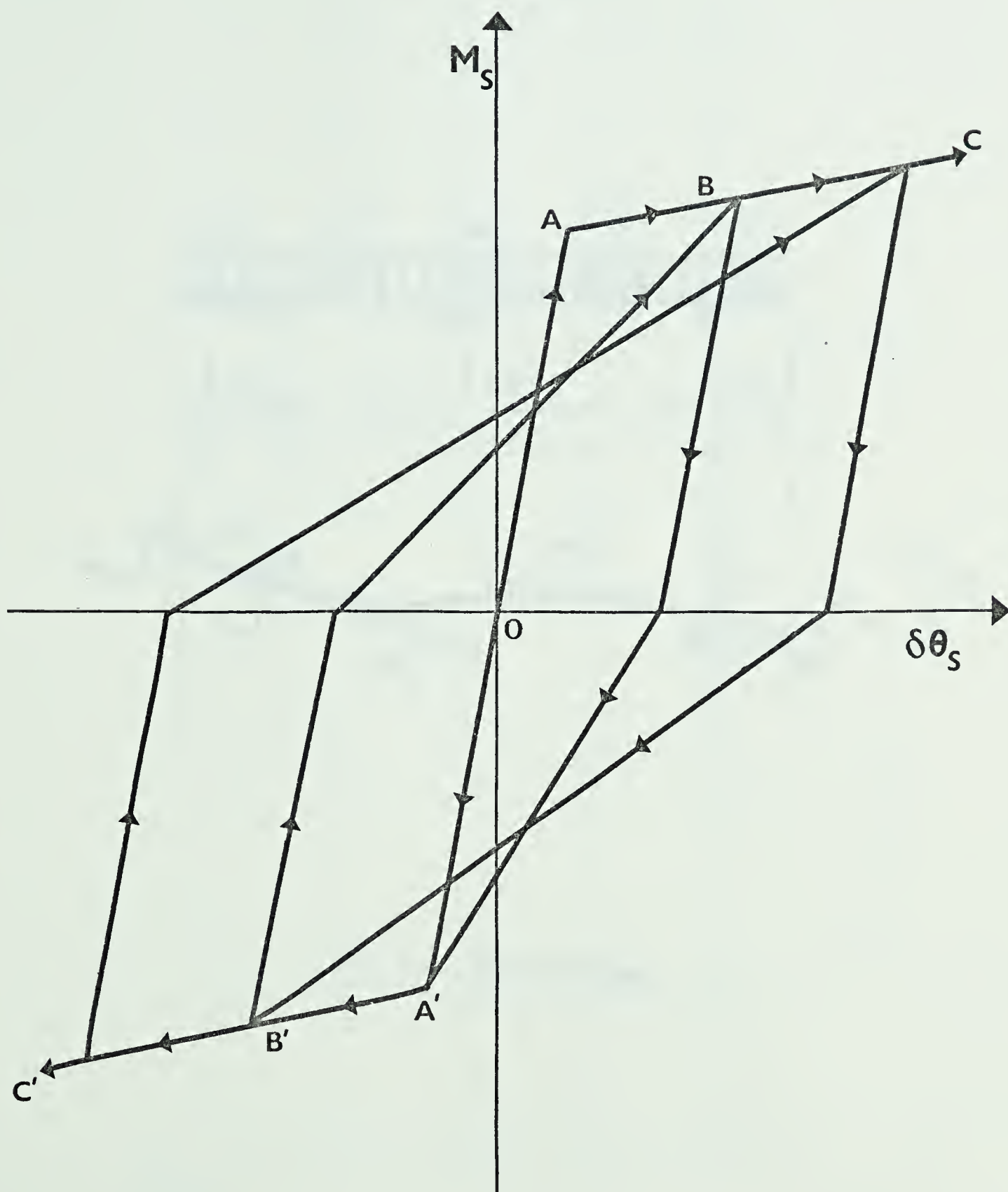


FIG. 4-5 Typical  $M_s$ - $\delta\theta_s$  Relationship for Reversing Cyclic Load



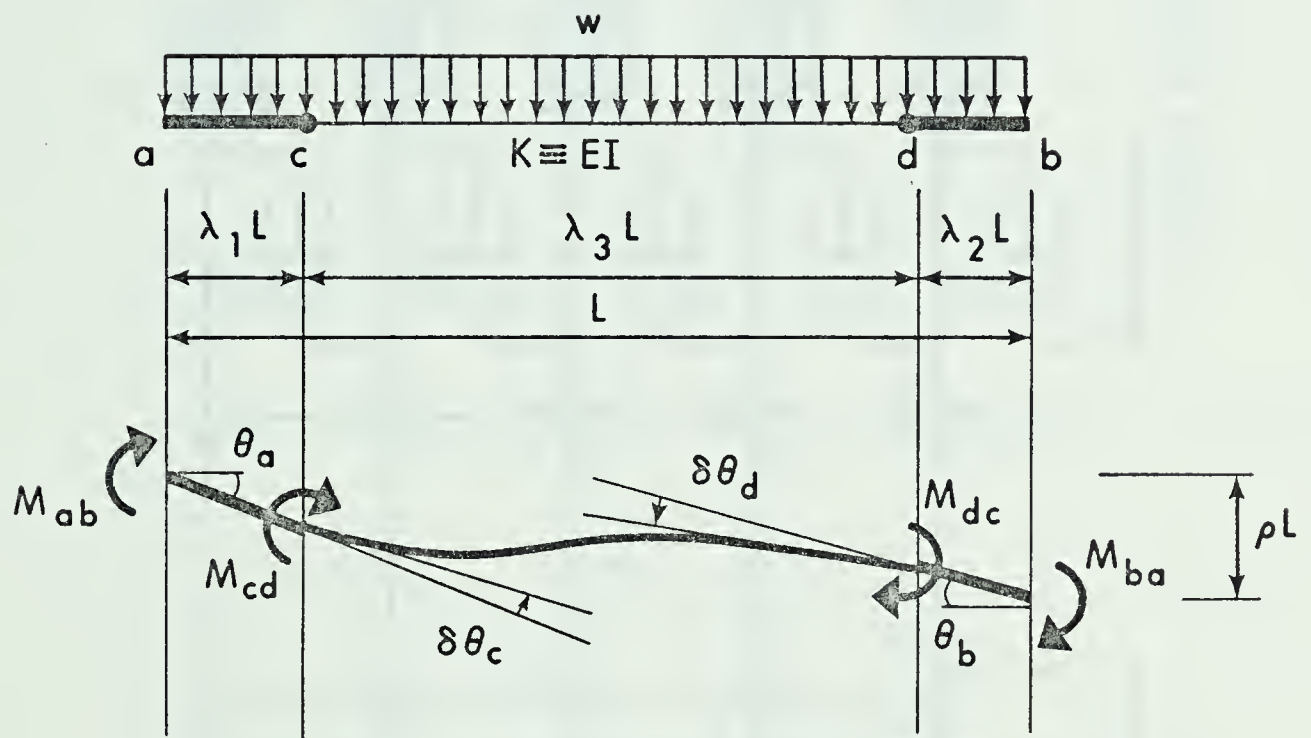


FIG. 4-6 TYPICAL MEMBER





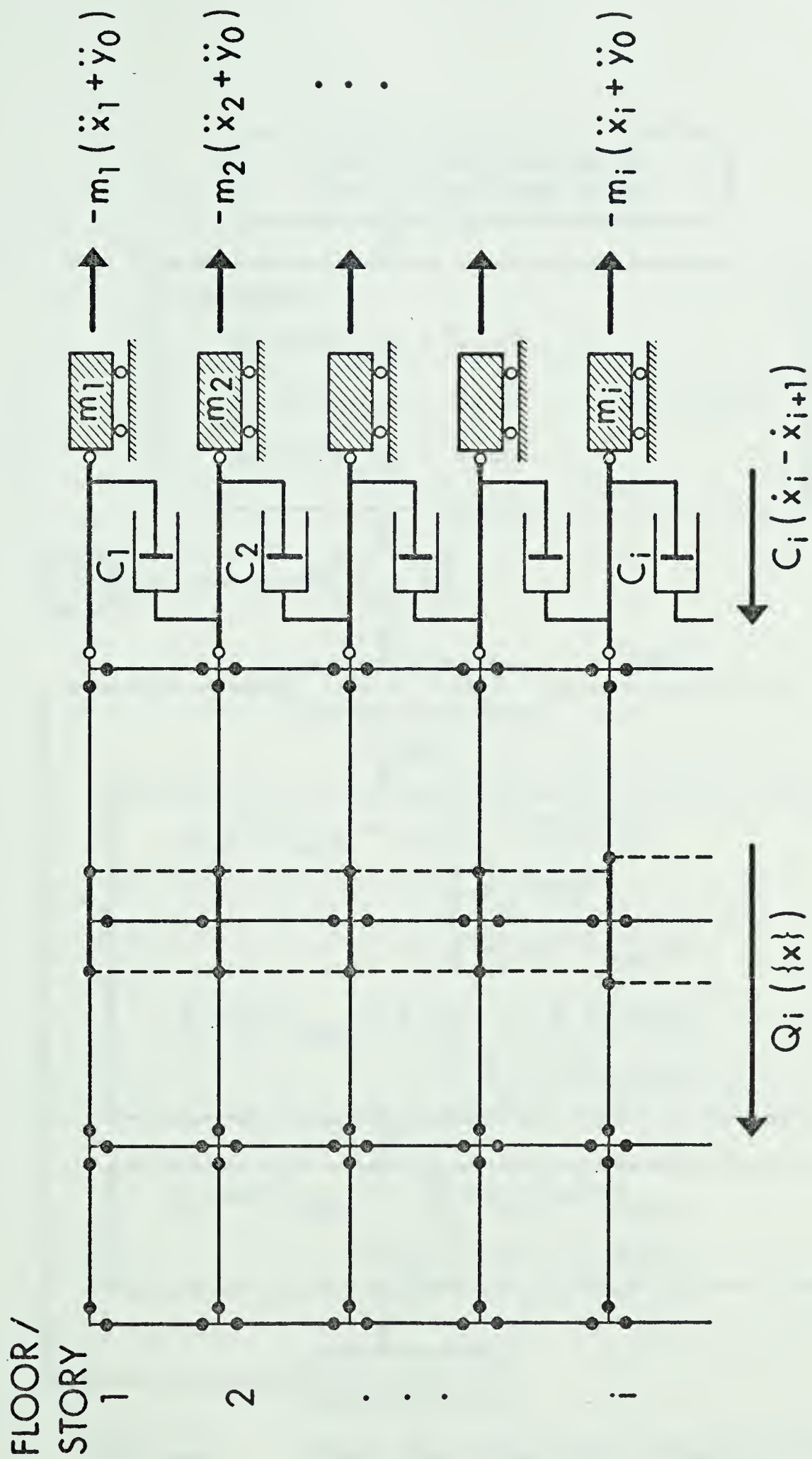


FIG. 4-7 EQUILIBRIUM OF FORCES IN MOTION



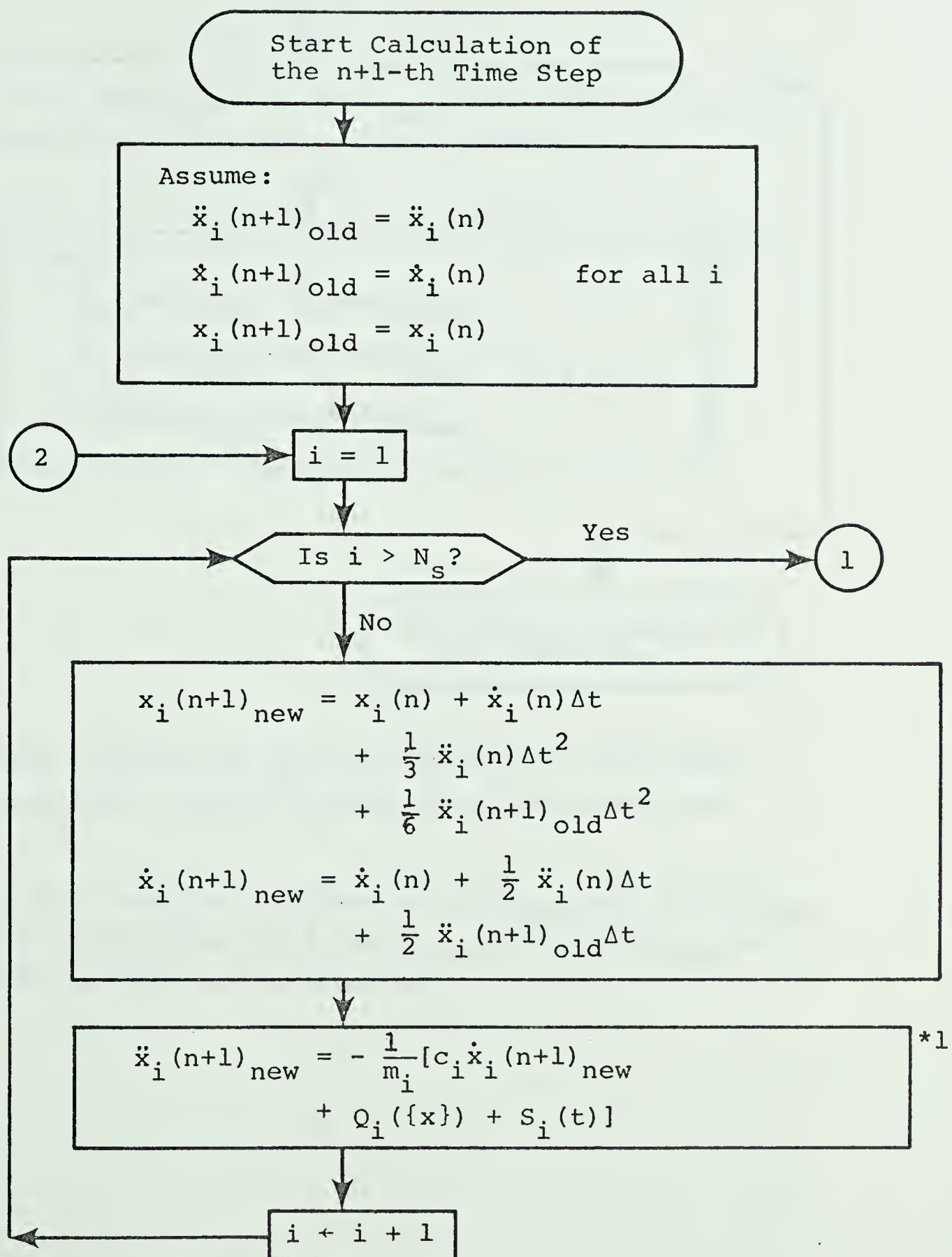
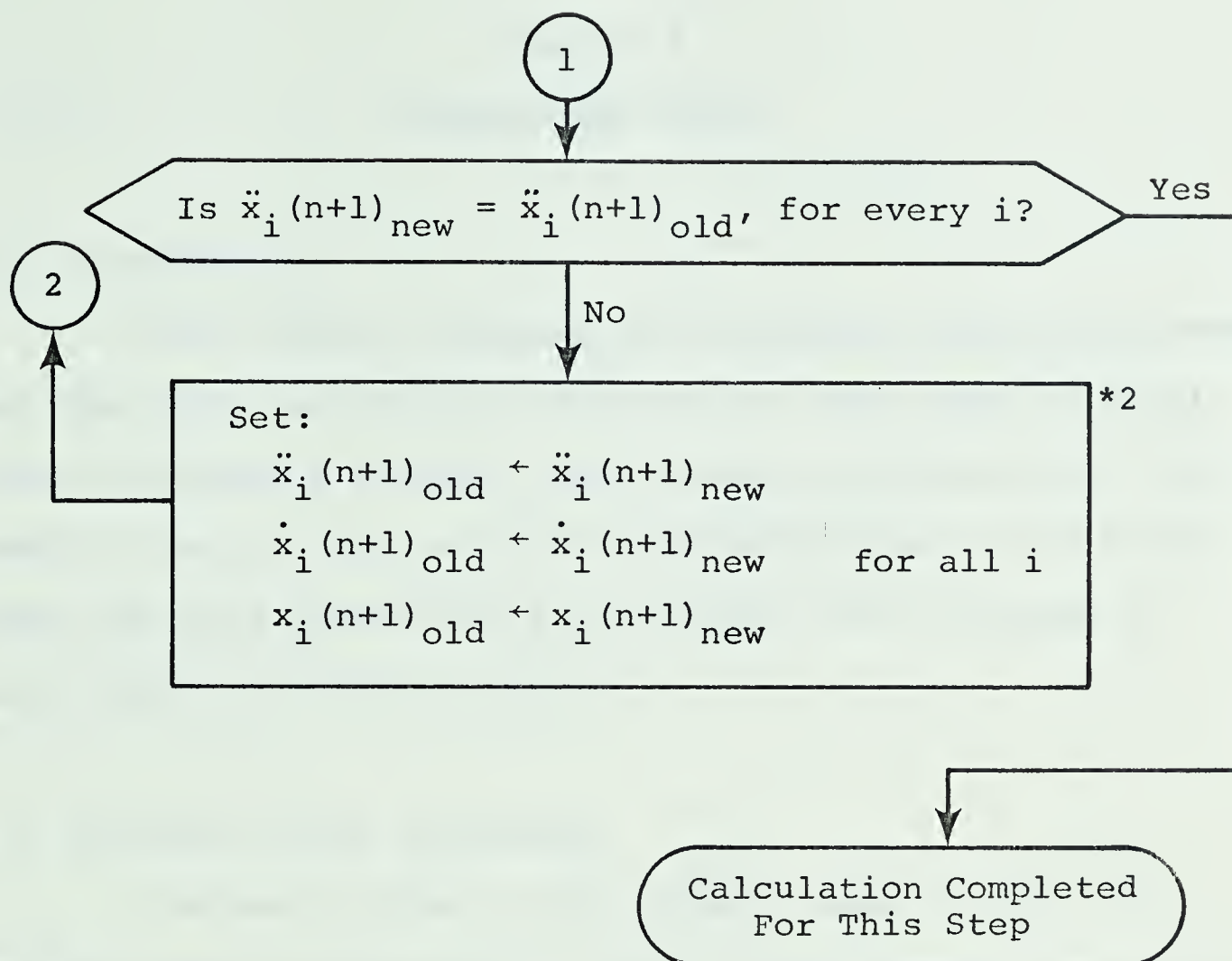


Fig. 4-8

Chart for Numerical Integration

(to be continued)





## Notes:

- \*1 When calculating  $Q_i(\{x\})$  and  $S_i(t)$ , new values of  $\ddot{x}_j(n+1)$ ,  $\dot{x}_j(n+1)$  and  $x_j(n+1)$  are used for  $j < i$ .
- \*2 In the computer program,  $\dot{x}_i(n+1)_{new}$  and  $x_i(n+1)_{new}$  are overwritten on  $\dot{x}_i(n+1)_{old}$  and  $x_i(n+1)_{old}$  as soon as they are calculated.

Fig. 4-8 (continued) Chart for Numerical Integration



## Chapter 5

### BEHAVIORAL STUDY

#### 5-1 Introduction

This chapter discusses the building frames considered, how they were selected and designed and the range of significant parameters studied. The results predicted for 6 seconds of the 1940 El Centro NS accelerogram using the earthquake analysis presented in this thesis are discussed in later sections of this chapter.

#### 5-2 Building Frame Considered

The basic frame of this study, shown in Fig. 5-1, was designed by engineers of the Portland Cement Association. The design was deemed to be typical of those used for high-rise apartment buildings. All axial and lateral forces are carried by the shear walls. This design could also represent a structure consisting of a shear wall connected to a hinged steel frame, which relies entirely on the shear wall for lateral resistance. A static earthquake analysis was carried out on this frame based on the equivalent earthquake loads presented in the 1973 Uniform Building Code. The base shear caused by the code specified earthquake loading, for one bent of the frame, was determined using the formula:

$$V_B = ZCKW \quad (5-1)$$





where

$$V_B = \text{base shear}$$

$$Z = \text{earthquake zone factor}$$

$$C = 0.05 \sqrt[3]{T}$$

$$T = \text{fundamental period of structure}$$

$$K = \text{Horizontal force factor reflecting type of construction}$$

$$W = \text{Total weight of bent}$$

The base shear,  $V_B$ , was distributed over the height of the building in accordance with the following formula:

$$F_X = V_B \frac{w_x h_x}{\sum w h} \quad (5-2)$$

where

$$F_X = \text{lateral force at level } x$$

$$w_x = \text{weight at level } x$$

$$h_x = \text{height of level } x \text{ above base}$$

$$\sum w h = \text{sum of all } w_x h_x$$

The shear, axial load, and moment for the code specified earthquake loading were determined using the above formulae and statics.

### 5-3 Building Parameters Studied

The most important parameter studied was the horizontal force factor,  $K$ , in Eqn. 5-1. Changes in the value of  $K$  are mirrored directly in changes of the values of design base shear and design seismic moment. Values of  $K$  listed in the Structural Engineers Association of California (1973)



code<sup>8</sup>, typical of those in other codes, are shown in Table 5-1.

Another parameter studied was the effect of tapering the size and stiffness of the shear wall from base to top of structure in contrast to having a prismatic shear wall with constant size and stiffness. In a normal building the shear walls "taper" either due to a relatively gradual reduction in wall thickness due to decreasing axial loads or due to the abrupt discontinuation of portions of the walls or elevator shafts. Studies, such as those of Giberson mentioned in Chapter 2, have shown differences in behavior between tapered and prismatic structures.

The third parameter studied was the influence of the cross-sectional shape of the shear wall upon the dynamic behavior of the building. Flanged sections having approximately the same flexural stiffness and yield moment as rectangular sections have correspondingly less web area to resist shearing deformations. Members which develop inclined cracking and thus significant shear deformations are approximately half as stiff as members without inclined cracking. Thus the effect of different shear stiffnesses within members of the frames studied on the dynamic behavior of cross-sections having equal flexural stiffness and yield moment was the third parameter studied.



### 5-3-1 Range of Building Parameters Studied

The capacity of the rectangular shear wall cross-section chosen for this building by Portland Cement Association engineers corresponded to a K value of 2.17 and a load factor,  $\frac{U}{\phi_{cap}}$ , of 1.75 against flexural yielding. This high value of K resulted from providing the minimum reinforcing for walls specified by ACI 318-71. Typical values of K given by building codes for this type of building range between 0.67 to 1.33, therefore dynamic behavior at these K values was also of interest.

The reduction in K value while maintaining base shear and seismic moment at the desired proportion of the wall capacity involved increasing the weight of each story of the structure as shown by Eqn. 5-1. A hypothetical pinned frame was added to the shear wall to provide support for the extra weight leaving the axial load level and capacity of the shear wall constant. The weight assumed at each floor level corresponded to the K value assumed for the frame and did not change for tapered or prismatic shear walls.

The building as originally designed was tapered. Prismatic buildings were formed by extending the first story shear wall cross-section and reinforcement to the top of the building.

I-shaped shear wall cross-sections were designed to have essentially the same moment of inertia and the same balanced moments as the basic rectangular shear wall cross-





sections. Cross-section capacities for both rectangular and I-shaped shear wall cross-sections are listed in Table 5-2.

The buildings were considered to be fixed at the base. No attempt was made to study the dynamic effects caused by soil-structure compliance.

The buildings were subjected to 6 seconds of the 1940 El Centro NS earthquake accelerogram. Since the structures studied had minimum natural periods of the order of 0.01 seconds, the time step used in solving the iterative process depicted in Fig. 4-8 was 0.0005 seconds. The necessity for this small time step is partially explained in Sec. 4-5-3. The small time step led to large computer time requirements thus it became necessary to choose an earthquake accelerogram having maximum peaks of acceleration and anticipated maximum dynamic effects within a limited time period. The first 6 seconds of the 1940 El Centro NS accelerogram was considered to best fit this requirement.

Three tapered rectangular shear wall structures, corresponding to the three K values, were first analyzed. Considering these results, it was found that there was no necessity of analyzing further shear wall structures with masses corresponding to the two larger K values as the shear wall structure with masses adjusted for a K value of 0.67 was responding elastically to the input earthquake accelerogram. The last four analyses were therefore for prismatic



rectangular, prismatic I and tapered I shear wall structures with masses adjusted for a K value of 0.67.

Structural properties of the seven shear wall structures analyzed are listed in Tables 5-3 to 5-9. The hinged steel frame was considered to be made up of stiff beams and columns with very weak rotational springs at their ends.

Henceforth each structure analyzed will be referred to using a series of letters and numbers. The series corresponds to taper, type of wall and K value. Two examples would be TR0.67 and PI0.67 which correspond to tapering rectangular and prismatic I-shaped shear wall structures with masses adjusted for a K value of 0.67. For the PI0.67 structure an additional variable is denoted in brackets to show the number of floors, counted from the base, which were assumed to develop inclined cracking and significant shear deformations. PI0.67(12) was analyzed to obtain a direct comparison between a tapered structure and a prismatic structure both of which were assumed to have inclined cracking within their lower 12 floors. The actual shear force on PI0.67 structure was only high enough to cause inclined cracking in the lower 6 floors of the structure thus PI0.67(6) was analyzed.

#### 5-4 Dynamic Response Spectrum for Elastic Systems

For a specific excitation of a simple elastic system having a particular percentage of critical damping, the



maximum response is a function of the natural period of vibration of the system. A plot of the maximum response against the period of vibration,  $T$ , is called a "response spectrum". The most useful response spectra are those for acceleration  $\ddot{x}$ , velocity  $\dot{x}$ , and displacement  $x$ . Since the response spectra give the maximum values of these quantities for each period considered, it is desirable to use a different symbol to indicate the spectral value. In the following, the spectral value of the displacement relative to ground is designated by the symbol  $S_D$ , the spectral value of the velocity relative to ground is denoted by the symbol  $S_V$ , and the spectral value of the absolute acceleration of the masses is denoted by the symbol  $S_A$ .

Fig. 5-2 is a response spectrum for elastic systems for the 1940 El Centro earthquake.<sup>46</sup> Consideration of this response spectrum reveals the following:

1. Structures responding essentially in their fundamental mode with fundamental periods from 0.15 to 1.5 seconds experience high accelerations during an El Centro type earthquake. Displacements are usually small.
2. Structures responding essentially in their fundamental mode with fundamental periods of from 1.5 to 7.0 seconds experience high displacements at comparatively low acceleration levels during an El Centro type earthquake.

Considering Table 5-10 which lists the fundamental and other periods of the structures analyzed, one can see





that the shear wall structures analyzed belong to the second category.

Results of modal analyses carried out on the shear wall structures of this dissertation using the mode shapes and natural periods produced by the dynamic analysis computer program and the response spectrum of Fig. 5-2 are listed in Table 5-11. The response listed represents the root mean square value of the participations of the first three modes. The participation of the second and third modes was negligible in all cases for these analyses.

The period of a one degree-of-freedom elastic system is given by:

$$T = \frac{2 \pi}{\sqrt{\kappa/M}}$$

where  $\kappa$  = stiffness of system

$M$  = mass of system

If one considers this equation as it applies to a one degree-of-freedom system with constant  $\kappa$  and varying mass due to variations in horizontal force factor  $K$ , one finds that as the value of  $K$  decreases, the value of  $M$  increases and the period  $T$ , of the structure increases and vice-versa.

This seems to have led to a desirable situation for the shear wall structures considered herein. As the value of  $K$  decreased and the masses of the system increased, the period lengthened and the accelerations of the system





dropped. The resulting force level was below the yield level of the system. In the opposite situation, as the value of  $K$  increased and the mass of the system decreased, the period shortened and the accelerations of the system increased. Resulting forces formed as a product of the masses and accelerations were still below the yield level of the system.

One can follow the above discussion directly on the response spectrum of Fig. 5-2. The response spectrum also tends to predict the larger than expected displacement of the TR1.33 structure which had a fundamental period of 3.221 seconds corresponding to a peak in the response spectrum.

Values of displacement predicted by modal analysis compare reasonably well with those found by the dynamic analysis program of this dissertation. Maximum moment values predicted by modal analysis exceed the yield moments of the rectangular shear wall structures by 10 to 20 percent and are close to yield for the I shaped structures.

## 5-5 Observed Structural Response

All structures analyzed responded elastically to the first 6 seconds of the 1940 El Centro NS accelerogram. Maximum displacements of each floor for each of the seven structures analyzed are shown in Fig. 5-3 and Fig. 5-4. Maximum interfloor displacements for each of the seven structures analyzed are shown in Fig. 5-5 and Fig. 5-6.



Similarly Fig. 5-7 and Fig. 5-8 show maximum rotations from vertical of the joints of each beam-column joint and Fig. 5-9 and Fig. 5-10 show maximum rotations from vertical of the joints where the beams frame into the shear wall. Observed structural responses will be discussed in the following sections.

#### 5-5-1 Presence of Various Modes in Observed Structural Responses

The time of occurrence of each floor's maximum displacement for each structure analyzed is listed in Tables 5-12 to 5-18. The shape of the maximum displacement responses and the fact that all maximum displacements within a structure occur almost concurrently seems to indicate that the participation of higher modes, usually out of phase with the fundamental mode, were very small. This observation was confirmed by the modal analysis of Sec. 5-4.

#### 5-5-2 Effect of Horizontal Force Factor $K$

Changes in response which could be attributed to changes in the value of the horizontal force factor  $K$ , are probably more correctly associated with changes in fundamental period of the structure. As  $K$  is increased, the fundamental period decreases and vice-versa.

As  $K$  decreases and the fundamental period increases, maximum displacements, maximum interfloor displacements, maximum shear wall joint rotations and maximum column rotations all tended to increase. If  $K$  is held constant and





the stiffness of the section of the building considered is held constant, maximum displacements, maximum interfloor displacements, maximum shear wall joint rotations and maximum column joint rotations tend to remain constant.

Fig. 5-3 shows that as  $K$  decreased maximum displacements tended to increase. The large maximum displacements of the TR1.33 building must be attributed to resonance caused by a matching of the fundamental period of the TR1.33 building and the period of the 1940 El Centro "forcing function". Fig. 5-4 shows that when  $K$  is held constant, maximum displacements tend to stay fairly constant. When the stiffness of the section of the building considered is also held constant as in the lower 6 stories of the 3 buildings of Fig. 5-4 the maximum displacements also remain quite constant.

Similar observations can be made concerning Fig. 5-5 and Fig. 5-6 relating to maximum interfloor displacements, concerning Fig. 5-7 and Fig. 5-8 relating to maximum column joint rotations and concerning Fig. 5-9 and Fig. 5-10 relating to maximum shear wall joint rotations.

### 5-5-3 Tapered Structures versus Prismatic Structures

Tapered structures experienced greater deformations than did their prismatic counterparts when subjected to the 1940 El Centro earthquake. Fig. 5-3 shows the TR0.67 building to have had larger maximum displacements than the PR0.67





building. Similarly Fig. 5-4 shows the TI0.67 building to have had larger maximum displacements in its upper 10 stories than either of the PI0.67 structures. Fig. 5-4 indicates that within stories of equal stiffness, the lower 6 stories in this case, the TI0.67 structure and both PI0.67 structures deformed essentially equal amounts. Fig. 5-7 and Fig. 5-9 show that the larger maximum displacements of the TR0.67 structure over those of the PR0.67 structure were due to the TR0.67 structure having greater curvatures in its bottom stories which led to larger maximum displacements and maximum interfloor displacements in this structure than in the PR0.67 structures.

Table 5-10 shows the fundamental periods of the three I-shaped shear wall structures to be virtually identical. The fundamental periods of the two rectangular shear wall structures are also virtually identical. The modal response of Table 5-11 shows the rectangular shear wall structure to be at higher force levels than the I-shaped shear wall structures. It may be then that differences between tapered and prismatic structures only become noticeable at force levels close to the yield level of these structures.

#### 5-5-4 Effect of Changing Shear Stiffness

Shear deformations were included in developed  $M_s - \delta\theta_s$  relationships for the lower parts of the TI0.67, PI0.67(6) and PI0.67(12) structures. In these structures, the shears



predicted by the 1973 Uniform Building Code static earthquake loadings were greater than the uncracked shear capacities of the I-shaped cross-sections within the first twelve stories for the TI0.67 structure and within the first 6 stories for the PI0.67(6) structure, and shear deformations were included in the cracked portions of the structure. The PI0.67(12) structure in which shear cracking was assumed to occur in the lower 12 stories was analyzed for comparison to the TI0.67 structure. Its first 12 stories were assumed to have shear deformations as did the TI0.67 structure.

I-shaped shear wall structures with shear deformations were contrasted to rectangular shear wall structures having the same flexural stiffness and moment capacity. Thus the TI0.67 structure was compared to the TR0.67 structure and the PI0.67 structures were compared to the PR0.67 structure.

Fig. 5-11 and Fig. 5-12 show that changing the shear stiffness of a structure did not significantly affect its maximum displacement response. Changing the shear stiffness did however change the magnitude and distribution of maximum interfloor displacements, column joint rotations and shear wall joint rotations. Maximum interfloor displacements are shown in Fig. 5-13 and Fig. 5-14. Maximum column joint rotations are shown in Fig. 5-15 and Fig. 5-16. Fig. 5-17 and Fig. 5-18 show maximum shear wall joint rotations. Deformations tended to concentrate at the upper end of the zone in which shear deformations occurred and then to



lessen to values less than those experienced by buildings which did not have shearing deformations.

This action seems to be analogous to that of the soft story concept proposed by Fintel and Khan.<sup>39</sup>

The author notes from Figs. 5-13 to Fig. 5-18 that the lower the number of stories with shear deformations the lower the differences between structures with and without shear deformations. This may be an argument for prismatic structures over tapered structures if shearing deformations are expected as prismatic structures will usually have fewer floors with shearing deformations.

## 5-6 Performance of Structures

The main deflection criterion for high rise buildings is lateral drift. This is the relative magnitude of the lateral displacement at the top of a building with respect to its height or alternatively, the ratio of the relative lateral story displacement to the story height, assuming a more or less uniform story height.

Limiting values of this ratio, commonly called deflection limits are usually about  $1/500$  for wind loading.<sup>41</sup> The performance of modern buildings designed in recent years to meet this criterion appears to have been satisfactory with respect to the following effects of sway under wind loading:

(1) the stability of the individual columns as well as the structure as a whole.





2. the integrity of nonstructural partitions and glazing.

3. the comfort of the occupants of such buildings.

Reference 8 recommends an allowable drift due to static earthquake forces twice that normally used in designing for wind.

Deflection limits for wind would correspond to approximate building tip deflections of 5 inches and interfloor deflections of 0.25 inches for the buildings analyzed. Allowable drifts due to static earthquake forces would then be 10 inches tip deflection and 0.5 inches of interfloor displacement.

Building deflections for the TR2.17 structure computed by Portland Cement Association engineers were 0.42 inches tip deflection under static earthquake loading and 0.10 inches tip deflection under wind loading.

As shown in the figures of this chapter, none of the structures analyzed met the deflection limits mentioned above under the 1940 El Centro earthquake except within their bottom stories. El Centro is classified as a catastrophic earthquake and has a Richter value of 7.7. Under a more moderate earthquake however, the structures analyzed would meet the desired deflection limits. This is revealed through consideration of the response spectrum of a Jennings's  $C^{40}$  earthquake with a Richter Magnitude of 5.5 to 6.0. Under this earthquake the structures analyzed would have





displacements and accelerations approximately  $1/10$  of those caused by El Centro. The performance of the structures analyzed thus appears to be within the bounds of Code philosophy stated in Section 1-2 of this dissertation.

It would appear to the author that if deflections are to be limited under a catastrophic earthquake, a substantial frame must act in conjunction with a shear wall to limit structural deflections in upper stories.



TABLE 5-1  
HORIZONTAL FORCE FACTOR "K" FOR BUILDINGS  
OR OTHER STRUCTURES<sup>2</sup>

Type of Arrangement of resisting Elements	Value of <sup>1</sup> K
All building framing systems except as hereinafter classified	1.00
Buildings with a box system i.e. a structural system without a complete vertical load carrying space-frame. In this system the required lateral forces are resisted by shear walls.	1.33
Buildings with a complete horizontal bracing system capable of resisting all lateral forces, which system includes a moment-resisting, space-frame which, when assumed to act independently is capable of resisting a maximum of 25% of the total required lateral force.	0.80
Buildings with a moment-resisting space-frame which when assumed to act independently of any other more rigid elements is capable of resisting 100% of the total required lateral forces in the frame alone	0.67
<sup>1</sup> The coefficients determined here are for use in the State of California and in other seismic areas of similar earthquake activity.	
<sup>2</sup> Where wind load would provide higher stresses, this load shall be used in lieu of the loads resulting from earthquake forces.	



TABLE 5-2  
PROPERTIES OF SHEAR WALLS

SHAPE		$M_{bal}$ Kip-ft.	$P_{bal}$ Kips
Rectangular	24" x 360"	130000.	16210.
Rectangular	20" x 360"	112110.	13000.
Rectangular	16" x 360"	88920.	10500.
I - shaped	12" x 288" *	124630.	13000.
I - shaped	10" x 288"	104610.	11000.
I - shaped	8" x 288"	85330.	8500.

\* 12" refers to thickness of flanges and web of I-shaped cross section drawn below.

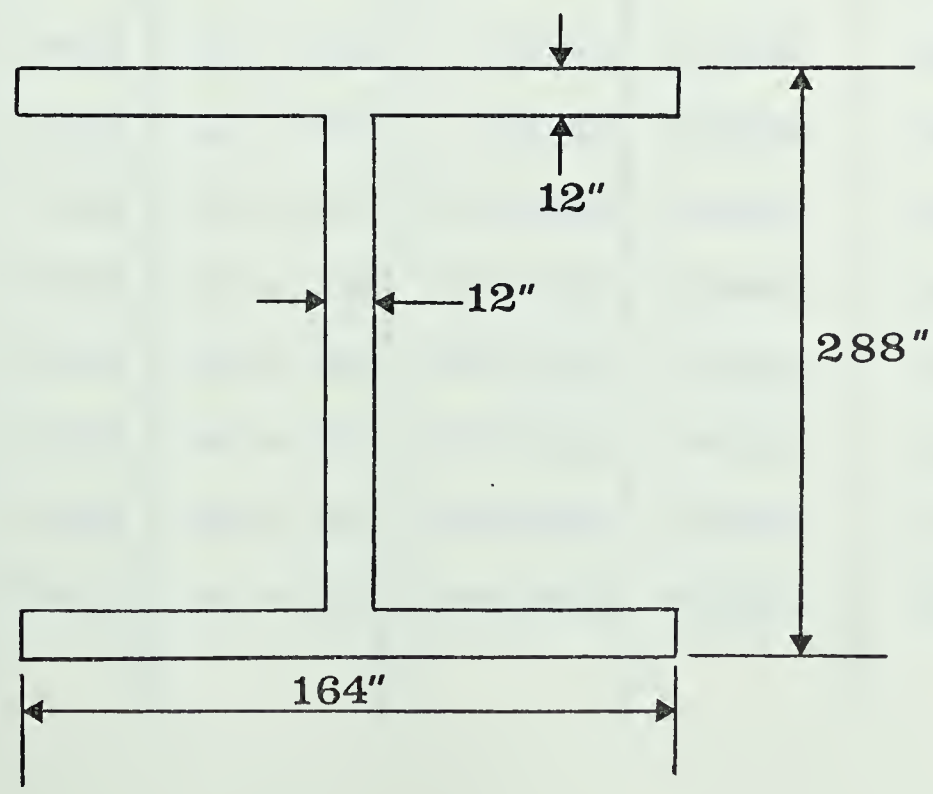






TABLE 5-3 PROPERTIES OF FRAME TR2.17

Story	Weight per floor (Kip)	Axial Load (Kip)	Cross Section	Moment of Inertia (in <sup>4</sup> )	M Yield (in-Kip)	Shear Deforma- tions
20	219	219	16 x 360	62208000	204190	No
19	219	438	16 x 360	62208000	236530	No
18	219	657	16 x 360	62208000	267750	No
17	219	876	16 x 360	62208000	277620	No
16	219	1095	16 x 360	62208000	306550	No
15	219	1314	16 x 360	62208000	334050	No
14	219	1533	16 x 360	62208000	362120	No
13	219	1752	16 x 360	62208000	385190	No
12	232	1984	20 x 360	77760000	469370	No
11	232	2216	20 x 360	77760000	496530	No
10	232	2448	20 x 360	77760000	522420	No
9	232	2680	20 x 360	77760000	551290	No
8	232	2912	20 x 360	77760000	571950	No
7	232	3144	20 x 360	77760000	599460	No
6	245	3389	24 x 360	93312000	672840	No
5	245	3634	24 x 360	93312000	694480	No
4	245	3879	24 x 360	93312000	715490	No
3	245	4124	24 x 360	93312000	746280	No
2	245	4369	24 x 360	93312000	766240	No
1	245	4614	24 x 360	93312000	787570	No



TABLE 5-4 PROPERTIES OF FRAME TR1.33

Story	Weight per floor (Kip)	Axial Load (Kip)	Cross Section	Moment of Inertia (in <sup>4</sup> )	M Yield (in-Kip)	Shear Deforma- tions
20	356.9	356.9	16 x 360	62208000	204190	No
19	356.9	713.8	16 x 360	62208000	236530	No
18	356.9	1070.7	16 x 360	62208000	267750	No
17	356.9	1427.6	16 x 360	62208000	277620	No
16	356.9	1784.5	16 x 360	62208000	306550	No
15	356.9	2141.4	16 x 360	62208000	334050	No
14	356.9	2498.3	16 x 360	62208000	362120	No
13	356.9	2855.2	16 x 360	62208000	385180	No
12	378.1	3233.3	20 x 360	77760000	469370	No
11	378.1	3611.4	20 x 360	77760000	496540	No
10	378.1	3989.5	20 x 360	77760000	522420	No
9	378.1	4367.6	20 x 360	77760000	544650	No
8	378.1	4745.7	20 x 360	77760000	471950	No
7	378.1	5123.8	20 x 360	77760000	582290	No
6	399.4	5523.2	24 x 360	93312000	644730	No
5	399.4	9922.6	24 x 360	93312000	634480	No
4	399.4	6322.4	24 x 360	93312000	715500	No
3	399.4	6721.4	24 x 360	93312000	737370	No
2	399.4	7120.8	24 x 360	93312000	757570	No
1	399.4	7520.2	24 x 360	93312000	778210	No



TABLE 5-5 PROPERTIES OF FRAME TRO.67

Story	Weight per floor (Kip)	Axial Load (Kip)	Cross Section	Moment of Inertia (in <sup>4</sup> )	M Yield (in-Kip)	Shear Deforma- tions
20	713.9	713.9	16 x 360	62208000	204190	No
19	713.9	1427.8	16 x 360	62208000	236830	No
18	713.9	2141.7	16 x 360	62208000	267780	No
17	713.9	2855.6	16 x 360	62208000	277620	No
16	713.9	3569.5	16 x 360	62208000	306540	No
15	713.9	4283.4	16 x 360	62208000	334040	No
14	713.9	7997.3	16 x 360	62208000	357570	No
13	713.9	5711.2	16 x 360	62208000	385140	No
12	756.3	6467.5	20 x 360	77760000	463500	No
11	756.3	7223.8	20 x 360	77760000	490410	No
10	756.3	7980.1	20 x 360	77760000	516030	No
9	756.3	8736.4	20 x 360	77760000	544650	No
8	756.3	9492.7	20 x 360	77760000	565040	No
7	756.3	10249.0	20 x 360	77760000	585160	No
6	798.7	11048.0	24 x 360	93312000	656580	No
5	798.7	11846.0	24 x 360	93312000	676770	No
4	798.7	12645.0	24 x 360	93312000	698260	No
3	798.7	13444.0	24 x 360	93312000	718590	No
2	798.7	14242.0	24 x 360	93312000	730170	No
1	798.7	15041.0	24 x 360	93312000	740600	No





TABLE 5-6 PROPERTIES OF FRAME PRO.67

Story	Weight per floor (Kip)	Axial Load (Kip)	Cross Section	Moment of Inertia (in <sup>4</sup> )	M Yield (in-Kip)	Shear Deforma- tions
20	713.9	713.9	24 x 360	93312000	299820	No
19	713.9	1427.8	24 x 360	93312000	332510	No
18	713.9	2141.7	24 x 360	93312000	363620	No
17	713.9	2855.6	24 x 360	93312000	396430	No
16	713.9	3569.5	24 x 360	93312000	424610	No
15	713.9	4283.4	24 x 360	93312000	424750	No
14	713.9	4997.3	24 x 360	93312000	453450	No
13	713.9	5711.2	24 x 360	93312000	479120	No
12	756.3	6467.5	24 x 360	93312000	504130	No
11	756.3	7223.8	24 x 360	93312000	538310	No
10	756.3	7980.1	24 x 360	93312000	564140	No
9	756.3	8736.4	24 x 360	93312000	586760	No
8	756.3	9492.7	24 x 360	93312000	613180	No
7	756.3	10248.9	24 x 360	93312000	635190	No
6	798.4	11048.0	24 x 360	93312000	656580	No
5	798.7	11846.0	24 x 360	93312000	677670	No
4	798.7	12645.0	24 x 360	93312000	698260	No
3	798.7	13440.0	24 x 360	93312000	719590	No
2	798.7	14242.0	24 x 360	93312000	730170	No
1	798.7	15041.0	24 x 360	93312000	740600	No





TABLE 5-7 PROPERTIES OF FRAME T10.67

Story	Weight per floor (Kip)	Axial Load (Kip)	Cross Section	Moment of Inertia (in <sup>4</sup> )	M Yield (in-Kip)	Shear Deforma- tions
20	639.9	639.9	8 x 288	63592448	126610	No
19	639.9	1279.8	8 x 288	63592448	157240	No
18	639.9	1919.7	8 x 288	63592448	186290	No
17	639.9	2559.6	8 x 288	63592448	216080	No
16	639.9	3185.5	8 x 288	63592448	244290	No
15	639.9	3838.4	8 x 288	63592448	266750	No
14	639.9	4479.3	8 x 288	63592448	295850	No
13	639.9	4119.2	8 x 288	63592448	322290	No
12	677.9	5797.1	10 x 288	78642400	361040	Yes
11	677.9	6475.0	10 x 288	78642400	386940	Yes
10	677.9	7152.9	10 x 288	78642400	408540	Yes
9	677.9	7830.8	10 x 288	78642400	432300	Yes
8	677.9	8508.7	10 x 288	78642400	446190	Yes
7	677.9	9186.6	10 x 288	78642400	480390	Yes
6	715.0	9901.6	12 x 288	93360384	533070	Yes
5	715.0	10617.0	12 x 288	93360384	556880	Yes
4	715.0	11332.0	12 x 288	93360384	575850	Yes
3	715.0	12047.0	12 x 288	93360384	594400	Yes
2	715.0	12762.0	12 x 288	93360384	607440	Yes
1	715.0	13477.0	12 x 288	93360384	626480	Yes



TABLE 5-8 PROPERTIES OF FRAME PI0.67 (12)

Story	Weight per floor (Kip)	Axial Load (Kip)	Cross Section	Moment of Inertia (in <sup>4</sup> )	M Yield (in-Kip)	Shear Deforma- tions
20	639.9	639.9	12 x 288	93360384	173510	No
19	639.9	1279.8	12 x 288	93360384	203360	No
18	639.9	1919.7	12 x 288	93360384	234970	No
17	639.9	2559.6	12 x 288	93360384	262230	No
16	639.9	3199.5	12 x 288	93360384	291800	No
15	639.9	3835.4	12 x 288	93360384	319560	No
14	639.9	4479.3	12 x 288	93360384	349770	No
13	639.9	5119.2	12 x 288	93360384	366890	No
12	677.9	5797.1	12 x 288	93360384	387700	Yes
11	677.9	6475.0	12 x 288	93360384	412430	Yes
10	677.9	7152.9	12 x 288	93360384	436580	Yes
9	677.9	7830.8	12 x 288	93360384	462120	Yes
8	677.9	8508.7	12 x 288	93360384	484420	Yes
7	677.9	9186.6	12 x 288	93360384	510380	Yes
6	715.0	9901.6	12 x 288	93360384	533070	Yes
5	715.0	10617.0	12 x 288	93360384	556880	Yes
4	715.0	11332.0	12 x 288	93360384	575850	Yes
3	715.0	12047.0	12 x 288	93360384	594400	Yes
2	715.0	12762.0	12 x 288	93360384	607440	Yes
1	715.0	13477.0	12 x 288	93360384	626480	Yes



TABLE 5-9 PROPERTIES OF FRAME PIO.67 (6)

Story	Weight per floor (Kip)	Axial Load (Kip)	Cross Section	Moment of Inertia (in <sup>4</sup> )	M Yield (in-Kip)	Shear Deforma- tions
20	639.9	639.9	12 x 288	93360384	173510	No
19	639.9	1279.8	12 x 288	93360834	203360	No
18	639.9	1919.7	12 x 288	93360834	234970	No
17	639.9	2559.6	12 x 288	93360834	262230	No
16	639.9	3199.5	12 x 288	93360834	291800	No
15	639.9	3839.4	12 x 288	93360834	319560	No
14	639.9	4479.3	12 x 288	93360834	349770	No
13	639.9	5119.2	12 x 288	93360834	366890	No
12	677.9	5797.1	12 x 288	93360834	396980	No
11	677.9	6475.0	12 x 288	93360834	427150	No
10	677.9	7182.9	12 x 288	93360834	452750	No
9	677.9	7830.8	12 x 288	93360834	479410	No
8	677.9	8508.7	12 x 288	93360834	508060	No
7	677.9	9186.6	12 x 288	93360834	529060	No
6	715.0	9901.6	12 x 288	93360834	533070	Yes
5	715.0	10617.0	12 x 288	93360834	556880	Yes
4	715.0	11332.0	12 x 288	93360834	575850	Yes
3	715.0	12047.0	12 x 288	93360834	594440	Yes
2	715.0	12762.0	12 x 288	93369834	607440	Yes
1	715.0	13477.0	12 x 288	93360834	626480	Yes







TABLE 5-10  
NATURAL PERIODS OF FRAMES

	Fundamental or 1st Mode	2nd Mode	3rd Mode	Minimum
TR2.17	2.508	0.524	0.196	0.004
TR1.33	3.221	0.672	0.251	0.004
TR0.67	4.605	0.957	0.358	0.011
PR0.67	4.591	0.920	0.328	0.005
TI0.67	5.351	1.485	0.540	0.010
PI0.67 (12)	5.340	1.433	0.510	0.017
PI0.67 (6)	5.302	1.021	0.372	0.007



TABLE 5-11

## MODAL ANALYSIS

STRUCTURE	MODAL ANALYSIS		COMPUTER PROGRAM
	Maximum Moment (KIP-INCHES)	Tip Deflection (INCHES)	Tip Deflection (INCHES)
TR2.17	904339.3	16.46	17.07
TR1.33	882911.0	20.96	22.71
TR0.67	955408.5	19.47	18.64
PR0.67	959053.9	19.47	17.16
TI0.67	607633.7	19.04	17.31
PI0.67 (6)	608128.0	19.22	15.47
PI0.67 (12)	607663.4	19.10	16.48



TABLE 5-12  
 MAXIMUM RESPONSES OF FRAME  
 TR2.17

Story	Displacement to Ground (IN)	Relative Displacement (IN)	Time of Occurrence (SEC)
20	17.07	1.07	4.773
19	16.03	1.07	4.773
18	15.01	1.08	4.772
17	14.00	1.08	4.772
16	13.01	1.09	4.772
15	12.02	1.09	4.771
14	11.04	1.08	4.770
13	10.04	1.07	4.766
12	9.04	1.05	4.754
11	8.03	1.03	4.674
10	7.02	1.02	4.654
9	6.02	1.00	4.640
8	5.03	0.96	4.629
7	4.07	0.91	4.618
6	3.17	0.84	4.608
5	2.33	0.75	4.600
4	1.58	0.69	4.591
3	0.95	0.59	4.583
2	0.45	0.32	4.573
1	0.12	0.12	4.563



TABLE 5-13  
MAXIMUM RESPONSES OF FRAME  
TR1.33

Story	Displacement to Ground(IN)	Relative Displacement (IN)	Time of Occurrence (SEC)
20	22.71	1.45	4.956
19	21.45	1.45	4.956
18	20.23	1.45	4.956
17	19.01	1.45	4.955
16	17.78	1.45	4.953
15	16.54	1.44	4.946
14	15.27	1.42	4.923
13	13.96	1.39	5.016
12	12.63	1.38	5.030
11	11.27	1.38	5.212
10	9.89	1.39	5.205
9	8.52	1.37	5.199
8	7.15	1.34	5.193
7	5.82	1.28	5.185
6	4.55	1.19	5.172
5	3.36	1.08	5.163
4	2.29	0.92	5.159
3	1.37	0.72	5.157
2	0.65	0.47	5.153
1	0.17	0.17	5.149





TABLE 5-14  
MAXIMUM RESPONSES OF FRAME  
TR0.67

Story	Displacement to Ground (IN)	Relative Displacement (IN)	Time of Occurrence (SEC)
20	18.64	1.36	4.377
19	17.42	1.36	4.378
18	16.29	1.36	4.377
17	15.26	1.36	4.376
16	14.33	1.35	4.372
15	13.42	1.33	4.367
14	12.50	1.29	4.357
13	11.57	1.24	4.307
12	10.60	1.20	4.261
11	9.59	1.16	4.226
10	8.55	1.14	4.172
9	7.46	1.12	4.135
8	6.36	1.12	4.044
7	5.26	1.10	4.034
6	4.16	1.05	4.025
5	3.12	0.97	4.010
4	2.16	0.85	3.984
3	1.32	0.68	3.966
2	0.63	0.46	3.961
1	0.17	0.17	3.960



TABLE 5-15

## MAXIMUM RESPONSES OF FRAME

PR0.67

Story	Displacement To Ground (IN)	Relative Displacement (IN)	Time of Occurrence (SEC)
20	17.16	1.19	4.330
19	16.14	1.19	4.331
18	15.15	1.19	4.330
17	14.20	1.19	4.330
16	13.27	1.19	4.327
15	12.36	1.18	4.320
14	11.44	1.15	4.285
13	10.52	1.13	4.252
12	9.58	1.11	4.234
11	8.64	1.08	4.217
10	7.68	1.05	4.181
9	6.69	1.02	4.147
8	5.68	1.02	4.005
7	4.67	0.99	3.998
6	3.68	0.95	3.992
5	2.75	0.86	3.981
4	1.89	0.75	3.954
3	1.15	0.59	3.934
2	0.55	0.40	3.925
1	0.15	0.15	3.919



TABLE 5-16  
MAXIMUM RESPONSES OF FRAME  
TI0.67

Story	Displacement To Ground (IN)	Relative Displacement (IN)	Time of Occurrence (SEC)
20	17.321	1.13	2.322
19	16.26	1.13	2.323
18	15.25	1.13	2.322
17	14.44	1.13	2.321
16	13.69	1.12	2.318
15	12.92	1.10	2.313
14	12.13	1.08	2.297
13	11.28	1.05	2.276
12	10.37	1.19	2.604
11	9.19	1.48	2.582
10	7.82	1.58	2.569
9	6.76	1.53	2.557
8	5.87	1.36	2.540
7	5.03	1.13	2.500
6	4.17	1.01	1.922
5	3.29	0.95	2.392
4	2.39	0.88	2.359
3	1.53	0.75	2.333
2	0.78	0.55	2.320
1	0.22	0.22	2.308





TABLE 5-17  
MAXIMUM RESPONSES OF FRAME  
PI0.67(12)

Story	Displacement To Ground (IN)	Relative Displacement (IN)	Time of Occurrence (SEC)
20	16.48	1.03	2.306
19	15.58	1.04	2.306
18	14.74	1.04	2.305
17	13.93	1.03	2.303
16	13.15	1.03	2.300
15	12.39	1.02	2.294
14	11.62	1.00	2.286
13	10.85	0.99	2.789
12	10.05	1.07	2.603
11	9.02	1.33	2.568
10	7.87	1.46	2.555
9	6.81	1.46	2.545
8	5.89	1.35	2.534
7	5.03	1.16	2.512
6	4.15	1.01	1.913
5	3.25	0.95	2.378
4	2.36	0.88	2.352
3	1.51	0.75	2.322
2	0.77	0.55	2.299
1	0.23	0.23	2.284



TABLE 5-18  
MAXIMUM RESPONSES OF FRAME  
PI0.67 (6)

Story	Displacement to Ground (IN)	Relative Displacement (IN)	Time of Occurrence (SEC)
20	15.47	1.00	2.224
19	14.62	1.00	2.223
18	13.78	1.00	2.220
17	12.97	1.00	2.214
16	12.29	1.00	2.207
15	11.63	0.99	2.198
14	10.94	0.98	2.190
13	10.23	0.96	4.436
12	9.48	0.94	4.429
11	8.68	0.92	4.422
10	7.81	0.94	2.492
9	6.88	0.99	2.480
8	5.90	1.04	2.472
7	4.89	1.05	2.466
6	4.02	1.05	2.544
5	3.12	0.96	2.438
4	2.24	0.84	2.627
3	1.40	0.71	2.617
2	0.69	0.49	2.604
1	0.19	0.19	2.588



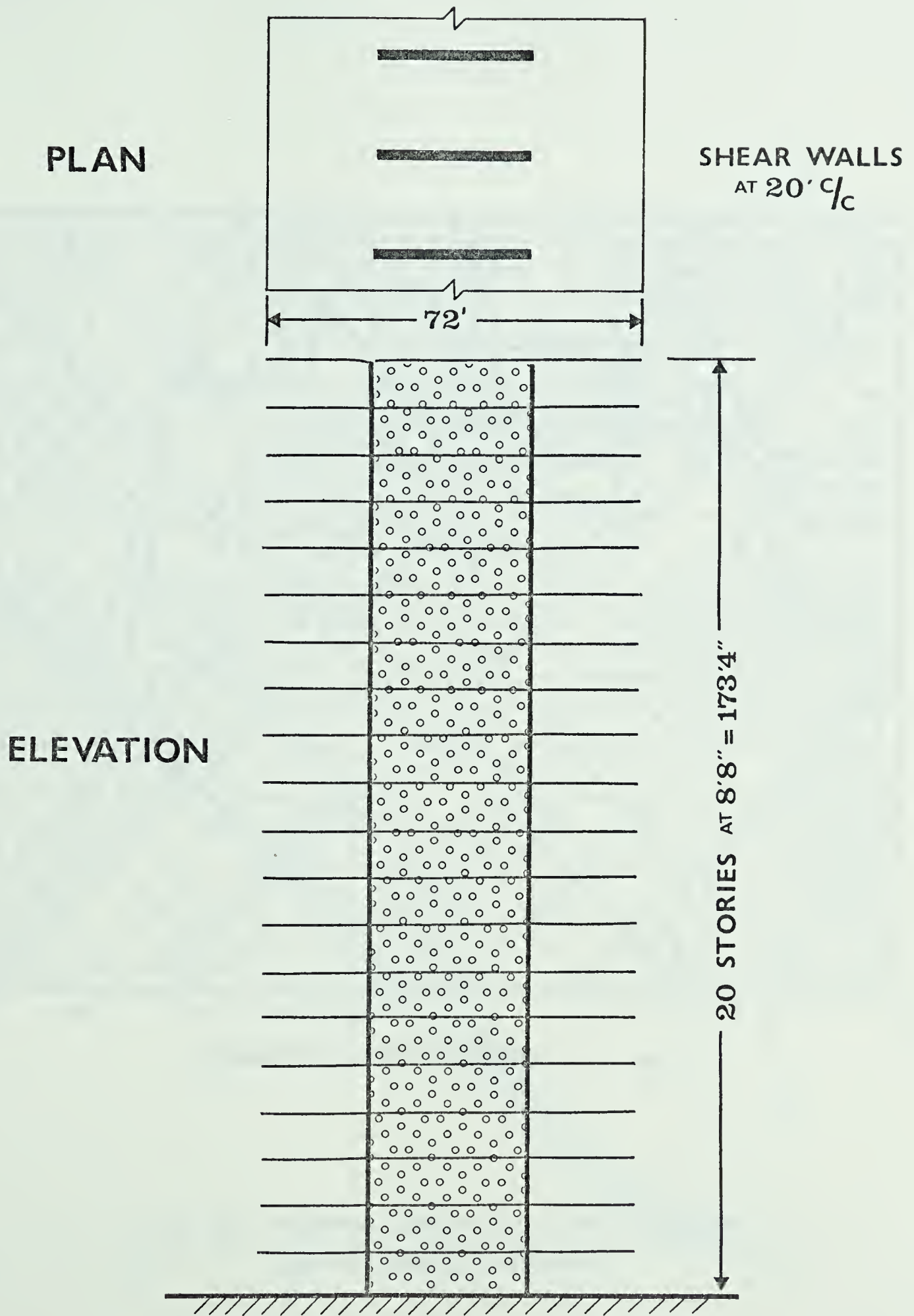


FIG. 5-1 Shear Wall Frame





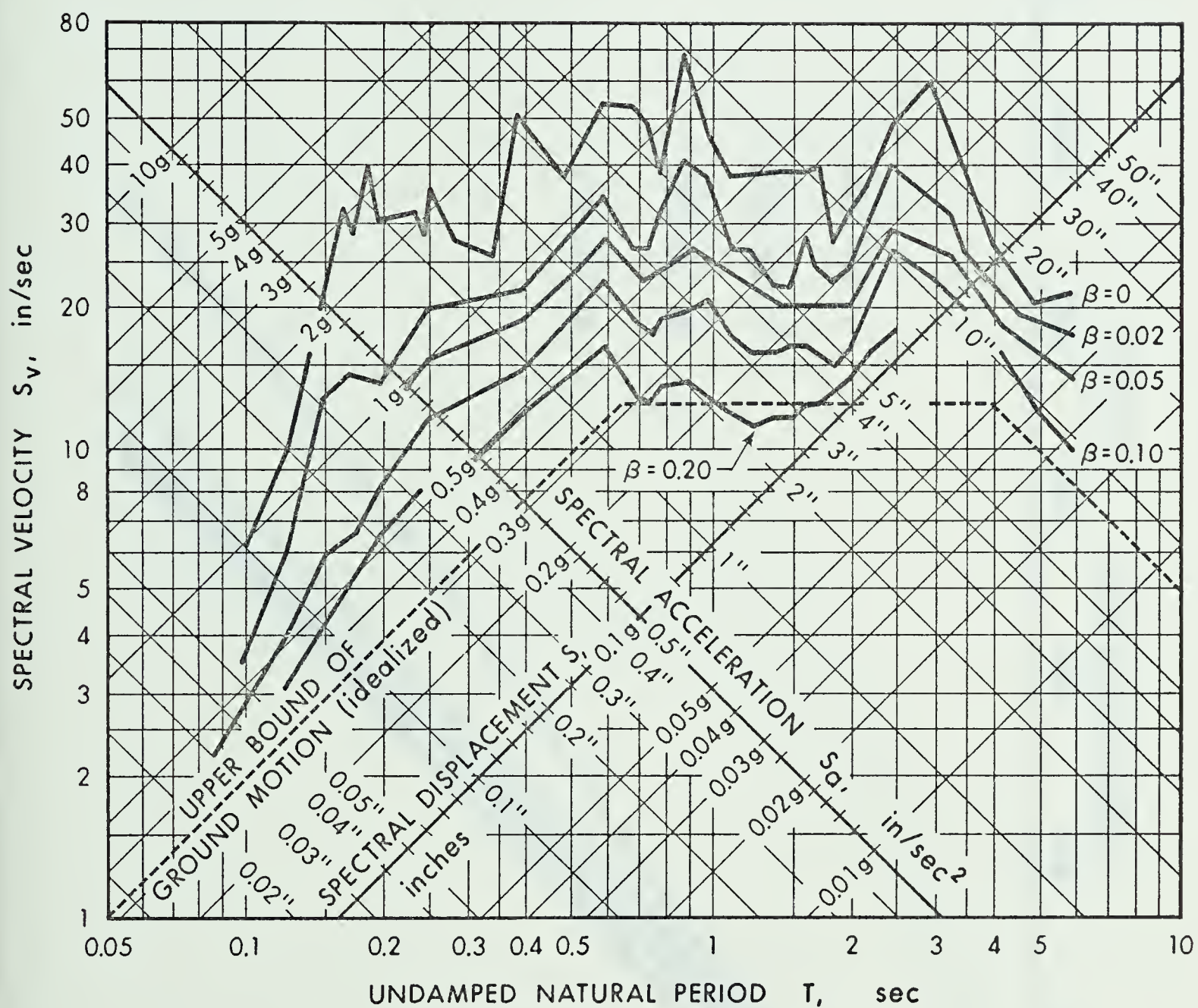


FIG. 5-2 Response Spectra for Elastic Systems,  
1940 El Centro Earthquake





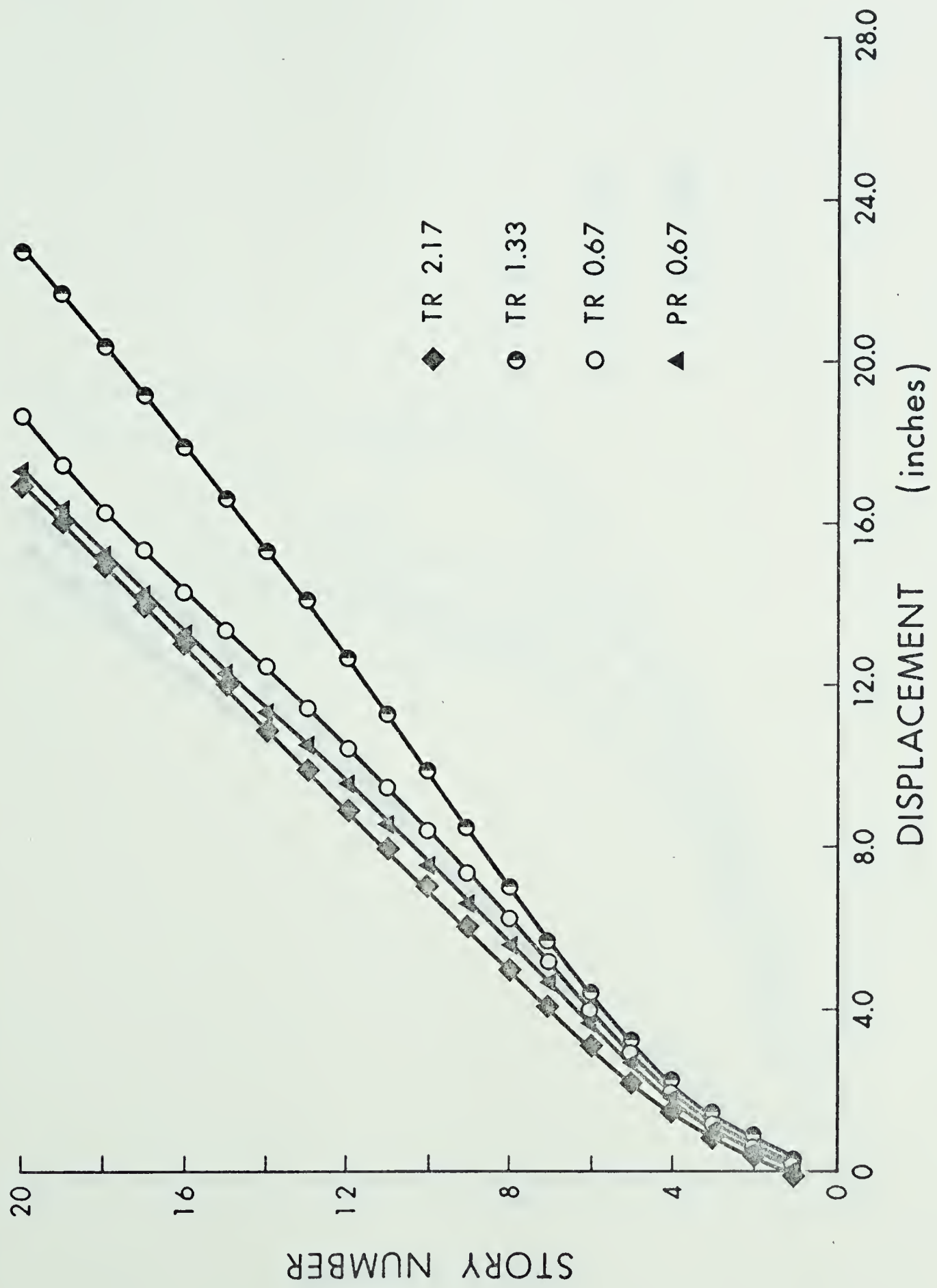


FIG. 5-3 MAXIMUM DISPLACEMENTS



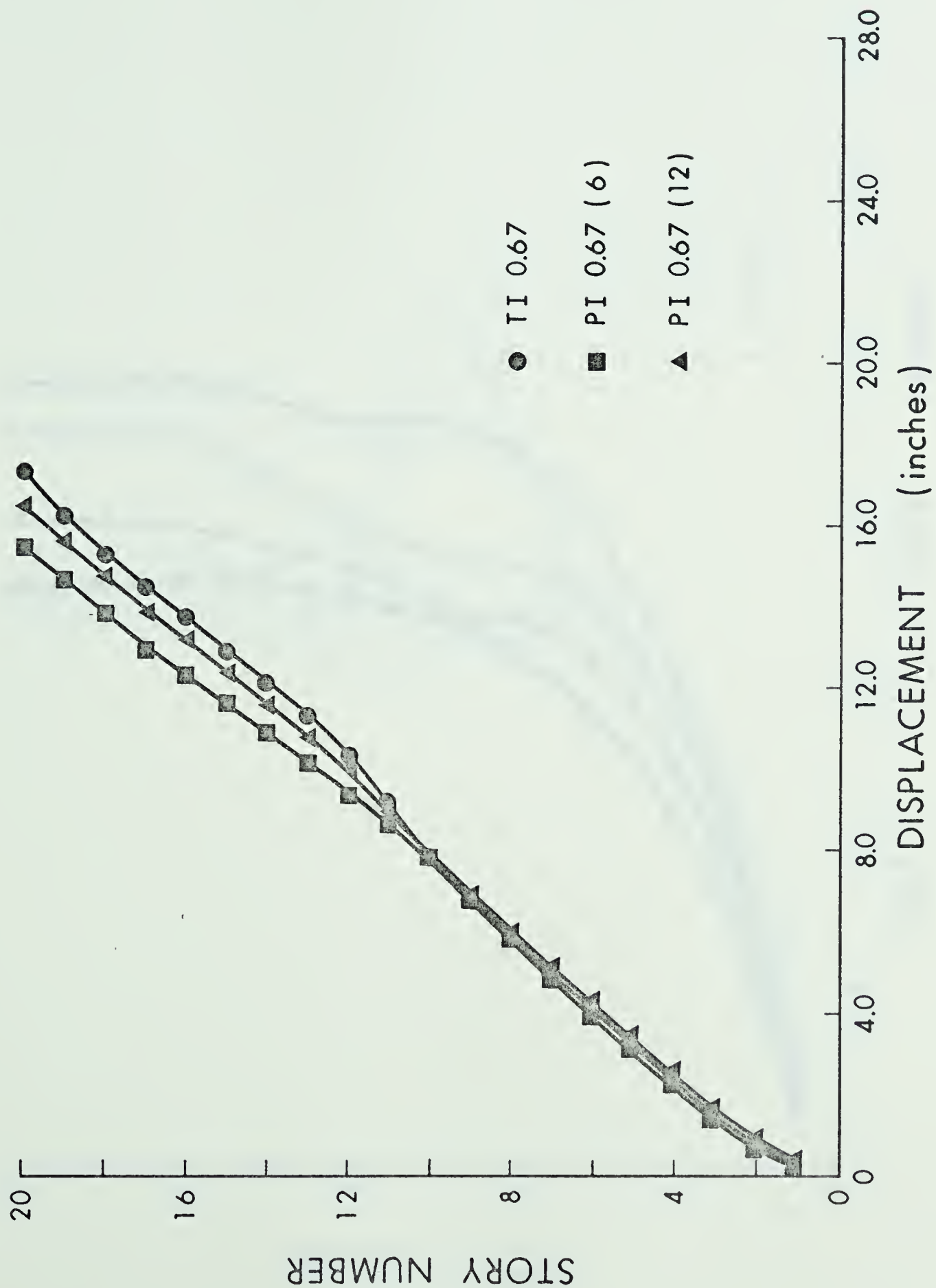


FIG. 5-4 MAXIMUM DISPLACEMENTS



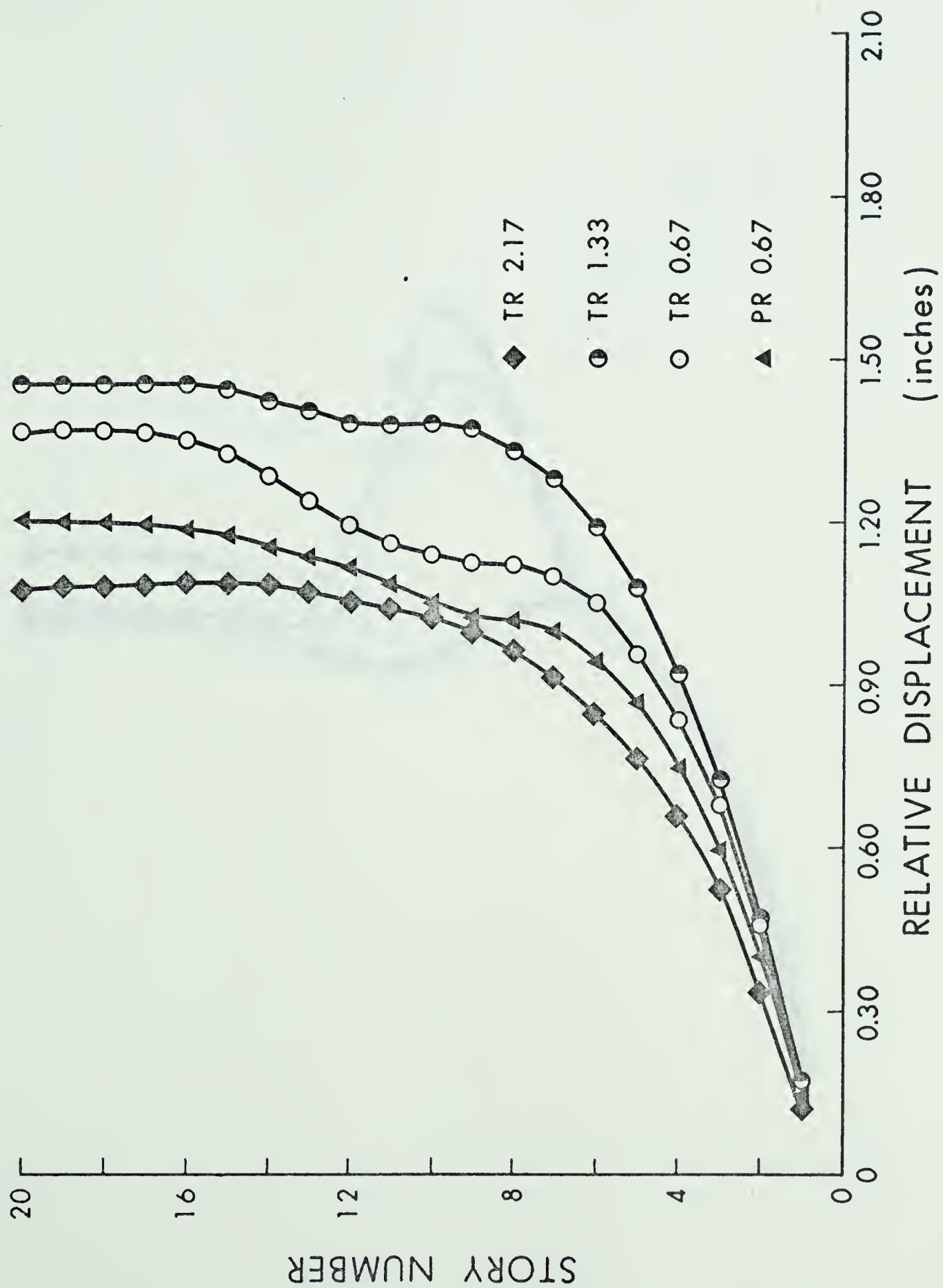


FIG. 5-5 MAXIMUM INTERFLOOR DISPLACEMENTS





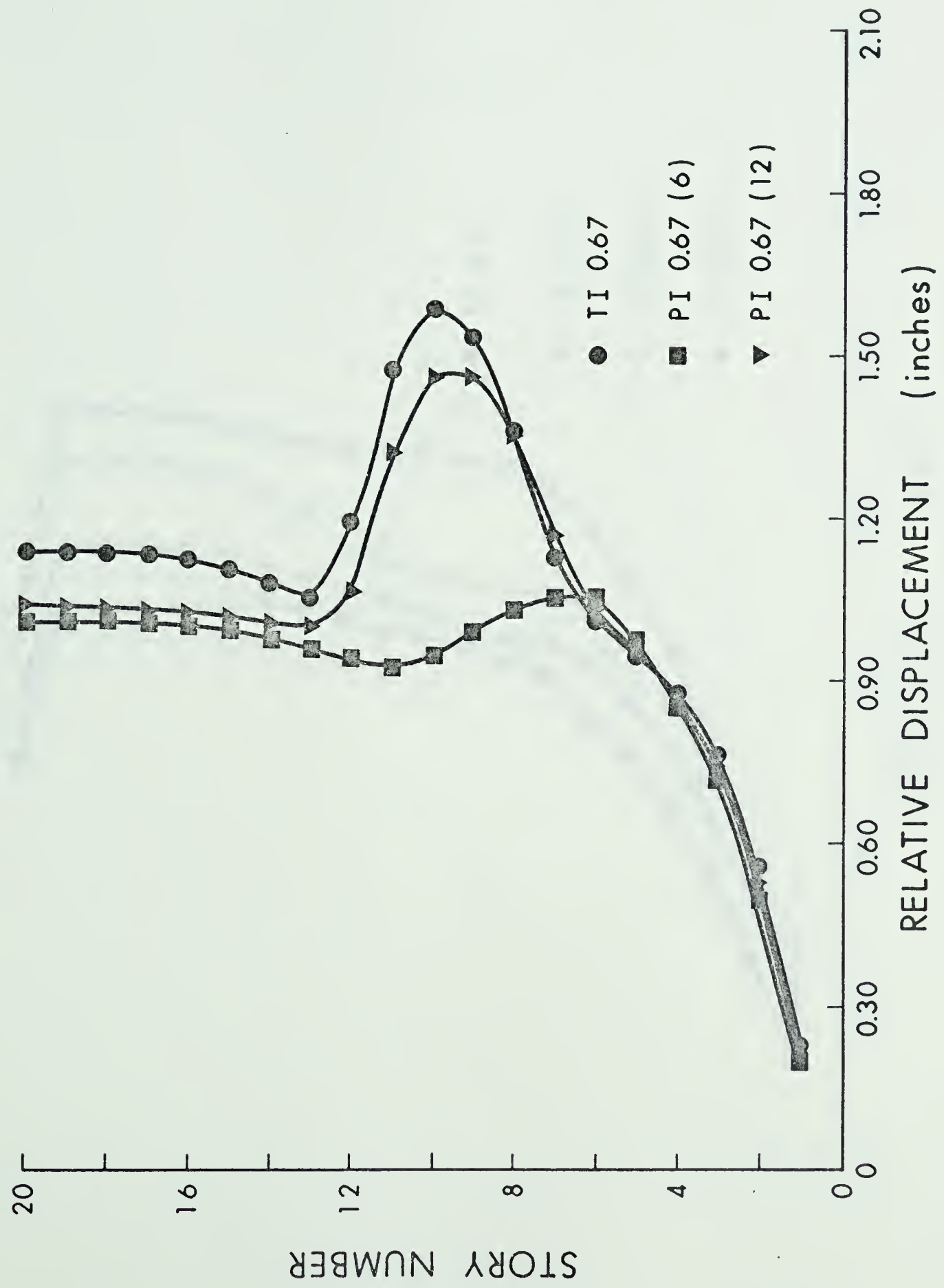


FIG. 5-6 MAXIMUM INTERFLOOR DISPLACEMENTS



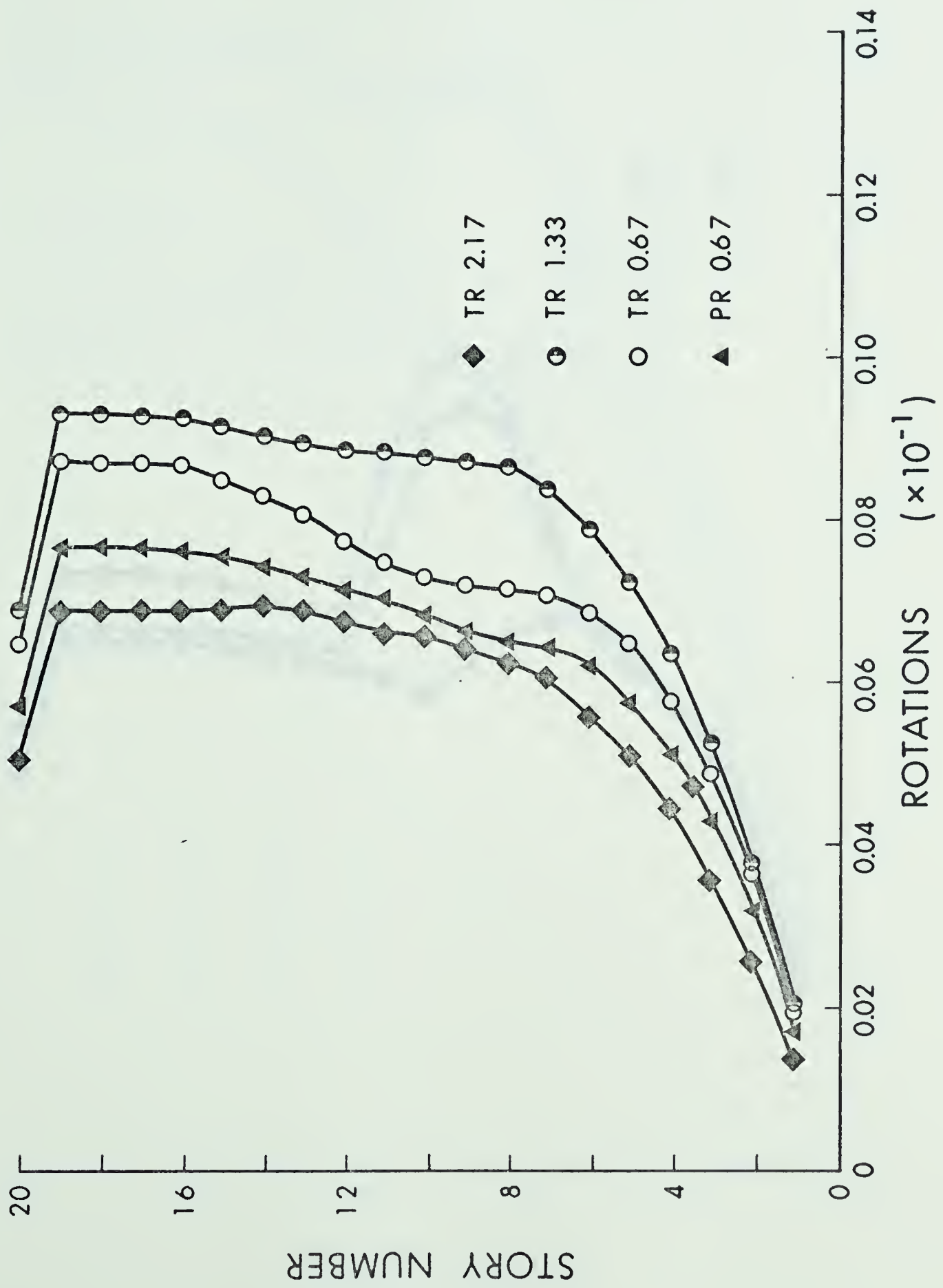


FIG. 5-7 MAXIMUM COLUMN ROTATIONS



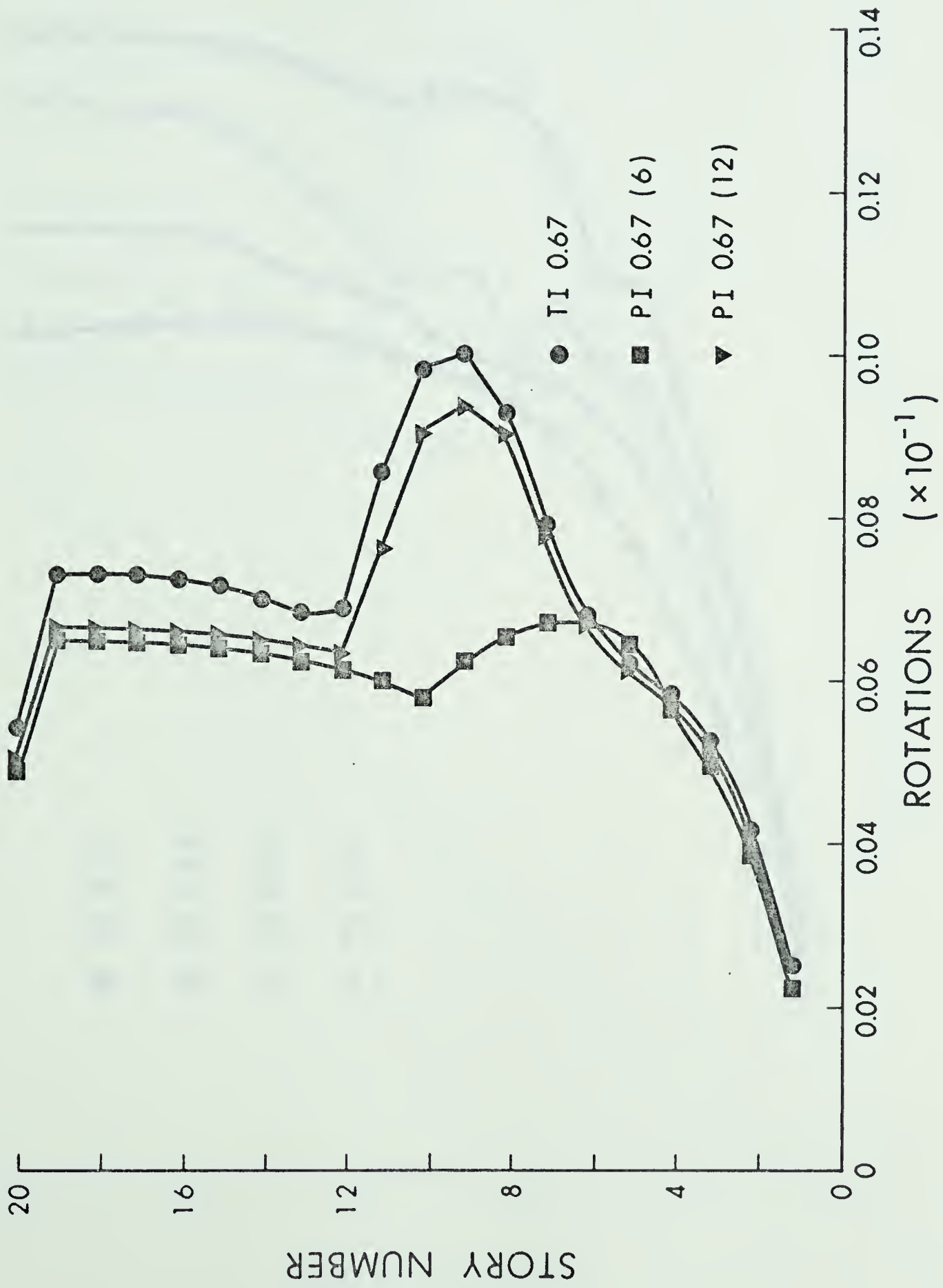


FIG. 5-8 MAXIMUM COLUMN ROTATIONS



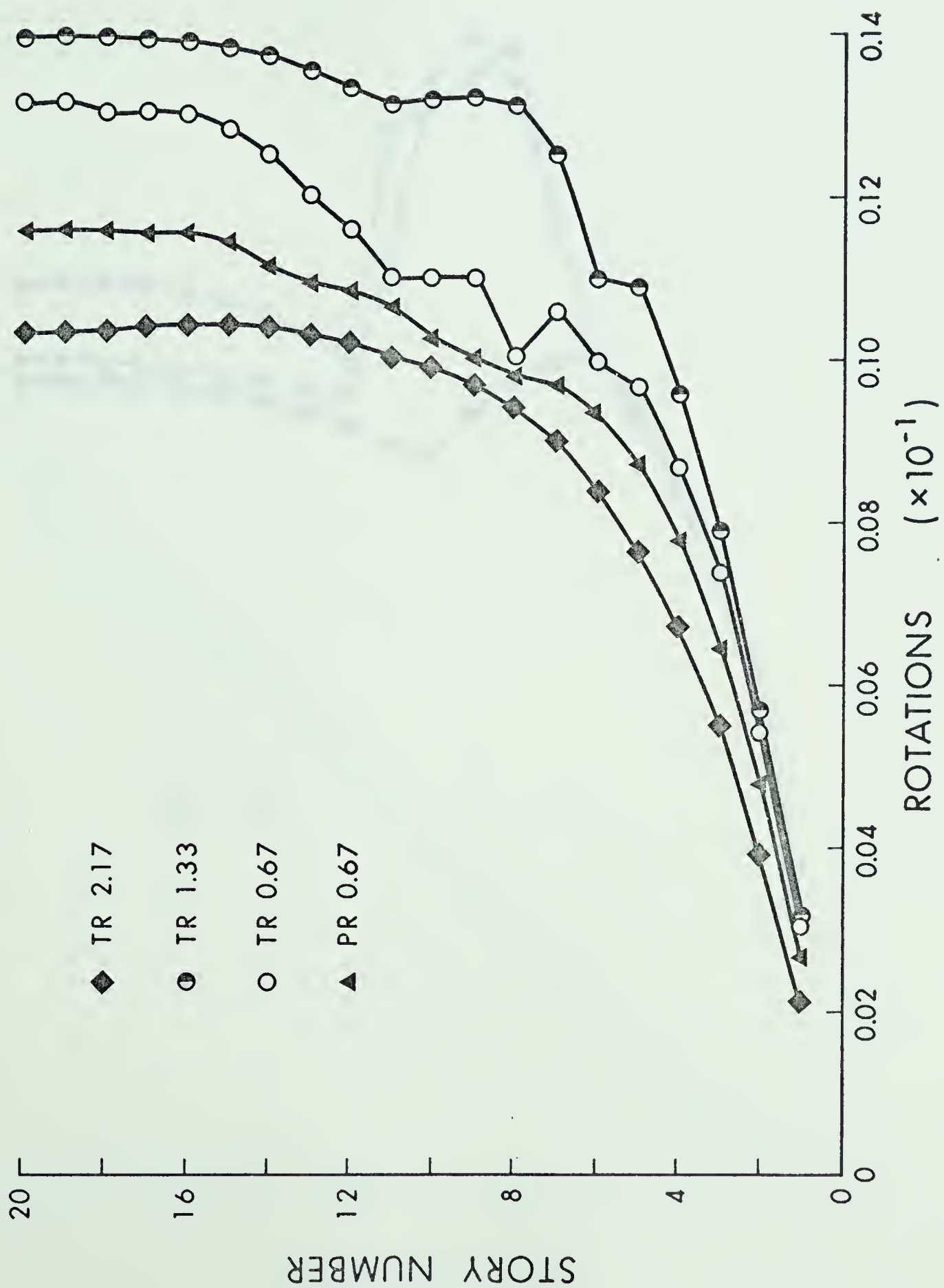


FIG. 5-9 MAXIMUM SHEAR WALL ROTATIONS





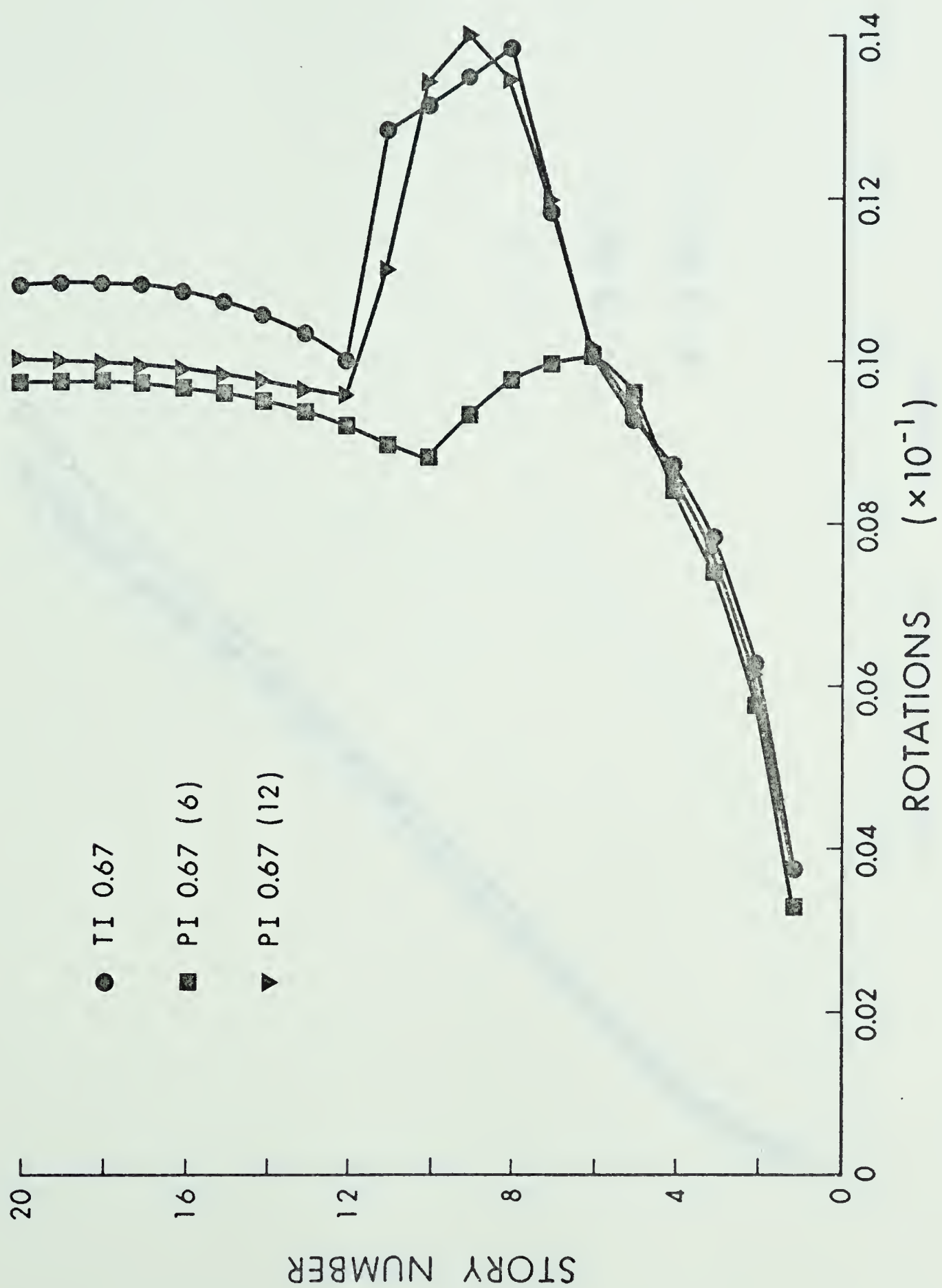


FIG. 5-10 MAXIMUM SHEAR WALL ROTATIONS



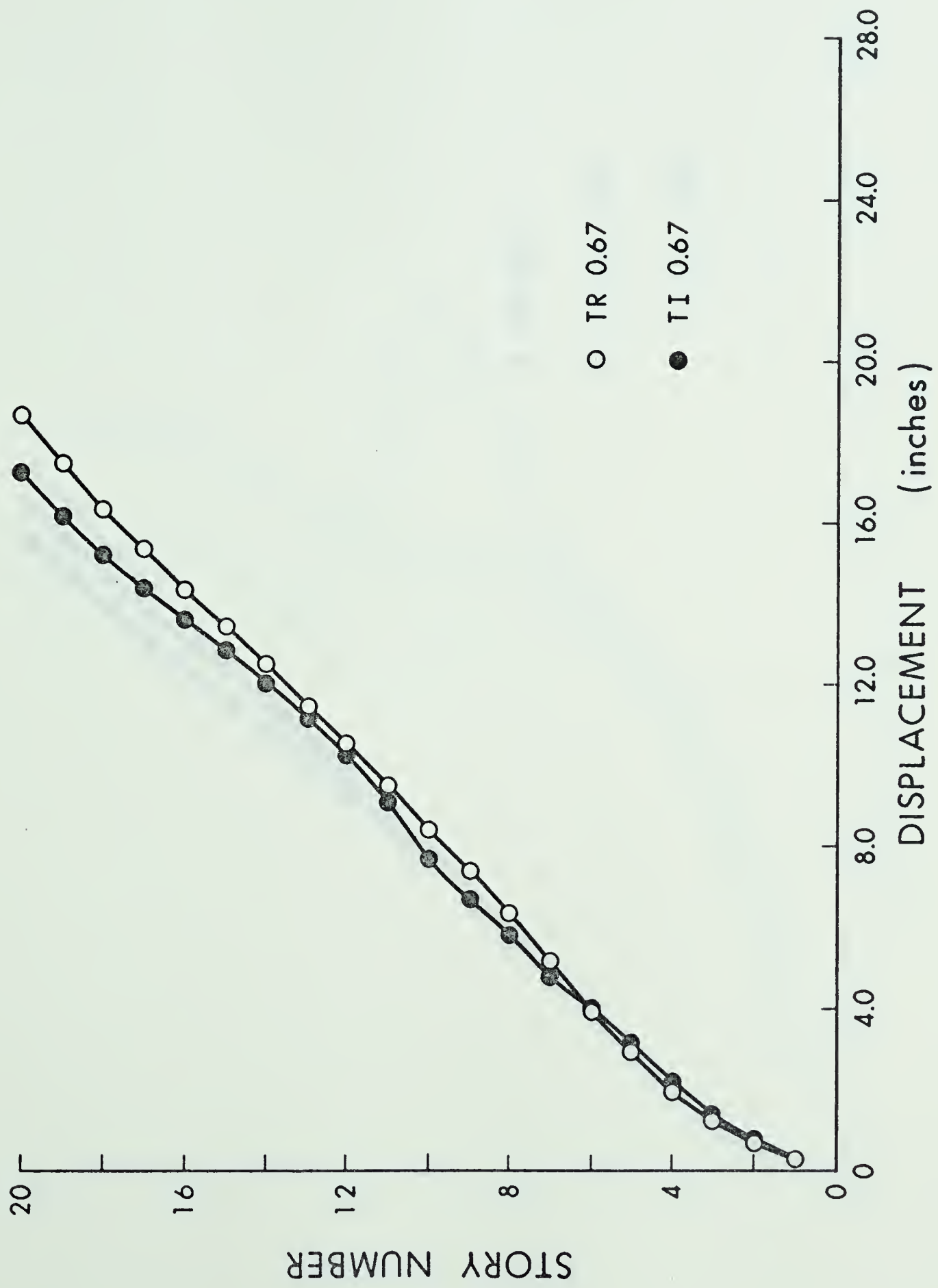


FIG. 5-11 MAXIMUM DISPLACEMENTS



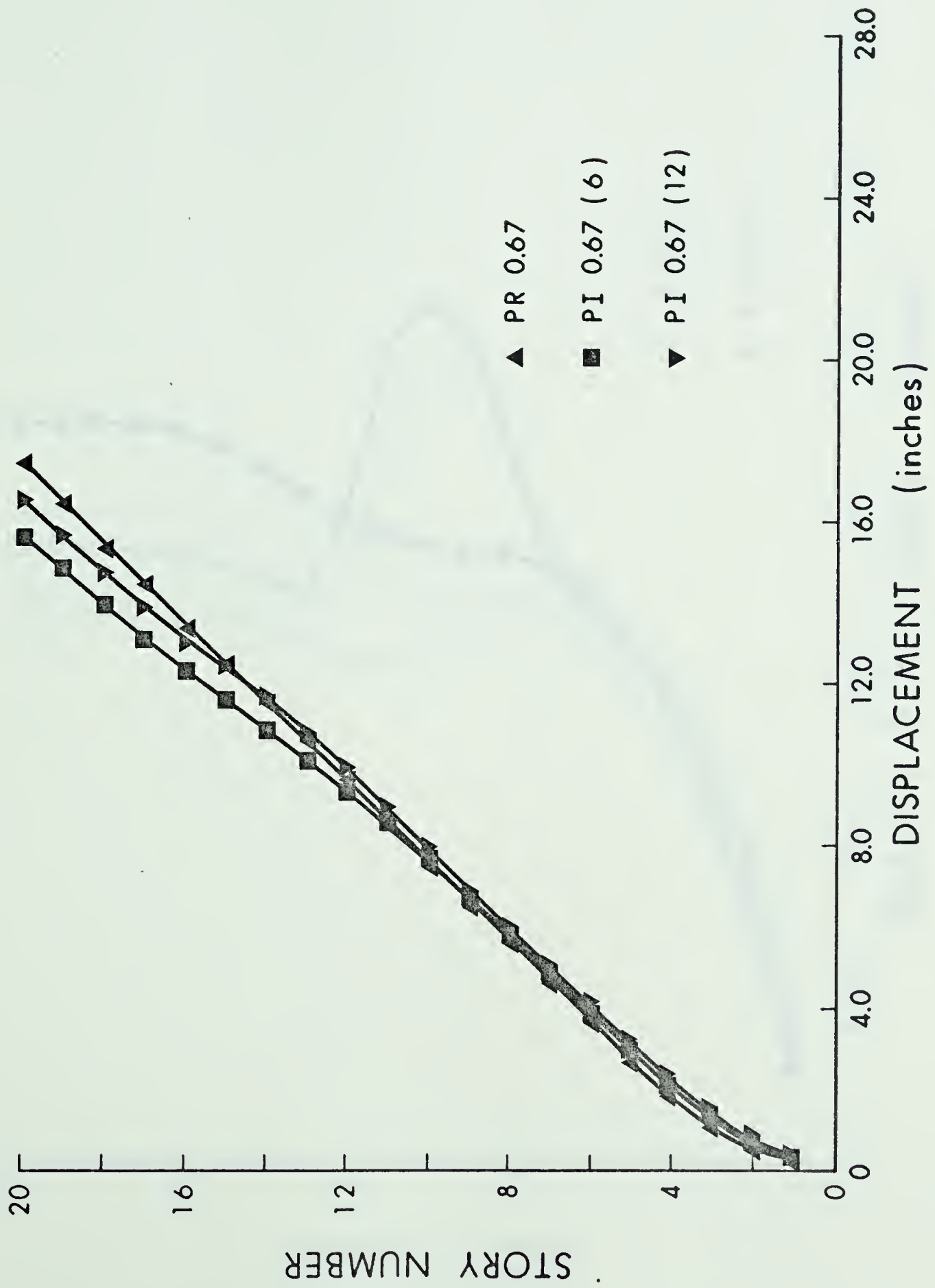


FIG. 5-12 MAXIMUM DISPLACEMENTS





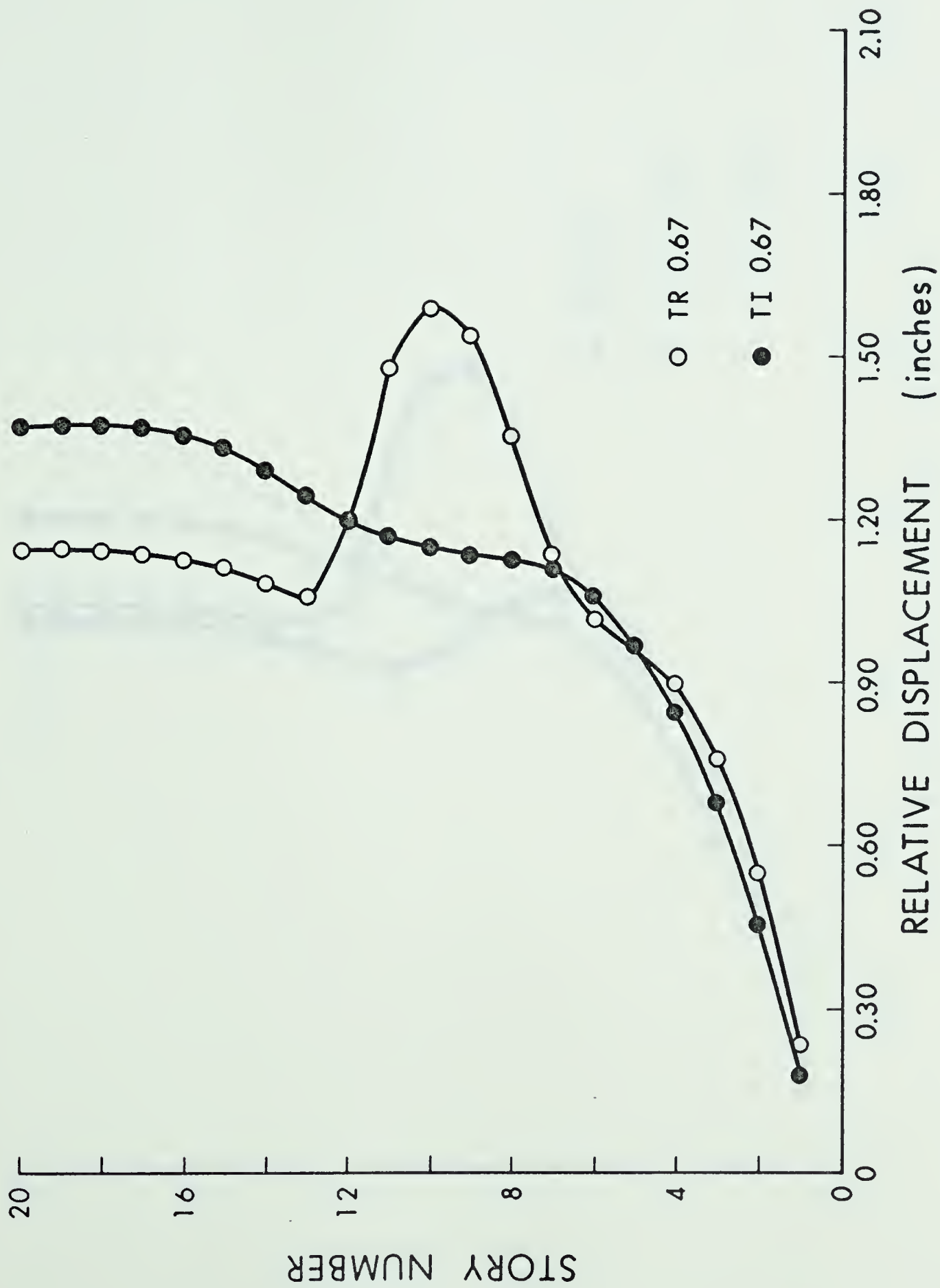


FIG. 5-13 MAXIMUM INTERFLOOR DISPLACEMENTS



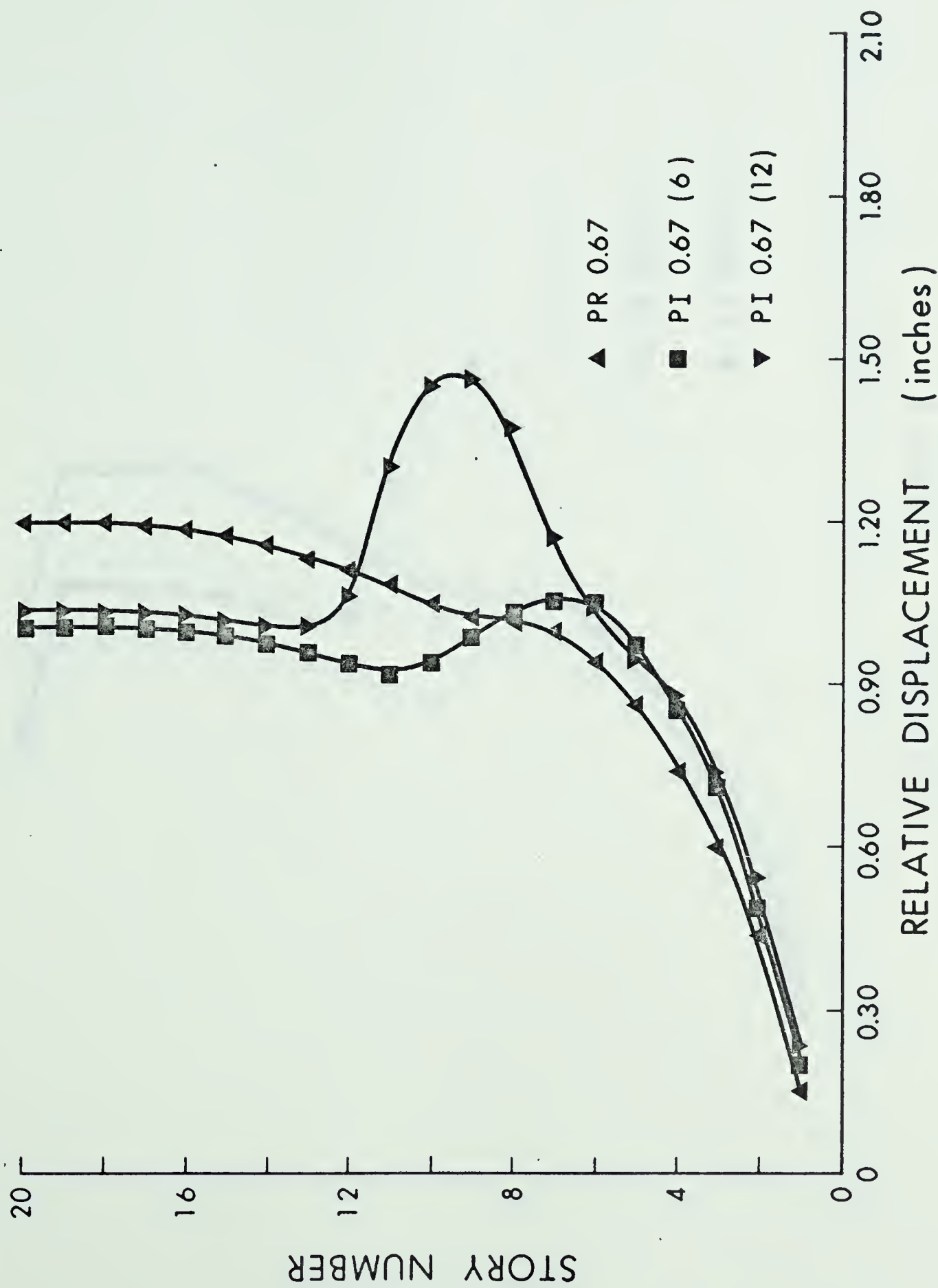


FIG. 5-14 MAXIMUM INTERFLOOR DISPLACEMENTS



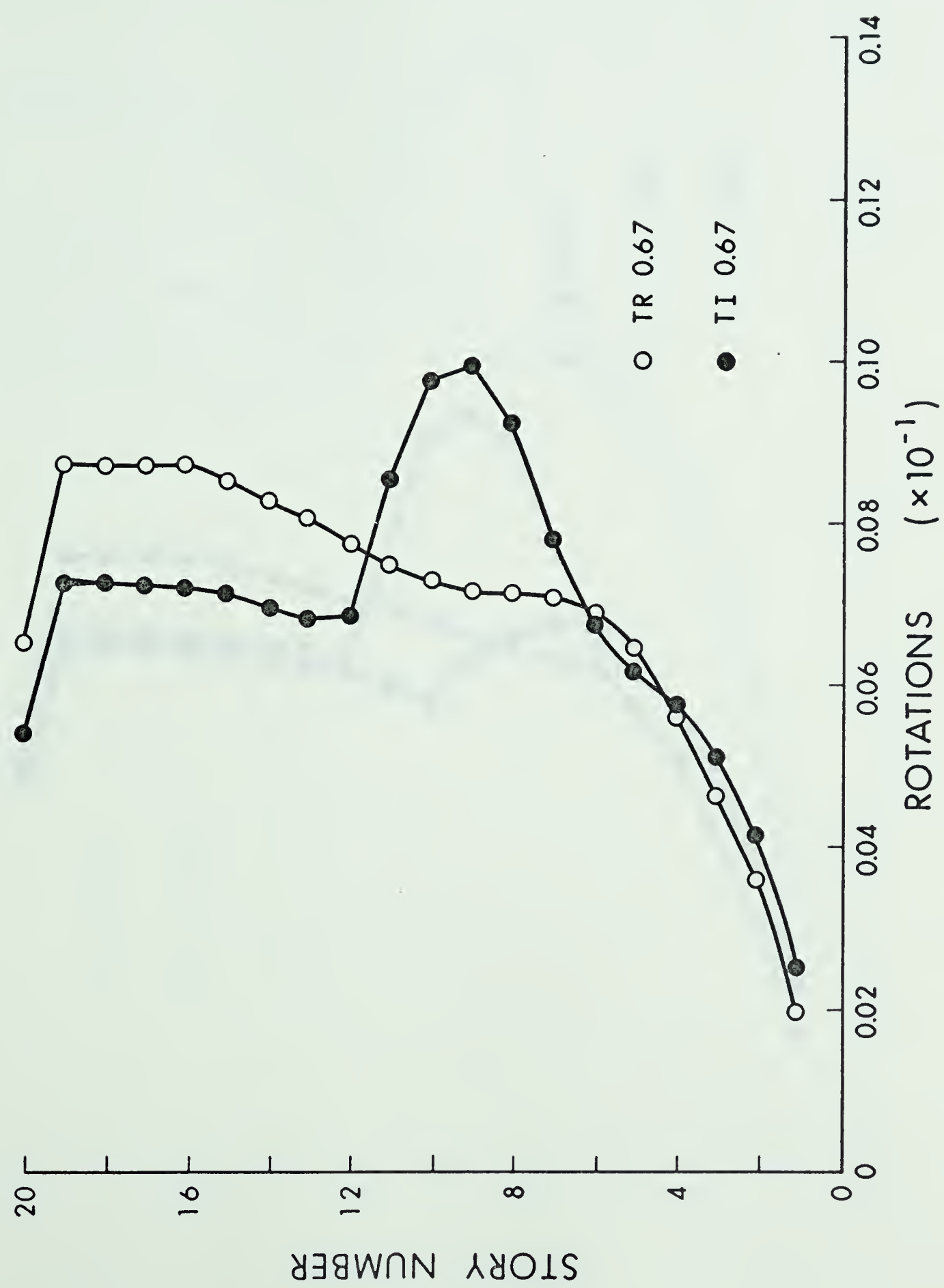


FIG. 5-15 MAXIMUM COLUMN ROTATIONS



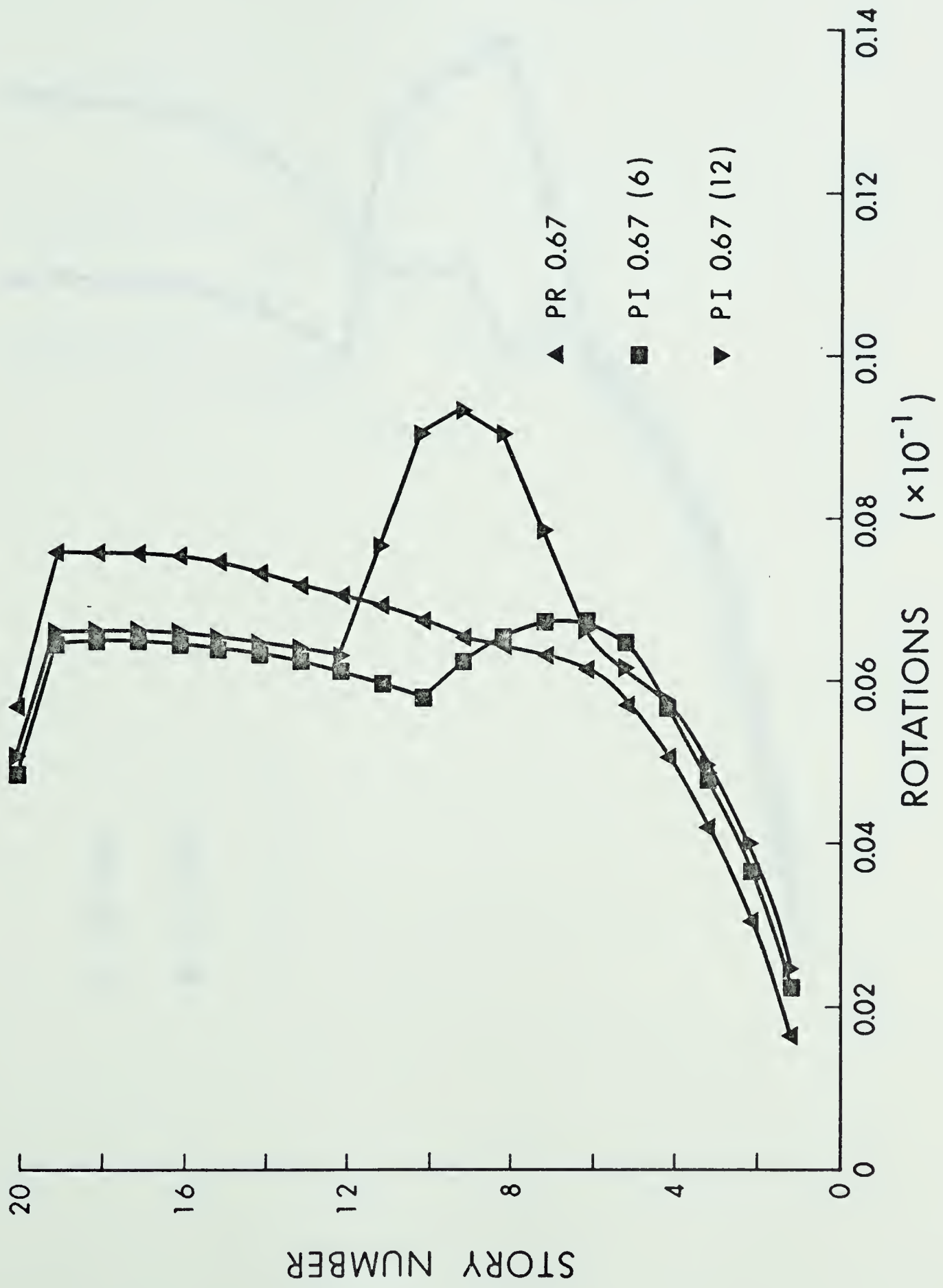


FIG. 5-16 MAXIMUM COLUMN ROTATIONS





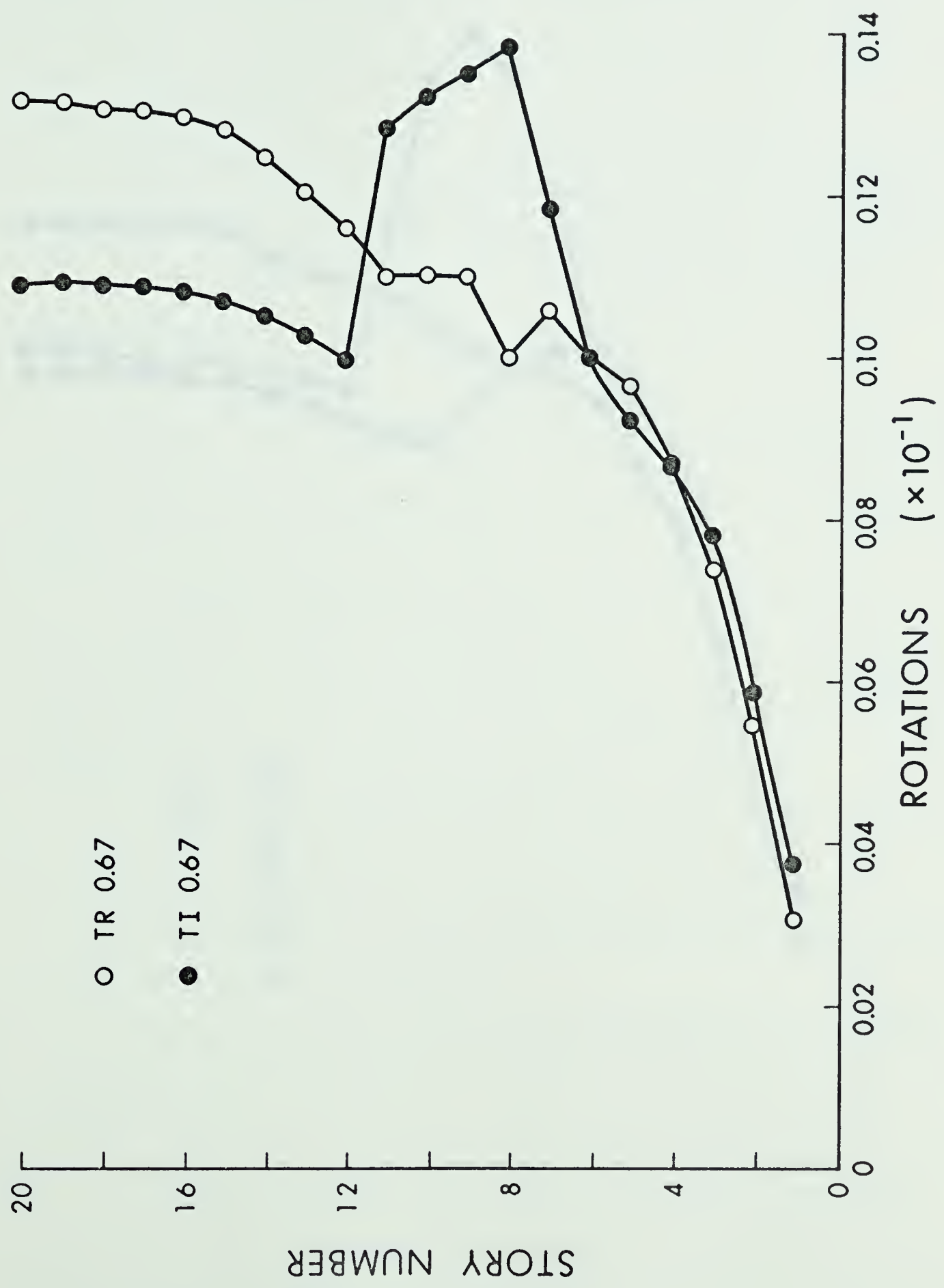


FIG. 5-17 MAXIMUM SHEAR WALL ROTATIONS



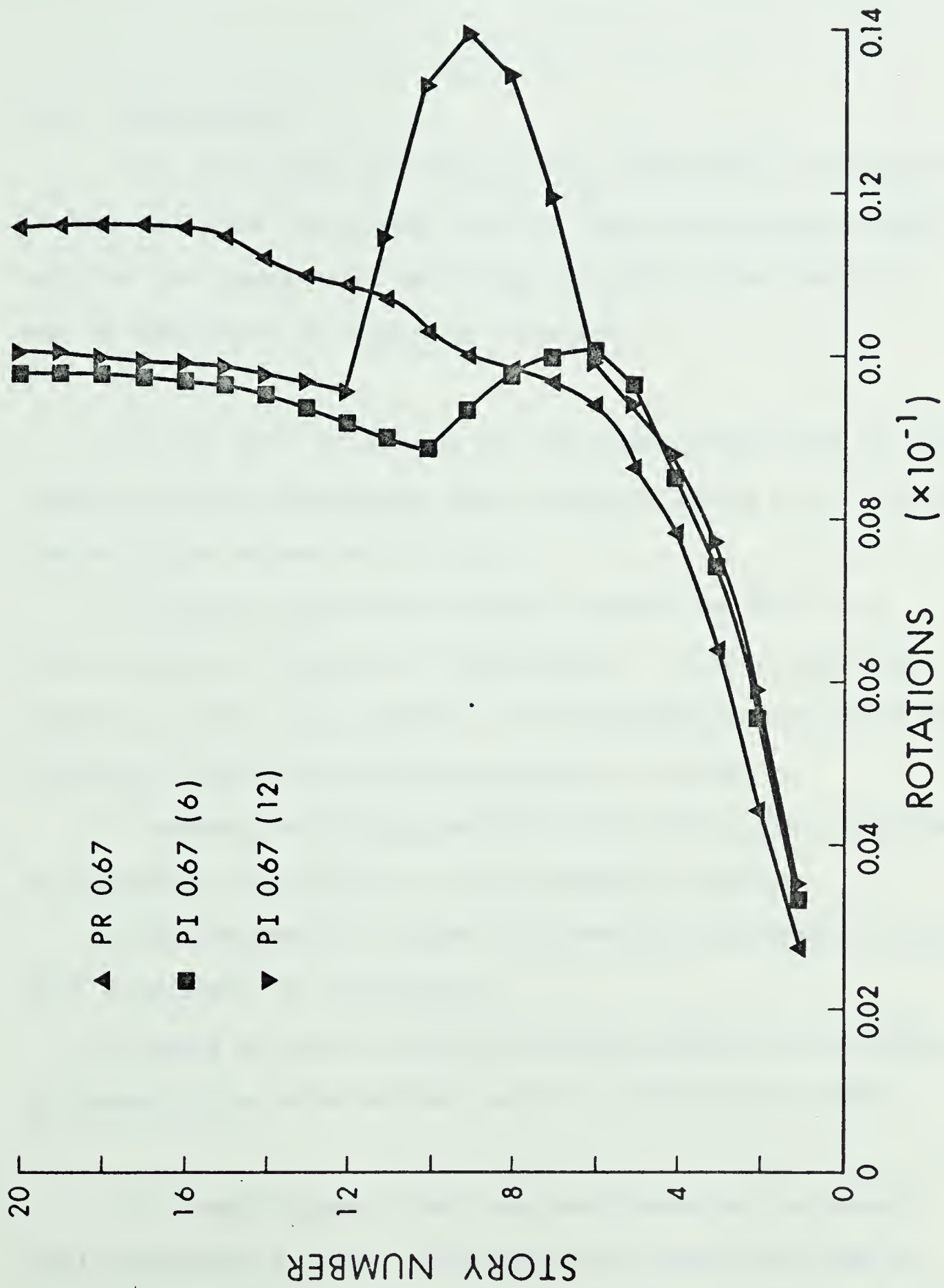


FIG. 5-18 MAXIMUM SHEAR WALL ROTATIONS



## Chapter 6

### CONCLUSIONS AND RECOMMENDATIONS

#### 6-1 Conclusions

The following conclusions are based on the results of the analyses performed herein. These conclusions apply only to the shear wall buildings of this investigation and to the range of behavior observed.

1. Shear wall buildings of the type considered in this thesis perform adequately when designed using a horizontal force factor value of  $K = 0.67$ .

2. Response spectrum analysis should be used as a first check on forces and deflections. If the structure remains elastic, the values of the response quantities predicted by spectrum analysis are quite accurate.

3. Tapered buildings perform adequately. The response of prismatic buildings is only minimally better.

4. The presence of shear deformations increases structural responses to earthquake.

5. Zones of great stiffness change should be avoided if possible as deformations tend to concentrate there.

It would appear that the good behavior of shear wall buildings in past earthquakes has resulted from a combination of over design and low force levels associated





with the long fundamental periods of these structures.

## 6-2 Recommendations for Future Research

1. The ratio of moment to shear upon a member may change as an earthquake progresses and the various modes interact. It is therefore recommended that an earthquake analysis procedure should be developed wherein the moment and shear and their respective deformations are kept separate. In this manner members would be allowed to change shear stiffness when their shear level exceeds their cracking shear and the combination of shear and flexural deformations would be in accord with the member's present moment to shear ratio.

2. Research should be performed to verify and predict the shear-shear deformation relationship of a member under repeated reversed cyclic loadings.

3. Response spectrum analysis is a valuable tool in earthquake engineering. In this connection more work should be done to develop average response spectra to be used in design. Results should be furnished for more values of critical damping and for larger values of fundamental period.



## REFERENCES

1. Fintel , M., "The Behavior of Reinforced Concrete Structures in the Caracas Earthquake of July 29, 1967", XS6731, Portland Cement Association, 1968, 52 pp.
2. Kunze, W.E., Sbarounis, J.A., and Amrhein, J.E., "The March 27, 1964, Alaskan Earthquake", XS6510, Portland Cement Association, 1965, 35 pp.
3. "The Behavior of Reinforced Concrete Buildings Subjected to the Chilean Earthquakes of May 1960", Advanced Engineering Bulletin #6, Portland Cement Association, 1963, 32 pp.
4. Fintel, M., "Quake Lesson from Managua: Revise Concrete Building Design?", Civil Engineering -ASCE. August, 1973, pp. 60-63.
5. Fintel, M., "Resistance to Earthquakes - Philosophy, Ductility and Details" Response of Multistory Concrete Structures to Lateral Forces, Publication SP-36, American Concrete Institute, 1973, pp 75-96.
6. Clough, R.W., and Benuska, K.L., "Non-Linear Earthquake Behavior of Tall Buildings". Paper 5292, ASCE Proceedings, Journal of the Engineering Mechanics Division, June, 1967.
7. Steinbrugge, K.V., "Earthquake Damage and Structural Performance in the United States", Earthquake Engineering, Prentice-Hall, Inc., Englewood Cliffs, N.J., 1970, pp 167-226.
8. Seismology Committee, "Recommended Lateral Force Requirements and Commentary" Structural Engineers Association of California, 1973.
9. "Uniform Building Code", 1970 Edition, published by the International Conference of Building Officials, California.
10. "National Building Code of Canada, 1970, Section 4.1, Structural Loads and Procedures", Associate Committee on the National Building Code, National Research Council of Canada, Ottawa, Canada.
11. ACI Committee 318, "Building Code Requirements for Reinforced Concrete (ACI 318-71)", American Concrete Institute, Detroit, 1971.





12. Popov, E.P., Bertero, V.V., and Krawinkler, H., "Cyclic Behavior of Three R.C. Flexural Members with High Shear", Report No. EERC 72-5, Earthquake Engineering Research Center, College of Engineering, University of California, Berkeley, California, October, 1972.
13. Burns, N.H., and Siess, C.P., "Repeated and Reversed Loading in Reinforced Concrete" Journal of the Structural Division, ASCE, Vol. 92, No ST 5, Proc. Paper 4931, October, 1966, pp. 45-64.
14. Burns, N.H., and Siess, C.P., "Plastic Hinging in Reinforced Concrete", Journal of the Structural Division, ASCE, Vol. 92, No. ST 5, Proc. Paper 4932, October, 1966, pp. 65-78.
15. Park, R.K., Kent, D.C., and Sampson, R.A., "Reinforced Concrete Members with Cyclic Loading" Journal of the Structural Division, ASCE, Vol. 98, No. St 7, Proc. Paper. 9011, July, 1972, pp. 1341-1360.
16. Brown, R.H., and Jirsa, J.O., "Reinforced Concrete Beams under Load Reversals". Structural Research at Rice Report No. 7, Department of Civil Engineering, Rice University, Houston, Texas, October, 1970.
17. Fenwick, R.C., and Paulay T., "Mechanism of Shear Resistance of Concrete Beams", Journal of the Structural Division, ASCE, Vol. 94, No. ST10, October, 1968.
18. Wight, J.K., and Sozen, M.A., "Shear Strength Decay in Reinforced Concrete Columns Subjected to Large Deflection Reversals," Structural Research Series No. 403, UILU-ENG-73-2017, University of Illinois, Urbana, Illinois, August, 1973.
19. Bertero, V.V., "Limit Design for Dynamic Loading", State of the Art Report TC 22-5, Proceedings ASCE - International Association for Bridge and Structural Engineering Conference on Tall Buildings, Volume DS, 1973.
20. Yamada, M., and Furui, S., "Shear Resistance and Explosive Cleavage Failure of Reinforced Concrete Members Subjected to Axial Load, " IABSE Eighth Congress, New York, September, 1968, Contribution to the Discussion of Theme IV, 12 pp.



21. Sinha, B.P., Gerstle, K.H., and Tulin, L.G., "Response of Singly Reinforced Beams to Cyclic Loading" Journal of the American Concrete Institute, August 1964.
22. Aoyama, H., "Moment-Curvature Characteristics of Reinforced Concrete Members Subjected to Axial Load and Reversal of Bending" Proceedings of the International Symposium, Flexural Mechanics of Reinforced Concrete, Miami, Florida, Nov. 10-12, 1964.
23. Agrawal, G.L., Tulin, L.G., and Gerstle, K.H., "Response of Doubly Reinforced Concrete Beams to Cyclic Loading" Journal of the American Concrete Institute, July, 1965.
24. Monnier, T. "The Moment-Curvature Relation of Reinforced Concrete", Institute TNO for Building Materials and Building Structures, Lange Kleiveg 5, Rijswijk (ZH), Delft, The Netherlands, September, 1969.
25. Takeda,, T., Sozen, M.A. and Nielson, N.N, "Reinforced Concrete Response to Simulated Earthquakes", Journal of the Structural Division, ASCE, Vol. 96, No ST12, Proc. Paper 7759, December, 1970, pp 2557-2573.
26. Imbeault, F.A., "Bilinear and Degrading Bilinear Seismic Response of Multistory Frames" Ph. D. thesis, University of Illinois, Urbana, Champaign, 1972.
27. Yamada, M., Kawamura, H., and Katagihara, K., "Reinforced Concrete Shear Walls with Openings: Tests and Analysis" Unpublished.
28. Yamada, M., Kawamura, H., and Katagihara, K., "Reinforced Concrete Shear Walls without Openings: Tests and Analysis" Unpublished.
29. Barda, F., "Shear Strength of Low-Rise Walls with Boundary Elements", Ph. D. Dissertation, Lehigh University, Bethlehem, Pennsylvania, 1972.
30. Zimmerli, B., "Model for Ultimate Strength of Shear Walls", ASCE-IABCE International Conference Preprints: Volume DS, August, 1972.
31. Dilger, W., "Antangliche und nachtragliche Durchbiegung infolge Querkraft bei Stahlbetonbalken in Zustand II, Beton und Stahlbeton bau, 62, Jahrgang, Heft 9, 1967.





32. Giberson, M.F., "The Response of Non-linear Multistory Structures Subjected to Earthquake Excitation", California Institute of Technology, Ph. D., 1967.
33. Husid, R., "Gravity Effects on the Earthquake Response of Yielding Structures", California Institute of Technology, Ph. D., 1967.
34. Otani, S., and Sozen, M.A., "Behavior of Multistory Reinforced Concrete Frames during Earthquakes". Structural Research Series No. 392. UILU-ENG-72-2018, University of Illinois, Urbana, Illinois, November, 1972.
35. Yamashiro, R., and Siess, C.P., "Moment-Rotation Characteristics of Reinforced Concrete Members Subjected to Bending, Shear and Axial Load. Structural Research Series No. 260, University of Illinois, Urbana, Illinois, December, 1962.
36. Karsan, I.D., and Jirsa, J.O., "Behavior of Concrete Under Compressive Loadings" Journal of the Structural Division, ASCE, Vol. 95, ST12, December, 1969. pp 2543-2563.
37. Kent, D.C., and Park, R., "Flexural Members with Confined Concrete" Journal of the Structural Division, ASCE, Vol. 97, No. ST7, Proc. Paper 8243, July, 1971, pp. 1969-1990.
38. Singh, A., Gerstle, L.H., and Tulin, L.G., "The Behavior of Reinforcing Steel Under Reversed Loading", Materials Research and Standards, January, 1965.
39. Fintel, M., and Khan, F.R., "Shock Absorbing Soft Story Concept for Multistory Earthquake Structures," ACI Journal, Proceedings V. 66, No. 5, May, 1969, pp. 381-390.
40. Jennings, P.C., Housner, G.W., and Tsai, N.C., "Simulated Earthquake Motions," Earthquake Engineering Research Laboratory, California Institute of Technology, Pasadena, California, April, 1968.
41. ACI Committee 435, "Allowable Deflections," ACI Journal, Proceedings V. 65, No. 6, June, 1968, pp. 433-444.
42. MacGregor, J.G., "Stress-Strain Curves for Concrete", Unpublished, August, 1966.



43. Nikhed, R.P., MacGregor, J.G., and Adams, P.F., "Studies of Reinforced Concrete Shear Wall-Frame Structures" Structural Engineering Report No. 25, Department of Civil Engineering, The University of Alberta, Edmonton. Canada, June, 1970.
44. Bachmann, H., "Influence of Shear and Bond on Rotational Capacity of Reinforced Concrete Beams," Publications 30-II, 1970, International Association for Bridge and Structural Engineering.
45. Suko, M., and Adams, P.F., "Inelastic Analysis of Multistory Multibay Frames Subjected to Dynamic Disturbances", Structural Engineering Report No. 44, Department of Civil Engineering, University of Alberta, Edmonton, Canada, June 1973.
46. Blume, J.A., Newmark, N.M., and Corning, L.H., "Design of Multistory Reinforced Concrete Buildings for Earthquake Motions", Portland Cement Association, Skokie, Illinois, 1961.
47. O'Leary, A.J., "Shear, Flexure and Axial Tension in Reinforced Concrete Members", University of Canterbury, Christchurch, New Zealand, Ph.D., 1970.



## APPENDIX A

### MOMENT - AXIAL LOAD - CURVATURE PROGRAM

#### A-1 Description of the Program

This program predicts the moment-axial load - curvature relationship of any general cross-section symmetric about its vertical axis. The theoretical background is described in Sec. 3-2.

#### A-2 Input Data

The cross-section is discretized into elements of desired thickness as shown in Fig. A-1. The points describing the extremities of each element are called nodes.

First Card: NNODES, NSTEEL, NELEMS

Input format: (3I5)

NNODES:        Number of nodes

NSTEEL:        Number of steel areas considered

NELEMS:        Number of elements

Second Card: NODE, X(NODE), Y(NODE)

Input format: (I5,2F 10.5)

NODE:            Node number as in Fig. A-1

X(NODE):        x - coordinate of node

Y(NODE):        y - coordinate of node





This card is repeated until all nodes are described.

Third Card: AS (I), YS(I)

Input Format: (2F 10.5)

AS(I): Area of steel (I)

YS(I): Y-coordinate of steel (I)

This card is repeated until all steel areas are described.

Fourth Card: NELEM, N1, N2, N3, N4

Input Format: (5I5)

NELEM: Number of element as shown in Fig. A-1.

N1: Lower left hand node

N2: Upper left hand node

N3: Upper right hand node

N4: Lower right hand node

This card is repeated until all elements and their respective nodes connected are described.

Fifth Card: DEPTH, AXIAL, FSUBC, XNAREA, PHIFAC

Input Format: (5F10.5)

DEPTH: Depth of cross-section

AXIAL LOAD: Axial load on cross-section

FSUBC: Concrete strength at 28 days

XNAREA: Cross-section area

PHIFAC: Multiple of  $1.0 \times 10^{-7}$  to be added to  $\phi$  at each step.



Sixth Card: YMOD, EYIELD, ESH, EULT, FYIELD,  
FULT, YSH

Input Format: (7F10.5)

Steel properties of Fig. A-2

YMOD: Young's modulus (E) of steel  
EYIELD: Strain at yield of steel  
ESH: Strain at start of strain hardening  
EULT: Strain at steel fracture  
FYIELD: Yield stress of steel  
FULT: Ultimate stress of steel  
YSH : Strain hardening modulus

### A-3 Description of Subprograms and Flow Charts

#### (1) Main Program:

Description: Main program calls subroutine XN which reads and calculates the cross-section properties. Main program then reads the last two input cards and calls subroutine STRAIN.

CALLS: XN and STRAIN subroutines.

#### (2) SUBROUTINE XN:

Description: XN reads the cross-sectional properties given on the first four data card series. XN calculates the areas and centroids of the elements and returns to Main.



Called by: Main

(3) SUBROUTINE STRAIN:

Description: STRAIN initiates  $\phi$  and makes an initial guess at the neutral axis position. Strains for each element and steel area are calculated. STRAIN calls subroutine CFORCE to calculate the force in each concrete area and subroutine SFORCE to calculate the force in each steel area. If equilibrium is reached between all forces on the cross-section STRAIN calls XCALC. If equilibrium is not reached the neutral axis position is adjusted up or down based on the sign of the sum of all forces calculated on cross-section.

Called by: MAIN

Calls : CFORCE, SFORCE, XCALC

(4) SUBROUTINE CFORCE:

Description: CFORCE takes the strain for each concrete area given by subroutine STRAIN and finds the corresponding stress from a concrete stress-strain curve such as that shown in Fig. A-2. The stress in each element is multiplied by the element's area to give the element force.

Called by: STRAIN

(5) SUBROUTINE SFORCE

Description, SFORCE takes the strain for each steel area given by subroutine STRAIN and finds the corresponding stress from a steel stress-strain curve such as that in Fig. A-2. The stress in each steel area is multiplied by the steel area to give the steel force.

Called by: STRAIN



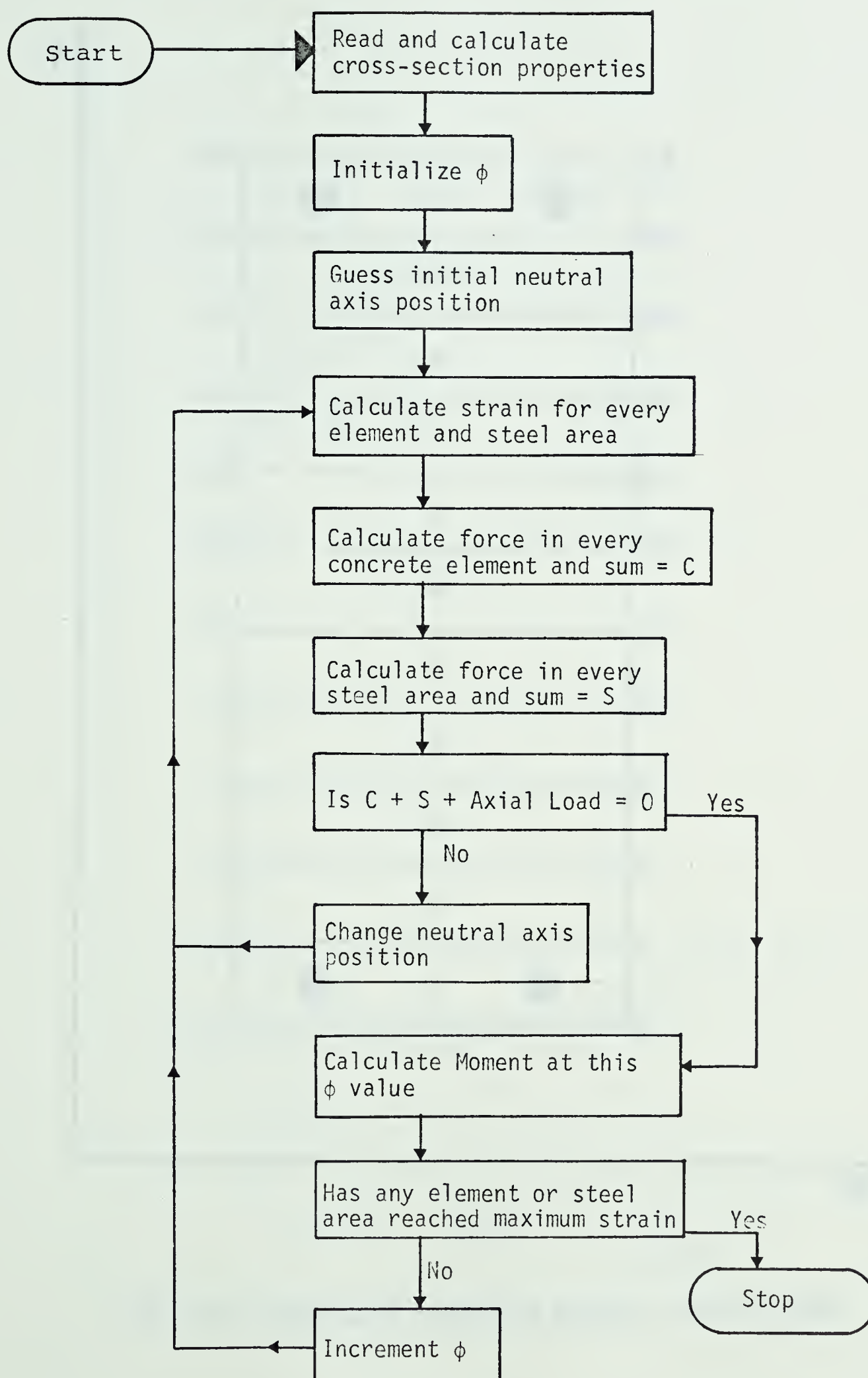
(6) SUBROUTINE XCALC

Description: XCALC calculates the moment corresponding to each equilibrium position and corresponding  $\phi$  value. The force of each element and steel area is multiplied by its distance to the centroid of the cross-section. The products are summed to give the moment value.

Called by: STRAIN





FIG. A-1 Flow Chart for M-P- $\phi$  Program



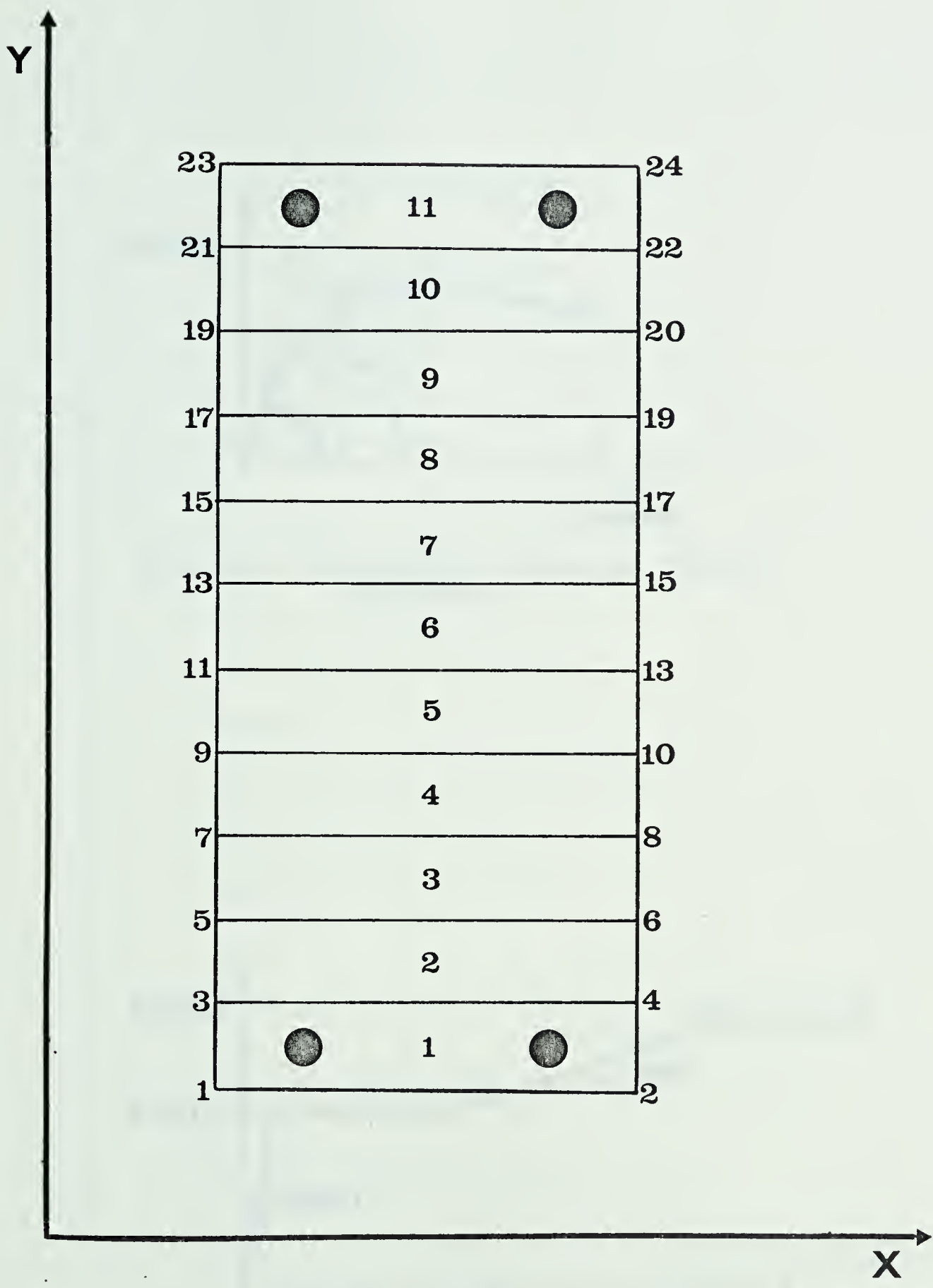
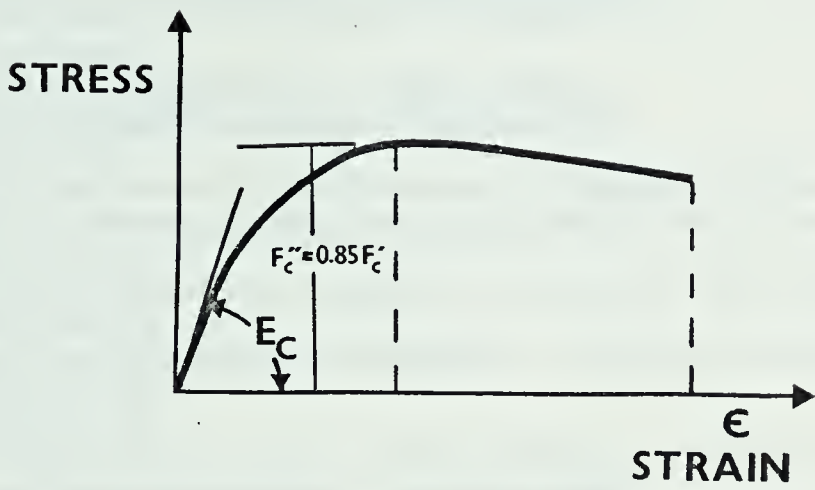
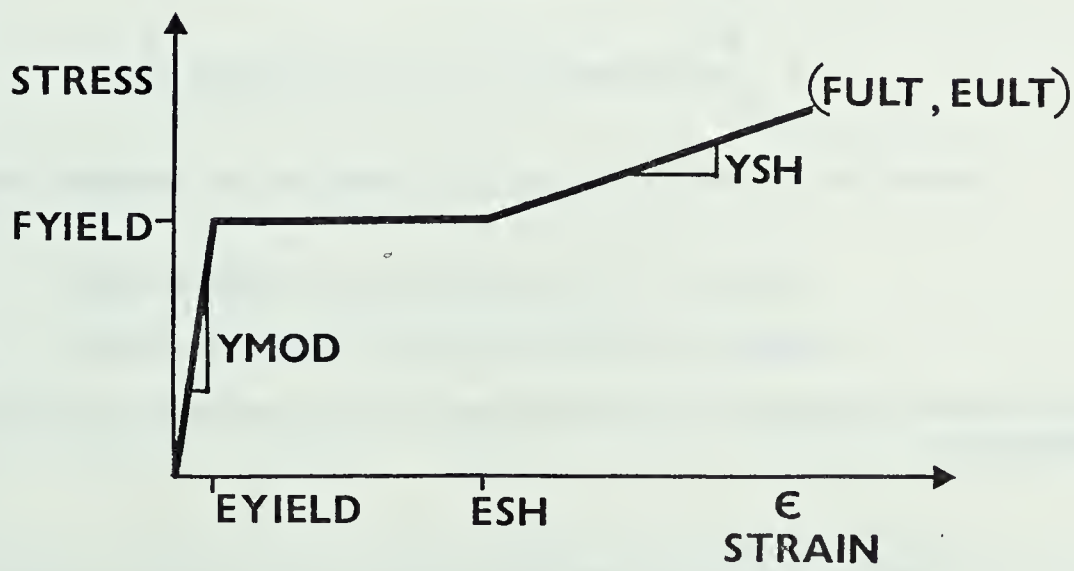


FIG. A-2 DISCRETIZED REINFORCED CONCRETE CROSS-SECTION





Hognestad's stress-strain diagram for flexure in concrete



Typical steel stress-strain diagram

FIG. A-3 STRESS-STRAIN DIAGRAMS





```

C
C      MOMENT--AXIAL LOAD--CURVATURE RESPONSE FOR GENERAL CROSS SECTION
C
C      UNITS ARE POUNDS AND INCHES
C
C      DIMENSION AS(20),YS(20),AREA(80),YC(80)
C      CALL XN(AS,YS,AREA,YC,NELEMS,NSTEEL)
C      WRITE(6,115)
C      READ(5,114)DEPTH,AXIAL,FSUBC,XNAREA
C      WRITE(6,116)DEPTH,AXIAL,FSUBC,XNAREA
C      WRITE(6,117)
C      READ(5,118)YMOD,EYIELD,ESH,EULT,FYIELD,FULT,YSH
C      WRITE(6,119)YMOD,EYIELD,ESH,EULT,FYIELD,FULT,YSH
114  FORMAT(4F10.5)
115  FORMAT(5X,'DEPTH',4X,'AXIAL',5X,'FSUBC',4X,'XNAREA')
116  FORMAT(4F10.2)
117  FORMAT('VARIOUS STEEL PROPERTIES  STRAINS AND STRESSES')
118  FORMAT(7F10.5)
119  FORMAT(7E12.5)
      CALL STRAIN(DEPTH,AXIAL,FSUBC,XNAREA,YMOD,EYIELD,ESH,EULT,FYIELD,
*FULT,AREA,NELEMS,NSTEEL,YC,YS,AS,YSH)
      CALL EXIT
      STOP
      END
      SUBROUTINE XN(AS,YS,AREA,YC,NELEMS,NSTEEL)
C
C      *
C      *
C      *      Y--COORDINATES
C      *
C      *      2 ***** 3
C      *      *
C      *      * 1 ELEMENT OF UP TO
C      *      *
C      *      * 80 ELEMENTS COMPRISING
C      *      *
C      *      * GENERAL CROSS-SECTION
C      *      *
C      *      *
C      *      *
C      *      1 ***** 4
C      *
C      *
C      ***** NUMBER OF ELEMENTS TO BE DIVISIBLE BY 3. *****
C      *
C      *
C      *      NODE NUMBERS CONNECTED MUST BE TAKEN
C      *
C      *      CLOCKWISE FROM LEFT HAND BOTTOM CORNER
C      *
C      *****
C
C      X--COORDINATES
C
C      DIMENSION X(150),Y(150),AS(20),YS(20),AREA(80),YC(80)
C

```



```

C      READ NUMBER OF NODES, STEEL AREAS, AND ELEMENTS
C
      READ(5,101)NNODES,NSTEEL,NELEMS
      WRITE(6,100)
      WRITE(6,102)NNODES,NSTEEL,NELEMS
      WRITE(6,103)
C
C      READ NODE AND ITS X AND Y COORDINATES
C
      DO 1 I=1,NNODES
      READ(5,104)NODE,X(NODE),Y(NODE)
1 WRITE(6,105)NODE,X(NODE),Y(NODE)
      WRITE(6,106)
C
C      READ STEEL AREA AND ITS Y COORDINATE
C
      DO 2 I=1,NSTEEL
      READ(5,107)AS(I),YS(I)
      WRITE(6,108)AS(I),YS(I)
2 CONTINUE
      WRITE(6,109)
C
C      READ NODES CONNECTED
C
      DO 3 I=1,NELEMS
      READ(5,110)NELEM,N1,N2,N3,N4
      WRITE(6,111)NELEM,N1,N2,N3,N4
      AREA(NELEM)=(Y(N2)-Y(N1))*(X(N4)-X(N1))
      YC(NELEM)=(Y(N1)+Y(N2))/2.0
      DO 4 J=1,NSTEEL
      IF((YS(J).LT.Y(N2)).AND.(YS(J).GT.Y(N1)))GO TO 5
4 CONTINUE
3 CONTINUE
      WRITE(6,113)
      DO 7 I=1,NELEMS
7 WRITE(6,112)I,AREA(I),YC(I)
      GO TO 6
5 AREA(NELEM)=AREA(NELEM)-AS(J)
      GO TO 4
6 CONTINUE
100 FORMAT(/'NUMBER OF NODES  NO.OF STEEL AREAS  NO.OF ELEMENTS')
101 FORMAT(3I5)
102 FORMAT(5X,I5,2(10X,I5))
103 FORMAT(/6X,'NODE',5X,'X COORDINATE',8X,'Y COORDINATE')
104 FORMAT(I5,2F10.5)
105 FORMAT(5X,I5,5X,F12.4,8X,F12.4)
106 FORMAT(/'STEEL AREA',5X,'Y COORDINATE')
107 FORMAT(2F10.5)
108 FORMAT(F10.5,5X,F12.4)
109 FORMAT('ELEMENT AND NODES CONNECTED')
110 FORMAT(5I5)
111 FORMAT(5I5)
112 FORMAT(10X,I5,3X,F7.3,7X,F12.4)
113 FORMAT(/'ELEMENT  NUMBER      AREA      AND      Y COORDINATE')
      RETURN
      END
      SUBROUTINE STRAIN(DEPTH,AXIAL,FSUBC,XNAREA,YMOD,EYIELD,ESH,EULT,F
      *YIELD,FULT,AREA,NELEMS,NSTEEL,YC,YS,AS,YSH)
      REAL MCALC
      REAL NADEEP

```



```

      DIMENSION ALPHA(20),X(1000),Y(1000)
      DIMENSION YC(80),YS(20),EELEM(80),EAS(20),AREA(80),AS(20),FC(80),
*FS(20)
      PHI=10.0E-07
      L=0
      PHIS=PHI*4.0
      NADEEP=-(((AXIALL/XNAREA)/(57000.0*SQRT(FSUBC)))/PHI)
      IF(AXIALL.EQ.0.0)NADEEP=DEPTH/2.
      C1S=0.25
      C3S=2.25
      XXX=0.0
8    COUNT=0.0
      C1=0.25
      NCROSS=0
      IF(NADEEP.GE.0.0)C1=0.00025
      IF(NADEEP.GE.0.0)C1S=0.00025
      IF(NADEEP.GE.0.0)C3S=.00225
      DIFF1=0.0
7    CONTINUE
      COUNT=COUNT+1.0
      IF(COUNT.GT.5000.)GO TO 200
201  GO TO 202
200  WRITE(6,203)
203  FORMAT('MORE THAN 5000 POSITIONS TRIED FOR NEUTRAL AXIS DEPTH'//)
      XXX=1.0
      I=-2
      GO TO 88
202  CONTINUE
      DO 1 I=1,NELEMS
      EELEM(I)=(NADEEP-YC(I))*PHI
1    CONTINUE
      DO 3 I=1,NSTEEL
3    EAS(I)=(NADEEP-YS(I))*PHI
      CALL CFORCE(NELEMS,EELEM,AREA,FSUBC,TOTALF,FC)
      CALL SFORCE(YMOD,YSH,EYIELD,ESH,EULT,FYIELD,NSTEEL,FULT,AS,EAS,FS,
*SUMF)
      TOTAL=TOTALF+SUMF
      DIFF=AXIALL+TOTAL
      IF(ABS(DIFF).LT.100.0)GO TO 4
      SIGN=-1.0
      IF(DIFF.LT.0.0)SIGN=1.0
      IF(DIFF1*DIFF)5,6,6
6    DIFF1=DIFF
      NADEEP=NADEEP+((C1*DEPTH)*SIGN)
      GO TO 7
5    NCROSS=NCROSS-1
      C1=C1S*(10.**NCROSS)
      C3=C3S*(10.**NCROSS)
      NADEEP=NADEEP+((C3*DEPTH)*SIGN)
      DIFF1=-DIFF
      GO TO 7
4    CONTINUE
      WRITE(6,131)
      I=-2
88   I=I+3
      I1=I
      I2=I+1
      I3=I+2
      IF(I1.GE.NELEMS)GO TO 89
90  WRITE(6,140)I1,EELEM(I1),FC(I1),I2,EELEM(I2),FC(I2),I3,EELEM(I3),F

```





```

      *C(I3)
140  FORMAT(I4,F14.8,4X,F14.4,I4,F14.8,4X,F14.4,I4,F14.8,4X,F14.4)
      GO TO 88
      89  CONTINUE
          WRITE(6,210)TOTALF
          WRITE(6,211)SUMF
210  FORMAT('SUM OF CONCRETE FORCES= ',F15.4//)
211  FORMAT('SUM OF STEEL FORCES= ',F15.4//)
          WRITE(6,132)DIFF
          WRITE(6,130)
          DO 11 I=1,NSTEEL
              WRITE(6,140)I,EAS(I),FS(I)
              IF(XXX.GT.0.1)CALL EXIT
      11  CONTINUE
          DO 77 I=1,NELEMS
              IF(ABS(EELEM(I)).GT.0.0039995)GO TO 55
      77  CONTINUE
          GO TO 69
      55  WRITE(6,122)
122  FORMAT('MAXIMUM CONCRETE STRAIN EXCEEDED')
          L=L/2
          DO 301 I=1,L
              J=I*2
              X(I)=X(J)
              Y(I)=Y(J)
              WRITE(6,303)I,X(I),Y(I)
      301  CONTINUE
          READ(5,501)(ALPHA(NX),NX=1,20)
          CALL CGPL(X,Y,Y,L,-129,1,1,2,0,
      * -9.9,-9.9,24.0,-9.9,-9.9,20.0,ALPHA,6)
          CALL EXIT
      69  CONTINUE
      501  FORMAT(20A4)
      303  FORMAT(I5,2X,E15.5,2X,F15.2)
          DO 66 I=1,NSTEEL
              IF(ABS(EAS(I)).GT.EULT)GO TO 67
      66  CONTINUE
          GO TO 74
      67  CONTINUE
          WRITE(6,123)
123  FORMAT('MAXIMUM STEEL STRAIN EXCEEDED')
          L=L/2
          DO 302 I=1,L
              J=I*2
              X(I)=X(J)
              Y(I)=Y(J)
              WRITE(6,303)I,X(I),Y(I)
      302  CONTINUE
          READ(5,501)(ALPHA(NX),NX=1,20)
          CALL CGPL(X,Y,Y,L,-129,1,1,2,0,
      * -9.9,-9.9,24.0,-9.9,-9.9,20.0,ALPHA,6)
          CALL EXIT
      74  CONTINUE
      130  FORMAT(/'STEEL STRAINS'/)
      131  FORMAT(/'CONCRETE STRAINS'/)
      132  FORMAT(F25.10)
          DEP=DEPTH
          CALL XCALC(FC,FS,NADEEP,YC,YS,AXIAL,NELEMS,NSTEEL,COUNT,PHI,DEP,A
      * REA,AS,MCALC)
          L=L+1

```





```

X(L)=PHI
Y(L)=MCALC
WRITE(6,151)L
151 FORMAT(/'INCREMENT NUMBER = ',I4/)
PHI=PHI+PHIS
GO TO 8
27 CONTINUE
RETURN
END
SUBROUTINE CFORCE(NELEMS,EELEM,AREA,FSUBC,TOTALF,FC)
DIMENSION EELEM(80),AREA(80),FC(80)
TOTALF=0.0
FCPP=0.85*FSUBC
EC=1800000.0+(500.*FCPP)
EO=(2.0*FCPP)/EC
FT=7.0*SQRT(FSUBC)
EMAXT=(2.0*FT)/EC
DO 1 I=1,NELEMS
IF(EELEM(I).GT.0.0)GO TO 2
3 CONTINUE
EELEM(I)=-EELEM(I)
IF(EELEM(I).GT.EO)GO TO 5
6 FC(I)=(2.0*(EELEM(I)/EO))-((EELEM(I)/EO)**2)
GO TO 7
5 SLOPE=-0.15*FCPP/(0.0038-EO)
FC(I)=FCPP+((EELEM(I)-EO)*SLOPE)
GO TO 15
7 CONTINUE
FC(I)=FC(I)*FCPP
15 CONTINUE
FC(I)=-FC(I)
EELEM(I)=-EELEM(I)
GO TO 4
2 IF(EELEM(I).GT.EMAXT)EELEM(I)=0.0
FC(I)=(2.0*(EELEM(I)/EMAXT))-((EELEM(I)/EMAXT)**3)
FC(I)=FC(I)*FT
4 CONTINUE
TOTALF=TOTALF+(FC(I)*AREA(I))
1 CONTINUE
RETURN
END
SUBROUTINE SFORCE(YMOD,YSH,EYIELD,ESH,EULT,FYIELD,NSTEEL,FULT,AS,
*EAS,FS,SUMF)
DIMENSION AS(20),EAS(20),FS(20)
SUMF=0.0
DO 4 I=1,NSTEEL
IF(EAS(I))1,2,3
1 CONTINUE
IF(EAS(I).GE.-EYIELD)GO TO 5
14 CONTINUE
IF(EAS(I).LT.-ESH)GO TO 6
15 CONTINUE
FS(I)=-FYIELD
GO TO 7
5 FS(I)=EAS(I)*YMOD
GO TO 7
6 FS(I)=((EAS(I)+ESH)*YSH)-FYIELD
GO TO 7
2 FS(I)=0.0
GO TO 7

```



```

3 IF(EAS(I).LE.EYIELD)GO TO 8
16 CONTINUE
   IF(EAS(I).GT.ESH)GO TO 9
17 CONTINUE
   FS(I)=FYIELD
   GO TO 7
8 CONTINUE
   FS(I)=YMOD*EAS(I)
   GO TO 7
9 FS(I)=FYIELD+(((EAS(I)-ESH  )*YSH)
7 CONTINUE
   SUMF=SUMF+(FS(I)*AS(I))
4 CONTINUE
   RETURN
   END
   SUBROUTINE XCALC(FC,FS,NADEEP,YC,YS,AXIALL,NELEMS,NSTEEL,COUNT,
*PHI,DEP,AREA,AS,MCALC)
   REAL MCALC
   REAL NADEEP
   DIMENSION AREA(80),AS(20)
   DIMENSION FC(80),FS(20),YC(80),YS(20)
   MCALC=0.0
4 DO 5 I=1,NELEMS
5 MCALC=MCALC-(((YC(I)-(DEP/2.))*FC(I))*AREA(I))
   DO 6 I=1,NSTEEL
6 MCALC=MCALC-(((YS(I)-(DEP/2.))*FS(I))*AS(I))
7 CONTINUE
   WRITE(6,149)NADEEP
149 FORMAT(/'NEUTRAL AXIS POSITION IS ',F6.1,' INCHES FROM THE BOTTOM
*EDGE OF THE CROSS-SECTION'/)
   WRITE(6,120)
   WRITE(6,121)PHI,MCALC,AXIALL,COUNT
120 FORMAT(6X,'PHI',8X,'MCALC',4X,'AXIALL',5X,'COUNT')
121 FORMAT(E11.4,E14.6,2F10.1)
   MCALC=MCALC/1000.
   WRITE(7,169)MCALC,PHI
169 FORMAT(F15.2,E11.4)
   RETURN
   END

```



## APPENDIX B

### DILGER SHEAR-GAMMA RELATIONSHIP

#### B-1 Introduction

This program has been developed to calculate the shear-gamma relationship of any general cross-section as given in formulae by Dilger. The background to the program is contained in Sec. 2-4.

#### B-2 Input Data

First Card: BETA, DEPTH, FSUBC, VCONC, T

Input Format: (8F10.5)

BETA = Inclination of cracks (degrees)

DEPTH =  $j$  x effective depth (in)

FSUBC = 28 day concrete compressive strength (psi)

VCONC = shear carried by concrete alone (pounds)

T = thickness of web (in)

Second Card: ALPHA, SPACE, AlSTIR, FY, FU, EUST

ESHST

Input Format: (8F10.5)

ALPHA = Inclination of stirrups (degrees)

SPACE = Spacing of stirrups (in)

AlSTIR = Area of 1 stirrup (all legs) (sq. in)

FY = Yield stress of steel (psi)

FU = Ultimate stress of steel (psi)

EUST = Ultimate strain of steel ( $\frac{\text{in}}{\text{in}}$ )





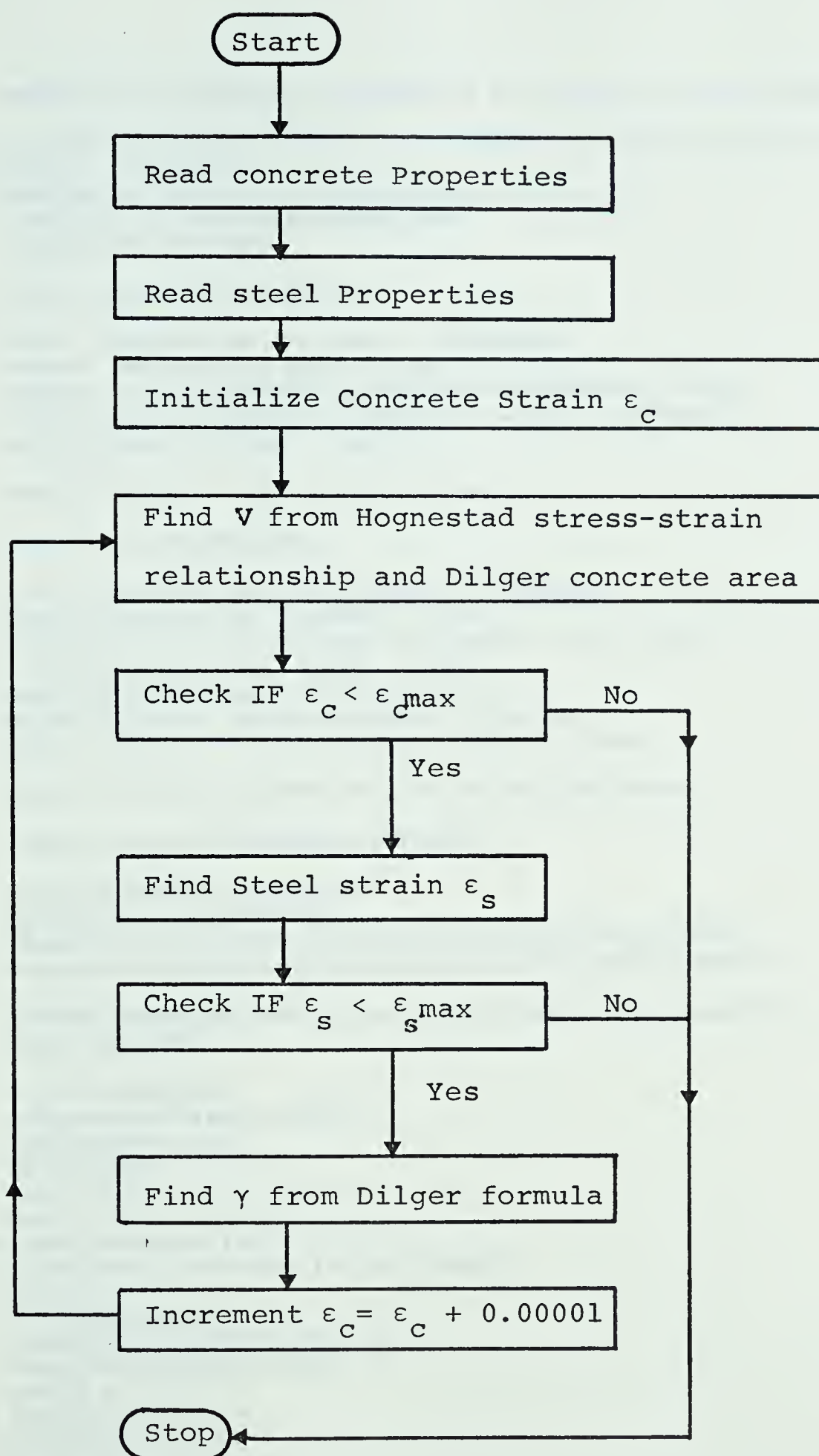
ESHST = Steel strain hardening steel ( $\text{in}/\text{in}$ )

### B-3 Description of Program

The program begins with an initial value of concrete strain and finds the shear,  $V$ , applied to the cross-section using Hognestad's concrete stress-strain curve and the concrete area value given by Dilger formula.

The value of  $V$  is then substituted into the Dilger formula for gamma. Steel strain corresponding to this applied shear is checked and if neither concrete or steel exceed their maximum strain, the initial concrete strain is increased and the procedure repeated.



FIG. B-1 Flow Chart for V- $\gamma$  Program



```

C      PROGRAM TO CALCULATE RESPONSE OF W. DILGER'S SHEAR DEFORMATION MODEL
C
C      DIMENSION VV(200),SIGMAE(200),GAMMA(200),VADD(200),GDILG(200),GSIG
C      *M(200),VSIGM(200)
C      DIMENSION SIGMEE(200),STRAIN(200),ECONC(200)
C      DIMENSION STST(200),STCONC(200)
C      DIMENSION ALPH(20)
C
C      READ CONCRETE PROPERTIES
C
C      BETA= INCLINATION OF CRACKS (DEGREES)
C      DEPTH= J*EFFECTIVE DEPTH (IN)
C      FSUBC= 28 DAY CONCRETE COMPRESSIVE STRENGTH (PSI)
C      VCONC= SHEAR CARRIED BY CONCRETE ALONE (POUNDS)
C      T= THICKNESS OF WEB (IN)
C
C      READ(5,100)BETA,DEPTH,FSUBC,VCONC,T
C
C      READ STEEL PROPERTIES
C
C      ALPHA= INCLINATION OF STIRRUPS (DEGREES)
C      SPACE= SPACING OF STIRRUPS (IN)
C      A1STIR= AREA OF 1 STIRRUP (ALL LEGS) (SQ. IN)
C      FY= YIELD STRESS OF STEEL (PSI)
C      FU= ULTIMATE STRESS OF STEEL (PSI)
C      EUST= ULTIMATE STRAIN OF STEEL (IN/IN)
C      ESHST= STEEL STRAIN HARDENING STRAIN (IN/IN)
C
C      READ(5,100)ALPHA,SPACE,A1STIR,FY,FU,EUST,ESHST
C
C      FIND STEEL AND CONCRETE STRAINS
C
C      ALPHA=ALPHA*3.14159/180.
C      BETA=BETA*3.14159/180.
C      AREAC=T*DEPTH*(COTAN(ALPHA)+COTAN(BETA))*SIN(BETA)
C      AREAS=A1STIR*DEPTH*(COTAN(ALPHA)+COTAN(BETA))/SPACE
C
C      DEFINE CONCRETE STRAIN AND FIND STRESS FROM HOGNESTAD STRESS-STRAIN
C      RELATIONSHIP
C
C      FCPP=0.85*FSUBC
C      EC=1800000.0+(500.*FCPP)
C      EO=(2.*FCPP)/EC
C      EU=0.0038
C      E=0.00001
C      I=1.
C      5 IF(E.GT.EO)GO TO 1
C      FC=FCPP*((2.0*(E/EO))-((E/EO)**2))
C      GO TO 3
C      1 IF(E.GT.EU)GO TO 2
C      SLOPE=(-0.15*FCPP)/(EU-EO)
C      FC=FCPP+((E-EO)*SLOPE)
C      GO TO 3
C      2 WRITE(6,900)
C      GO TO 9
C      3 V=FC*AREAC
C

```



```

C      FIND STEEL STRESS AND STRAIN
C
FSTEEL=V/AREAS
IF(FSTEEL.GT.FY)GO TO 6
ESV=FSTEEL/29000000.0
GO TO 7
6 IF(FSTEEL.GT.FU)GO TO 8
ESH=(FU-FY)/(EUST-ESHST)
ESV=ESHST+(FSTEEL-FY)/ESH
GO TO 7
8 WRITE(6,901)
GO TO 9
7 CONTINUE

C
C      GAMMA FOUND USING STRESS STRAIN CURVES
C
SIGMAE(I)=(ESV/(SIN(ALPHA)**2))+(E/(SIN(BETA)**2))
ECONC(I)=E
STRAIN(I)=ESV

C
C      FIND DILGER GAMMA
C
PV=A1STIR/(SPACE*T*SIN(ALPHA))
GAMMA(I)=V/(T*DEPTH*((COTAN(ALPHA)+COTAN(BETA))**2))*(1./(PV*
*29000000.0*(SIN(ALPHA)**4))+1./(EC*(SIN(BETA)**4)))
VV(I)=V
E=E+0.00001
I=I+1
GO TO 5

C
C      FIND ELASTIC GAMMA
C
9 EGAMMA= VCONC/((EC/2.36)*DEPTH*T)
II=I+1
DO 10 J=3,II
VADD(J)=VV(J-2)+VCONC
GDILG(J)=GAMMA(J-2)+EGAMMA
10 GSIGM(J)=SIGMAE(J-2)+EGAMMA
VADD(2)=VCONC
GDILG(2)=EGAMMA
GSIGM(2)=EGAMMA
VADD(1)=0.0
GDILG(1)=0.0
GSIGM(1)=0.0
DO 11 JJ=2,I
VSIGM(JJ)=VV(JJ-1)
STCONC(JJ)=ECONC(JJ-1)
STST(JJ)=STRAIN(JJ-1)
11 SIGMEE(JJ)=SIGMAE(JJ-1)
VSIGM(1)=0.0
VSIGM(I+1)=0.0
SIGMEE(1)=0.0
SIGMEE(I+1)=0.0
STST(1)=0.0
STST(I+1)=0.0
STCONC(1)=0.0
STCONC(I+1)=0.0
WRITE(6,902)
DO 12 K=1,II
12 WRITE(6,903)VSIGM(K),SIGMEE(K),VADD(K),GDILG(K),GSIGM(K)

```





```
*,STCONC(K),STST(K)
100 FORMAT(8F10.5)
900 FORMAT(/'MAXIMUM CONCRETE STRAIN EXCEEDED'/)
901 FORMAT(/'MAXIMUM STEEL STRESS EXCEEDED'/)
902 FORMAT(/'SHEARS AND GAMMAS'/)
903 FORMAT(7(2X,F16.5))
501 FORMAT(20A4)
STOP
END
```



## APPENDIX C

### DERIVATION OF MODIFIED SLOPE DEFLECTION EQUATIONS

The standard slope deflection equations have been modified in order to accommodate the special end conditions incurred during the modeling process of a frame for the dynamic analysis, as discussed in Chapter 4. In the model, a member end is restrained by a rotational spring. The member end may also consist of a rigid stub, as shown in Fig. 4-6. The final formats of such equations are shown in Eqs. 4-5 and 4-6. The derivation of these equations is shown in this appendix.

The sway rotation,  $\rho$ , between points a and b in Fig. 4-6 is temporarily assumed to be zero. If the joint rotations at points a and b are  $\theta_a$  and  $\theta_b$ , respectively, the end rotations of the member cd at points c and d are

$$\theta_a = \frac{M_{cd} - \beta_1}{\alpha_1},$$

and

$$\theta_b = \frac{M_{dc} - \beta_2}{\alpha_2}$$

respectively as explained in Eqs. 4-3 and 4-4. If  $\rho$  is zero, the sway rotation between points c and d,  $\rho_{cd}$ , is given by:

$$\rho_{cd} = - \frac{\lambda_1 L \theta_a + \lambda_2 L \theta_b}{\lambda_3 L}$$



$$= - \frac{\lambda_1 \theta_a = \lambda_2 \theta_b}{\lambda_3}$$

Therefore the end moments,  $M_{cd}$  and  $M_{dc}$ , are expressed by:

$$\begin{aligned} M_{cd} = & \frac{2EI}{\lambda_3 L} \left\{ 2 \left( \theta_a - \frac{M_{cd}^{-\beta_1}}{\alpha_1} \right) + \left( \theta_b - \frac{M_{dc}^{-\beta_2}}{\alpha_2} \right) \right. \\ & \left. + 3 \frac{\lambda_1 \theta_a + \lambda_2 \theta_b}{\lambda_3} \right\} + C_{cd} \end{aligned} \quad (C-1)$$

$$\begin{aligned} M_{dc} = & \frac{2EI}{\lambda_3 L} \left\{ \left( \theta_a - \frac{M_{cd}^{-\beta_1}}{\alpha_1} \right) + 2 \left( \theta_b - \frac{M_{dc}^{-\beta_2}}{\alpha_2} \right) \right. \\ & \left. + 3 \frac{\lambda_1 \theta_a + \lambda_2 \theta_b}{\lambda_3} \right\} + C_{dc} \end{aligned} \quad (C-2)$$

where  $C_{cd}$  and  $C_{dc}$  are defined in Eqs. 4-7 and 4-8, respectively. Solving Eqs. C-1 and C-2 for  $M_{cd}$  and  $M_{dc}$ ,

$$\begin{aligned} M_{cd} = & \left[ \frac{2EI}{\lambda_3 L} \left\{ \left( 2 + 3 \frac{\lambda_1}{\lambda_3} + \frac{6EI}{\alpha_2 \lambda_3 L} + \frac{6\lambda_1 EI}{\alpha_2 \lambda_3^2 L} \right) \theta_a \right. \right. \\ & + \left( 1 + 3 \frac{\lambda_2}{\lambda_3} + \frac{6\lambda_2 EI}{\alpha_2 \lambda_3^2 L} \right) \theta_b + \left( 2 + \frac{6EI}{\alpha_2 \lambda_3 L} \right) \frac{\beta_1}{\alpha_1} + \frac{\beta_2}{\alpha_2} \left. \right\} \\ & + \left( 1 + \frac{4EI}{\alpha_2 \lambda_3 L} \right) C_{cd} - \frac{2EI}{\alpha_2 \lambda_3 L} C_{dc} \left. \right] / A_7 \end{aligned} \quad (C-3)$$

$$M_{dc} = \left[ -\frac{2EI}{\lambda_3 L} \left\{ \left( 1 + 3 \frac{\lambda_1}{\lambda_3} + \frac{6\lambda_1 EI}{\alpha_1 \lambda_3^2 L} \right) \theta_a + \left( 2 + 3 \frac{\lambda_2}{\lambda_3} \right) \right. \right.$$





$$\begin{aligned}
& + \frac{6EI}{\alpha_1 \lambda_3 L} + \frac{6\lambda_2 EI}{\alpha_1 \lambda_3^2 L} \theta_b + \frac{\beta_1}{\alpha_1} + \left(2 + \frac{6EI}{\alpha_1 \lambda_3 L}\right) \frac{\beta_2}{\alpha_2} \} \\
& - \frac{2EI}{\alpha_1 \lambda_3 L} C_{cd} + \left(1 + \frac{4EI}{\alpha_1 \lambda_3 L}\right) C_{dc} \} / A_7 \quad (C-4)
\end{aligned}$$

where  $A_7$  is defined in Eq. 4-22.

The end moments,  $M_{ab}$  and  $M_{ba}$ , and the end moments,  $M_{cd}$  and  $M_{dc}$ , are related as follows.

In general, shear forces at the member ends (see Fig. C-1) are given, ignoring the secondary moments produced by axial force, by:

$$V_1 = -\frac{1}{L}(M_1 + M_2) + \frac{1}{2}wL \quad (C-5)$$

$$V_2 = -\frac{1}{L}(M_1 + M_2) - \frac{1}{2}wL \quad (C-6)$$

Here the uniformly distributed load,  $w$ , is assumed to be applied throughout the member length,  $L$ . Therefore the shear force at the right end of the member  $ac$ ,  $V_{ac}$ , is

$$V_{ac} = -\frac{1}{\lambda_1 L}(M_{ab} + M_{ca}) - \frac{1}{2}w\lambda_1 L$$

and the shear force at the left end of the member  $cd$ ,  $V_{cd}$ , is:

$$V_{cd} = -\frac{1}{\lambda_3 L}(M_{cd} + M_{dc}) + \frac{1}{2}w\lambda_3 L$$

The equilibrium condition at this point requires that the above two shear forces are the same. Thus,

$$\begin{aligned}
M_{ab} = M_{cd} + \frac{\lambda_1}{\lambda_3}(M_{cd} + M_{dc}) - \frac{1}{2}w\lambda_1(1-\lambda_2)L^2 \\
\ldots (C-7)
\end{aligned}$$



In the above, the equilibrium of moments:

$$M_{ca} + M_{cd} = 0 \quad (C-8)$$

is used. A similar process at point d yields:

$$M_{ba} = M_{dc} + \frac{\lambda_2}{\lambda_3}(M_{cd} + M_{dc}) + \frac{1}{2}w\lambda_2(1-\lambda_1)L^2 \quad \dots (C-9)$$

As  $M_{cd}$  and  $M_{dc}$  are calculated in Eqs. C-3 and C-4, the end moments  $M_{ab}$  and  $M_{ba}$  are obtained using Eqs. C-7 and C-9. Substituting Eqs. C-3 and C-4 into C-7,  $M_{ab}$  is obtained as:

$$M_{ab} = \frac{\frac{2EI}{\lambda_3 L}(A_1^\theta a + A_2^\theta b + A_4 \frac{\beta_1}{\alpha_1} + A_5 \frac{\beta_2}{\alpha_2}) + A_6 C_{cd}}{A_7} + A_8 D_{ab} \quad \dots (C-10)$$

and similarly,  $M_{ba}$  as:

$$M_{ba} = \frac{\frac{2EI}{\lambda_3 L}(A_2^\theta a + A_1'^\theta b + A_5' \frac{\beta_1}{\alpha_1} + A_4' \frac{\beta_2}{\alpha_2}) + A_6 C_{cd}}{A_7} + A_8 D_{ab} \quad \dots (C-11)$$

where  $A_1, A_1', A_2, A_4, A_4', A_5, A_5', A_6, A_6', A_7, A_8 D_{ab}$  and  $A_8' D_{ba}$  are as defined in Sec. 4-4-1. When deriving these equations, the relationship,

$$C_{cd} = -C_{dc} \quad (C-12)$$

was used.



If the sway rotation,  $\rho$ , is present, the end moments,  $M_{ab}$  and  $M_{ba}$ , will be expressed in the forms shown in Eqs. 4-5 and 4-6. The end moments observed when the joint rotations at both ends of the member are zero and only the sway rotation,  $\rho$ , exists are the same as the moments observed when the joint rotations at both ends are equal to  $-\rho$  and the sway rotation is zero. Therefore the coefficients of  $\rho$ ,  $A_3$  and  $A'_3$ , in Eqs. 4-5 and 4-6, respectively, are given by:

$$A_3 = -(A_1 + A_2)$$

and

$$A'_3 = -(A'_1 + A_2)$$

as shown in Eqs. 4-14 and 4-15. In other words, Eqs. 4-5 and 4-6 are the expressions for the end moments under an arbitrary member position as shown in Fig. 4-6.

The lower ends of the bottom story columns are connected to the foundation through elastic rotational springs. The slope deflection equations must be modified to accommodate this situation. The derivation of modified slope deflection equations for this case is, however, similar to that shown above, thus the explanation has been omitted here.



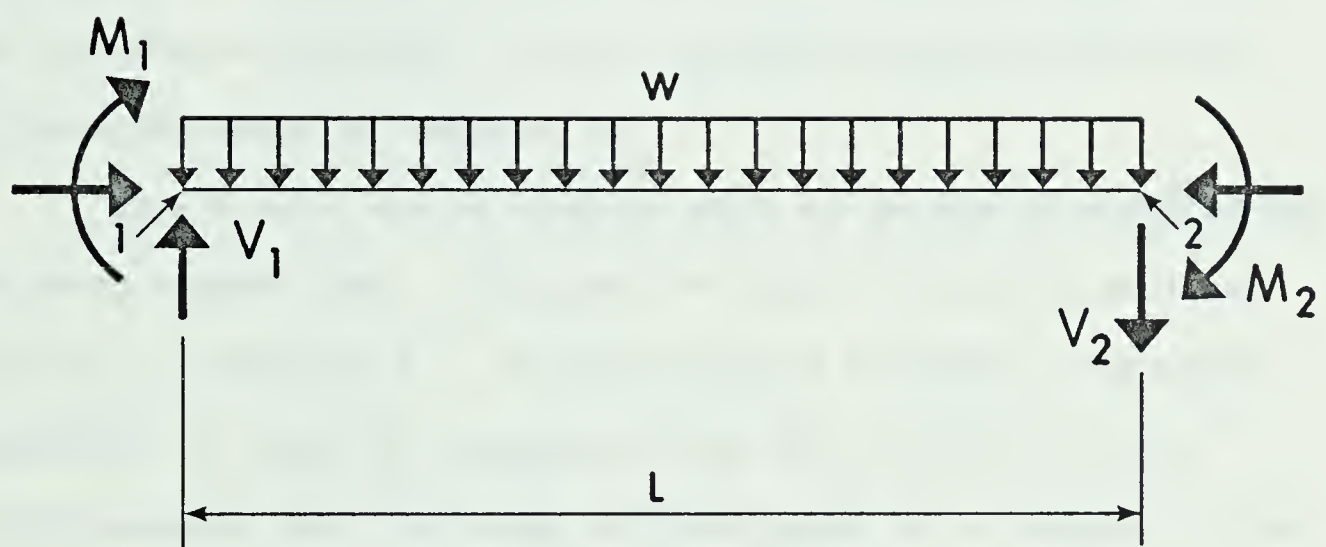


FIG. C-1 Equilibrium of Forces





## Appendix D

### MAIN COMPUTER PROGRAM

#### D-1 Description of the Program

This program has been developed to perform an inelastic dynamic analysis of a multistory, multibay frame subjected to either a blast load or an earthquake motion. The procedure employed in the program complies with the statements made in Chapter 4.

The  $M_s - \delta\theta_s$  relationship must be prepared beforehand for each member end. This may be done using the program listed in Appendix E. In the present program, the input statement is made by assuming that the initial  $M_s - \delta\theta_s$  relationships are the same at both ends of a member. The data describing the external disturbance may be input through a deck of cards or through a file stored in the computer disk.

The results of the entire response may be printed out or may be either punched out or stored in the disk so that the results can be plotted by CalComp Plotter using a program written especially for this purpose.

#### D-2 Input Data

Card Group 1: NS, NB, NCAL, MXIT, NTOBU, NSAI, LTP, IGPH, TIMELT, DELTAT, GOSA. The input format is (8I5,10X, 3F10.0). The numbering convention and other symbols are as



defined in Chapter 4. The variables used here are as follows.

- NS : Number of stories ( $N_s$ ),
- NB : Number of bays ( $N_b$ ),
- NCAL : Number of integration steps,
- MXIT : Maximum number of iterations allowed for each step of integration procedure.  
( $20 \leq \text{MXIT} \leq 50$ ),
- NTOBU : Results are printed out for every NTOBU-step of integration,
- NSAI : Number of subdivisions. If there is any change in the value of  $\alpha_1$ ,  $\beta_1$ ,  $\alpha_2$ , or  $\beta_2$  in the modified slope deflection equation or if convergence was not obtained, integration is done for smaller time increments as specified by this. ( $2 \leq \text{NSAI} \leq 5$ )
- LTP : Type of external disturbance.  
 $\text{LTP} \leq 4$  ... Earthquake  
 $\text{LTP} \geq 5$  ... Blast Load
- IGPH : Indicates the type of output.  
 $\text{IGPH} \geq 6$  ... Results are printed out; however they are neither punched out nor stored in the disk.  
 $\text{IGPH} = 1$  ... Results are punched out.  
 $\text{IGPH} = 2$  ... Results are stored in the disk.



Two files must be created in the disk, and the output code numbers must be assigned in the following manner.

2 = file name 1

3 = file name 2

In the file name 1, entire behavior is stored; and in file name 2, the maximum values are stored.

**TIMELT** : This value must be equal to the prepared total computation time minus 0.3 or 0.4 minutes. If the total computation time assigned for this job is not enough to perform all the response calculation, the response calculation is cut off after TIMELT (min) is spent, and the maximum values so far obtained are printed out and the results stored in the disk are saved in the tape.

**DELTAT** : Incremental time step in the integration step ( $\Delta t$ ),

**GOSA** : Convergence limit. It is usually adequate to specify this value between 0.001 and 0.0001.

Card Group 2: EM, GR, SEICO, IDISC, THAJI, TOWA.

FORMAT (3F10.0, 15, 25X, 2F10.0).

**EM** : Modulus of elasticity (E)





- GR : Acceleration of gravity (g)
- SEICO : Input data of external disturbance is multiplied by this value. If the input data for an earthquake is prepared so that the maximum value of acceleration is equal to the acceleration of gravity, SEICO corresponds to the seismic design coefficient in a static analysis. If the input data for a blast load is prepared so that the maximum value is 1.0, SEICO shows the maximum load at the standard floor.
- IDISC : Indicates if the data describing the external disturbance are input through a deck of cards (IDISC  $\neq$  0) or through a file stored in the disk (IDISC = 0). If the data are given through the disk, the file must be called by the input code number 4.
- THAJI and TOWA : The results for every story are printed out regardless of the indication of IP(i) (See Card Group 4) for the time period from THAJI (sec) to TOWA (sec).  
If these places are left blank, the function is ignored.

Card Group 3: SB(j), for j = 1 to N<sub>b</sub>. FORMAT  
((8F10.0)).



SB(j) : Length of the j-th bay (from column center to column center)

Card Group 4: For  $i = 1$  to  $N_s$ ; SM(i), H (i), SH(i), IP(i). FORMAT (3F10.0, 15).

SM(i) : Weight concentrated at the i-th floor  
( $m_i \times g$ )

H(i) : Damping factor ( $h_i$ )

SH(i) : Story height of the i-th story

IP(i) : Indicates if the print out of the result for the i-th floor is required ( $IP(i) \geq 0$ ) or not ( $IP(i) \leq -1$ ).

Card Group 5: For  $i = 1$  to  $N_s$ ; RP(i,j), for  $j = 1$  to  $N_b + 1$ . FORMAT ((8F10.0)).

RP (i,j) : Length of the rigid stub at the right end of the beam at the i-th floor and the j-1 th bay which is assumed to be equal to the length of rigid stub at the left end of the beam at the i-th floor and the j-th bay.

Card Group 6: For  $i = 1$  to  $N_s$ ; BMI(i,j), for  $j = 1$  to  $N_b$ . FORMAT ((8F10.0)).

BMI(i,j) : Moment of inertia of the beam at the i-th floor and the j-th bay.

Card Group 7: For  $i = 1$  to  $N_s$ ; CMI(i,j), for  $j = 1$



to  $N_b + 1$ . FORMAT ((8F10.0)).

CMI(i,j) : Moment of inertia of the column at the  
i-th story and the j-th row.

Card Group 8: SPR(j), for  $j = 1$  to  $N_b + 1$ .

FORMAT ((8F10.0)).

SPR(j) : Spring constant of the foundation at  
the bottom of the j-th column. (For  
fixed end  $\rightarrow 1.0 \times 10^{30}$ ).

Card Group 9: For  $i = 1$  to  $N_s$ ; UDL(i,j), for  
 $j = 1$  to  $N_b$ . FORMAT ((8F10.0)).

UDL(i,j) : Uniformly distributed load applied to  
the beam at the i-th floor and the  
j-th bay.

Card Group 10: Part a; IKUTSU, NES(k), for  $K$   
 $= 1$  to IKUTSU. FORMAT ((16I5)).

Part b; TEMPO(i), for  $i = 1$  to  
6.

FORMAT (6F10.0).

IKUTSU : Number of members which have the same  
 $M_s - \delta \theta_s$  relationships.

NES(k) : Member number which was referred above.

TEMPO(i): Temporary variable. Used to show the  
coordinates of points A, B and C in Fig.  
4-5, i.e.

(TEMPO(1), TEMPO(2)) ... Point A

(TEMPO(3), TEMPO(4)) ... Point B



(TEMPO(5), TEMPO (6)).... Point C

POINT B is any point on line A-C.

The next relationship must be satisfied.

TEMPO(5) > TEMPO(3) > TEMPO(1) > 0.

If the theoretical value of TEMPO(1) is zero, a value like  $1.0 \times 10^{-30}$  should be input in the computer.

Part a and part b are repeated until the  $M_s - \delta\theta_s$  relationships are input for all members.

Card Group 11 (Only when IGPH = 1 or 2): MSKIP, INSA, NPCH, IPCH(j), for j = 1 to NPCH. FORMAT 10I5).

MSKIP : Results are either punched out (if IGPH = 1) or stored in the disk (if IGPH = 2) for every MSKIP-steps of integration.

INSA : Indicates if the print out of results is required ( $INSA \geq 5$ ) or not ( $INSA \leq 4$ ) together with punched out cards or files stored in the disk.

NPCH : Number of floors for which results are punched out. ( $NPCH \leq 5$ ).

INPCH(j) : Floor number for which the results are punched out.

If IGPH = 2, neither NPCH nor IPCH(j) need to be specified as the results of every floor is stored in the disk.





Card Group 12: TSEI(i), for i = 1 to 20. FORMAT  
(20A4).

TSEI(i) : Identification of external disturbance.

Card Group 13: GA(j), for j = 1 to NCAL. FORMAT  
((7F10.0)).

GA(j) : Data of external disturbance. Seven  
data are input at a time.

Some general remarks are listed as follows:

1. One unit each for length, mass and time should be used throughout the preparation of data. As far as this regulation is observed, either customary (English) system or the SI (international) system may be used.
2. If IDISC = 0 in Card Group 2, the data given in Card Groups 12 and 13 are assumed to be stored in the disk in the same formats as shown here.
3. Total time for which the response calculation is preformed is NCAL X DELTAT.

### D-3 Presentation of Results

The results of response calculation are presented in various manners according to the specified values of IGPH and INSA in the preparation of input data.

- (1) Those which are printed out regardless of the values of IGPH and INSA.

a. First three natural periods and the smallest



natural period.

- b. Locations of member end where inelastic action was experienced.
- c. Locations of member ends where collapse was indicated.
- d. Maximum values in displacement relative to the ground, displacement relative to the lower floor, velocity relative to the lower floor, absolute acceleration, resisting force due to damping, resisting force due to frame action, shear coefficient and the total (damping and frame action combined) resisting force; for every floor.

(2) Additional results which are printed out when  $IGPH \geq 6$ ; or  $IGPH = 1$  or  $2$ , and  $INSA \geq 5$ .

- e. Displacement relative to the ground, displacement relative to the lower floor, velocity relative to the lower floor, absolute acceleration, resisting force due to damping, resisting force due to frame action and shear coefficient; for the specified floors by  $IP(i)$ , for every NTOBU-steps of integration.

(3) Results which are punched out when  $IGPH = 1$ .

- f. Floor number (counted from the bottom--only in this case), time, displacement relative to the ground, displacement relative to the lower floor, velocity relative to the lower floor, absolute



acceleration, resisting force due to damping, resisting force due to frame action and shear coefficient for the specified floors by IPCH(j), for every MSKIP-steps of integration. The output format is (12,F8.3, 1P7E 10.3).

- g. Maximum values in displacement relative to the lower floor, the time it was recorded, velocity relative to the lower floor, the time it was recorded, shear coefficient and the time it was recorded; for every floor starting from the bottom. The output format is (3(1PE10.4, OPF10.3)).

(4) The results stored in the disk when IGPH = 2.

- h. The same variables as listed in article f above, by the same output format; except that they are recorded for every floor.
- i. The same variables indicated in article g above, by the same output format.

#### D-4 Description of Subprograms and Flow Charts

##### (1) MAIN PROGRAM

Description: MAIN PROGRAM is functioned to set initial values for some variables and to assemble subroutines.

Calls: TIME, SAKURA, STIFF, SHUKI, KIKU and JISHIN.

Flow Chart: Shown in Fig. D-1.





Variables in Common Statements (in order of appearance):

NS, NB, SH(i), SPR(I), SB(i), RP(i,j), UDL(i,j) and  
SLPLS(i) : As explained in the preparation of input  
data,

STF(i) : Stiffness of the i-th member,  $2EI/L$ , where  
L is either column length or bay length  
(column center to center),

SLP(i,j,k):  $\alpha_1$  or  $\alpha_2$  as appears in Eqs. 4-3 and 4-4  
for the i-th member and j-th member end.  
K corresponds to the branch number as  
depicted in Fig. D-2.

BETA(i,j,k) :  $\beta_j$  as appears in Eq. 4-3 and 4-4, for  
the i-th member. Subscript k indicates  
the branch number as shown in Fig. D-2,

THETA(i,j,k) : The value of  $\delta\theta_s$  at points A,B,C,A',B'  
and C', respectively, corresponding to  $K = 1,$   
... 6 at the i-th member and the j-th end,

IMA(i,j) : Indicates the branch in the  $M_s - \delta\theta_s$   
relationship where the present values of  
( $M_s, \delta\theta_s$ ) lie, at the i-th member and the j-th  
end. If they are on branch #1, IMA = 0; if  
on branch #2, IMA = 1; if on branch #3,  
IMA = 2; if on branch #4, IMA = -1; and if  
on branch #5, IMA = -2, in Fig. D-2,

PMO(i,j,k) : The values of  $M_s$  at points A and A' in



Fig. D-2, for  $k = 1$  and  $2$ , respectively,  
at the  $i$ -th member and the  $j$ -th end.

HXD( $i$ ) : Vector  $\{\xi\}$  defined in Eq. 4-27, and

HNL( $i$ ) : Vector  $\{\eta\}$  defined in Eq. 4-27.

#### Other Variables (Only the important ones)

GOSA, NCAL, MXIT, NTOBU, NSAI, GR, DELTAT,

SEICO, IP( $i$ ), THAJI, TOWA, LTP, IGPH and IDISC:

As explained in the preparation of input  
data,

C( $i$ ) : Identical to H( $i$ ) as explained in the  
preparation of input data until KIKU is  
called; thereafter,  $c_i$  as defined in Eq.  
4-28.

SM( $i$ ) : Mass concentrated at the  $i$ -th floor,

CSM( $i$ ) : CSM <sub>$i$</sub>  as defined in Eq. 4-34.

ITIME : TIMELT expressed in terms of milli-  
seconds,

IA : Number of unknowns ( dimension of  $\{\theta\}$  )  
in Eq. 4-23,

Q( $i,i$ ) : Stiffness matrix  $[G]$  in Eq. 4-27,

A( $i,j$ ) : Matrix  $[R]$  in Eq. 4-23. Stored for  
only the band width of  $2N_b + 3$ ,

ISHUT : Indicates if the Gaussian elimina-  
tion process was done without having numer-  
ical problems (ISHUT = 0) or not (ISHUT =  
1), and



GOME :  $1/\omega_1$ , where  $\omega_1$  is defined in Sec.  
4-5-1.

(2) SUBROUTINE SAKURA

Description: SAKURA reads in most of the input data and prints out the important frame properties necessary for the identification of the problem.

Called By: MAIN

Flow Chart: Omitted

New Variables:

SM(i) : Weight at first, later converted to mass, concentrated at the i-th floor, and

TEMPO(i) : Temporary variables.

(3) SUBROUTINE STIFF

Description: STIFF is called whenever a new stiffness matrix [G] as in Eq. 4-27 is necessary to be calculated. Matrix [R] as in Eq. 4-23 is constructed by calling FUJI. LU decomposition (Gaussian elimination) of matrix [R] using Doolittle's method (without pivoting) is performed. Then, by calling YURI, Eq. 4-23 is solved for the stiffness matrix in the manner as described in Sec. 4-4-2.

Called By: MAIN, JISHIN and SAIBUN.



Calls: FUJI and YURI

Flow Chart: Shown in Fig. D-3.

New Variable:

INIT : Indicates if this subroutine is called to calculate the initial stiffness matrix by MAIN (INIT = 0) or not (INIT = 1).

(4) SUBROUTINE FUJI

Description: FUJI assembles the elements of matrix [R] defined in Sec. 4-4-2. The coefficients of  $\theta_a$  and  $\theta_b$  in the modified slope deflection equations as in Eqs. 4-5 and 4-6 are obtained by calling IZU.

Called By: STIFF

Calls: IZU.

Flow Chart: Omitted.

New Variables:

VA : Coefficient of  $\theta_a$  in Eq. 4-5 or 4-6,

VB : Coefficient of  $\theta_b$  in Eq. 4-5 or 4-6,

MA : Member number indicating the column which connects from above to the joint where the equilibrium of moments is being considered,

ML : Member number indicating the beam which connects from left to such a joint,





MR : Member number indicating the beam  
 which connects from right to such a joint,  
 MB : Member number indicating the column  
 which connects from below to such a joint,  
 FR1 :  $\lambda_1$  as defined in Sec. 4-4-1, and  
 FR2 :  $\lambda_2$  as defined in Sec. 4-4-1.

(5) SUBROUTINE IZU

Description: IZU calculates the coefficients of  $\theta_a$  and  $\theta_b$  in Eq. 4-5 or 4-6 when called by FUJI, or those in Eq. C-3 or C-4 when called by KYOTO. If IZU is called with respect to the equilibrium of story shears by FUJI, the corresponding values are calculated from the combined equation,  $M_{ab} + M_{ba}$ , obtained from Eqs. 4-5 and 4-6. The formulae used in the actual computation sometimes look different than given in the mentioned equations, depending upon the values of  $\alpha_1$  and  $\alpha_2$ .

Called By: FUJI and KYOTO.

Flow Chart: Omitted.

New Variables:

II : Indicates if the present calculation should be done using Eq. 4-5 or C-3 (II = 1), or using Eq. 4-6 or C-4 (II = 2). Further, if II = 3, the combined equation,



$M_{ab} + M_{ba}$ , should be used,

IASHI : Indicates if the member being considered is the column of bottom story (IASHI = -1) or not (IASHI = 1), and

IGO : Indicates if this subroutine was called by FUJI (IGO = 1) or by KYOTO (IGO = -1).

#### (6) SUBROUTINE YURI

Description: YURI assembles the right hand side,  $\{B\}$ , of Eq. 4-23 by calling B, and solves for  $\{\theta\}$  by calling SOLVE. It then constructs the stiffness matrix  $[G]$  as described in Sec. 4-4-2. If it is the calculation of the initial stiffness matrix, the vector  $\{\eta_o\}$  defined in Sec. 4-4-2 is also evaluated.

Called By: Stiff.

Calls: B and SOLVE

Flow Chart: Omitted.

#### (7) FUNCTION B

Description: B assembles the i-th element of vector  $\{B\}$  in Eq. 4-23 by calling UHEN for given values for vector  $\{x\}$ .

Called By: YURI and KYOTO.

Calls: UHEN

Flow Chart : Omitted.



New Variables:

MA, ML, MR, MB FR1 and FR2: As defined in IZU,

IJ : Indicates the element number in vector {B} ,

SXD(i) : Displacement relative to the ground;

i.e., the vector {x} defined in Sec. 4-4-2

and

R : Sway rotation,  $\rho$ , as defined in Sec. 4-4-1.

(8) FUNCTION UHEN

Description: UHEN sums the rest of the terms that are excluded either by  $\theta_a$  term or  $\theta_b$  term in Eq. 4-5 or 4-6 when called by B, or the corresponding terms in Eq. C-3 or C-4 when called by KYOTO. If UHEN is called with respect to the equilibrium of story shears by B, the corresponding value is calculated from the combined equation,  $M_{ab} + M_{ba}$ , obtained from Eqs. 4-5 or 4-6. The formulae used in the actual computation, sometimes looks different than given in the mentioned equations depending upon the values of  $\alpha_1$  and  $\alpha_2$ .

Called By: B and KYOTO.

Flow Chart: Omitted.

New Variables:

II and IASHI: as defined in IZU,

M : Member number,





S: Member length, and

IGO : Indicates if this function was called  
by B (IGO = 1) or by KYOTO (IGO = -1).

(9) SUBROUTINE SOLVE

Description: SOLVE solves for  $\{\theta\}$  in Eq. 4-23 by back substitutions.

Called By: YURI and KYOTO.

Flow Chart: Omitted.

New Variables:

A(i,j) : Lower and upper matrices that have  
been obtained by LU decomposition of  
matrix [R] in Eq. 4-23 (done in STIFF) are  
now stored, instead of [R] itself,

W(i) : Vector  $\{B\}$  in Eq. 4-23 at the be-  
ginning; then changed to  $[L]^{-1} \{B\}$  using  
forward elimination. When the calculation  
is finished, it is the solution  $\{\theta\}$  in Eq.  
4-23, and

C(i) : Story shear terms in the solution  
 $\{\theta\}$  in Eq. 4-23.

(10) SUBROUTINE SHUKI

Description: SHUKI computes the first three undamped  
natural periods and the minimum natural period;  
and corresponding modes.

Called By: MAIN



Calls: TOKYO1

Flow Chart: Omitted.

(11) SUBROUTINE TOKYO1

Description: TOKYO1 is used to change a matrix to its inverse matrix as it goes through.

Called By: SHUKI and KIKU.

Flow Chart: Omitted.

(12) SUBROUTINE KIKU

Description: KIKU calculates the damping coefficients,  $c_i$ , as defined in Eq. 4-28. It also calculates the initial deflection,  $\{\xi_o\}$  as in Eq. 4-26.

Called by: MAIN

Calls: TOKYO1.

Flow Chart: Omitted.

(13) SUBROUTINE JISHIN

Description: JISHIN is the most important subroutine as it solves the equations of motion by calling SUCHI, checks member end moments,  $M_s$ , and relaxation angles,  $\delta\theta_s$ , if they are within the assumed branches of the  $M_s$ - $\delta\theta_s$  relationship by calling KYOTO and if they are not, a new stiffness matrix is calculated in SAIBUN. The  $M_s$ - $\delta\theta_s$  relationships are updated in the manner as described in Sec. 2-3, by calling NARA. The results are output in various formats according to input specifications.



Called By: MAIN

Calls: STIFF, SUCHI, SAIBUN, KYOTO, NARA and TIME.

Flow Chart: Shown in Fig. D-4.

New Variables:

GA(i), TSEI (i) : As defined in the preparation of input data,

AX(i) : Acceleration relative to the ground ( $\{\ddot{x}\}$  as in Sec. 4-5-1),

VX(i) : Velocity relative to the ground ( $\{\dot{x}\}$ ),

XD(i) : Displacement relative to the ground ( $\{x\}$ ),

RX(i) : Displacement at the i-th floor relative to the i+1-th floor,

RV(i) : Velocity at the i-th floor relative to the i+1-th floor,

AA(i) : Absolute acceleration ( $\{\ddot{x}\} + \ddot{Y}_0$ ) for an earthquake;  $\{\ddot{x}\}$  for a blast load),

CQ(i) : Shear coefficient,

RESC(i) : Resisting force due to damping,

RESQ(i) : Resisting force due to frame action,

RXXM(i) : Maximum value in relative displacement,

RVMX(i) : Maximum value in relative velocity,

CQMX(i) : Maximum value in shear coefficient,



XDMX(i) : Maximum value in displacement relative  
 to the ground ,  
 AAMX(i) : Maximum value in absolute acceleration,  
 RCMX(i) : Maximum value in resisting force due  
 to damping,  
 RQMX(i) : Maximum value in resisting force due  
 to frame action,  
 TRMX(i) : Maximum value in total resisting force,  
 TRX(i) : Time when the maximum relative dis-  
 placement was recorded,  
 TRV(i) : Time when the maximum relative velocity  
 was recorded,  
 TCQ(i) : Time when the maximum shear coefficient  
 was recorded,  
 OAX(i) : Acceleration ( $\{\ddot{x}\}$ ) obtained in the  
 previous step of integration,  
 OVX(i) : Velocity ( $\{\dot{x}\}$ ) obtained in the previous  
 step of integration,  
 OXD(i) : Displacement ( $\{x\}$ ) obtained in the  
 previous step of integration,  
 FT(i,j) : Present value of relaxation angle,  $\delta\theta_s$ ,  
 at the i-th member and the j-th end,  
 KOSAN(i,j) : Indicates if the rotational spring  
 has experienced inelastic action (KOSAN =  
 1) or not (KOSAN = 0) at the i-th member





and the  $j$ -th end,

GA1 : External disturbance at  $t = t_p - 2\Delta t$

where  $t_p$  is the value of time axis for which the present step of calculation is being done,

GA2 : External disturbance at  $t = t_p - \Delta t$ ,

GA3 : External disturbance at  $t = t_p$ ,

GA4 : External disturbance at  $t = t_p + \Delta t$ ,

and

TP : Value of time axis for which the present step of calculation is being done.

#### (14) SUBROUTINE SAIBUN

Description: SAIBUN reperforms the numerical integration by calling SUCHI with a smaller value of time increment, when the calculations failed to converge with regular value of  $t$  or when the  $M_s - \delta\theta_s$  relationships at any member ends are being changed from one branch to another.

Called by JISHIN.

Calls: SUCHI, KYOTO, STIFF and NARA.

Flow Chart: Shown in Fig. D-5.

New Variable:

GAP : Present value of external disturbance obtained by interpolating GA1, GA2,



GA3 and GA4.

(15) SUBROUTINE SUCHI

Description: SUCHI solves the equations of motion using the linear acceleration method as explained in Sec. 4-5-2.

Called By: JISHIN and SAIBUN.

Calls: QQ.

Flow Chart: Shown in Fig. D-6.

New Variable:

ISAI : Indicates if the equations of motion were solved successfully; i.e., numerical integration procedure converged (ISAI = 10) or not (ISAI = - 10).

(16) FUNCTION QQ

Description: QQ calculates  $Q_i$  ( $\{x\}$ ) in Eq. 4-32.

Called By: SUCHI.

Flow Chart: Omitted.

(17) SUBROUTINE KYOTO

Description: KYOTO calculates the present value of relaxation angle at every member end and checks if it is within the assumed branch of the  $M_s - \delta\theta_s$  relationship (set ICHI = 0) or not (Set ICHI  $\geq$  1).

Called By: JISHIN and SAIBUN.

Calls: B, SOLVE, IZU and UHEN.



Flow Chart: Shown in Fig. D-7.

New Variables:

EM(j) : End moment at the j-th end of the member being considered; i.e.,  $M_{cd}$  and  $M_{dc}$  as defined in Eqs. C-3 and C-4, and

IIQ : Indicates if this subroutine was called by JISHIN (IIQ = 1) or by SAIBUN (IIQ = 2).

#### (18) SUBROUTINE NARA

Description: NARA updates the  $M_s - \delta\theta_s$  relationships by using the procedure described in Sec. 2-3. It also prints out the location of member end when it experiences the inelastic action for the first time or when the collapse is indicated.

Called By: JISHIN and SAIBUN.

Flow Chart: Shown in Fig. D-8.

New Variable:

KDIS : Indicates if any rotational springs have indicated collapses (KDIS = -10) or not (KDIS = 10).

#### (19) SUBROUTINE TIME

Description: TIME is a standard MTS (Michigan Terminal System - IBM/360 at the University of





Alberta) subroutine which allows the user easy access to the elapsed time, CPU time used, time of day, and the date in convenient units.

Called By: MAIN and JISHIN.

D-5 Listing of Program.

The listing of the program appears on pages through



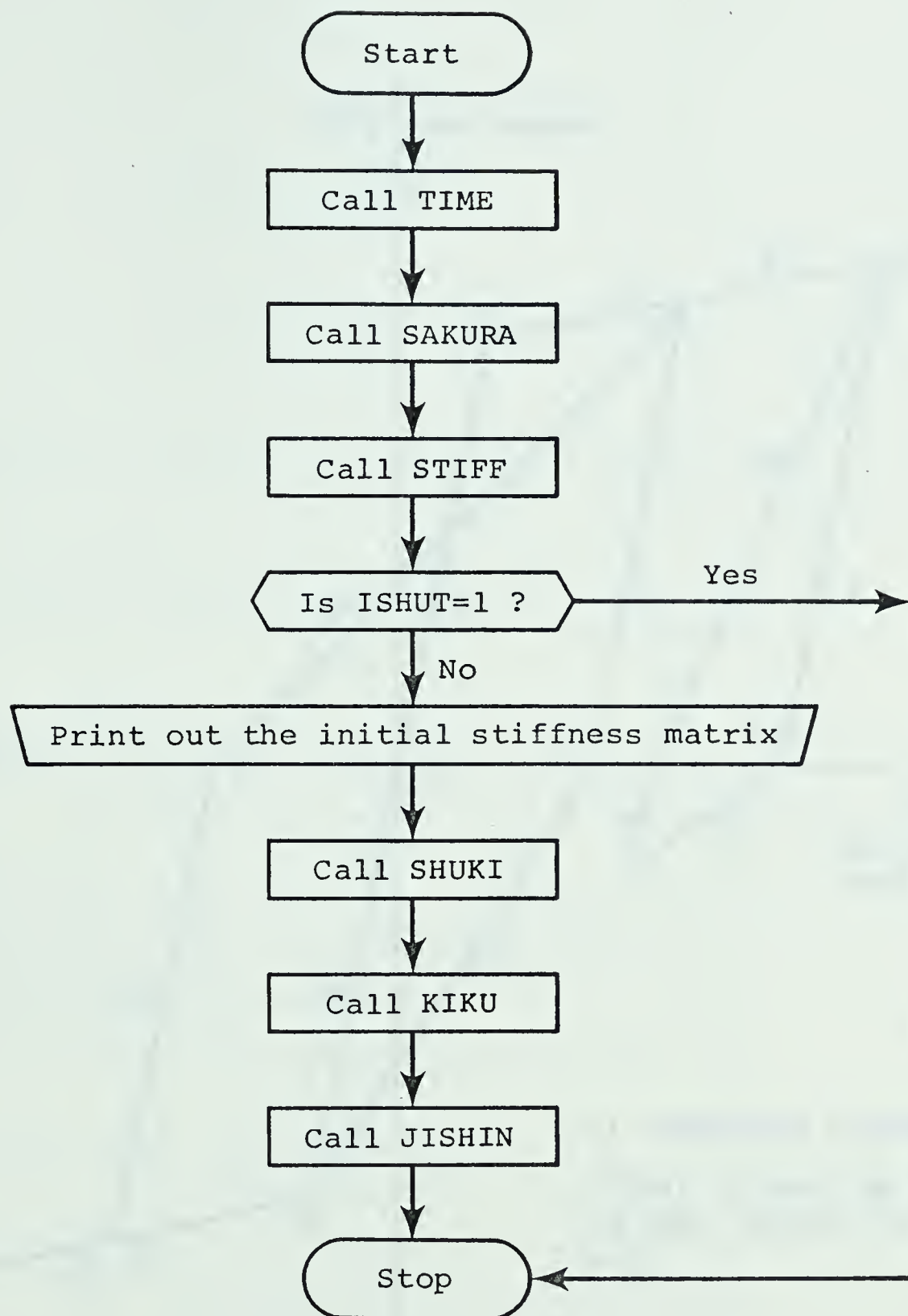


Fig. D-1 MAIN PROGRAM



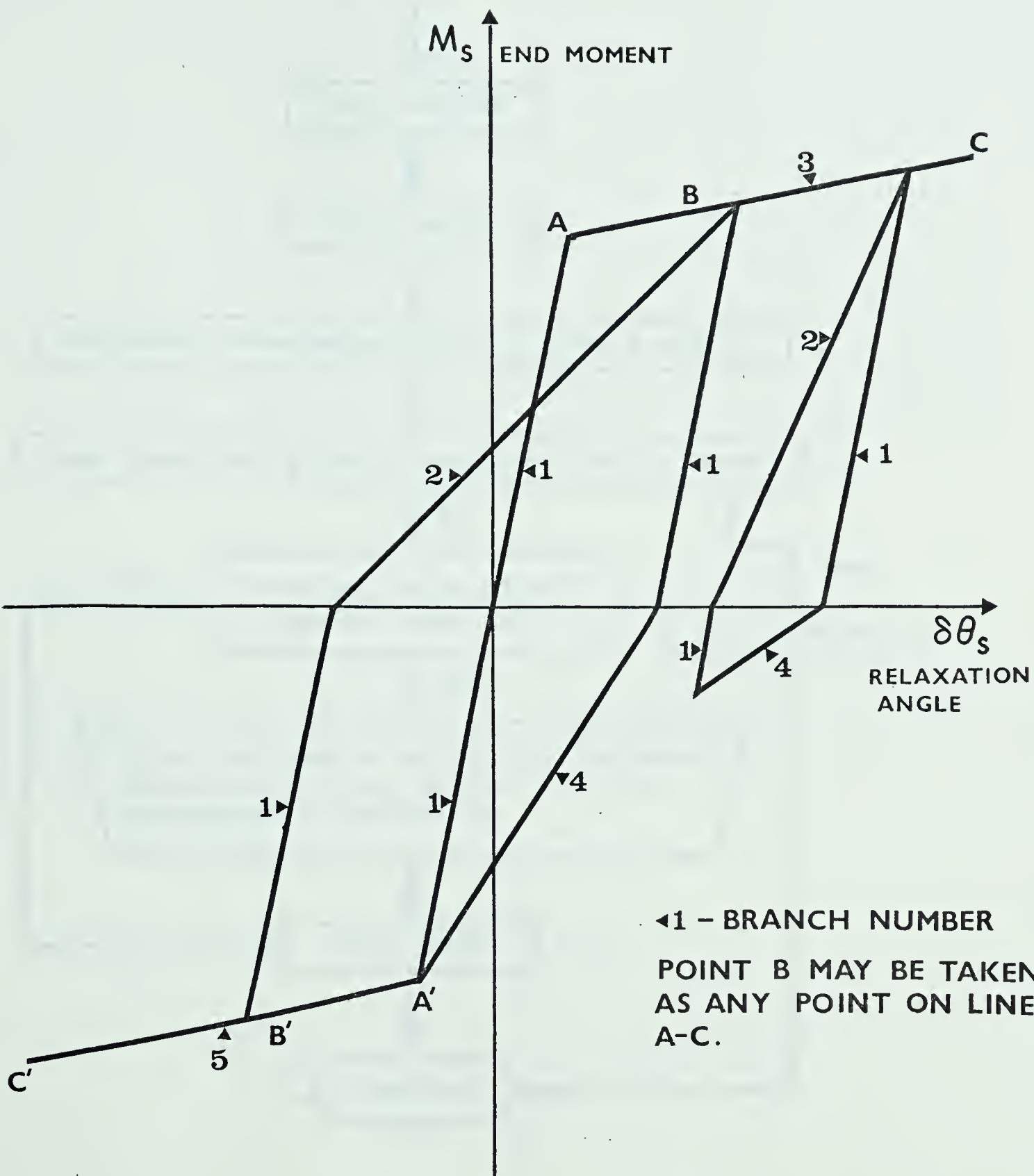


FIG. D-2  $M_S - \delta\theta_s$  Relationship in General Situation



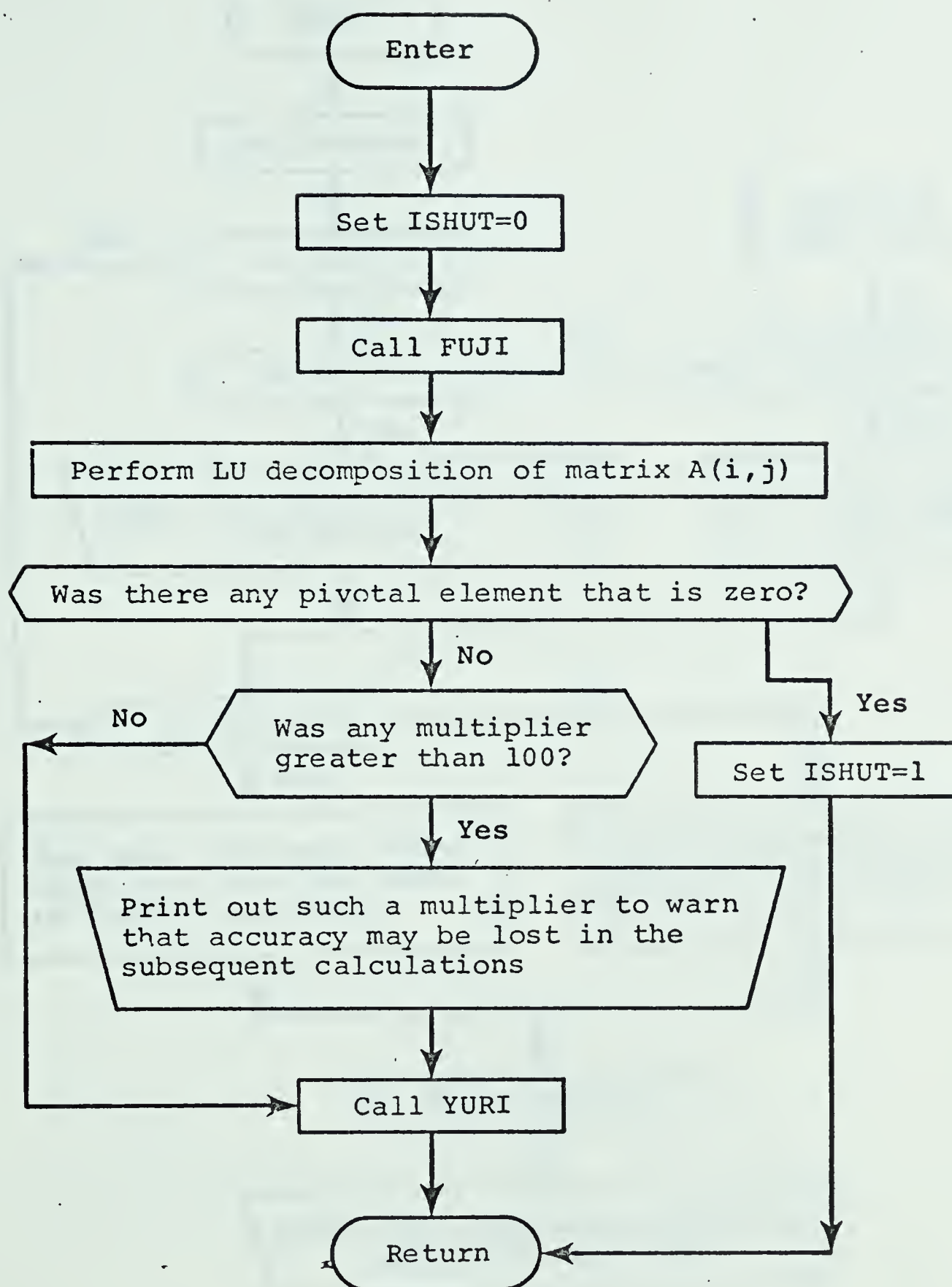


Fig. D-3 SUBROUTINE STIFF





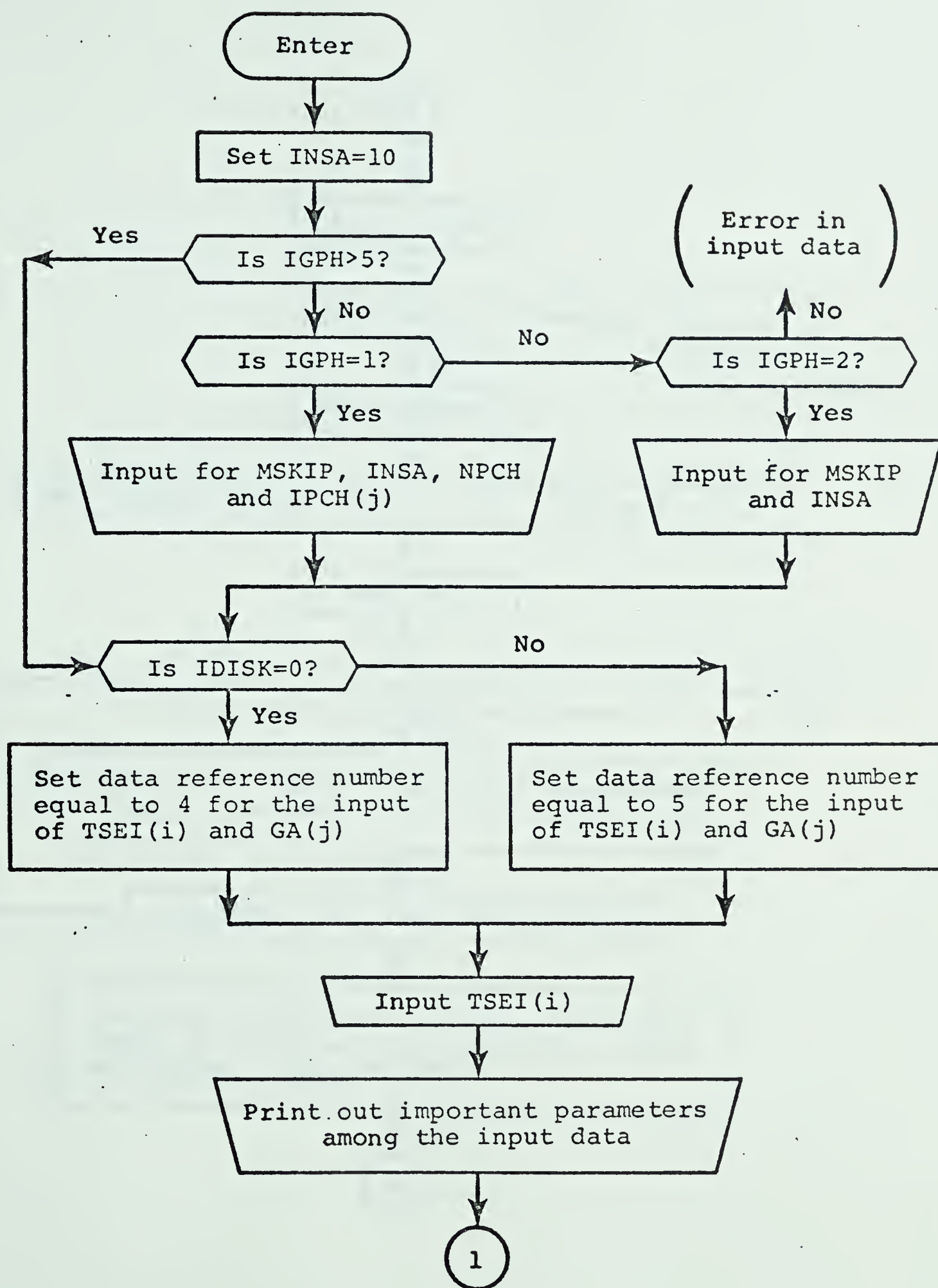


Fig. D-4 SUBROUTINE JISHIN (to be continued)



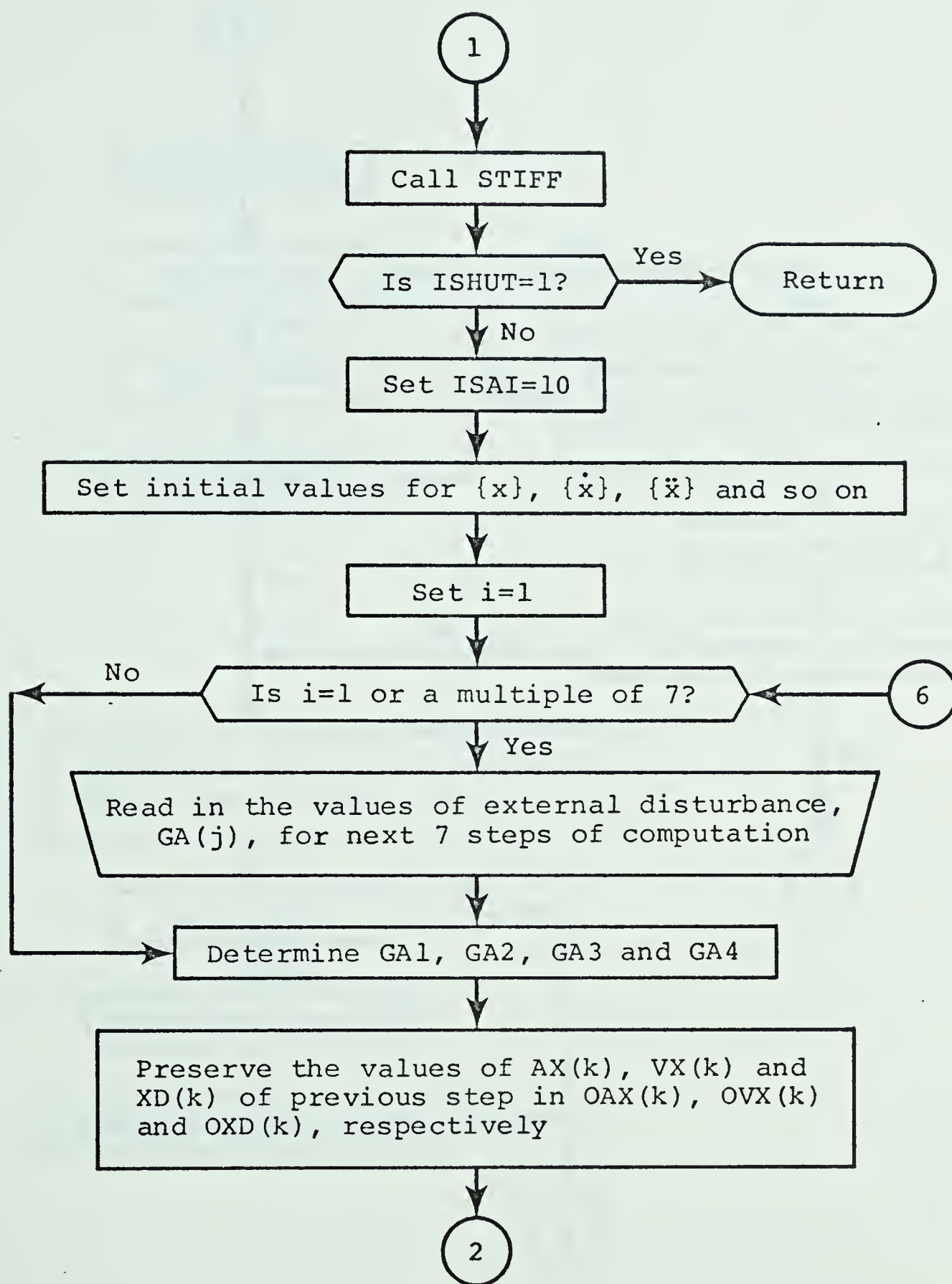


Fig. D-4 (continued) SUBROUTINE JISHIN



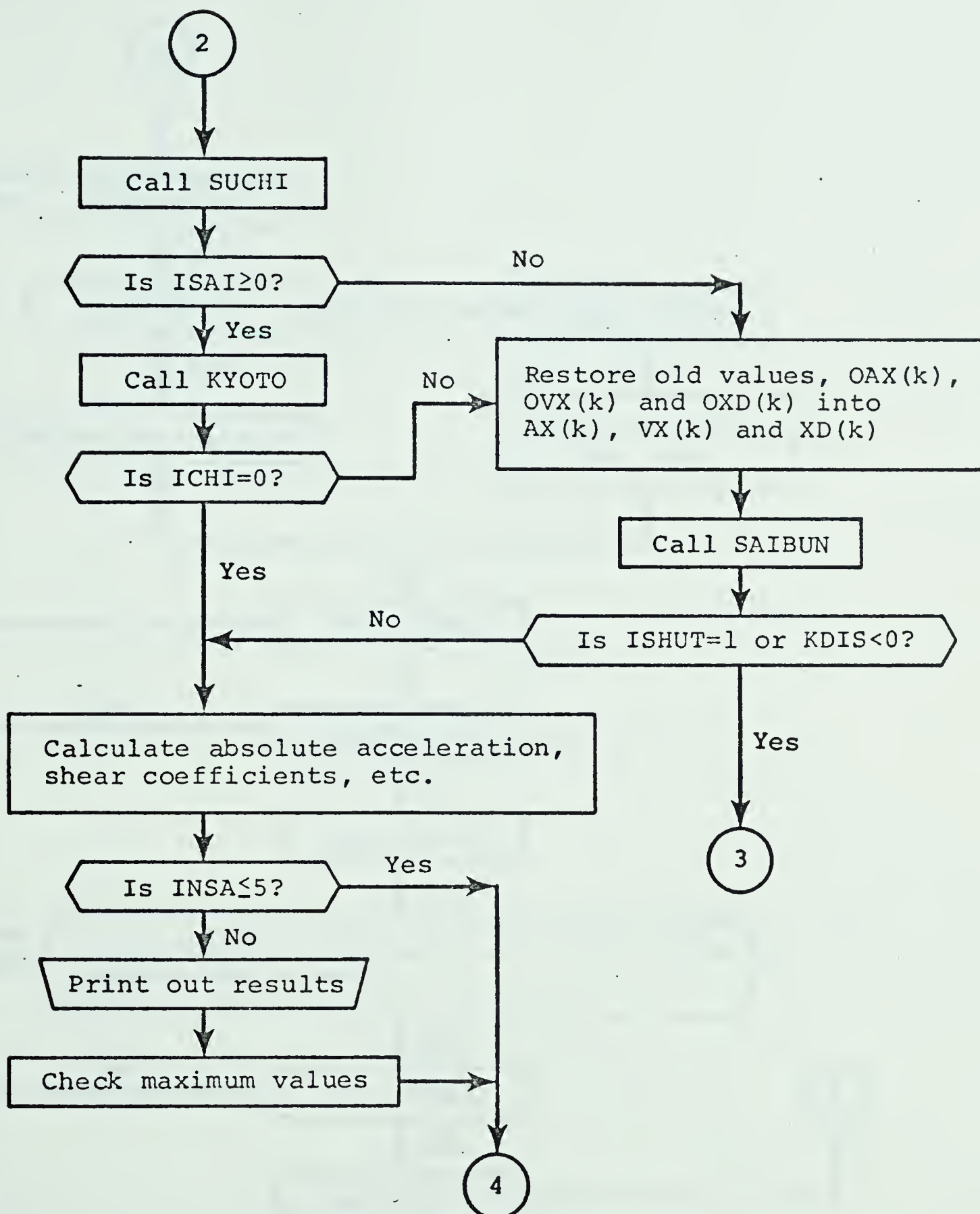


Fig. D-4 (continued) SUBROUTINE JISHIN





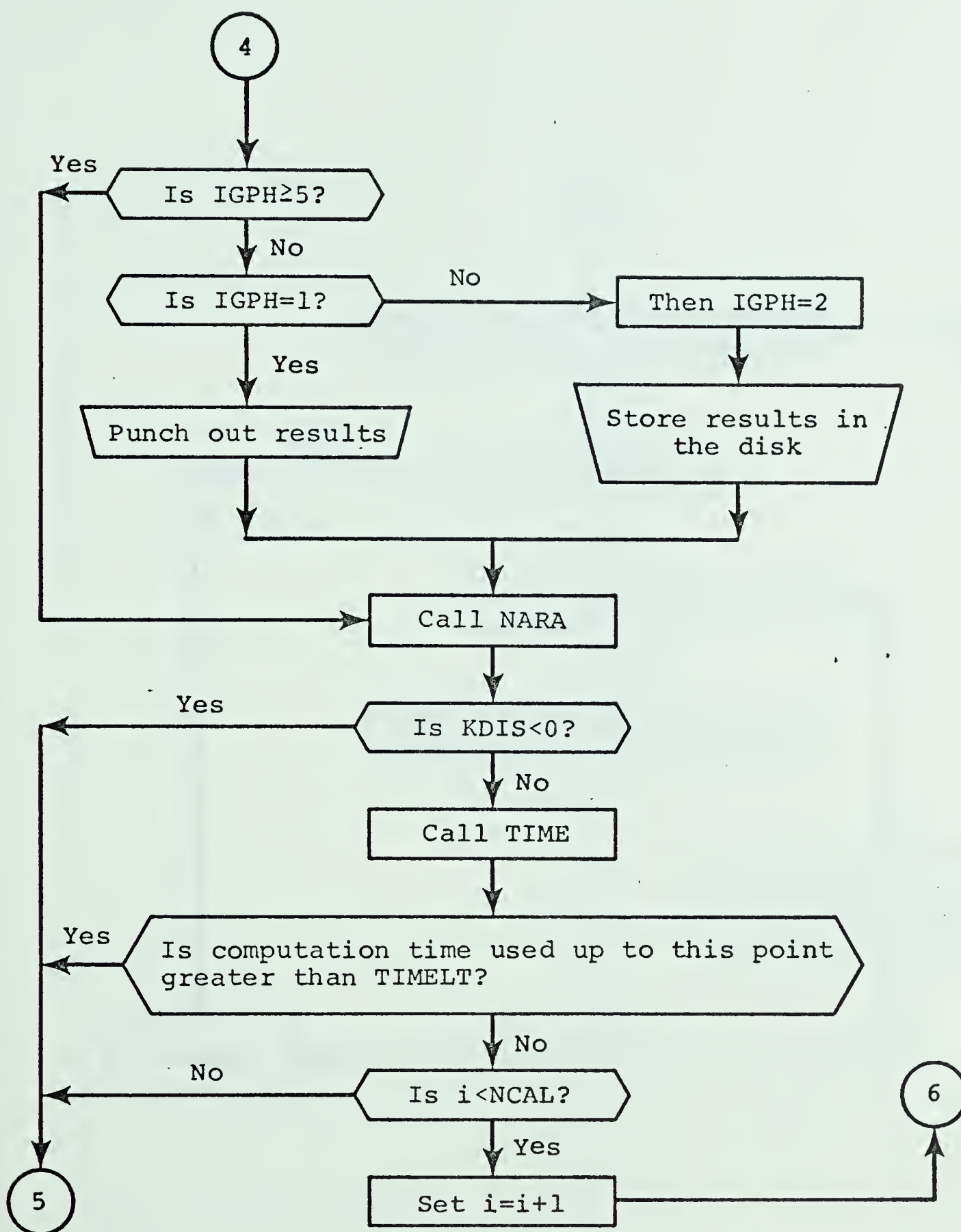


Fig. D-4 (continued) SUBROUTINE JISHIN



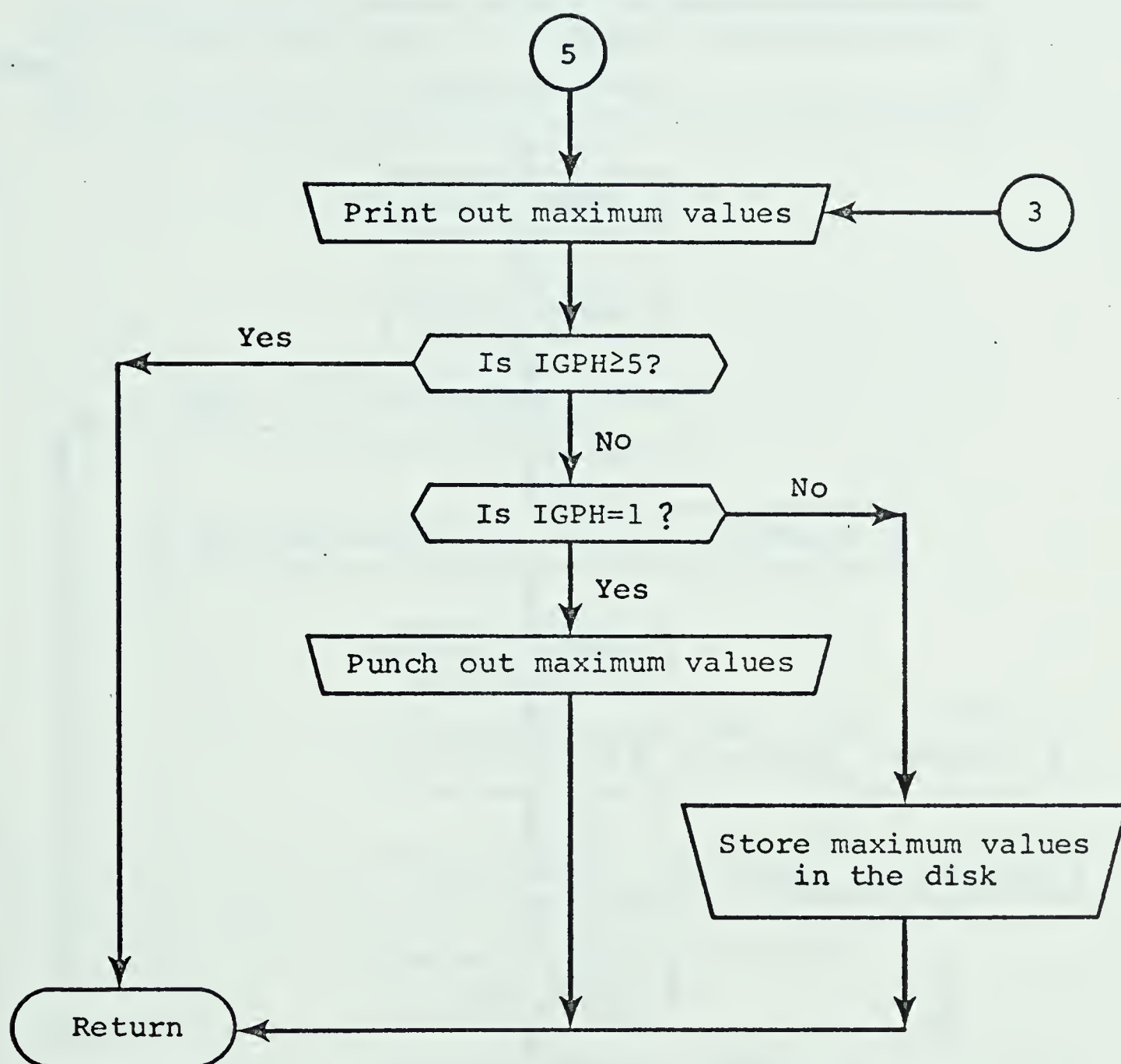


Fig. D-4 (continued) SUBROUTINE JISHIN



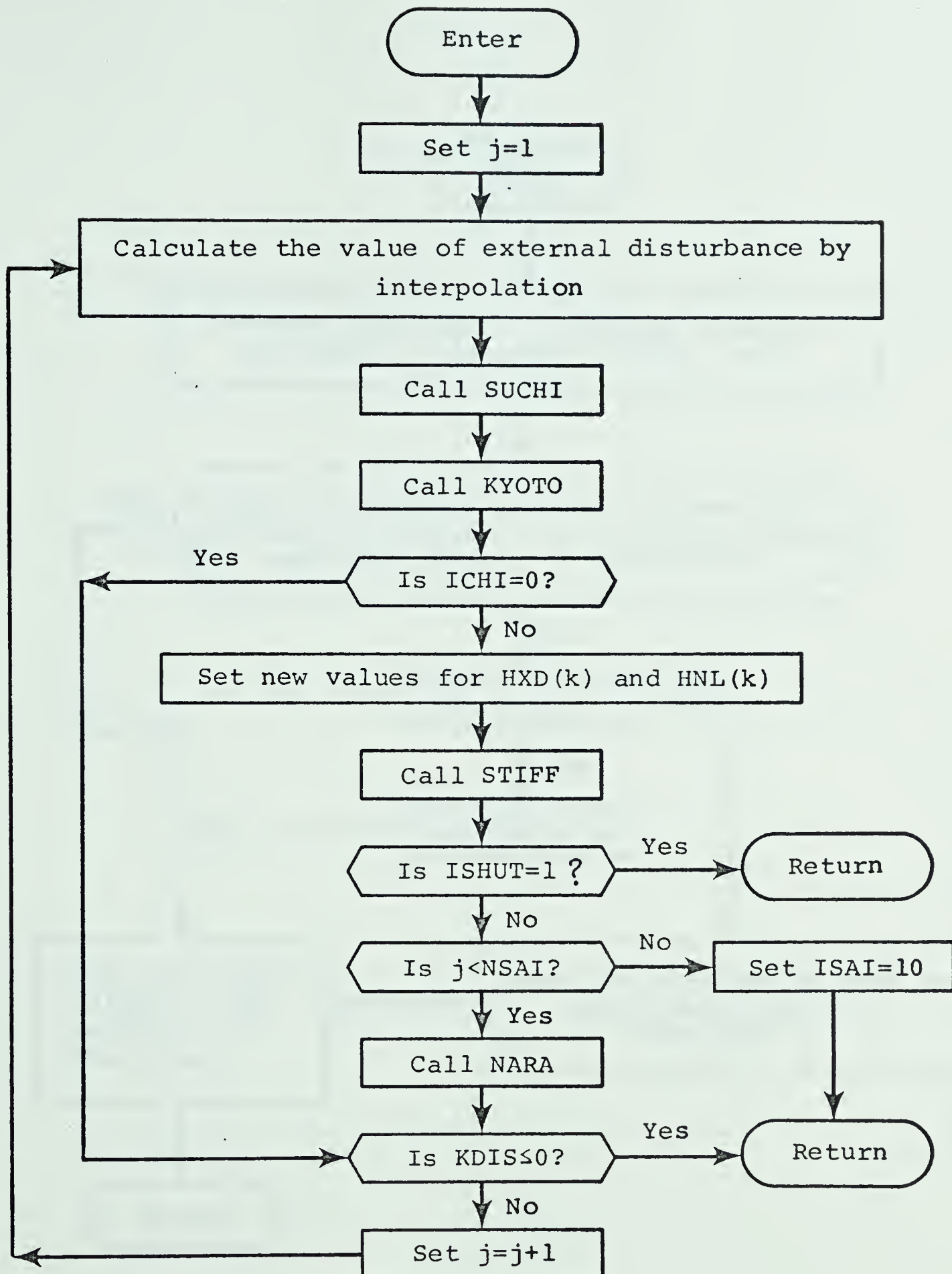


Fig. D-5 SUBROUTINE SAIBUN



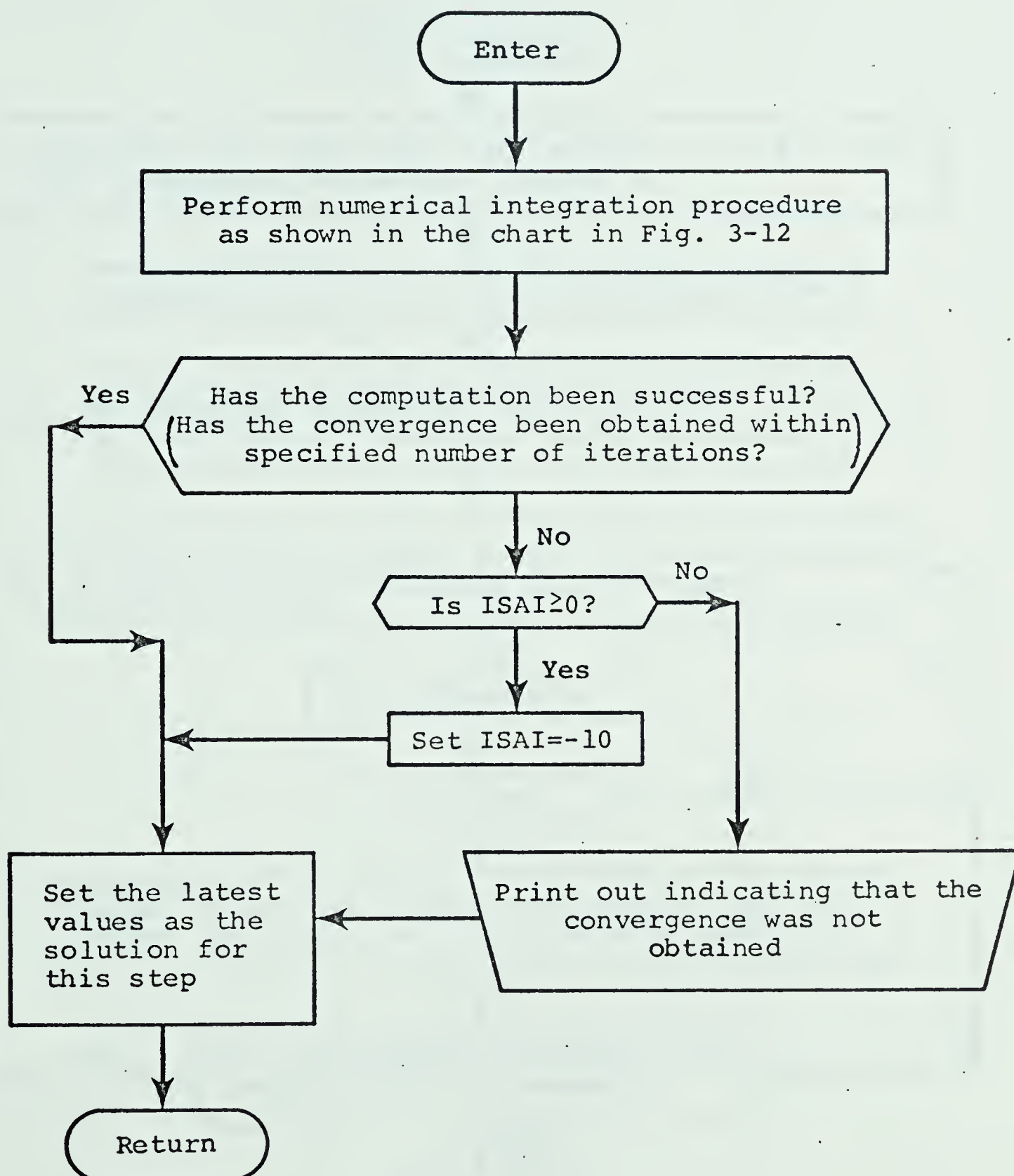


Fig. D-6 SUBROUTINE SUCHI





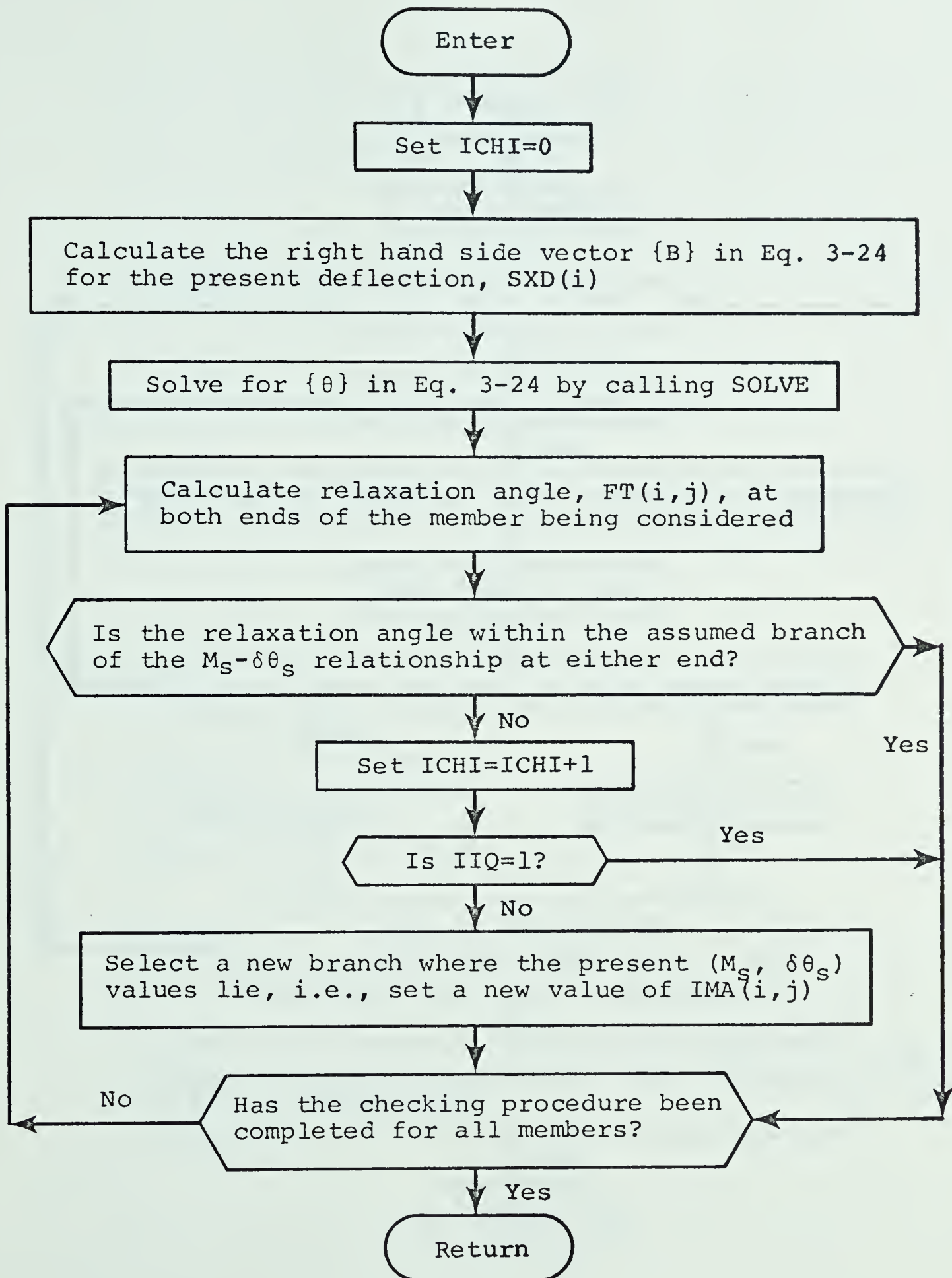


Fig. D-7 SUBROUTINE KYOTO



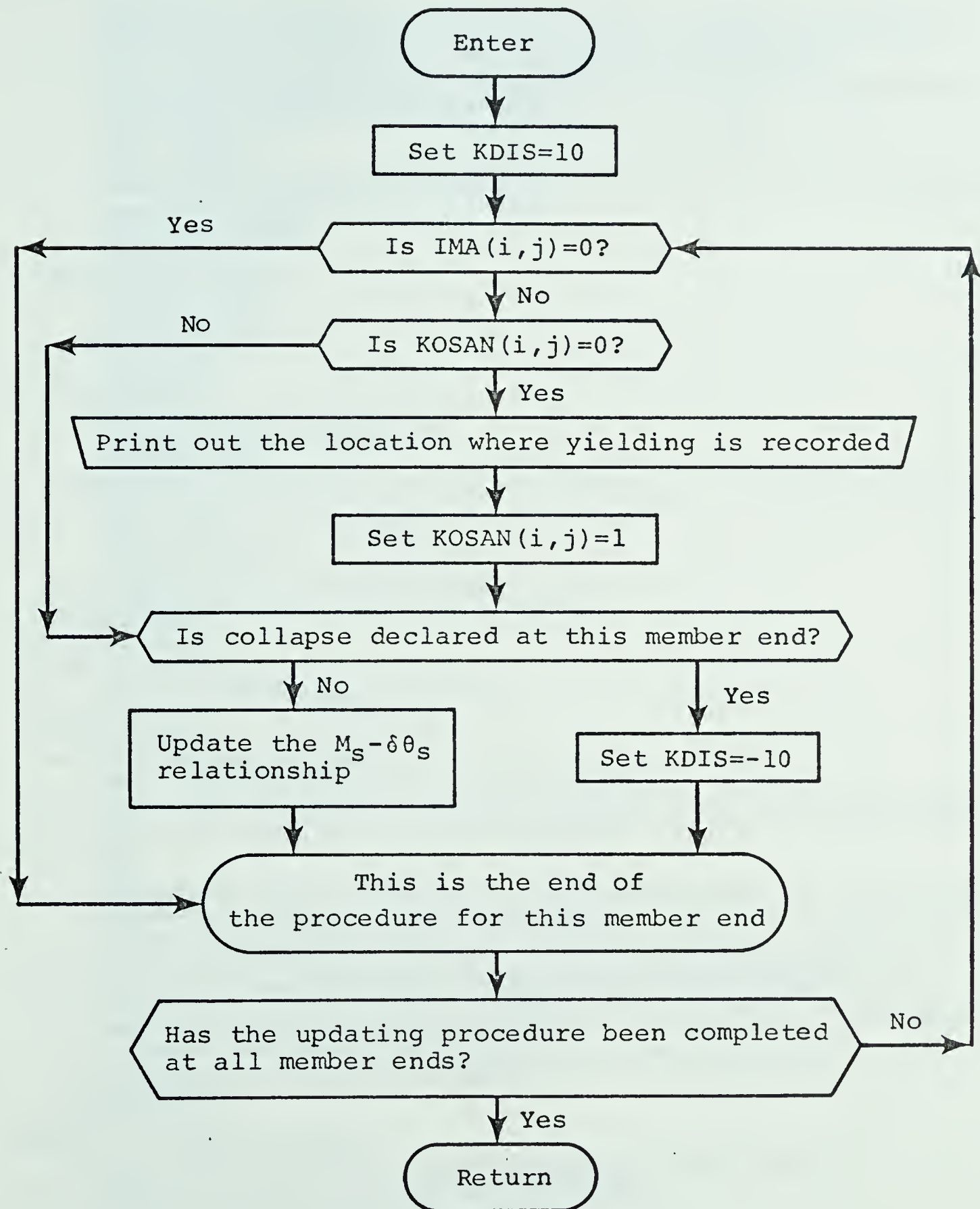


Fig. D-8 SUBROUTINE NARA



```

COMMON NS,NB,STF(225),SH(25),SPR( 5),SB( 4),RP(25, 5),UDL(25, 4)
*,IOP(225,2),ION(225,2),SLPLS(225),SLP(225,2,5),BETA(225,2,7),
1THETA(225,2,6),IMA(225,2),PMO(225,2,2),HXD(25),HNL(25)
2,EMLAST(225,2),KOSSAN(225,2),INEG(225,2),IPOS(225,2),PMC(225,2,2)
3,ROTN(225),ROTMAX(225),RCTMIN(225)
DIMENSION A(150, 11),CSM(25),Q(25,25),C(25),SM(25),IP(25)
CALL TIME(0)
CALL SAKURA (GOSA,NCAL,MXIT,NTOBU,NSAI,GR,DELTAT,SEICO,C,SM,IP,CSM
1,THAJI,TOWA,LTP,IGPH,ITIME,IDISC)
NMEB=(2*NB+1)*NS
DO 302 M=1,NMEB
DO 302 K=1,2
302 EMLAST(M,K)=0.0
IA=(NB+2)*NS
DO 100 I=1,NS
HXD(I)=0.0
HNL(I)=0.0
100 CONTINUE
CALL STIFF(Q,0,A,IA,ISHUT)
IF(ISHUT.EQ. 1) STOP
WRITE(6,200)
200 FORMAT(/1X,'STIFFNESS MATRIX FOR THE FRAME -- IN TERMS OF TOTAL ST
1OREY SHEAR.')
IF(NS.LE. 8) GO TO 230
DO 220 I=1,NS
WRITE(6,210) I,(Q(I,J),J=1,NS)
210 FORMAT(3X,'ROW',I3,8E15.6/(9X,8E15.6))
220 CONTINUE
GO TO 260
230 DO 250 I=1,NS
WRITE(6,240) I,(Q(I,J),J=1,NS)
240 FORMAT(3X,'ROW',I3,8E15.6)
250 CONTINUE
260 CALL SHUKI(Q,SM,GOME)
CALL KIKU (DELTAT,C,GOME,Q,GOSA,GR,NCAL)
CALL JISHIN (SM,CSM,C,IP,IGPH,GR,GOSA,NCAL,DELTAT,MXIT,NSAI,NTOBU,
1THAJI,TOWA,SEICO,Q,IA,A,LTP,ITIME,IDISC)
STOP
END
SUBROUTINE SAKURA (GOSA,NCAL,MXIT,NTOBU,NSAI,GR,DELTAT,SEICO,H,SM,
1IP,CSM,THAJI,TOWA,LTP,IGPH,ITIME,IDISC)
COMMON NS,NB,STF(225),SH(25),SPR( 5),SB( 4),RP(25, 5),UDL(25, 4)
*,IOP(225,2),ION(225,2),SLPLS(225),SLP(225,2,5),BETA(225,2,7),
1THETA(225,2,6),IMA(225,2),PMO(225,2,2),HXD(25),HNL(25)
2,EMLAST(225,2),KOSSAN(225,2),INEG(225,2),IPOS(225,2),PMC(225,2,2)
3,ROTN(225),ROTMAX(225),ROTMIN(225)
DIMENSION BMI(25,4),CMI(25,5),SM(25),IP(25),H(25),CSM(2
15),NES(225),TEMPO(225),NESS(225)
10 FORMAT(1H1)
20 FORMAT(1H )
COMMENT : INPUT STATEMENT
READ(5,100) NS,NB,NCAL,MXIT,NTOBU,NSAI,LTP,IGPH,TIMELT,
1DELTAT,GOSA,EM,GR,SEICO,IDISC,THAJI,TOWA
100 FORMAT( 8I5,10X,3F10.0/3F10.0,I5,25X,2F10.0)
IF(TIMELT.LT. 0.000001) TIMELT=60.0
ITIME=1FIX(TIMELT*60000.0)
NB1=NB+1

```





```

      NBB=2*NB+1
      NBBT=NBB*NS
COMMENT : INPUT STATEMENT
      READ(5,110) (SB(J),J=1,NB)
      110 FORMAT((8F10.0))
      DO 130 I=1,NS
COMMENT : INPUT STATEMENT
      READ(5,120) SM(I),H(I),SH(I),IP(I)
      120 FORMAT(3F10.0,I5)
      130 CONTINUE
      DO 140 I=1,NS
COMMENT : INPUT STATEMENT
      READ(5,110) (RP(I,J),J=1,NB1)
      140 CONTINUE
      DO 150 I=1,NS
COMMENT : INPUT STATEMENT
      READ(5,110) (BMI(I,J),J=1,NB)
      150 CONTINUE
      DO 160 I=1,NS
COMMENT : INPUT STATEMENT
      READ(5,110) (CMI(I,J),J=1,NB1)
      160 CONTINUE
      DO 190 I=1,NS
      DO 170 J=1,NB
      IJ=NBB*(I-1)+J
      STF(IJ)=2.0*EM*BMI(I,J)/SB(J)
      170 CONTINUE
      DO 180 J=1,NB1
      IJ=NBB*(I-1)+NB+J
      STF(IJ)=2.0*EM*CMI(I,J)/SH(I)
      180 CONTINUE
      190 CONTINUE
COMMENT : INPUT STATEMENT
      READ(5,110) (SPR(I),I=1,NB1)
      CSM(1)=SM(1)
      IF(NS .EQ. 1) GO TO 220
      DO 210 I=2,NS
      CSM(I)=CSM(I-1)+SM(I)
      210 CONTINUE
      220 DO 230 I=1,NS
COMMENT : INPUT STATEMENT
      READ(5,110) (UDL(I,J),J=1,NB)
      230 CONTINUE
      ITSU=0
      KUMI=0
COMMENT : INPUT STATEMENT
      240 READ(5,241) IKUTSU,(NES(K),K=1,IKUTSU)
      241 FORMAT((16I5))
      K=10000000
      DO 231 J=1,IKUTSU
      IF(NES(J) .GE. K) GO TO 231
      K=NES(J)
      IF(J .EQ. 1) GO TO 231
      NES(J)=NES(1)
      NES(1)=K
      231 CONTINUE
COMMENT : INPUT STATEMENT
      READ(5,242) (TEMPO(I),I=1,6),SLPLS(K)
      242 FORMAT(7E10.5)
      KUMI=KUMI+1

```



```

DO 245 J=1,IKUTSU
JJ=NES(J)
NESS(JJ)=KUMI
245 CONTINUE
SLP(K,1,1)=TEMPO(2)/TEMPO(1)
SLP(K,1,2)=(TEMPO(4)-TEMPO(2))/(TEMPO(3)-TEMPO(1))
SLP(K,1,3)=(TEMPO(6)-TEMPO(4))/(TEMPO(5)-TEMPO(3))
SLP(K,1,4)=SLP(K,1,2)
SLP(K,1,5)=SLP(K,1,3)
BETA(K,1,1)=0.0
BETA(K,1,2)=(TEMPO(3)*TEMPO(2)-TEMPO(1)*TEMPO(4))/(TEMPO(3)-TEMPO(
11))
BETA(K,1,3)=(TEMPO(5)*TEMPO(4)-TEMPO(3)*TEMPO(6))/(TEMPO(5)-TEMPO(
13))
BETA(K,1,4)=-BETA(K,1,2)
BETA(K,1,5)=-BETA(K,1,3)
TEMPO(4)=TEMPO(2)
THETA(K,1,1)=0.0
THETA(K,1,2)=TEMPO(1)
THETA(K,1,3)=TEMPO(5)
THETA(K,1,4)=0.0
THETA(K,1,5)=-TEMPO(1)
THETA(K,1,6)=-TEMPO(5)
PMO(K,1,1)=TEMPO(2)
PMO(K,1,2)=-TEMPO(2)
DO 270 I=1,IKUTSU
KI=NES(I)
DO 260 J=1,2
IOP(KI,J)=1
ION(KI,J)=1
IMA(KI,J)=0
EMLAST(KI,J)=0.0
INEG(KI,J)=5
IPDS(KI,J)=2
IF(I.EQ.1.AND.J.EQ.1) GO TO 260
DO 255 L=1,7
IF(L.GE.7) GO TO 256
THETA(KI,J,L)=THETA(K,1,L)
256 CONTINUE
IF(L.GE.6) GO TO 257
BETA(KI,J,L)=BETA(K,1,L)
257 CONTINUE
IF(L.GE.3) GO TO 255
PMO(KI,J,L)=PMO(K,1,L)
255 CONTINUE
SLPLS(KI)=SLPLS(K)
DO 265 L=1,5
SLP(KI,J,L)=SLP(K,1,L)
265 CONTINUE
260 CONTINUE
270 CONTINUE
THETA(K,1,5)=TEMPO(4)
THETA(K,1,6)=TEMPO(6)
ITSU=ITSU+IKUTSU
IF(ITSU.EQ.NBBT) GO TO 275
GO TO 240
275 WRITE(6,10)
WRITE(6,280)
280 FORMAT(1X,'** INPUT DATA **')
WRITE(6,290)

```



```

290 FORMAT(/1X,'BEAMS ',5X,' PLASTIC MOMENT ** STIFFNESS(2EI/L) ** U.D
1.L.')
KAKU=1
300 JS=(KAKU-1)*3+1
IF(NB .LE. KAKU*3) GO TO 301
JE=JS+2
KAKU=KAKU+1
GO TO 302
301 JE=NB
KAKU=-1
JES=JE+1-JS
GO TO (304,303,302), JES
304 WRITE(6,307) (J,J=JS,JE)
GO TO 308
303 WRITE(6,306) (J,J=JS,JE)
GO TO 308
302 WRITE(6,305) (J,J=JS,JE)
305 FORMAT(3X,'FLOOR',3(10X,'---- BAY NO. (' ,I3,' ) ----',7X))
306 FORMAT(3X,'FLOOR',2(10X,'---- BAY NO. (' ,I3,' ) ----',7X))
307 FORMAT(3X,'FLOOR', 10X,'---- BAY NO. (' ,I3,' ) ----')
308 DO 320 I=1,NS
IJ=NBB*(I-1)+JS
IJJ=IJ+JE-JS
DO 310 K=JS,JE
KK=IJ-JS+K
TEMPO(KK)=UDL(I,K)
310 CONTINUE
WRITE(6,315) I,((PMO(J,1,1),STF(J),TEMPO(J)),J=IJ,IJJ)
315 FORMAT(1X,I6,1X,3(2X,3E13.5))
320 CONTINUE
WRITE(6,325) (SB(J),J=JS,JE)
325 FORMAT(3X,'BAY LENGTH',10X,E13.5,2(28X,E13.5))
IF(KAKU .GE. 0) GO TO 300
WRITE(6,330)
330 FORMAT(/1X,'COLUMNS',5X,' PLASTIC MOMENT ** STIFFNESS(2EI/H) ** LE
NGTH OF RIGID ZONE (EACH SIDE OF COLUMN)')
KAKU=1
340 JS=(KAKU-1)*3+1
IF(NB1 .LE. KAKU*3) GO TO 341
JE=JS+2
KAKU=KAKU+1
GO TO 342
341 JE=NB1
KAKU=-1
JES=JE+1-JS
GO TO (344,343,342), JES
344 WRITE(6,347) (J,J=JS,JE)
GO TO 348
343 WRITE(6,346) (J,J=JS,JE)
GO TO 348
342 WRITE(6,345) (J,J=JS,JE)
345 FORMAT(3X,'STOREY',3(9X,'--- COLUMN NO. (' ,I3,' ) ---',7X))
346 FORMAT(3X,'STOREY',2(9X,'--- COLUMN NO. (' ,I3,' ) ---',7X))
347 FORMAT(3X,'STOREY', 9X,'--- COLUMN NO. (' ,I3,' ) ---')
348 DO 360 I=1,NS
IJ=NBB*(I-1)+NB+JS
IJJ=IJ+JE-JS
DO 350 K=JS,JE
KK=IJ-JS+K
TEMPO(KK)=RP(I,K)

```





```

350 CONTINUE
  WRITE(6,315) I,((PMO(J,1,1),STF(J),TEMPO(J)),J=1J,IJJ)
360 CONTINUE
  WRITE(6,370) (SPR(I),I=JS,JE)
370 FORMAT(3X,'BASE SPRING CONST.',2X,E13.5,2(28X,E13.5))
  IF(KAKU .GE. 0) GO TO 340
  WRITE(6,380)
380 FORMAT(/,1X,'CTHER STRUCTURAL PROPERTIES')
  IF(LTP .GE. 5) GO TO 420
  WRITE(6,390)
390 FORMAT( 3X,'STOREY',5X,'HEIGHT',9X,'WEIGHT',4X,'CUMULATIVE WT.',2
1X,'DAMPING COEF.')
```

DO 410 I=1,NS

```

  WRITE(6,400) I,SH(I),SM(I),CSM(I),H(I)
400 FORMAT(1X,I6,8E15.5)
  SM(I)=SM(I)/GR
  CSM(I)=CSM(I)/GR
410 CONTINUE
  GO TO 445
```

COMMENT : INPUT STATEMENT (ONLY WHEN BLAST LOADING)

```

420 READ(5,110) (CSM(I),I=1,NS)
  WRITE(6,430)
430 FORMAT( 3X,'STOREY',5X,'HEIGHT',9X,'WEIGHT',5X,'DAMPING COEF.',3X
1,'LOAD FACTOR')
  DO 440 I=1,NS
  WRITE(6,400) I,SH(I),SM(I),H(I),CSM(I)
  SM(I)=SM(I)/GR
  CSM(I)=-CSM(I)
  IF(I .EQ. 1) GO TO 440
  CSM(I)=CSM(I-1)+CSM(I)
440 CONTINUE
445 WRITE(6,450)
450 FORMAT(/,1X,'THE SPRING TO SIMULATE THE PLASTIC BEHAVIOUR AND/OR A
1XIAL LOAD EFFECT HAS A MOMENT-THETA RELATION GIVEN BELOW')
  DO 500 L=1,KUMI
  IKUTSU=0
  DO 460 LL=1,NBBT
  IF(NESS(LL) .NE. L) GO TO 460
  IKUTSU=IKUTSU+1
  NES(IKUTSU)=LL
460 CONTINUE
  K=NES(1)
  IF(IKUTSU .LE. 22) GO TO 481
  WRITE(6,480) (NES(I),I=1,IKUTSU)
480 FORMAT(3X,'FOR THE MEMBER NO.',22(I4,', '))/(6X,25(I4,', ')))
  GO TO 490
481 WRITE(6,482) (NES(I),I=1,IKUTSU)
482 FORMAT(3X,'FOR THE MEMBER NO.',22(I4,', '))
490 WRITE(6,491) THETA(K,1,1),PMO(K,1,1),THETA(K,1,2),THETA(K,1,5),
1THETA(K,1,3),THETA(K,1,6),SLPLS(K)
491 FORMAT(3X,'THETA-MOMENT',3(2X,2E13.5,'; '),3X,'PLASTIC SLOPE',E14.5
1)
  THETA(K,1,5)=-THETA(K,1,2)
  THETA(K,1,6)=-THETA(K,1,3)
500 CONTINUE
  DO 501 M=1,NBBT
  DO 501 K=1,2
  PMC(M,K,1)=PMO(M,K,1)
  PMC(M,K,2)=PMO(M,K,2)
501 CONTINUE
```





```

RETURN
END
SUBROUTINE STIFF(Q,INIT,A,IA,ISHUT)
COMMON NS,NB,STF(225),SH(25),SPR( 5),SB( 4),RP(25, 5),UDL(25, 4)
*,IOP(225,2),ION(225,2),SLPLS(225),SLP(225,2,5),BETA(225,2,7),
1THETA(225,2,6),IMA(225,2),PMO(225,2,2),HXD(25),HNL(25)
2,EMLAST(225,2),KOSSAN(225,2),INEG(225,2),IPOS(225,2),PMC(225,2,2)
3,ROTN(225),ROTMAX(225),ROTMIN(225)
DIMENSION A(150,11),Q(25,25)
ISHUT=0
CALL FUJI(A,IA)
N1=NB+1
N2=NB+2
N3=NB+3
NE=2*NB+3
DO 260 I=1,NS
DO 250 J=1,N1
IJ=N2*(I-1)+J
DO 240 K=1,N2
IK=IJ+K
N2S=N2*NS+1
IF(IK .GE. N2S) GO TO 250
NK=N2-K
N3J=N3-J
IF(K .GE. N3J) NK=NK+1
IF(ABS(A(IK,NK)) .LT. 1.0E-30) GO TO 240
IF(ABS(A(IJ,N2)) .LT. 1.0E-30) GO TO 270
A(IK,NK)=-A(IK,NK)/A(IJ,N2)
IF(ABS(A(IK,NK)) .LT. 1.0E2) GO TO 220
WRITE(6,210) A(IK,NK)
210 FORMAT(/1X,'WARNING - ACCURACY LOSS IN CALCULATING STIFFNESS MATRI
1X - MULTIPLIER=',E12.4)
220 DO 230 L=N3,NE
NL=NK+L-N2
A(IK,NL)=A(IK,NL)+A(IK,NK)*A(IJ,L)
230 CONTINUE
240 CONTINUE
250 CONTINUE
260 CONTINUE
GO TO 290
270 WRITE(6,280)
280 FORMAT(/1X,'DIVISION BY ZERO WHEN FINDING STIFFNESS MATRIX')
ISHUT=1
RETURN
290 CALL YURI(Q,A,IA,INIT)
RETURN
END
SUBROUTINE FUJI(A,IA)
COMMON NS,NB,STF(225),SH(25),SPR( 5),SB( 4),RP(25, 5),UDL(25, 4)
*,IOP(225,2),ION(225,2),SLPLS(225),SLP(225,2,5),BETA(225,2,7),
1THETA(225,2,6),IMA(225,2),PMO(225,2,2),HXD(25),HNL(25)
2,EMLAST(225,2),KOSSAN(225,2),INEG(225,2),IPOS(225,2),PMC(225,2,2)
3,ROTN(225),ROTMAX(225),ROTMIN(225)
DIMENSION A(150,11)
N1=NB+1
N2=NB+2
N3=NB+3
NBB=2*NB+1
NE=NBB+2
DO 100 I=1,IA

```



```

      DO 90 J=1,NE
      A(I,J)=0.0
90    CONTINUE
100   CONTINUE
      DO 260 I=1,NS
      DO 250 J=1,N2
      IJ=N2*(I-1)+J
      IF(J .EQ. N2) GO TO 200
      IF(I .EQ. 1) GO TO 110
      MA=NBB*(I-1)-N1+J
      CALL IZU(VA,VB,MA,2,0.0,0.0,1,1)
      A(IJ, 1)=VA
      A(IJ,N2)=VB
110   IF(J .EQ. 1) GO TO 120
      ML=NBB*(I-1)+J-1
      FR1=RP(I,J-1)/SB(J-1)
      FR2=RP(I,J)/SB(J-1)
      CALL IZU(VA,VB,ML,2,FR1,FR2,1,1)
      A(IJ,N1)=VA
      A(IJ,N2)=A(IJ,N2)+VB
120   IF(J .EQ. N1) GO TO 130
      MR=NBB*(I-1)+J
      FR1=RP(I,J)/SB(J)
      FR2=RP(I,J+1)/SB(J)
      CALL IZU(VA,VB,MR,1,FR1,FR2,1,1)
      A(IJ,N3)=VB
      A(IJ,N2)=A(IJ,N2)+VA
130   MB=NBB*I-N1+J
      IF(I .EQ. NS) GO TO 140
      CALL IZU(VA,VB,MB,1,0.0,0.0,1,1)
      A(IJ,NE)=VB
      A(IJ,N2)=A(IJ,N2)+VA
      GO TO 250
140   CALL IZU(VA,VB,MB,1,0.0,0.0,-1,1)
      A(IJ,N2)=A(IJ,N2)+VA
      GO TO 250
200   DO 220 K=1,N1
      KK=NBB*I-N1+K
      KB=N1+K
      IF(I .EQ. NS) GO TO 210
      CALL IZU(VA,VB,KK,3,0.0,0.0,1,1)
      A(IJ, K)=VA
      A(IJ,KB)=VB
      GO TO 220
210   CALL IZU(VA,VB,KK,3,0.0,0.0,-1,1)
      A(IJ, K)=VA
220   CONTINUE
      A(IJ,NE)=SH(I)
250   CONTINUE
260   CONTINUE
      RETURN
      END
      SUBROUTINE IZU(VA,VB,M,II,FR1,FR2,IASHI,IGO)
      COMMON NS,NB,STF(225),SH(25),SPR( 5),SB( 4),RP(25, 5),UDL(25, 4)
      *,IOP(225,2),ION(225,2),SLPLS(225),SLP(225,2,5),BETA(225,2,7),
      1THETA(225,2,6),IMA(225,2),PMO(225,2,2),HXD(25),HNL(25)
      2,EMLAST(225,2),KOSSAN(225,2),INEG(225,2),IPOS(225,2),PMC(225,2,2)
      3,ROTN(225),ROTMAX(225),RCTMIN(225)
      FR3=1.0-FR1-FR2
      FRA=FR1

```



```

FRB=FR2
IF(IGO .LT. 0 .AND. II .EQ. 1) FR1=0.0
IF(IGO .LT. 0 .AND. II .EQ. 2) FR2=0.0
IF(IASHI .LT. 0) J=M-(2*NB+1)*(NS-1)-NB
IF(IMA(M,1) .LE. -1) GO TO 111
ICON=IMA(M,1)+1
W=SLP(M,1,ICON)
GO TO 112
111 ICON=3-IMA(M,1)
W=SLP(M,1,ICON)
112 IF(IMA(M,2) .LE. -1) GO TO 113
ICON=IMA(M,2)+1
Y=SLP(M,2,ICON)
GO TO 120
113 ICON=3-IMA(M,2)
Y=SLP(M,2,ICON)
120 IF(ABS(W) .LT. STF(M) .OR. ABS(Y) .LT. STF(M)) GO TO 130
IF(W .LT. 1.0E30 .AND. Y .LT. 1.0E30) GO TO 105
BUN=ALOG(W)+ALOG(Y)
IF(BUN .LT. 150.0) GO TO 105
DEN=1.0+2.0*STF(M)*(1.0/W+1.0/Y)/FR3
GO TO 110
105 DEN=1.0+2.0*STF(M)*(1.0/W+1.0/Y)/FR3+3.0*(STF(M)/FR3/W)*(STF(M)/FR
13/Y)
110 IF(IASHI .LT. 0) GO TO 125
VC=(1.0+3.0*(FR1+FR2)/FR3+6.0*FR1*FR2/FR3**2+3.0*STF(M)*(FR1/W+FR2
1/Y)/FR3**2+3.0*FR1*FR2*STF(M)*(1.0/W+1.0/Y)/FR3**3)*STF(M)/FR3/DEN
IF(II .EQ. 2) GO TO 122
VB=VC
IF(IGO .LT. 0) FR1=FRA
VA=2.0+3.0*FR1/FR3+3.0*STF(M)*(1.0+FR1/FR3)/FR3/Y
IF(IGO .LT. 0) GO TO 121
VA=VA+3.0*(1.0+2.0*FR1/FR3)*FR1/FR3+3.0*STF(M)*((1.0+FR1/FR3)*FR1/
1FR3**2/Y+FR1**2/FR3**3/W)
121 VA=VA*STF(M)/FR3/DEN
IF(II .EQ. 1) RETURN
VA=VA+VC
GO TO 123
122 VA=VC
IF(IGO .LT. 0) FR2=FRB
123 VB=2.0+3.0*FR2/FR3+3.0*STF(M)*(1.0+FR2/FR3)/FR3/W
IF(IGO .LT. 0) GO TO 124
VB=VB+3.0*(1.0+2.0*FR2/FR3)*FR2/FR3+3.0*STF(M)*((1.0+FR2/FR3)*FR2/
1FR3**2/W+FR2**2/FR3**3/Y)
124 VB=VB*STF(M)/FR3/DEN
IF(II .EQ. 2) RETURN
VB=VB+VC
RETURN
125 G=SPR(J)*DEN+STF(M)*(2.0+3.0*STF(M)/W)
VA=(2.0+3.0*STF(M)/Y-STF(M)/G)*STF(M)/DEN
IF(II .LE. 2) RETURN
IF(SPR(J) .GT. STF(M)) GO TO 126
VA=VA+SPR(J)*STF(M)/G
RETURN
126 G=DEN+STF(M)*(2.0+3.0*STF(M)/W)/SPR(J)
VA=VA+STF(M)/G
RETURN
130 IF(ABS(W) .LE. STF(M)) GO TO 140
DEN=Y+2.0*STF(M)*(Y/W+1.0)/FR3+3.0*(STF(M)/FR3/W)*STF(M)/FR3
IF(IASHI .LT. 0) GO TO 135

```





```

VC=(Y*(1.0+3.0*(FR1+FR2)/FR3+6.0*FR1*FR2/FR3**2)+3.0*STF(M)*((FR1*Y
1/W+FR2)/FR3**2+3.0*FR1*FR2*STF(M)*(Y/W+1.0)/FR3**3)*STF(M)/FR3/DEN
IF(II .EQ. 2) GO TO 132
VB=VC
IF(IGO .LT. 0) FR1=FRA
VA=Y*(2.0+3.0*FR1/FR3)+3.0*STF(M)*((1.0+FR1/FR3)/FR3
IF(IGO .LT. 0) GO TO 131
VA=VA+3.0*Y*(1.0+2.0*FR1/FR3)*FR1/FR3+3.0*STF(M)*((1.0+FR1/FR3)*FR
11/FR3**2+Y*FR1**2/FR3**3/W)
131 VA=VA*STF(M)/FR3/DEN
IF(II .EQ. 1) RETURN
VA=VA+VC
GO TO 133
132 VA=VC
IF(IGO .LT. 0) FR2=FRB
133 VB=Y*(2.0+3.0*FR2/FR3+3.0*STF(M)*((1.0+FR2/FR3)/FR3/W)
IF(IGO .LT. 0) GO TO 134
VB=VB+3.0*Y*(1.0+2.0*FR2/FR3)*FR2/FR3+3.0*STF(M)*(Y*(1.0+FR2/FR3)*
1FR2/FR3**2/W+FR2**2/FR3**3)
134 VB=VB*STF(M)/FR3/DEN
IF(II .EQ. 2) RETURN
VB=VB+VC
RETURN
135 G=SPR(J)*DEN+Y*STF(M)*((2.0+3.0*STF(M)/W)
VA=(2.0*Y+3.0*STF(M)-Y**2*STF(M)/G)*STF(M)/DEN
IF(II .LE. 2) RETURN
IF(SPR(J) .GT. STF(M)) GO TO 136
VA=VA+SPR(J)*Y*STF(M)/G
RETURN
136 G=DEN+Y*STF(M)*((2.0+3.0*STF(M)/W)/SPR(J)
VA=VA+Y*STF(M)/G
RETURN
140 IF(ABS(Y) .LE. STF(M)) GO TO 150
DEN=W+2.0*STF(M)*((1.0+W/Y)/FR3+3.0*(STF(M)/FR3)*(STF(M)/FR3/Y)
IF(IASHI .LT. 0) GO TO 145
VC=(W*(1.0+3.0*(FR1+FR2)/FR3+6.0*FR1*FR2/FR3**2)+3.0*STF(M)*((FR1+F
1R2*W/Y)/FR3**2+3.0*FR1*FR2*STF(M)*((1.0+W/Y)/FR3**3)*STF(M)/FR3/DEN
IF(II .EQ. 2) GO TO 142
VB=VC
IF(IGO .LT. 0) FR1=FRA
VA=W*(2.0+3.0*FR1/FR3+3.0*STF(M)*((1.0+FR1/FR3)/FR3/Y)
IF(IGO .LT. 0) GO TO 141
VA=VA+3.0*W*(1.0+2.0*FR1/FR3)*FR1/FR3+3.0*STF(M)*(W*(1.0+FR1/FR3)*
1FR1/FR3**2/Y+FR1**2/FR3**3)
141 VA=VA*STF(M)/FR3/DEN
IF(II .EQ. 1) RETURN
VA=VA+VC
GO TO 143
142 VA=VC
IF(IGO .LT. 0) FR2=FRB
143 VB=W*(2.0+3.0*FR2/FR3)+3.0*STF(M)*((1.0+FR2/FR3)/FR3
IF(IGO .LT. 0) GO TO 144
VB=VB+3.0*W*(1.0+2.0*FR2/FR3)*FR2/FR3+3.0*STF(M)*((1.0+FR2/FR3)*FR
12/FR3**2+W*FR2**2/FR3**3/Y)
144 VB=VB*STF(M)/FR3/DEN
IF(II .EQ. 2) RETURN
VB=VB+VC
RETURN
145 G=SPR(J)*DEN+STF(M)*((2.0*W+3.0*STF(M))
VA=W*(2.0+3.0*STF(M)/Y-W*STF(M)/G)*STF(M)/DEN

```



```

      IF(II .LE. 2) RETURN
      IF(SPR(J) .GT. STF(M)) GO TO 146
      VA=VA+SPR(J)*W*STF(M)/G
      RETURN
146  G=DEN+STF(M)*(2.0*W+3.0*STF(M))/SPR(J)
      VA=VA+W*STF(M)/G
      RETURN
150  DEN=W*Y+2.0*STF(M)*(W+Y)/FR3+3.0*(STF(M)/FR3)**2
      IF(IASHI .LT. 0) GO TO 155
      VC=(W*Y*(1.0+3.0*(FR1+FR2)/FR3+6.0*FR1*FR2/FR3**2)+3.0*STF(M)*(FR1
1  *Y+FR2*W)/FR3**2+3.0*FR1*FR2*STF(M)*(W+Y)/FR3**3)*STF(M)/FR3/DEN
      IF(II .EQ. 2) GO TO 152
      VB=VC
      IF(IGO .LT. 0) FR1=FRA
      VA=W*(Y*(2.0+3.0*FR1/FR3)+3.0*STF(M)*(1.0+FR1/FR3)/FR3)
      IF(IGO .LT. 0) GO TO 151
      VA=VA+3.0*W*Y*(1.0+2.0*FR1/FR3)*FR1/FR3+3.0*STF(M)*(W*(1.0+FR1/FR3
1  )*FR1/FR3**2+Y*FR1**2/FR3**3)
151  VA=VA*STF(M)/FR3/DEN
      IF(II .EQ. 1) RETURN
      VA=VA+VC
      GO TO 153
152  VA=VC
      IF(IGO .LT. 0) FR2=FRB
153  VB=Y*(W*(2.0+3.0*FR2/FR3)+3.0*STF(M)*(1.0+FR2/FR3)/FR3)
      IF(IGO .LT. 0) GO TO 154
      VB=VB+3.0*W*Y*(1.0+2.0*FR2/FR3)*FR2/FR3+3.0*STF(M)*(Y*(1.0+FR2/FR3
1  )*FR2/FR3**2+W*FR2**2/FR3**3)
154  VB=VB*STF(M)/FR3/DEN
      IF(II .EQ. 2) RETURN
      VB=VB+VC
      RETURN
155  G=SPR(J)*DEN+Y*STF(M)*(2.0*W+3.0*STF(M))
      VA=W*(2.0*Y+3.0*STF(M)-W*Y**2*STF(M)/G)*STF(M)/DEN
      IF(II .LE. 2) RETURN
      IF(SPR(J) .GT. STF(M)) GO TO 156
      VA=VA+SPR(J)*W*Y*STF(M)/G
      RETURN
156  G=DEN+Y*STF(M)*(2.0*W+3.0*STF(M))/SPR(J)
      VA=VA+W*Y*STF(M)/G
      RETURN
      END
      SUBROUTINE YURI (O,AI,IA,INIT)
      COMMON NS,NB,STF(225),SH(25),SPR( 5),SB( 4),RP(25, 5),UDL(25, 4)
      *,IOP(225,2),ION(225,2),SLPLS(225),SLP(225,2,5),BETA(225,2,7),
      1THETA(225,2,6),IMA(225,2),PMO(225,2,2),HXD(25),HNL(25)
      2,EMLAST(225,2),KCSSAN(225,2),INEG(225,2),IPOS(225,2),PMC(225,2,2)
      3,ROTN(225),ROTMAX(225),ROTMIN(225)
      DIMENSION SXD(25),Q(25,25),AI(150,11),BH(150),BB(150),QTEM(25)
      IF(INIT .NE. 0) GO TO 130
      DO 100 I=1,NS
      SXD(I)=0.0
100  CONTINUE
      DO 110 J=1,IA
      BB(J)=B(J,SXD)
110  CONTINUE
      CALL SOLVE (AI,BB,QTEM)
      DO 120 I=1,NS
      HNL(I)=QTEM(I)
120  CONTINUE

```



```

130 DO 140 I=1,NS
    SXD(I)=HXD(I)
140 CONTINUE
    DO 150 I=1,IA
        BH(I)=B(I,SXD)
150 CONTINUE
    DO 180 I=1,NS
        SXD(I)=HXD(I)+1.0
        DO 160 K=1,IA
            BB(K)=B(K,SXD)-BH(K)
160 CONTINUE
        CALL SOLVE (AI,BB,QTEM)
        DO 170 J=1,NS
            Q(J,I)=QTEM(J)
170 CONTINUE
        SXD(I)=HXD(I)
180 CONTINUE
    RETURN
    END
    FUNCTION B(IJ,SXD)
        COMMON NS,NB,STF(225),SH(25),SPR( 5),SB( 4),RP(25, 5),UDL(25, 4)
        *,IOP(225,2),ION(225,2),SLPLS(225),SLP(225,2,5),BETA(225,2,7),
        1THETA(225,2,6),IMA(225,2),PMO(225,2,2),HXD(25),HNL(25)
        2,EMLAST(225,2),KOSSAN(225,2),INEG(225,2),IPOS(225,2),PMC(225,2,2)
        3,ROTN(225),ROTMAX(225),ROTMIN(225)
        DIMENSION SXD(25)
        B=0.0
        NB1=NB+1
        NB2=NB+2
        I=(IJ-1)/NB2+1
        J=IJ-NB2*(I-1)
        IF(J .EQ. NB2) GO TO 200
        IF(I .EQ. 1) GO TO 110
        MA=(2*NB+1)*(I-1)-NB1+J
        S=SH(I-1)
        R=(SXD(I-1)-SXD(I))/SH(I-1)
        B=UHEN(MA,S,2,0.0,R,0.0,0.0,1,1)
110 IF(J .EQ. 1) GO TO 120
        ML=(2*NB+1)*(I-1)+J-1
        FR1=RP(I,J-1)/SB(J-1)
        FR2=RP(I,J)/SB(J-1)
        UL=UDL(I,J-1)
        S=SB(J-1)
        B=B+UHEN(ML,S,2,UL,0.0,FR1,FR2,1,1)
120 IF(J .EQ. NB1) GO TO 130
        MR=(2*NB+1)*(I-1)+J
        FR1=RP(I,J)/SB(J)
        FR2=RP(I,J+1)/SB(J)
        UL=UDL(I,J)
        S=SB(J)
        B=B+UHEN(MR,S,1,UL,0.0,FR1,FR2,1,1)
130 MB=(2*NB+1)*I-NB1+J
        S=SH(I)
        IF(I .EQ. NS) GO TO 140
        R=(SXD(I)-SXD(I+1))/SH(I)
        B=B+UHEN(MB,S,1,0.0,R,0.0,0.0,1,1)
        RETURN
140 R=SXD(NS)/SH(NS)
        B=B+UHEN(MB,S,1,0.0,R,0.0,0.0,-1,1)
        RETURN

```





```

200 DO 220 K=1,NB1
   KK=(2*NB+1)*I-NB1+K
   S=SH(I)
   IF(I .EQ. NS) GO TO 210
   R=(SXD(I)-SXD(I+1))/SH(I)
   B=B+UHEN(KK,S,3,0.0,R,0.0,0.0,1,1)
   GO TO 220
210 R=SXD(NS)/SH(NS)
   B=B+UHEN(KK,S,3,0.0,R,0.0,0.0,-1,1)
220 CONTINUE
   RETURN
   END
   FUNCTION UHEN(M,S,II,UL,R,FR1,FR2,IASHI,IGO)
   COMMON NS,NB,STF(225),SH(25),SPR( 5),SB( 4),RP(25, 5),UDL(25, 4)
   *,IOP(225,2),ION(225,2),SLPLS(225),SLP(225,2,5),BETA(225,2,7),
   1THETA(225,2,6),IMA(225,2),PMO(225,2,2),HXD(25),HNL(25)
   2,EMLAST(225,2),KCSSAN(225,2),INEG(225,2),IPOS(225,2),PMC(225,2,2)
   3,ROTN(225),ROTMX(225),POTMIN(225)
   UHEN=0.0
   FR3=1.0-FR1-FR2
   IF(IGO .LT. 0 .AND. II .EQ.1) FR1=0.0
   IF(IGO .LT. 0 .AND. II .EQ.2) FR2=0.0
   FEMD=UL*(FR3*S)**2/12.0
   FEMC=-FEMD
   AFC=-0.5*UL*FR1*(1.0-FR2)*S**2
   AFD=0.5*UL*FR2*(1.0-FR1)*S**2
   IF(IASHI .LT. 0) J=M-(2*NB+1)*(NS-1)-NB
   CER=2.01*STF(M)
   IF(IMA(M,1) .LE. -1) GO TO 111
   ICON=IMA(M,1)+1
   W=SLP(M,1,ICON)
   IF(IMA(M,1) .EQ. 0 .AND. W .GE. CER) GO TO 112
   X=BETA(M,1,ICON)
   GO TO 112
111 ICON=3-IMA(M,1)
   W=SLP(M,1,ICON)
   X=BETA(M,1,ICON)
112 IF(IMA(M,2) .LE. -1) GO TO 113
   ICON=IMA(M,2)+1
   Y=SLP(M,2,ICON)
   IF(IMA(M,2) .EQ. 0 .AND. Y .GE. CER) GO TO 115
   Z=BETA(M,2,ICON)
   GO TO 115
113 ICON=3-IMA(M,2)
   Y=SLP(M,2,ICON)
   Z=BETA(M,2,ICON)
115 CER=2.0*STF(M)
   IF(ABS(W) .LT. STF(M) .OR. ABS(Y) .LT. STF(M)) GO TO 130
   IF(W .LT. 1.0E30 .AND. Y .LT. 1.0E30) GO TO 105
   BUN=ALOG(W)+ALOG(Y)
   IF(BUN .LT. 150.0) GO TO 105
   DEN=1.0+2.0*STF(M)*(1.0/W+1.0/Y)/FR3
   GO TO 110
105 DEN=1.0+2.0*STF(M)*(1.0/W+1.0/Y)/FR3+3.0*(STF(M)/FR3/W)*(STF(M)/FR
   13/Y)
110 IF(IMA(M,1) .EQ. 0 .AND. W .GE. CER) GO TO 116
   XOW=X/W
   GO TO 117
116 IP=IOP(M,1)
   XOW=PMO(M,1,1)/W-THETA(M,1,IP)

```





```

117 IF(IMA(M,2) .EQ. 0 .AND. Y .GE. CER) GO TO 118
    ZOY=Z/Y
    GO TO 120
118 IP=IOP(M,2)
    ZOY=PMO(M,2,1)/Y-THETA(M,2,IP)
120 IF(IASHI .LT. 0) GO TO 125
    IF(II .EQ. 2) GO TO 121
    VD=3.0*(1.0+STF(M)/Y)*R
    VD=VD-(2.0+3.0*FR1/FR3+3.0*STF(M)*(1.0+FR1/FR3)/FR3/Y)*XOW
    VD=VD-(1.0+3.0*FR1/FR3+3.0*STF(M)*FR1/FR3**2/W)*ZOY
    VD=VD*STF(M)/FR3
    UHEN=(VD-FEMC*(1.0+3.0*STF(M)*(1.0+FR1/FR3)/FR3/Y-3.0*STF(M)*FR1/FR3**2/W))/DEN-AFC
    IF(II .EQ. 1) RETURN
121 VD=3.0*(1.0+STF(M)/W)*R
    VD=VD-(1.0+3.0*FR2/FR3+3.0*STF(M)*FR2/FR3**2/Y)*XOW
    VD=VD-(2.0+3.0*FR2/FR3+3.0*STF(M)*(1.0+FR2/FR3)/FR3/W)*ZOY
    VD=VD*STF(M)/FR3
    UHEN=UHEN+(VD-FEMD*(1.0+3.0*STF(M)*(1.0+FR2/FR3)/FR3/W-3.0*STF(M)*FR2/FR3**2/Y))/DEN-AFD
    RETURN
125 G=SPR(J)*DEN+STF(M)*(2.0+3.0*STF(M)/W)
    VD=3.0*(1.0+STF(M)/Y-STF(M)*(1.0+STF(M)/W)/G)*R
    VD=VD-(2.0+STF(M)*(3.0/Y-1.0/G))*XOW
    VD=VD-(1.0-STF(M)*(2.0+3.0*STF(M)/W)/G)*ZOY
    UHEN=VD*STF(M)/DEN
    IF(II .LE. 2) RETURN
    VD=3.0*(1.0+STF(M)/W)*R-XOW-(2.0+3.0*STF(M)/W)*ZOY
    IF(SPR(J) .GT. STF(M)) GO TO 126
    UHEN=UHEN+VD*STF(M)*SPR(J)/G
    RETURN
126 G=DEN+STF(M)*(2.0+3.0*STF(M)/W)/SPR(J)
    UHEN=UHEN+VD*STF(M)/G
    RETURN
130 IF(ABS(W) .LE. STF(M)) GO TO 140
    DEN=Y+2.0*STF(M)*(Y/W+1.0)/FR3+3.0*(STF(M)/FR3/W)*STF(M)/FR3
    IF(IMA(M,1) .EQ. 0 .AND. W .GE. CER) GO TO 132
    XOW=X/W
    GO TO 133
132 IP=IOP(M,1)
    XOW=PMO(M,1,1)/W-THETA(M,1,IP)
133 IF(IASHI .LT. 0) GO TO 135
    IF(II .EQ. 2) GO TO 131
    VD=3.0*(Y+STF(M))*R
    VD=VD-(Y*(2.0+3.0*FR1/FR3)+3.0*STF(M)*(1.0+FR1/FR3)/FR3)*XOW
    VD=VD-(1.0+3.0*FR1/FR3+3.0*STF(M)*FR1/FR3**2/W)*Z
    VD=VD*STF(M)/FR3
    UHEN=(VD-FEMC*(Y+3.0*STF(M)*(1.0+FR1/FR3)/FR3-3.0*Y*STF(M)*FR1/FR3**2/W))/DEN-AFC
    IF(II .EQ. 1) RETURN
131 VD=3.0*Y*(1.0+STF(M)/W)*R
    VD=VD-(Y*(1.0+3.0*FR2/FR3)+3.0*STF(M)*FR2/FR3**2)*XOW
    VD=VD-(2.0+3.0*FR2/FR3+3.0*STF(M)*(1.0+FR2/FR3)/FR3/W)*Z
    VD=VD*STF(M)/FR3
    UHEN=UHEN+(VD-FEMD*(Y*(1.0+3.0*STF(M)*(1.0+FR2/FR3)/FR3/W)-3.0*STF(M)*FR2/FR3**2))/DEN-AFD
    RETURN
135 G=SPR(J)*DEN+Y*STF(M)*(2.0+3.0*STF(M)/W)
    VD=3.0*(Y+STF(M)-Y**2*STF(M)*(1.0+STF(M)/W)/G)*R
    VD=VD-(2.0*Y+STF(M)*(3.0-Y**2/G))*XOW

```



```

VD=VD-(1.0-Y*STF(M)*(2.0+3.0*STF(M)/W)/G)*Z
UHEN=VD*STF(M)/DEN
IF(II .LE. 2) RETURN
VD=3.0*Y*(1.0+STF(M)/W)*R-Y*XOW-(2.0+3.0*STF(M)/W)*Z
IF( (SPR(J) .GT. STF(M)) GO TO 136
UHEN=UHEN+VD*STF(M)*SPR(J)/G
RETURN
136 G=DEN+Y*STF(M)*(2.0+3.0*STF(M)/W)/SPR(J)
UHEN=UHEN+VD*STF(M)/G
RETURN
140 IF(ABS(Y) .LE. STF(M)) GO TO 150
DEN=W+2.0*STF(M)*(1.0+W/Y)/FR3+3.0*(STF(M)/FR3)*(STF(M)/FR3/Y)
IF( (IMA(M,2) .EQ. 0 .AND. Y .GE. CER) GO TO 142
ZOY=Z/Y
GO TO 143
142 IP=IOP(M,2)
ZOY=PMO(M,2,1)/Y-THETA(M,2,IP)
143 IF( (IASHI .LT. 0) GO TO 145
IF(II .EQ. 2) GO TO 141
VD=3.0*W*(1.0+STF(M)/Y)*R
VD=VD-(2.0+3.0*FR1/FR3+3.0*STF(M)*(1.0+FR1/FR3)/FR3/Y)*X
VD=VD-(W*(1.0+3.0*FR1/FR3)+3.0*STF(M)*FR1/FR3**2)*ZOY
VD=VD*STF(M)/FR3
UHEN=(VD-FEMC*(W*(1.0+3.0*STF(M)*(1.0+FR1/FR3)/FR3/Y)-3.0*STF(M)*FR
1R1/FR3**2))/DEN-AFC
IF(II .EQ. 1) RETURN
141 VD=3.0*(W+STF(M))*R
VD=VD-(1.0+3.0*FR2/FR3+3.0*STF(M)*FR2/FR3**2/Y)*X
VD=VD-(W*(2.0+3.0*FR2/FR3)+3.0*STF(M)*(1.0+FR2/FR3)/FR3)*ZOY
VD=VD*STF(M)/FR3
UHEN=UHEN+(VD-FEMD*(W+3.0*STF(M)*(1.0+FR2/FR3)/FR3-3.0*W*STF(M)*FR
12/FR3**2/Y))/DEN-AFD
RETURN
145 G=SPR(J)*DEN+STF(M)*(2.0*W+3.0*STF(M))
VD=3.0*(W*(1.0+STF(M)/Y)-W*STF(M)*(W+STF(M))/G)*R
VD=VD-(2.0+STF(M)*(3.0/Y-W/G))*X
VD=VD-W*(1.0-STF(M)*(2.0*W+3.0*STF(M))/G)*ZOY
UHEN=VD*STF(M)/DEN
IF(II .LE. 2) RETURN
VD=3.0*(W+STF(M))*R-X-(2.0*W+3.0*STF(M))*ZOY
IF( (SPR(J) .GT. STF(M)) GO TO 146
UHEN=UHEN+VD*STF(M)*SPR(J)/G
RETURN
146 G=DEN+STF(M)*(2.0*W+3.0*STF(M))/SPR(J)
UHEN=UHEN+VD*STF(M)/G
RETURN
150 DEN=W*Y+2.0*STF(M)*(W+Y)/FR3+3.0*(STF(M)/FR3)**2
IF( (IASHI .LT. 0) GO TO 155
IF(II .EQ. 2) GO TO 151
VD=3.0*W*(Y+STF(M))*R
VD=VD-(Y*(2.0+3.0*FR1/FR3)+3.0*STF(M)*(1.0+FR1/FR3)/FR3)*X
VD=VD-(W*(1.0+3.0*FR1/FR3)+3.0*STF(M)*FR1/FR3**2)*Z
VD=VD*STF(M)/FR3
UHEN=(VD-FEMC*(W*Y+3.0*W*STF(M)*(1.0+FR1/FR3)/FR3-3.0*Y*STF(M)*FR
1/FR3**2))/DEN-AFC
IF(II .EQ. 1) RETURN
151 VD=3.0*Y*(W+STF(M))*R
VD=VD-(Y*(1.0+3.0*FR2/FR3)+3.0*STF(M)*FR2/FR3**2)*X
VD=VD-(W*(2.0+3.0*FR2/FR3)+3.0*STF(M)*(1.0+FR2/FR3)/FR3)*Z
VD=VD*STF(M)/FR3

```





```

      UHEN=UHEN+(VD-FEMD*(W*Y+3.0*Y*STF(M)*(1.0+FR2/FR3)/FR3-3.0*W*STF(M
1) *FR2/FR3**2))/DEN-AFD
      RETURN
155 G=SPR(J)*DEN+Y*STF(M)*(2.0*W+3.0*STF(M))
      VD=3.0*(W*(Y+STF(M))-Y**2*W*STF(M)*(W+STF(M))/G)*R
      VD=VD-(2.0*Y+STF(M)*(3.0-W*Y**2/G))*X
      VD=VD-W*(1.0-Y*STF(M)*(2.0*W+3.0*STF(M))/G)*Z
      UHEN=VD*STF(M)/DEN
      IF(II .LE. 2) RETURN
      VD=3.0*Y*(W+STF(M))*R-X*Y-(2.0*W+3.0*STF(M))*Z
      IF(SPR(J) .GT. STF(M)) GO TO 156
      UHEN=UHEN+VD*STF(M)*SPR(J)/G
      RETURN
156 G=DEN+Y*STF(M)*(2.0*W+3.0*STF(M))/SPR(J)
      UHEN=UHEN+VD*STF(M)/G
      RETURN
      END
      SUBROUTINE SOLVE(A,W,C)
      COMMON NS,NB,STF(225),SH(25),SPR( 5),SB( 4),RP(25, 5),UDL(25, 4)
*,IOP(225,2),ION(225,2),SLPLS(225),SLP(225,2,5),BETA(225,2,7),
1THETA(225,2,6),IMA(225,2),PMO(225,2,2),HXD(25),HNL(25)
2,EMLAST(225,2),KOSSAN(225,2),INEG(225,2),IPOS(225,2),PMC(225,2,2)
3,ROTN(225),ROTMAX(225),ROTMIN(225)
      DIMENSION A(150,11),W(150),C(25)
      N1=NB+1
      N2=NB+2
      N3=NB+3
      NE=2*NB+3
      DO 300 I=1,NS
      DO 290 J=1,N2
      IJ=N2*(I-1)+J
      K1=IJ-N2
      IF(J .EQ. N2) K1=K1+1
      K2=K1+N1
      IF(I .EQ. 1 .AND. J .LE. N1) GO TO 240
      M=0
      L=0
      LS=N3-J
      IF(J .EQ. N2) LS=N2
      DO 230 K=K1,K2
      L=L+1
      IF(L .EQ. LS) GO TO 230
      M=M+1
      W(IJ)=W(IJ)+A(IJ,M)*W(K)
230 CONTINUE
      GO TO 290
240 IF(J .EQ. 1) GO TO 290
      W(J)=W(J)+A(J,N1)*W(J-1)
290 CONTINUE
300 CONTINUE
      DO 500 II=1,NS
      I=NS-II+1
      DO 490 JJ=1,N2
      J=N3-JJ
      IJ=N2*(I-1)+J
      IF(I .EQ. NS) GO TO 450
      K1=IJ+1
      IF(J .EQ. N2) GO TO 440
      K2=IJ+N2
      L=N2

```





```

M=N2
LS=NE-J+1
DO 430 K=K1,K2
L=L+1
IF(L .EQ. LS) GO TO 430
M=M+1
W(IJ)=W(IJ)-A(IJ,M)*W(K)
430 CONTINUE
W(IJ)=W(IJ)/A(IJ,N2)
GO TO 490
440 K2=IJ+N1
L=N1
DO 445 K=K1,K2
L=L+1
W(IJ)=W(IJ)-A(IJ,L)*W(K)
445 CONTINUE
GO TO 480
450 IF(J .EQ. N2) GO TO 480
K1=IJ+1
K2=IJ+N1-J
IF(J .EQ. N1) GO TO 470
L=N2
DO 460 K=K1,K2
L=L+1
W(IJ)=W(IJ)-A(IJ,L)*W(K)
460 CONTINUE
470 W(IJ)=W(IJ)/A(IJ,N2)
GO TO 490
480 W(IJ)=W(IJ)/A(IJ,NE)
C(I)=W(IJ)
490 CONTINUE
500 CONTINUE
RETURN
END
SUBROUTINE SHUKI(Q,SM,GOME)
COMMON NS,NB,STF(225),SH(25),SPR( 5),SB( 4),RP(25, 5),UDL(25, 4)
*,IOP(225,2),ION(225,2),SLPLS(225),SLP(225,2,5),BETA(225,2,7),
1THETA(225,2,6),IMA(225,2),PMO(225,2,2),HXD(25),HNL(25)
2,EMLAST(225,2),KOSSAN(225,2),INEG(225,2),IPOS(225,2),PMC(225,2,2)
3,ROTN(225),ROTMAX(225),ROTMIN(225)
DIMENSION SM(25),Y(25),YY(25),H(25,25),HH(25,25),C(25,25),D(25,25)
1,Z(25),Q(25,25)
N=NS
PI=3.141593
IF(N .EQ. 1) GO TO 210
DO 110 I=1,N
DO 100 J=1,N
C(I,J)=Q(I,J)
D(I,J)=SM(J)
IF(J .GT. 1) D(I,J)=0.0
100 CONTINUE
110 CONTINUE
CALL TOKYO1 (N,C)
DO 140 I=1,N
DO 140 K=1,N
ABC=0.0
DO 150 J=1,N
ABC=ABC+C(I,J)*D(J,K)
150 CONTINUE
HH(I,K)=ABC

```



```

      H(I,K)=ABC
140  CONTINUE
      KK=0
      NA=N
10   DO 20 I=1,NA
      Y(I)=1.0
20   CONTINUE
      KK=KK+1
      KA=2*(KK/2)
      IF(KK .EQ. KA) Y(NA)=-1.0
      B=0.000001
40   DO 50 I=1,NA
      YY(I)=0.0
      DO 60 J=1,NA
      YY(I)=YY(I)+H(I,J)*Y(J)
60   CONTINUE
      IF(I .EQ. 1) A=YY(I)
50   CONTINUE
      IF(ABS(A) .GT. 10.0E-15) GO TO 56
      DO 55 I=1,NA
      Y(I)=Y(I)+FLOAT(I)
55   CONTINUE
      GO TO 40
56   DO 70 I=1,NA
      Y(I)=YY(I)/A
70   CONTINUE
      S=A/B
      B=A
      IF(S .GT. 1.00001) GO TO 40
      IF(S .LT. 0.99999) GO TO 40
      IF(KK .EQ. KA) GO TO 75
      AA=A
      DO 71 I=1,NA
      Z(I)=Y(I)
71   CONTINUE
      GO TO 10
75   IF(A .GE. AA) GO TO 80
      A=AA
      DO 76 I=1,NA
      Y(I)=Z(I)
76   CONTINUE
80   IF(KK .EQ. 2) GO TO 200
      IF(KK .EQ. 4) GO TO 300
      IF(KK .EQ. 6) GO TO 400
      IF(KK .EQ. 12) GO TO 510
200  A1=A
      GOME=SQRT(A)
      GO TO 220
210  A=SM(1)/O(1,1)
      GOME=SQRT(A)
220  T=2.0*PI*GOME
      WRITE(6,230) T
230  FORMAT(/1X,'NATURAL PERIOD OF FIRST MODE  IS',F7.3,' SEC.')
      IF(N .EQ. 1) RETURN
      WRITE(6,240) (Y(I),I=1,N)
240  FORMAT( 3X,'CORRESPONDING MODE -- TOP TO BASE'/(3X,7E18.6))
      IF(N .EQ. 2) GO TO 280
      DO 260 I=1,NA
      DO 250 J=1,NA
      C(I,J)=H(I,J)

```



```

250 CONTINUE
  C(I,I)=C(I,I)-A1
  Z(I)=H(1,I)
260 CONTINUE
  NA=NA-1
  DO 275 I=1,NA
  DO 270 J=1,NA
    H(I,J)=H(I+1,J+1)-Y(I+1)*Z(J+1)
270 CONTINUE
275 CONTINUE
  GO TO 10
280 DO 285 I=1,NA
  H(I,I)=H(I,I)-A1
285 CONTINUE
  GO TO 10
300 IF(N .EQ. 2) GO TO 375
  A2=A
  A=SQRT(A)
  T=2.0*PI*A
  WRITE(6,310) T
310 FORMAT(/1X,'NATURAL PERIOD OF SECOND MODE IS',F7.3,' SEC.')
315 DO 320 I=1,NA
  Z(I+1)=Y(I)
320 CONTINUE
  Z(1)=0.0
  DO 340 I=1,N
  Y(I)=0.0
  DO 330 J=1,N
    Y(I)=Y(I)+C(I,J)*Z(J)
330 CONTINUE
  IF(I .EQ. 1) A=Y(1)
  Y(I)=Y(I)/A
340 CONTINUE
  WRITE(6,240) (Y(I),I=1,N)
  IF(KK .EQ. 6) GO TO 500
  IF(N .EQ. 3) GO TO 365
  DO 350 I=1,NA
  Y(I)=Z(I+1)
  DO 345 J=1,NA
  D(I,J)=H(I,J)
345 CONTINUE
  D(I,I)=D(I,I)-A2
  Z(I)=H(1,I)
350 CONTINUE
  NA=NA-1
  DO 360 I=1,NA
  DO 355 J=1,NA
    H(I,J)=H(I+1,J+1)-Y(I+1)*Z(J+1)
355 CONTINUE
360 CONTINUE
  GO TO 10
365 DO 370 I=1,NA
  H(I,I)=H(I,I)-A2
370 CONTINUE
  GO TO 10
375 A=A+A1
  A=SQRT(A)
  T=2.0*PI*A
  WRITE(6,310) T
  WRITE(6,240) (Y(I),I=1,N)

```



```

      RETURN
400  IF(N .EQ. 3) GO TO 440
      A3=A
      A=SQRT(A)
      T=2.0*PI*A
      WRITE(6,410) T
410  FORMAT(/1X,'NATURAL PERIOD OF THIRD MODE  IS',F7.3,' SEC.')
      DO 420 I=1,NA
      Z(I+1)=Y(I)
420  CONTINUE
      Z(1)=0.0
      N2=NA+1
      DO 435 I=1,N2
      Y(I)=0.0
      DO 430 J=1,N2
      Y(I)=Y(I)+D(I,J)*Z(J)
430  CONTINUE
435  CONTINUE
      NA=N2
      GO TO 315
440  A=A+A2
      A=SQRT(A)
      T=2.0*PI*A
      WRITE(6,410) T
      GO TO 315
500  IF(N .LE. 3) RETURN
      CALL TOKYO1 (N,HH)
      NA=N
      DO 506 I=1,N
      DO 505 J=1,N
      H(I,J)=HH(I,J)
505  CONTINUE
506  CONTINUE
      KK=10
      GO TO 10
510  A=SQRT(A)
      T=2.0*PI/A
      WRITE(6,520) T
520  FORMAT(/1X,'THE MINIMUM NATURAL PERIOD  IS',F7.3,' SEC.')
      WRITE(6,240) (Y(I),I=1,N)
      RETURN
      END
      SUBROUTINE TOKYO1 (NO,A)
      DIMENSION AC(25),AB(25),A(25,25)
      NO1=NO-1
      A(1,1)=1.0/A(1,1)
      IF (NO .EQ. 1) RETURN
      DO 80 N=1, NO1
      DO 50 I=1,N
      AB(I)=0.0
      AC(I)=0.0
      DO 50 J=1,N
      AB(I)=AB(I)+A(I,J)*A(J,N+1)
      AC(I)=AC(I)+A(N+1,J)*A(J,I)
50  CONTINUE
      ACB=0.0
      DO 60 I=1,N
      ACE=ACB+AC(I)*A(I,N+1)
60  CONTINUE
      A(N+1,N+1)=1.0/(A(N+1,N+1)-ACB)

```





```

DO 70 I=1,N
A(N+1,I)=-A(N+1,N+1)*AC(I)
A(I,N+1)=-AB(I)*A(N+1,N+1)
70 CONTINUE
DO 80 I=1,N
DO 80 J=1,N
A(I,J)=A(I,J)-A(I,N+1)*AC(J)
80 CONTINUE
RETURN
END
SUBROUTINE KIKU (DELTAT,C,GOME,O,GOSA,GR,NCAL)
COMMON NS,NB,STF(225),SH(25),SPR( 5),SB( 4),RP(25, 5),UDL(25, 4)
*,IOP(225,2),ION(225,2),SLPLS(225),SLP(225,2,5),BETA(225,2,7),
1THETA(225,2,6),IMA(225,2),PMO(225,2,2),HXD(25),HNL(25)
2,EMLAST(225,2),KOSSAN(225,2),INEG(225,2),IPOS(225,2),PMC(225,2,2)
3,ROTN(225),ROTMAX(225),ROTMIN(225)
DIMENSION C(25),O(25,25)
DO 100 I=1,NS
C(I)=2.0*C(I)*O(I,I)*GOME
100 CONTINUE
NOST=NS
CALL TOKYO1(NOST,O)
DO 140 I=1,NS
HXD(I)=0.0
DO 130 J=1,NS
HXD(I)=HXD(I)-O(I,J)*HNL(J)
130 CONTINUE
140 CONTINUE
DO 150 I=1,NS
HNL(I)=0.0
150 CONTINUE
WRITE(6,160) (HXD(I),I=1,NS)
160 FORMAT(/1X,'INITIAL DEFORMATION -- TOP TO BOTTOM'/(6X,8E14.5))
TLAST=DELTAT*FLCAT(NCAL)
WRITE(6,340) DELTAT,TLAST,GR,GOSA
340 FORMAT(/1X,'CALCULATIONS WILL BE DONE EVERY',F6.3,' SEC. UNTIL',
1F5.1,' SEC.',
4X,'ACCE
2LERATION OF GRAVITY IS',F8.3,4X,'CONVERGENCE LIMIT IS',F9.6)
RETURN
END
SUBROUTINE JISHIN (SM,CSM,C,IF,IGPH,GR,GOSA,NCAL,DELTAT,MXIT,NSAI,
1INTOBU,THAJI,TCWA,SEICO,Q,IA,AI,LTP,ITIME,IDISC)
COMMON NS,NB,STF(225),SH(25),SPR( 5),SB( 4),RP(25, 5),UDL(25, 4)
*,IOP(225,2),ION(225,2),SLPLS(225),SLP(225,2,5),BETA(225,2,7),
1THETA(225,2,6),IMA(225,2),PMO(225,2,2),HXD(25),HNL(25)
2,EMLAST(225,2),KOSSAN(225,2),INEG(225,2),IPOS(225,2),PMC(225,2,2)
3,ROTN(225),ROTMAX(225),ROTMIN(225)
DIMENSION GA(7),SM(25),CSM(25),C(25),IP(25),TSEI(25),AX(25),VX(25)
1,XD(25),RX(25),RV(25),AA(25),CO(25),RESC(25),RESQ(25),RXMX(25),RVM
2X(25),COMX(25),TRX(25),TRV(25),TCQ(25),OAX(25),OVX(25),OXD(25),
3O(25,25),AI(150, 11),FT(225,2),KOSAN(225,2),IPCH(5),XDMX(25),AAMX(
425),RCMX(25),RQMX(25),TR(25),TRMX(25),ZZ(25)
INSA=10
IF(IGPH .GT. 5) GO TO 10
GO TO (1,2), IGPH
COMMENT : INPUT STATEMENT (ONLY WHEN PUNCHING OUT THE RESULTS)
1 READ(5,100) MSKIP,INSA,NPCH,(IPCH(J),J=1,NPCH)
GO TO 10
2 READ(5,100) MSKIP,INSA
NPCH=NS

```



```

100 FORMAT(10I5)
COMMENT : INPUT STATEMENT
10 INP=5
   IF(IDISC .EQ. 0) INP=4
   READ(INP,15) (TSEI(I),I=1,20)
15 FORMAT(20A4)
   IF(LTP .LT. 5) GO TO 30
   WRITE(6, 20) (TSEI(I),I=1,20)
20 FORMAT(/1X,'BLAST LOADING MODEL USED IN THIS CALCULATION : ',20A4)
   WRITE(6, 25) SEICO
25 FORMAT(/1X,'MAXIMUM BLAST LOAD IS',F8.2,' AT THE LEVEL WHERE THE L
   LOAD FACTOR IS EQUAL TO 1.0'/)
   GO TO 45
30 WRITE(6, 35) (TSEI(I),I=1,20)
35 FORMAT(/1X,'SEISMIC MODEL USED IN THIS CALCULATION : ',20A4)
   WRITE(6, 40) SEICO
40 FORMAT(/1X,'MAXIMUM GROUND ACCELERATION IS',F6.3,' OF GRAVITY ACCE
   LERATION'/)
45 IF(IGPH .GT. 5) GO TO 60
   TKAN=DELTAT*FLOAT(MSKIP)
   GO TO (46,56), IGPH
46 WRITE(6,50) TKAN,(IPCH(J),J=1,NPCH)
50 FORMAT( 1X,'THIS PROGRAM PUNCHES OUT THE RESULTS OF EVERY',F6.3,
   1' SEC. FOR THE STOREY NO.',5(I5,' ')/)
   WRITE(7,55) TKAN,NS,NPCH,(IPCH(J),J=1,NPCH)
   GO TO 60
56 WRITE(6,57) TKAN
57 FORMAT(1X,'THE RESULT OF EVERY',F6.3,'SEC.,FOR EVERY STOREY IS STO
   1RED IN THE DISK'/)
   WRITE(2,55) TKAN ,NS
55 FORMAT(F10.3, 9X,'PRODUCED BY PROG.# 40',5X,7I5)
60 WRITE(6, 65)
65 FORMAT( /1X,'** RESPONSE **')
   IF(INSA .LT. 5) GO TO 111
   IF(LTP .GE. 5) GO TO 75
   WRITE(6, 70)
70 FORMAT(/2X,'TIME',3X,'GRND ACC/',3X,'DISP TO GRND',3X,'RELTV DISP'
   1,4X,'RELTV VELO',4X,'ABS ACCEL',3X,'RESIS (DAMP)',2X,'RESIS (SPRN)
   2',3X,'SHEAR COEF',3X,'TIME',7X,'ITER')
   GO TO 85
75 WRITE(6, 80)
80 FORMAT(/2X,'TIME',3X,'BLAST LD/',3X,'DISP TO GRND',3X,'RELTV DISP'
   1,4X,'RELTV VELO',4X,'ABS ACCEL',3X,'RESIS (DAMP)',2X,'RESIS (SPRN)
   2',3X,'SHEAR COEF',3X,'TIME',7X,'ITER')
85 WRITE(6, 90)
90 FORMAT(12X,'STOREY')
111 CALL STIFF(Q,1,AI,IA,ISHUT)
   IF(ISHUT .EQ. 1) RETURN
   ISAI=10
   DO 120 K=1,NS
   AX(K)=0.0
   VX(K)=0.0
   IF(ABS(HXD(K)) .LT. 1.0E-06) HXD(K)=0.0
   XD(K)=HXD(K)
   RXMX(K)=0.0
   TRX(K)=0.0
   RVMX(K)=0.0
   TRV(K)=0.0
   CQM(K)=0.0
   TCQ(K)=0.0

```



```

      TRMX(K)=0.0
      XDMX(K)=0.0
      AAMX(K)=0.0
      RCMX(K)=0.0
      RQMX(K)=0.0
      ZZ(K)=GR/1.0E+15
120  CONTINUE
      MEMB=(2*NB+1)*NS
      DO 125 I=1, MEMB
      DO 124 K=1, 2
      KOSAN(I,K)=0
      KOSSAN(I,K)=0
124  CONTINUE
125  CONTINUE
      DO 500 I=1, NCAL
      IF(I .EQ. 1) READ(INP,130) (GA(J),J=1,7)
130  FORMAT(7F10.0)
      IYOMU=7*(I/7)
      IF(I .EQ. IYOMU .AND. I .LT. NCAL) READ(INP,130) (GA(J),J=1,7)
      II=I-7*((I-1)/7)
      IF(I-1) 140,140,150
140  GA1=0.0
      GA2=0.0
      GA3=GA(II)*SEICO
      IF(NCAL .GT. 1) GO TO 141
      GA4=0.0
      GO TO 160
141  GA4=GA(II+1)*SEICO
      GO TO 160
150  GA1=GA2
      GA2=GA3
      GA3=GA4
      IF(I .EQ. NCAL) GO TO 151
      IF(II .EQ. 7) GO TO 152
      GA4=GA(II+1)*SEICO
      GO TO 160
151  GA4=0.0
      GO TO 160
152  GA4=GA(1)*SEICO
160  GAP=GA3
      TP=FLOAT(I)*DELTAT
      DO 190 K=1, NS
      OAX(K)=AX(K)
      OVX(K)=VX(K)
      OXD(K)=XD(K)
190  CONTINUE
      CALL SUCHI (AX,VX,XD,RX,RV,SM,C,CSM,GAP,DELTAT,KAZU,RESC,RESQ,MXIT
1,TP,ISAI,GOSA,Q,ZZ)
      IF(ISAI .GE. 0) GO TO 210
205  DO 206 K=1, NS
      AX(K)=OAX(K)
      VX(K)=OVX(K)
      XD(K)=OXD(K)
206  CONTINUE
      CALL SAIBUN (ISAI,AX,VX,XD,NSAI,TP,DELTAT,RX,RV,SM,C,CSM,KAZU,RESC
1,RESQ,MXIT,GOSA,GA1,GA2,GA3,GA4,Q,IA,AI,KDIS,FT,KOSAN,ISHUT,ZZ)
      IF(ISHUT .EQ. 1) GO TO 510
      IF(KDIS .LE. 0) GO TO 510
      GO TO 214
210  CALL KYOTO(XD,IA,AI,ICHI,FT,1)

```





```

      IF( ICHI .LE. 0) GO TO 214
      GO TO 205
214  IF( LTP .GE. 5) GO TO 225
      DO 215 K=1, NS
      AA(K)=AX(K)+GAP
215  CONTINUE
      CQN=0.0
      DO 220 N=1, NS
      CQN=CQN-SM(N)*AA(N)
      TR(N)=CQN
      CQ(N)=RESQ(N)/CSM(N)/GR
220  CONTINUE
      GO TO 230
225  DO 226 K=1, NS
      AA(K)=AX(K)
226  CONTINUE
      TOTM=0.0
      CQN=0.0
      DO 228 N=1, NS
      TOTM=TOTM+SM(N)
      CQN=CQN-SM(N)*AA(N)
      TR(N)=CQN-CSM(N)*GAP
      CQ(N)=RESQ(N)/TOTM/GR
228  CONTINUE
230  IF( INSA .LT. 5) GO TO 275
      IF( NTOBU .EQ. 0) GO TO 239
      NTO=I/NTOBU
      NTO=NTC*NTOBU
      IF( NTO .NE. 1) GO TO 275
239  DO 270 K=1, NS
      IF( K .NE. 1) GO TO 250
      WRITE(6,240) TP,GAP,XD(1),RX(1),RV(1),AA(1),RESC(1),RESQ(1),CQ(1),
1 TP,KAZU
240  FORMAT(1X,F6.3,1X,F10.5,1P7E14.5,0PF7.3,I10)
      GO TO 270
250  IF( TP .GT. THAJI .AND. TP .LT. TOWA) GO TO 255
      IF( IP(K) .LT. 0) GO TO 270
255  WRITE(6,260) K,XD(K),RX(K),RV(K),AA(K),RESC(K),RESQ(K),CQ(K)
260  FORMAT(13X,I5,1P7E14.5)
270  CONTINUE
275  DO 350 K=1, NS
      IF( ABS(RXMX(K)) .GE. ABS(RX(K))) GO TO 310
      RXMX(K)=RX(K)
      TRX(K)=TP
310  IF( ABS(RVMX(K)) .GE. ABS(RV(K))) GO TO 320
      RVMX(K)=RV(K)
      TRV(K)=TP
320  IF( ABS(TRMX(K)) .GE. ABS(TR(K))) GO TO 325
      TRMX(K)=TR(K)
325  IF( ABS(XDMX(K)) .GE. ABS(XD(K))) GO TO 326
      XDMX(K)=XD(K)
326  IF( ABS(AAMX(K)) .GE. ABS(AA(K))) GO TO 327
      AAMX(K)=AA(K)
327  IF( ABS(PCMX(K)) .GE. ABS(RESC(K))) GO TO 328
      RCMX(K)=RESC(K)
328  IF( ABS(ROMX(K)) .GE. ABS(RESQ(K))) GO TO 330
      ROMX(K)=RESQ(K)
      CQMX(K)=CQ(K)
      TCQ(K)=TP
330  IF( ZZ(K) .GE. ABS(AX(K))) GO TO 350

```



```

      ZZ(K)=ABS(AX(K))
350  CONTINUE
      IF(IGPH .GT. 5) GO TO 450
      NTO=MSKIP*(I/MSKIP)
      IF(NTO .NE. 1) GO TO 450
      DO 380 N=1,NPCH
      GO TO (335,360), IGPH
335  K=IPCH(N)
      KBTM=NS-K+1
      WRITE(7,370) KBTM,TP,XD(K),RX(K),RV(K),AA(K),RESC(K),RESQ(K),CQ(K)
      GO TO 380
360  K=NS-N+1
      KBTM=N
      WRITE(2,370) KBTM,TP,XD(K),RX(K),RV(K),AA(K),RESC(K),RESQ(K),CQ(K)
370  FORMAT(I2,F8.3,1P7E10.3)
380  CONTINUE
450  CALL NARA(KDIS,FT,KOSAN,TP)
      IF(KDIS .LE. 0) GO TO 510
      CALL TIME(1,0,LTIME)
      IF(LTIME .GE. ITIME) GO TO 510
500  CONTINUE
510  WRITE(6,520)
520  FORMAT(/,1X,'LIST OF MAXIMUM VALUES')
      WRITE(6,530)
530  FORMAT(/,3X,'STRY',2X,'DISP TO GND',3X,'RELTV DISP - WHEN',4X,'RELT
      1 V VELO - WHEN',4X,'ABS ACCEL',3X,'DAMP RESIS',3X,'SPRN RESIS',3X,'
      2 SHEAR COEF-WHEN',2X,'TOTAL SHEAR')
      DO 550 K=1,NS
      WRITE(6,540) K,XDMX(K),RXMX(K),TRX(K),RVMX(K),TRV(K),AAMX(K),RCMX(
      1 K),RQMX(K),COMX(K),TCQ(K),TRMX(K)
540  FORMAT(2X,I4,1P2E13.3,2(0PF8.3,1PE13.3),1P2E13.3,0PF10.4,F8.3,
      11PE13.3)
550  CONTINUE
      IF(IGPH .GT. 5) GO TO 600
      IF(IGPH .EQ. 1) GO TO 553
      IXXXXX=0
      XXXXXX=0.0
      DO 552 J=1,NS
      DO 551 JJ=1,4
      WRITE(2,370) IXXXXX,XXXXXX
551  CONTINUE
552  CONTINUE
      WRITE(3,555)
      GO TO 557
553  WRITE(7,555)
555  FORMAT(T55,'MAXIMUM VALUES, PROG.# 40')
557  DO 570 J=1,NS
      K=NS-J+1
      RXMX(K)=ABS(RXMX(K))
      RVMX(K)=ABS(RVMX(K))
      COMX(K)=ABS(COMX(K))
      IF(IGPH .EQ. 2) GO TO 558
      WRITE(7,560) RXMX(K),TRX(K),RVMX(K),TRV(K),COMX(K),TCQ(K)
      GO TO 570
558  WRITE(3,560) RXMX(K),TRX(K),RVMX(K),TRV(K),COMX(K),TCQ(K)
560  FORMAT(3(1PE10.4,0PF10.3))
570  CONTINUE
600  IF(LTIME .GE. ITIME) WRITE(6,610) TP
      NJOINT=(NB+1)*NS
      DO 1100 IXE=1,NJOINT

```



```

      WRITE(6,1102)
      SUMROT=ROTMAX(IXE)+ABS(ROTMIN(IXE))
1100 WRITE(6,1101)IXE,ROTMAX(IXE),ROTMIN(IXE),SUMROT
1101 FORMAT(I5,3E15.6)
1102 FORMAT(/2X,'JOINT  MAX POS.  ROT.  MAX NEG.  ROT  SUM OF POS.+NEG.')
```

610 FORMAT(/1X,'\*\* CALCULATION OF RESPONSE WAS TERMINATED BECAUSE PRE  
 1PARED COMPUTATION TIME HAD BEEN EXPIRED. \*\* TP=',F7.3/)

```

      WRITE(6,999)
999  FORMAT(1H1)
      RETURN
      END

      SUBROUTINE SAIBUN (ISAI,AX,VX,XD,NSAI,TP,DELTAT,RX,RV,SM,C,CSM,
1KAZU,RESC,RESQ,MXIT,GCSA,GA1,GA2,GA3,GA4,Q,IA,AI,KDIS,FT,KOSAN,
2ISHUT,ZZ)
      COMMON NS,NB,STF(225),SH(25),SPR( 5),SB( 4),RP(25, 5),UDL(25, 4)
*,IOP(225,2),ION(225,2),SLPLS(225),SLP(225,2,5),BETA(225,2,7),
1THETA(225,2,6),IMA(225,2),PMO(225,2,2),HXD(25),HNL(25)
2,EMLAST(225,2),KOSSAN(225,2),INEG(225,2),IPOS(225,2),PMC(225,2,2)
3,ROTN(225),ROTMAX(225),ROTMIN(225)
      DIMENSION AX(25),VX(25),XD(25),RX(25),RV(25),SM(25),C(25),CSM(25),
1RESC(25),RESQ(25),Q(25,25),AI(150, 11),FT(225,2),KOSAN(225,2),
2ZZ(25)
      SAIN=FLOAT(NSAI)
      TP=TP-DELTAT
      DO 460 J=1,NSAI
      TBUN=FLOAT(J)/SAIN
      TP=TP+DELTAT/SAIN
      GAP=(GA4-3.0*GA3+3.0*GA2-GA1)*TBUN**3/6.0+(GA3-2.0*GA2+GA1)*TBUN**
12/2.0-(GA4-6.0*GA3+3.0*GA2+2.0*GA1)*TBUN/6.0+GA2
      CALL SUCHI (AX,VX,XD,RX,RV,SM,C,CSM,GAP,DELTAT/SAIN,KAZU,RESC,RESQ
1,MXIT,TP,ISAI,GOSA,Q,ZZ)
      CALL KYOTO(XD,IA,AI,ICHI,FT,2)
      IF(ICHI .LE. 0) GO TO 456
      DO 455 K=1,NS
      HXD(K)=XD(K)
      HNL(K)=RESQ(K)
455  CONTINUE
      CALL STIFF(Q,1,AI,IA,ISHUT)
      IF(ISHUT .EQ. 1) RETURN
456  IF(J .EQ. NSAI) GO TO 460
      CALL NARA(KDIS,FT,KOSAN,TP)
      IF(KDIS .LE. 0) RETURN
460  CONTINUE
      ISAI=10
      RETURN
      END

      SUBROUTINE SUCHI (SAX,SVX,SXD,RX,RV,SM,C,CSM,GAP,DELTAT,KAZU,RESC,
1RESQ,MXIT,TP,ISAI,GOSA,Q,ZZ)
      COMMON NS,NB,STF(225),SH(25),SPR( 5),SB( 4),RP(25, 5),UDL(25, 4)
*,IOP(225,2),ION(225,2),SLPLS(225),SLP(225,2,5),BETA(225,2,7),
1THETA(225,2,6),IMA(225,2),PMO(225,2,2),HXD(25),HNL(25)
2,EMLAST(225,2),KCSSAN(225,2),INEG(225,2),IPOS(225,2),PMC(225,2,2)
3,ROTN(225),ROTMAX(225),ROTMIN(225)
      DIMENSION UX(25),UA(25),RX(25),RV(25),SAX(25),SXD(25),SVX(25),
1SM(25),C(25),CSM(25),ICOL(25),RESC(25),RESQ(25),UV(25),U(25),
2Q(25,25),ZZ(25)
      KAZU=0
      MXIJ=MXIT/2
      DO 100 N=1,NS
      UA(N)=SAX(N)

```





```

100 CONTINUE
110 KAZU=KAZU+1
    DO 120 N=1,NS
        UV(N)=SVX(N)+(SAX(N)+UA(N))*DELTAT/2.0
        UX(N)=SXD(N)+(SVX(N)+(SAX(N)/3.0+UA(N)/6.0)*DELTAT)*DELTAT
120 CONTINUE
    DO 200 N=1,NS
        NN=N-1
        CMA=0.0
        IF(N .EQ. 1) GO TO 140
        DO 130 K=1,NN
            CMA=CMA+SM(K)*UA(K)
130 CONTINUE
140 IF(N .NE. NS) GO TO 150
        ST=CMA+GAP*CSM(N)
        GO TO 160
150 ST=CMA+GAP*CSM(N)-C(N)*UV(N+1)
160 RESQ(N)=QQ(N,Q,UX)
        U(N)=-(C(N)*UV(N)+RESQ(N)+ST)/SM(N)
200 CONTINUE
        JHAN=0
        DO 400 N=1,NS
            ICOL(N)=0
            BUNBO=ABS(U(N)-UA(N))/GOSA/100.0+1.0E-35
            SHI=1.01*ABS(U(N)-UA(N))/(ABS(U(N))+BUNBO)
            IF(SHI .LT. GOSA) GO TO 400
            SHI=10.0*ABS(U(N)-UA(N))/ZZ(N)
            IF(SHI .LT. GOSA) GO TO 400
            JHAN=JHAN+1
            ICOL(N)=ICOL(N)+1
400 CONTINUE
        IF(JHAN .EQ. 0) GO TO 450
        IF(KAZU .LT. MXIT) GO TO 420
        IF(ISAI .LT. 0) GO TO 405
        ISAI=-10
        GO TO 450
405 MXII=MXIT+1
        IF(KAZU .EQ. MXII) GO TO 411
        DO 410 N=1,NS
            IF(ICOL(N) .EQ. 0) GO TO 410
            WRITE(6,406) N
406 FORMAT(1X,'CONVERGENCE IS NOT ENOUGH AT STOREY NO.',I3)
410 CONTINUE
411 DO 415 N=1,NS
            IF(ICOL(N) .EQ. 0) GO TO 415
            WRITE(6,412) TP,N,UX(N),UV(N),U(N),RESQ(N),KAZU
412 FORMAT(1X,F6.3,6X,I5,1PE14.5,7X,E14.5,7X,E14.5,14X,E14.5,21X,0PI10
1)
415 CONTINUE
        IF(KAZU .EQ. MXII) GO TO 450
420 IF(KAZU .EQ. MXIJ) GO TO 440
        DO 430 N=1,NS
            UA(N)=U(N)
430 CONTINUE
        GO TO 110
440 DO 445 N=1,NS
            UA(N)=(UA(N)+U(N))/2.0
445 CONTINUE
        MXIJ=MXIJ+(MXIT-MXIJ)/2
        GO TO 110

```





```

450 DO 455 N=1,NS
    SAX(N)=U(N)
    SVX(N)=UV(N)
    SXD(N)=UX(N)
455 CONTINUE
    DO 470 N=1,NS
        IF(N .EQ. NS) GO TO 460
        RX(N)=SXD(N)-SXD(N+1)
        RV(N)=SVX(N)-SVX(N+1)
        GO TO 465
460 RX(NS)=SXD(NS)
    RV(NS)=SVX(NS)
465 RESC(N)=C(N)*RV(N)
470 CONTINUE
    RETURN
    END
    FUNCTION QQ (N,Q,SXD)
        COMMON NS,NB,STF(225),SH(25),SPR( 5),SB( 4),RP(25, 5),UDL(25, 4)
        *,IOP(225,2),ION(225,2),SLPLS(225),SLP(225,2,5),BETA(225,2,7),
        1THETA(225,2,6),IMA(225,2),PMO(225,2,2),HXD(25),HNL(25)
        2,EMLAST(225,2),KCSSAN(225,2),INEG(225,2),IPOS(225,2),PMC(225,2,2)
        3,ROTN(225),ROTMAX(225),RCTMIN(225)
        DIMENSION Q(25,25),SXD(25)
        QQ=0.0
        DO 100 I=1,NS
            SHXD=SXD(I)-HXD(I)
            QQ=QQ+Q(N,I)*SHXD
100 CONTINUE
        QQ=HNL(N)+QQ
        RETURN
        END
        SUBROUTINE KYOTO (SXD,IA,AI,ICHI,FT,IIQ)
            COMMON NS,NB,STF(225),SH(25),SPR( 5),SB( 4),RP(25, 5),UDL(25, 4)
            *,IOP(225,2),ION(225,2),SLPLS(225),SLP(225,2,5),BETA(225,2,7),
            1THETA(225,2,6),IMA(225,2),PMO(225,2,2),HXD(25),HNL(25)
            2,EMLAST(225,2),KCSSAN(225,2),INEG(225,2),IPOS(225,2),PMC(225,2,2)
            3,ROTN(225),ROTMAX(225),RCTMIN(225)
            DIMENSION SXD(25),BB(150),AI(150,11),FT(225,2),EM(2),CCC(25)
            DIMENSION EMSAVE(10),FTSAVE(10)
            DIMENSION EMTEMP(225,2)
            DIMENSION FTKEPT(225,2)
            ICHI=0
            DO 100 I=1,IA
                BB(I)=B(I,SXD)
100 CONTINUE
                NB1=NB+1
                NB2=NB+2
                NBB=2*NB+1
                CALL SOLVE(AI,BB,CCC)
                DO 181 IXA=1,NS
                    DO 181 IXB=1,NB1
                        J=((IXA-1)*3)+IXB
                        JK=((IXA-1)*2)+IXB
181 ROTN(JK)=BB(J)
                    DO 300 I=1,NS
                        IF(I .EQ. NS) GO TO 110
                        R=(SXD(I)-SXD(I+1))/SH(I)
                        GO TO 120
110 R=SXD(NS)/SH(NS)
120 DO 250 J=1,NBB

```



```

M=NBB*(I-1)+J
IF(STF(M) .LT. 1.0E-30) GO TO 250
JJ=J-NB
IF(J .GE. NB1) GO TO 130
KA=NB2*(I-1)+J
KB=KA+1
GO TO 140
130 KA=NB2*(I-1)+J-NB
IF(I .EQ. NS) GO TO 140
KB=KA+NB2
140 PA=BB(KA)
IF(I .EQ. NS .AND. J .GE. NB1) GO TO 150
PB=BB(KB)
150 IF(J .GE. NB1) GO TO 160
SS=SB(J)
FR1=RP(I,J)/SS
FR2=RP(I,J+1)/SS
FR3=1.0-FR1-FR2
UL=UDL(I,J)
DO 155 K=1,2
CALL IZU (VA,VB,M,K,FR1,FR2,1,-1)
EM(K)=VA*PA+VB*PB-UHEN(M,SS,K,UL,0.0,FR1,FR2,1,-1)
155 CONTINUE
FEM=-UL*(FR3*SS)**2/12.0
FT(M,1)=-((2.0*EM(1)-EM(2)-3.0*FEM)*FR3/STF(M)/3.0+(1.0+FR1/FR3)*PA
1+FR2*PB/FR3
FT(M,2)=-((2.0*EM(2)-EM(1)+3.0*FEM)*FR3/STF(M)/3.0+FR1*PA/FR3+(1.0+
1FR2/FR3)*PB
GO TO 180
160 SS=SH(I)
IF(I .EQ. NS) GO TO 170
DO 165 K=1,2
CALL IZU (VA,VB,M,K,0.0,0.0,1,-1)
EM(K)=VA*PA+VB*PB-UHEN(M,SS,K,0.0,R,0.0,0.0,1,-1)
165 CONTINUE
GO TO 175
170 CALL IZU (VA,VB,M,1,0.0,0.0,-1,-1)
EM(1)=VA*PA-UHEN(M,SS,1,0.0,R,0.0,0.0,-1,-1)
CALL IZU (VA,VB,M,3,0.0,0.0,-1,-1)
EM(2)=VA*PA-UHEN(M,SS,3,0.0,R,0.0,0.0,-1,-1)-EM(1)
IF(SCR(JJ) .LE. 1.0E-5) GO TO 175
PB=-EM(2)/SCR(JJ)
175 FT(M,1)=-((2.0*EM(1)-EM(2))/STF(M)/3.0+PA-R
IF(I .EQ. NS .AND. SCR(JJ) .LE. 1.0E-5) GO TO 180
FT(M,2)=-((2.0*EM(2)-EM(1))/STF(M)/3.0+PB-R
180 CONTINUE
DO 182 K=1,2
EMTEMP(M,K)=EM(K)
182 FTKEPT(M,K)=FT(M,K)
DO 220 K=1,2
IF(I .EQ. NS .AND. J .GE. NB1 .AND. SCR(JJ) .LE. 1.0E-5) GO TO 220
IF(IMA(M,K)) 210,200,190
190 ICON=IMA(M,K)
IPOS(M,K)=ICON
IF(FT(M,K) .GE. THETA(M,K,ICON) .AND. FT(M,K) .LE. THETA(M,K,ICON+
1)) GO TO 220
IF(FT(M,K) .GE. THETA(M,K,ICON+1)) GO TO 195
ICHI=ICHI+1
IF(II0 .EQ. 1) GO TO 220
IMA(M,K)=0

```



```

      GO TO 220
195 IF(IMA(M,K) .EQ. 2) GO TO 220
      ICHI=ICHI+1
      IF(IIG .EQ. 1) GO TO 220
      IMA(M,K)=IMA(M,K)+1
      GO TO 220
200 IF(EM(K))211,220,191
211 IF(KOSSAN(M,K).EQ.0)GO TO 214
212 IF(FT(M,K).GT.THETA(M,K,INEG(M,K)))GO TO 220
      ICHI=ICHI+1
      IF(IIQ.EQ.1)GO TO 220
      IMA(M,K)=3-INEG(M,K)
      GO TO 220
214 IF(EM(K).GE.PMC(M,K,2))GO TO 220
      ICHI=ICHI+1
      IF(IIQ.EQ.1)GO TO 220
      IMA(M,K)=-2
      GO TO 220
191 IF(KOSSAN(M,K).EQ.0)GO TO 194
192 IF(FT(M,K).LT.THETA(M,K,IPOS(M,K)))GO TO 220
      ICHI=ICHI+1
      IF(IIQ.EQ.1)GO TO 220
      IMA(M,K)=IPOS(M,K)
      GO TO 220
194 IF(EM(K).LE.PMC(M,K,1))GO TO 220
      ICHI=ICHI+1
      IF(IIQ.EQ.1)GO TO 220
      IMA(M,K)=2
      GO TO 220
210 ICON=3-IMA(M,K)
      INEG(M,K)=ICON
      IF(FT(M,K) .GE. THETA(M,K,ICON+1) .AND. FT(M,K) .LE. THETA(M,K,ICO
1N)) GO TO 220
      IF(FT(M,K) .LE. THETA(M,K,ICON+1)) GO TO 215
      ICHI=ICHI+1
      IF(IIG .EQ. 1) GO TO 220
      IMA(M,K)=0
      GO TO 220
215 IF(IMA(M,K) .EQ. -2) GO TO 220
      ICHI=ICHI+1
      IF(IIG .EQ. 1) GO TO 220
      IMA(M,K)=IMA(M,K)-1
220 CONTINUE
250 CONTINUE
300 CONTINUE
      IF(ICHI.EQ.0)GO TO 303
306 GO TO 304
303 CONTINUE
      DO 305 IXC=1,NS
      DO 305 IXD=1,NB1
      JK=((IXC-1)*2)+IXD
      IF(ROTN(JK))310,305,311
310 IF(ROTN(JK).LT.ROTMIN(JK))ROTMIN(JK)=ROTN(JK)
      GO TO 305
311 IF(ROTN(JK).GT.ROTMAX(JK))ROTMAX(JK)=ROTN(JK)
305 CONTINUE
304 CONTINUE
      RETURN
      END
      SUBROUTINE NARA (KDIS,FT,KOSAN,TP)

```





```

COMMON NS,NB,STF(225),SH(25),SPR( 5),SB( 4),RP(25, 5),UDL(25, 4)
*,IOP(225,2),ION(225,2),SLPLS(225),SLP(225,2,5),BETA(225,2,7),
1THETA(225,2,6),[MA(225,2),PMO(225,2,2),HxD(25),HNL(25)
2,EMLAST(225,2),KOSSAN(225,2),INEG(225,2),IPOS(225,2),PMC(225,2,2)
3,ROTN(225),ROTMAX(225),RCTMIN(225)
DIMENSION FT(225,2),KOSAN(225,2)
KDIS=10
NB1=NB+1
NB2=NB+2
NBB=2*NB+1
DO 360 I=1,NS
DO 350 J=1,NBB
M=NBB*(I-1)+J
CER=2.5*STF(M)
DO 340 K=1,2
IF(IMA(M,K)) 100,340,100
100 IF(KOSAN(M,K) .EQ. 0) GO TO 110
IF(IMA(M,K) .GT. 0) GO TO 130
GO TO 170
110 KOSAN(M,K)=1
KOSSAN(M,K)=1
IF(J .GE. NB1) GO TO 120
GO TO (111,115), K
111 WRITE(6,112) I,J,TP
112 FORMAT(1X,'YIELD AT THE LEFT END OF THE BEAM -- STOREY NO.',I3,',
1 BAY NO.',I3,'; TIME',F7.3,' SEC.')
GO TO 128
115 WRITE(6,116) I,J,TP
116 FORMAT(1X,'YIELD AT THE RIGHT END OF THE BEAM -- STOREY NO.',I3,',
1 BAY NO.',I3,'; TIME',F7.3,' SEC.')
GO TO 128
120 JC=J-NB
GO TO (121,125), K
121 WRITE(6,122) I,J,TP
122 FORMAT(1X,'YIELD AT THE TOP OF THE COLUMN -- STOREY NO.',I3,',
1 COL. NO.',I3,'; TIME',F7.3,' SEC.')
GO TO 128
125 WRITE(6,126) I,J,TP
126 FORMAT(1X,'YIELD AT THE BOTTOM OF THE COLUMN -- STOREY NO.',I3,',
1 COL. NO.',I3,'; TIME',F7.3,' SEC.')
128 IF(IMA(M,K) .GT. 0) GO TO 130
GO TO 170
130 IF(FT(M,K) .GE. THETA(M,K,3)) GO TO 210
IP=IMA(M,K)
THETA(M,K,IP)=FT(M,K)
IF(IP.EQ.2) THETA(M,K,1)=FT(M,K)
YA=SLP(M,K,IP+1)*FT(M,K)+BETA(M,K,IP+1)
YB=SLP(M,K,3)*THETA(M,K,2)+BETA(M,K,3)
PMO(M,K,1)=YA
PMC(M,K,1)=YB
IF(SLP(M,K,1) .GE. (2.5*STF(M))) GO TO 131
BETA(M,K,1)=YA-(SLP(M,K,1)*FT(M,K))
131 CONTINUE
THETA(M,K,4)=FT(M,K)-(YA/SLP(M,K,1))
SLP(M,K,4)=-PMC(M,K,2)/(THETA(M,K,4)-THETA(M,K,5))
BETA(M,K,4)=-THETA(M,K,4)*SLP(M,K,4)
INEG(M,K)=4
GO TO 340
170 IF(FT(M,K) .LE. THETA(M,K,6)) GO TO 210
PMO(M,K,1)=0.0

```



```

      IN=-IMA(M,K)
      THETA(M,K,IN+3)=FT(M,K)
      YC=SLP(M,K,IN+3)*FT(M,K)+BETA(M,K,IN+3)
      YD=SLP(M,K,5)*THETA(M,K,5)+BETA(M,K,5)
      PMC(M,K,2)=YD
      IF(SLP(M,K,1).GE.(2.5*STF(M)))GO TO 171
      BETA(M,K,1)=YC-SLP(M,K,1)*FT(M,K)
171  CONTINUE
      THETA(M,K,1)=FT(M,K)-(YC/SLP(M,K,1))
      SLP(M,K,2)=PMC(M,K,1)/(THETA(M,K,2)-THETA(M,K,1))
      BETA(M,K,2)=-THETA(M,K,1)*SLP(M,K,2)
      IPOS(M,K)=1
      GO TO 340
210  KDIS=-10
      IF(J .GE. NB1) GO TO 260
      GO TO (220,240), K
220  WRITE(6,230) I,J,TP
230  FORMAT(/1X,'COLLAPSE AT THE LEFT END  OF THE BEAM -- STOREY NO.',I
      13,', BAY NO.',I3,'; TIME',F7.3,' SEC.')
      GO TO 340
240  WRITE(6,250) I,J,TP
250  FORMAT(/1X,'COLLAPSE AT THE RIGHT END OF THE BEAM -- STOREY NO.',I
      13,', BAY NO.',I3,'; TIME',F7.3,' SEC.')
      GO TO 340
260  JC=J-NB
      GO TO (270,290), K
270  WRITE(6,280) I,J,TP
280  FORMAT(/1X,'COLLAPSE AT THE TOP    OF THE COLUMN -- STOREY NO.',I
      13,', COL. NO.',I3,'; TIME',F7.3,' SEC.')
      GO TO 340
290  WRITE(6,300) I,J,TP
300  FORMAT(/1X,'COLLAPSE AT THE BOTTOM  OF THE COLUMN -- STOREY NO.',I
      13,', COL. NO.',I3,'; TIME',F7.3,' SEC.')
340  CONTINUE
350  CONTINUE
360  CONTINUE
      RETURN
      END

```



## APPENDIX #

 $M_s - \delta \theta_s$  PROGRAM

## E-1 Introduction

This program has been developed to predict and combine the deformations due to flexure and shear of the cantilever column shown in Fig. 4-3. The background to the program is contained in Sec. 4-3.

## E-2 Input Data

First Card: NUMBER, HEIGHT, INTYPE

Input format: (I5, F10.5, I5)

NUMBER = Member number

HEIGHT = Height of cantilever

INTYPE = Input type (usually = 1)

Second Card: VULT

Input format: (F10.5)

VULT = ultimate shear to be applied.

Third Card: (C(I,J), J = 1,8)

Fourth Card: (C(I,J), J = 9,16)

Fifth Card : (C(I,J), J = 17,24)

Sixth Card : (C(I,J), J = 25,30)

Input format:(8F10.5)

(C(I,J), J = 1,20) describe the input M-P- $\phi$  relationship as shown in Fig. E-3.

C(I,21) = Axial load



$C(I,22)$  = Cross section moment of inertia  
 $C(I,23)$  = Cross-section section modulus  
 $C(I,24)$  = Height of cross-section  
 $C(I,25)$  = 28 day concrete compressive strength

$(C(I,J), J = 26,29)$  describes the input  $M-P-\phi$   
 relationship as shown in Fig. E-3.

Seventh Card: GAMMA 1, V1, GAMMA 2, V2, GAMMA 3, V3

GAMMA 1, V1 Coordinates of first point of input  
 $V-\gamma$  relationship of Fig. E-2.

GAMMA 2, V2 Coordinates of second point of Fig. E-2

GAMMA 3, V3 Coordinates of third point of Fig. E-2

### E-3 Description of Program

The program is described in Sec. 4-3 of this dissertation.





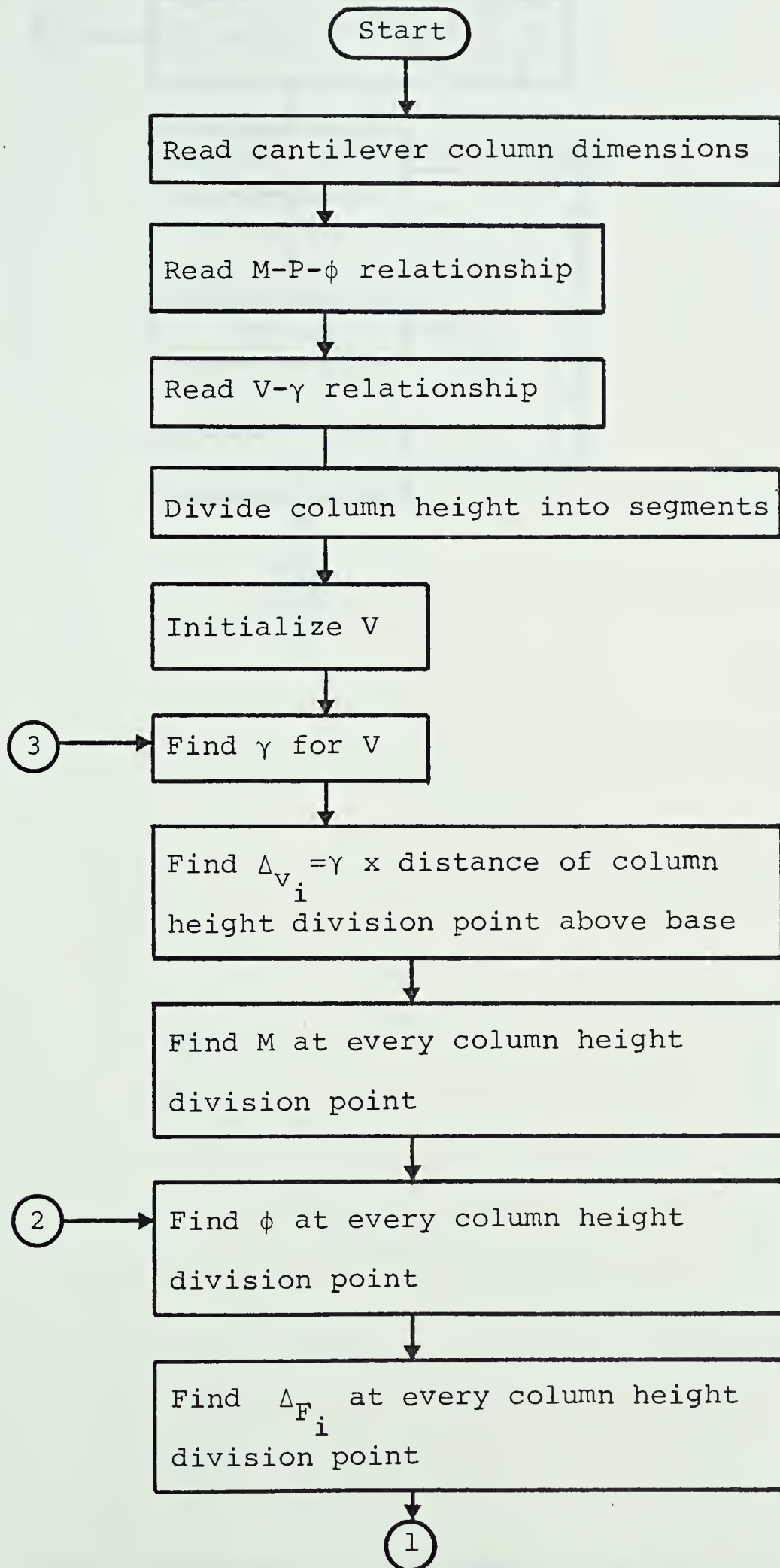


FIG. E-1 Flow Chart for  $M_S-\delta\theta_S$  Program



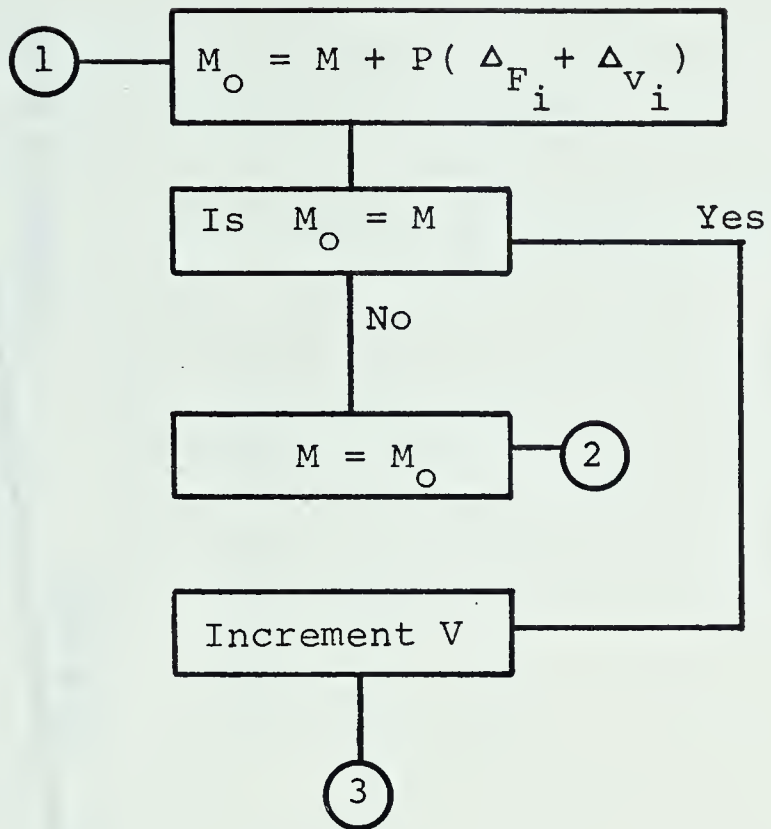


FIG. E-1 (Cont'd) Flow Chart for  $M_s - \delta\theta_s$  Program



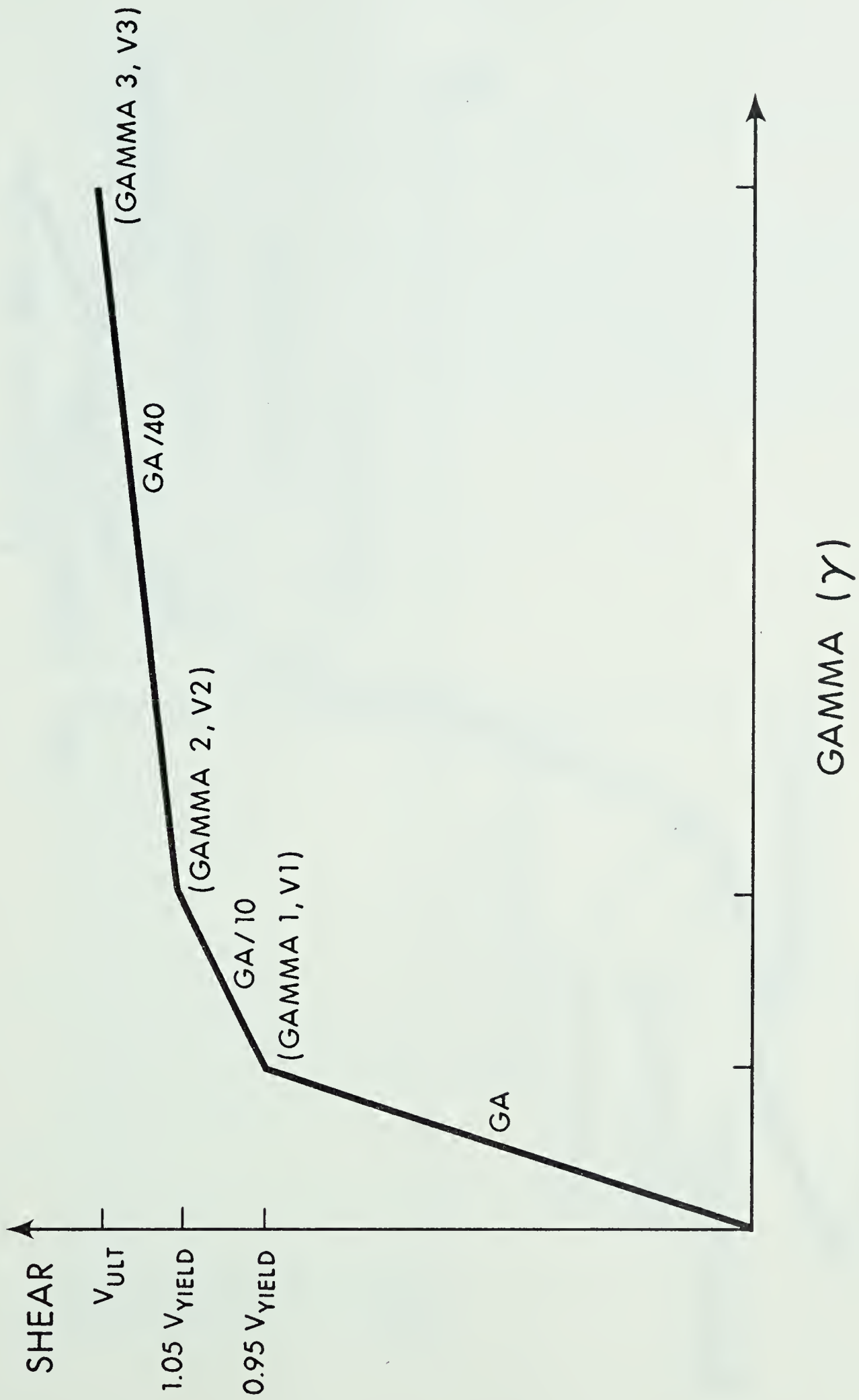


FIG. E-2 Input V- $\gamma$  Relationship





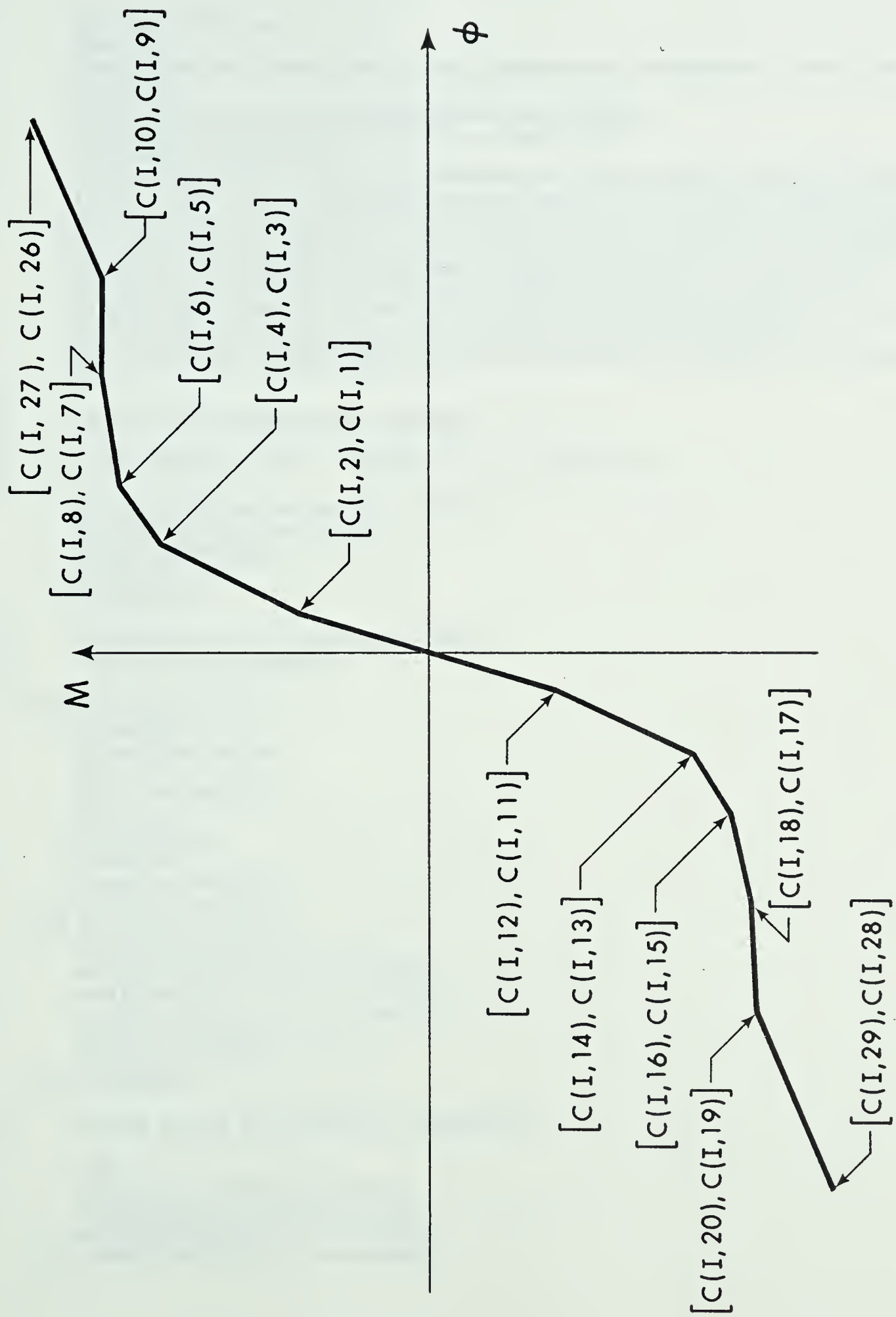


FIG. E-3 Input  $M$ - $P$ - $\phi$  Relationship



```

      IMPLICIT REAL(M)
      REAL KV
      DIMENSION XPHI(300),YMPHI(300),XGAMMA(300),YVGAM(300),DEXPT(300),D
      *MAX(300)
      DIMENSION DELTA(300),MMDATA(300),DFDATA(300)
      DIMENSION VDATA(300),PDATA(300),GDATA(300)
      DIMENSION SLOPE(100)
      DIMENSION MORIG(30),SS(30),DTKEPT(300),AVGRAT(30),BDMID(300),MKEPT
      1(30),DL(30),V(30),GAMMA(30),DV(30),DF(30),DT(30),MDATA(300),ALPHA(
      220),MSTORE(30),COUNT2(30),COUNT3(30),COUNT4(30),COUNT5(30),COUNT6(
      330),COUNT7(30),COUND8(30),PATH(30),PLASTO(30),MLAST(30),PLAST(30),
      4MSAVE(30),PSAVE(30),MSAVE1(30),PSAVE1(30),S(30),H(30),PHI(30),M(30
      5),CTROID(30),SPC(30),AREAM(30),C(6,30),COUNT(30),COUNT1(30)
      DIMENSION VKEPT(30),VLAST(30),GLAST(30),VPATH(30),VSAVE(30),GSAVE(
      *30),VSAVE1(30),GSAVE1(30),GLASTO(30),COONT(30),COONT1(3
      $0),COONT3(30),COONT4(30),COONT5(30),COONT6(30),COONT7(30),COOND8(3
      *0)

C
C      UNITS ARE KIPS, INCHES, 1/INCHES
C
C      READ MEMBER NUMBER, HEIGHT, AND V INPUT TYPE
C
      READ(5,100)NUMBER,HEIGHT,INTYPE
      IF(INTYPE.LT.1)GO TO 13
      READ(5,901)VULT
13  CONTINUE
      VINC=0.60

C
C      DISCRETIZATION OF MEMBER HEIGHT
C      AUTOMATIC DIVISIONS
C
202  NDIV=20
      DIVN=NDIV
      DIV=HEIGHT/DIVN
      F=-1.0
      DO 9 I=1,NDIV
      F=F+1.0
      S(I)=F*DIV
9  CONTINUE
      S(NDIV+1)=HEIGHT
      DO 109 I=1,NDIV
109  H(I)=S(I+1)-S(I)
      WRITE(6,128)NDIV
      WRITE(6,130)(S(I),I=1,NDIV)
      WRITE(6,132)
      WRITE(6,134)(H(I),I=1,NDIV)
      DO 151 I=1,NDIV
      COUNT2(I)=0.0
151  CONTINUE

C
C      READS M, PHI AND SECTION PROPERTIES
C
      I=1
      READ(5,901)(C(I,J),J=1,8)
      READ(5,901)(C(I,J),J=9,16)
      READ(5,901)(C(I,J),J=17,24)
      READ(5,901)(C(I,J),J=25,30)

```



```

WRITE(8,939)
WRITE(8,937)NUMBER,C(I,21)
WRITE(8,926)C(I,1),C(I,2)
WRITE(8,927)C(I,3),C(I,4)
WRITE(8,928)C(I,5),C(I,6)
WRITE(8,929)C(I,7),C(I,8)
WRITE(8,930)C(I,9),C(I,10)
WRITE(8,931)C(I,11),C(I,12)
WRITE(8,932)C(I,13),C(I,14)
WRITE(8,933)C(I,15),C(I,16)
WRITE(8,934)C(I,17),C(I,18)
WRITE(8,935)C(I,19),C(I,20)
WRITE(8,940)C(I,26),C(I,27)
WRITE(8,941)C(I,28),C(I,29)
WRITE(8,938)C(I,22),C(I,23),C(I,24),C(I,25)
WRITE(8,939)
NNODES=NDIV+1
C
C   READ V-GAMMA RELATIONSHIP
C
READ(5,901)GAMMA1,V1,GAMMA2,V2,GAMMA3,V3
WRITE(8,4567)GAMMA1,V1,GAMMA2,V2,GAMMA3,V3
4567 FORMAT(6E20.10)
WRITE(8,970)
970 FORMAT(// 'THE V - GAMMA RELATIONSHIP USED ' //)
WRITE(8,939)
GA1=V1/GAMMA1
GA2=(V2-V1)/(GAMMA2-GAMMA1)
GA3=(V3-V2)/(GAMMA3-GAMMA2)
COONT2=0.0
GAT=GA1
GAT1=GA1
GAMM11=-GAMMA1
GAMM21=-GAMMA2
GAMM31=-GAMMA3
V11=-V1
V21=-V2
V31=-V3
DO 780 I=1,NNODES
M(I)=0.0
MKEPT(I)=0.0
MLAST(I)=0.0
780 MSTORE(I)=0.0
K1=1
717 CONTINUE
C
C   STORE MOMENT AND DEFLECTION DATA
C
IF(K1.EQ.1)GO TO 310
DTKEPT(K1-1)=DT(NNODES)
DFDATA(K1-1)=DF(NNODES)
DEXPT(K1-1)=DTOP
BDMID(K1-1)=DV(NNODES)
MDATA(K1-1)=MLAST(1)
VDATA(K1-1)=VLAST(1)
PDATA(K1-1)=PLAST(1)
GDATA(K1-1)=GLAST(1)
310 CONTINUE
704 VINC=VINC+0.01
960 FORMAT(3F10.5)

```



```

      IF (INTYPE.GT.0.0) VTOP=VINC*VULT
      IF (K1.GT.1) GO TO 315
925 IC=1
      MCR=C(IC,1)
      PHICR=C(IC,2)
      MY=C(IC,3)
      PHIY=C(IC,4)
      MFY=C(IC,5)
      PHIFY=C(IC,6)
      MWY=C(IC,7)
      PHIWY=C(IC,8)
      MULT=C(IC,9)
      PHIULT=C(IC,10)
      MCR1=C(IC,11)
      PHICR1=C(IC,12)
      MY1=C(IC,13)
      PHIY1=C(IC,14)
      MFY1=C(IC,15)
      PHIFY1=C(IC,16)
      MWY1=C(IC,17)
      PHIWY1=C(IC,18)
      MULT1=C(IC,19)
      PHIUL1=C(IC,20)
      AXIAL1=C(IC,21)
      XNI=C(IC,22)
      XNS=C(IC,23)
      FSUBC=C(IC,25)
      MSSH=C(IC,26)
      PHISSH=C(IC,27)
      MSSH1=C(IC,28)
      PHSSH1=C(IC,29)
      EIO=MCR/PHICR
      MODR=ESTEEL*XNI/EIO
      EIG=(MY-MCR)/(PHIY-PHICR)
      ESH=(MFY-MY)/(PHIFY-PHIY)
      EFY=(MWY-MFY)/(PHIWY-PHIFY)
      EWY=(MULT-MWY)/(PHIULT-PHIWY)
      EIO1=MCR1/PHICR1
      EIG1=(MY1-MCR1)/(PHIY1-PHICR1)
      ESH1=(MFY1-MY1)/(PHIFY1-PHIY1)
      EFY1=(MWY1-MFY1)/(PHIWY1-PHIFY1)
      EWY1=(MULT1-MWY1)/(PHIUL1-PHIWY1)
      ESSH=(MSSH-MULT)/(PHISSH-PHIULT)
      ESSH1=(MSSH1-MULT1)/(PHSSH1-PHIUL1)
      IF (MSSH1.EQ.0.0) ESSH1=EWY1
      IF (MSSH.EQ.0.0) ESSH=EWY
      IF (MSSH.EQ.0.0) MSSH=MULT
      IF (MSSH1.EQ.0.0) MSSH1=MULT1
      IF (PHISSH.EQ.0.0) PHISSH=PHIULT
      IF (PHSSH1.EQ.0.0) PHSSH1=PHIUL1
8 EIT=EIO
      EIT1=EIO1
315 CONTINUE
      WRITE(6,950) K1, VTOP
      IF (COUNT8.GT.0.1) GO TO 311
      GO TO 314
C
C      WRITE STORED MOMENT AND DEFLECTION DATA
C
311 WRITE(8,313)

```





```

      K1=K1-1
      DO 16 IA=1,K1
16 WRITE(6,316) MDATA(IA),DTKEPT(IA),VDATA(IA),GDATA(IA),MDATA(IA),PDA
      *TA(IA)
      DO 4100 NA=1,K1
      DEL=VDATA(NA)*((HEIGHT**3)/(3.*EIO))
      DELTA(NA)=(DTKEPT(NA)-DEL)/HEIGHT
4100 MMDATA(NA)=MDATA(NA)-(AXI ALL*DTKEPT(NA))
      DO 4400 NA=1,K1
      WRITE(6,316)DEXPT(NA),DTKEPT(NA),DFDATA(NA),BDMID(NA),MMDATA(NA),
      *DELTA(NA)
4400 CONTINUE
      WRITE(8,4409)
4409 FORMAT(/9X,'MOMENT',14X,'DELTA-THETA',9X,'SLOPE'/)
      CONTR=0.0
      DO 4401 NB=2,K1
      SLOPE(NB)=(MMDATA(NB)-MMDATA(NB-1))/(DELTA(NB)-DELTA(NB-1))
      IF(MDATA(NB).GE.MFY)GO TO 4403
      GO TO 4404
4403 IF(CONTR.GT.0.1)GO TO 4404
      SM1=MMDATA(NB-1)
      SD1=DELTA(NB-1)
      CONTR=1.0
4404 CONTINUE
4401 WRITE(8,318)NB,MMDATA(NB),DELTA(NB),SLOPE(NB),MDATA(NB),DTKEPT(NB)
318 FORMAT(I5,5(2X,E20.12))
      SM2=(MMDATA(K1)+SM1)/2.
      SD2=(DELTA(K1)+SD1)/2.
      WRITE(7,4408)SD1,SM1,SD2,SM2,DELTA(K1),MMDATA(K1)
4408 FORMAT(F10.7,F10.1,F10.7,F10.1,F10.7,F10.1)
C
C   INPUT AND OUTPUT PLOTS
C
      XPHI(1)=PHSSH1
      YMPHI(1)=MSSH1
      XPHI(2)=C(1,20)
      YMPHI(2)=C(1,19)
      XPHI(3)=C(1,18)
      YMPHI(3)=C(1,17)
      XPHI(4)=C(1,16)
      YMPHI(4)=C(1,15)
      XPHI(5)=C(1,14)
      YMPHI(5)=C(1,13)
      XPHI(6)=C(1,12)
      YMPHI(6)=C(1,11)
      XPHI(7)=0.0
      YMPHI(7)=0.0
      XPHI(8)=C(1,2)
      YMPHI(8)=C(1,1)
      XPHI(9)=C(1,4)
      YMPHI(9)=C(1,3)
      XPHI(10)=C(1,6)
      YMPHI(10)=C(1,5)
      XPHI(11)=C(1,8)
      YMPHI(11)=C(1,7)
      XPHI(12)=C(1,10)
      YMPHI(12)=C(1,9)
      XPHI(13)=PHISSH
      YMPHI(13)=MSSH
      XGAMMA(1)=GAMM31

```



```

YVGAM(1)=V31
XGAMMA(2)=GAMM21
YVGAM(2)=V21
XGAMMA(3)=GAMM11
YVGAM(3)=V11
XGAMMA(4)=0.0
YVGAM(4)=0.0
XGAMMA(5)=GAMMA1
YVGAM(5)=V1
XGAMMA(6)=GAMMA2
YVGAM(6)=V2
XGAMMA(7)=GAMMA3
YVGAM(7)=V3
314 CONTINUE
K1=K1+1
YYY=0.0
CHECK=0.0
COUNTF=0.0
IF(COUNT8.GT.0.1)CALL EXIT
DO 520 I=1,NNODES
COUNT3(I)=0.0
COUNT4(I)=0.0
COUNT5(I)=0.0
COUNT6(I)=0.0
DL(I)=0.0
520 CONTINUE
720 CONTINUE
C
C   COMPUTE V AT EACH NODE
C
DO 701 I=1,NNODES
701 V(I)=VTOP
C
C   CALCULATE GAMMA FOR EACH DIVISION
C
VCHECK=0.0
DO 1520 I=1,NNODES
COONT3(I)=0.0
COONT4(I)=0.0
COONT5(I)=0.0
COONT6(I)=0.0
1520 CONTINUE
WRITE(6,1160)
1160 FORMAT(18X,'V',13X,'GAMMA',3X,'GLASTO',8X,'GSAVE',8X,'VSAVE',5X,
*'GSAVE1',5X,'VSAVE1'/)
DO 1063 I=1,NDIV
COONT2=COONT2+1.0
IF(COONT2.GT.1.0)GO TO 1051
DO 1050 KK=1,NNODES
GAMMA(KK)=0.0
VLAST(KK)=0.0
GLAST(KK)=0.0
VSAVE(KK)=0.0
GSAVE(KK)=0.0
VSAVE1(KK)=0.0
GSAVE1(KK)=0.0
VKEPT(KK)=0.0
COONT7(KK)=0.0
COOND8(KK)=0.0
1050 GLASTO(KK)=0.0

```



```

1051 CONTINUE
    IF(V(I))1017,1032,1019
1019 IF(V(I)*VLAST(I))1046,1046,1047
1046 COONT(I)=0.0
    IF(VKEPT(I).GE.VLAST(I))GO TO 1215
1261 CONTINUE
    IF(VLAST(I).LT.VSAVE(I))GO TO 1423
    GO TO 1047
1423 COONT5(I)=1.0
    GO TO 1215
1047 CONTINUE
    IF(V(I).LT.VLAST(I))GO TO 1030
1591 CONTINUE
    IF(COONT4(I).GT.0.1)GO TO 1028
1207 IF(ABS(GLASTO(I)).GT.1.0E-09)GO TO 1031
1048 IF(V(I).LE.V1)GO TO 1020
1208 IF(V(I).LE.V2)GO TO 1021
1598 CONTINUE
    GAMMA(I)=GAMMA2+((V(I)-V2)/GA3)
    VPATH(I)=18.
    GO TO 1023
1020 GAMMA(I)=V(I)/GA1
    GLASTO(I)=0.0
    VPATH(I)=1.
    GO TO 1023
1021 GAMMA(I)=GAMMA1+((V(I)-V1)/GA2)
    VPATH(I)=2.
    GO TO 1023
1031 IF(COOND8(I).LT.0.9)GO TO 1248
    GO TO 1631
1248 VSAVE(I)=V1
    GSAVE(I)=GAMMA1
1631 IF(V(I).GT.VSAVE(I))GO TO 1048
1499 CONTINUE
    GANOW=VSAVE(I)/(GSAVE(I)-GLASTO(I))
    GAMMA(I)=V(I)/GANOW+GLASTO(I)
    VPATH(I)=3.
    GO TO 1023
1030 COONT(I)=COONT(I)+1.0
    IF(COONT(I).GT.1.1)GO TO 1028
1209 VSAVE(I)=VLAST(I)
    GSAVE(I)=GLAST(I)
    COONT4(I)=1.0
1028 IF(GSAVE(I).LE.GAMMA1)GO TO 1035
1210 IF(GSAVE(I).LE.GAMMA2)GO TO 1033
1211 GATX=GAT.
    GAMMA(I)=GSAVE(I)-((VSAVE(I)-V(I))/GATX)
    GLASTO(I)=GSAVE(I)-(VSAVE(I)/GATX)
    IF(COONT6(I).GT.0.1)GO TO 1049
1490 CONTINUE
    VPATH(I)=4.
    GO TO 1023
1033 GATY=(VSAVE(I)-V11)/(GSAVE(I)-GAMM11)
    GAMMA(I)=GSAVE(I)-((VSAVE(I)-V(I))/GATY)
    GLASTO(I)=GSAVE(I)-(VSAVE(I)/GATY)
    IF(COONT6(I).GT.0.1)GO TO 1049
1491 CONTINUE
    VPATH(I)=5.
    GO TO 1023
1035 CONTINUE

```





```

      IF(COONT6(I).GT.0.1)GO TO 1049
1492  CONTINUE
      GAMMA(I)=V(I)/GA1
      GLASTO(I)=0.0
      VPATH(I)=11.
1023  CONTINUE
      IF(V(I).LE.0.0)GO TO 1262
      IF(VCHECK.GT.0.1)GO TO 1301
1302  CONTINUE
      VKEPT(I)=VLAST(I)
1301  CONTINUE
      VLAST(I)=V(I)
      GLAST(I)=GAMMA(I)
      COOND8(I)=1.0
      GO TO 1044
1017  IF(V(I)*VLAST(I))1098,1098,1049
1098  COONT1(I)=0.0
      IF(VKEPT(I).LE.VLAST(I))GO TO 1209
1262  CONTINUE
      IF(VLAST(I).GT.VSAVE(I))GO TO 1422
      GO TO 1049
1422  COONT6(I)=1.0
      GO TO 1209
1049  CONTINUE
      IF(V(I).GT.VLAST(I))GO TO 1039
1592  CONTINUE
      IF(COONT3(I).GT.0.1)GO TO 1041
1212  IF(GSAVE(I).LE.GAMMA1)GO TO 1036
1213  GO TO 1037
1036  IF(V(I).LT.V11)GO TO 1040
1214  GAMMA(I)=V(I)/GA1
      VPATH(I)=6.
      GO TO 1024
1040  IF(V(I).LT.V21)GO TO 1404
3100  CONTINUE
      GAMMA(I)=GAMM11+((V(I)-V11)/GA2)
      VPATH(I)=7.
      GO TO 1024
1404  CONTINUE
      GAMMA(I)=GAMM21+((V(I)-V21)/GA3)
      VPATH(I)=19.
      GO TO 1024
1037  IF(COONT7(I).LT.0.9)GO TO 1236
      GO TO 1632
1236  VSAVE1(I)=V11
      GSAVE1(I)=GAMM11
1632  IF(V(I).LT.VSAVE1(I))GO TO 1036
1237  GANOW1=VSAVE1(I)/(GSAVE1(I)-GLASTO(I))
      GAMMA(I)=GLASTO(I)+(V(I)/GANOW1)
      VPATH(I)=8.
      GO TO 1024
1039  COONT1(I)=COONT1(I)+1.0
      IF(COONT1(I).GT.1.1)GO TO 1041
1215  GSAVE1(I)=GLAST(I)
      VSAVE1(I)=VLAST(I)
      COONT3(I)=1.0
1041  IF(GSAVE1(I).GE.GAMM11)GO TO 1042
1216  IF(GSAVE1(I).GE.GAMM21)GO TO 1043
1217  GAT1X=GAT1
      GAMMA(I)=GSAVE1(I)-((VSAVE1(I)-V(I))/GAT1X)

```



```

        GLASTO(I)=GSAVE1(I)-(VSAVE1(I)/GAT1X)
        IF(COONT5(I).GT.0.1)GO TO 1047
1493  CONTINUE
        VPATH(I)=9.
        GO TO 1024
1042  CONTINUE
        GAMMA(I)=V(I)/GA1
        GLASTO(I)=0.0
        IF(COONT5(I).GT.0.1)GO TO 1047
1494  CONTINUE
        VPATH(I)=14.
        GO TO 1024
1043  GATY1=(V1-VSAVE1(I))/(GAMMA1-GSAVE1(I))
        GAMMA(I)=GSAVE1(I)-((VSAVE1(I)-V(I))/GATY1)
        GLASTO(I)=GSAVE1(I)-(VSAVE1(I)/GATY1)
        IF(COONT5(I).GT.0.1)GO TO 1047
1495  CONTINUE
        VPATH(I)=10.
1024  CONTINUE
        IF(V(I).GE.0.0)GO TO 1261
        IF(VCHECK.GT.0.1)GO TO 1303
1304  CONTINUE
        VKEPT(I)=VLAST(I)
1303  CONTINUE
        VLAST(I)=V(I)
        GLAST(I)=GAMMA(I)
        COONT7(I)=1.0
        GO TO 1044
1032  IF(VLAST(I))1045,1044,1096
1045  GAT3=(V1-VSAVE1(I))/(GAMMA1-GSAVE1(I))
        IF(VSAVE1(I).LE.V21)GAT3=GAT1
        GLASTO(I)=GSAVE1(I)-(VSAVE1(I)/GAT3)
        IF(VSAVE1(I).GE.V11)GLASTO(I)=0.0
        GAMMA(I)=GLASTO(I)
        VPATH(I)=12.
        IF(VCHECK.GT.0.1)GO TO 1322
1326  CONTINUE
        VKEPT(I)=VLAST(I)
1322  CONTINUE
        VLAST(I)=V(I)
        GO TO 1044
1096  GAT2=(VSAVE(I)-V11)/(GSAVE(I)-GAMM11)
        IF(VSAVE(I).GE.V2)GAT2=GAT
        GLASTO(I)=GSAVE(I)-(VSAVE(I)/GAT2)
        IF(VSAVE(I).LE.V1)GLASTO(I)=0.0
        GAMMA(I)=GLASTO(I)
        IF(VCHECK.GT.0.1)GO TO 1324
1328  CONTINUE
        VKEPT(I)=VLAST(I)
1324  CONTINUE
        VLAST(I)=V(I)
        VPATH(I)=13.
1044  CONTINUE
        WRITE(6,150)I,VPATH(I),V(I),GAMMA(I),GLASTO(I),GSAVE(I),VSAVE(I),
        *GSAVE1(I),VSAVE1(I)
1063  CONTINUE
        DO 421 I=1,NNODES
421   DV(I)=0.0
        DO 709 I=2,NNODES
        K=I-1

```



```

      DO 709 J=1,K
      DV(I)=DV(I)+(GAMMA(J)*H(J))
709  CONTINUE
C
C      COMPUTE M AT EACH NODE
C
      M(NNODES)=0.0
      M(1)=VTOP*HEIGHT
      DO 14 I=2,NNODES
14  M(I)=M(1)*(HEIGHT-S(I))/HEIGHT
418  CONTINUE
      WRITE(6,907)
      DO 799 I=1,NNODES
      MSTORE(I)=M(I)
799  WRITE(6,909)I,V(I),GAMMA(I),MKEPT(I),MLAST(I),MSTORE(I)
C      CALCULATE PHI AT EACH NODE
C
718  WRITE(6,160)
      PHI(NNODES)=0.0
      PLASTC(NNODES)=0.0
      KA=1
      DO 63 I=KA,NDIV
      IF(M(I).GE.MULT)GO TO 3331
      GO TO 3332
3331  K1=K1-1
      COUNT8=1.0
      IF(COUNT8.E0.1.0)GO TO 311
3332  CONTINUE
      COUNT2(I)=COUNT2(I)+1.0
      IF(COUNT2(I).GT.1.1)GO TO 27
754  CONTINUE
      PLASTO(I)=0.0
      MLAST(I)=0.0
      PLAST(I)=0.0
      MSAVE(I)=0.0
      PSAVE(I)=0.0
      PSAVE1(I)=0.0
      MSAVE1(I)=0.0
      COUNT7(I)=0.0
      COUNO8(I)=0.0
27  CONTINUE
      IF(M(I))17,32,19
19  IF(M(I)*MLAST(I))46,46,47
46  COUNT(I)=0.0
      IF(MKEPT(I).GE.MLAST(I))GO TO 215
261  CONTINUE
      IF(MLAST(I).LT.MSAVE1(I))GO TO 423
      GO TO 47
423  COUNT5(I)=1.0
      GO TO 215
47  CONTINUE
      IF(M(I).LT.MLAST(I))GO TO 30
591  CONTINUE
      IF(COUNT4(I).GT.0.1)GO TO 28
207  IF(ABS(PLASTO(I)).GT.0.0000000001)GO TO 31
48  IF(M(I).LE.MCR)GO TO 20
208  IF(M(I).LE.MY)GO TO 21
598  CONTINUE
      IF(M(I).GT.MFY)GO TO 800
801  PHI(I)=PHIY+((M(I)-MY)/ESH)

```



```

    PATH(I)=18.
    GO TO 23
800 IF(M(I).GT.MWY)GO TO 802
    PHI(I)=PHIFY+((M(I)-MFY)/EFY)
    PATH(I)=20.
    GO TO 23
802 IF(M(I).GT.MULT)GO TO 880
    PHI(I)=PHIWIY+((M(I)-MWY)/EWY)
    PATH(I)=21.
    GO TO 23
880 PHI(I)=PHIULT+((M(I)-MULT)/ESSH)
    PATH(I)=24.
    GO TO 23
20 PHI(I)=M(I)/EIO
    PLASTO(I)=0.0
    PATH(I)=1.
    GO TO 23
21 PHI(I)=PHICR+((M(I)-MCR)/EIG)
    PATH(I)=2.
    GO TO 23
31 IF(COUND8(I).LT.0.9)GO TO 248
    GO TO 631
248 MSAVE(I)=MCR
    PSAVE(I)=PHICR
631 IF(M(I).GT.MSAVE(I))GO TO 48
499 CONTINUE
    EINOW=MSAVE(I)/(PSAVE(I)-PLASTO(I))
    PHI(I)=M(I)/EINOW+PLASTO(I)
    PATH(I)=3.
    GO TO 23
30 COUNT(I)=COUNT(I)+1.0
    IF(COUNT(I).GT.1.1)GO TO 28
209 PSAVE(I)=PLAST(I)
    MSAVE(I)=MLAST(I)
    COUNT4(I)=1.0
28 IF(PSAVE(I).LE.PHICR)GO TO 35
210 IF(PSAVE(I).LE.PHIY)GO TO 33
211 EITX=EIT
    PHI(I)=PSAVE(I)-((MSAVE(I)-M(I))/EITX)
    PLASTO(I)=PSAVE(I)-(MSAVE(I)/EITX)
    IF(COUNT6(I).GT.0.1)GO TO 49
490 CONTINUE
    PATH(I)=4.
    GO TO 23
33 EITY=(MSAVE(I)-MCR1)/(PSAVE(I)-PHICR1)
    PHI(I)=PSAVE(I)-((MSAVE(I)-M(I))/EITY)
    PLASTO(I)=PSAVE(I)-(MSAVE(I)/EITY)
    IF(COUNT6(I).GT.0.1)GO TO 49
491 CONTINUE
    PATH(I)=5.
    GO TO 23
35 CONTINUE
    IF(COUNT6(I).GT.0.1)GO TO 49
492 CONTINUE
    PHI(I)=M(I)/EIO
    PLASTO(I)=0.0
    PATH(I)=11.
23 CONTINUE
    IF(M(I).LE.0.0)GO TO 262
    IF(CHECK.GT.0.1)GO TO 301

```





```

302 CONTINUE
   MKEPT(I)=MLAST(I)
301 CONTINUE
   MLAST(I)=M(I)
   PLAST(I)=PHI(I)
   COUNDO(I)=1.0
   GO TO 44
17 IF(M(I)*MLAST(I))98,98,49
98 COUNT1(I)=0.0
   IF(MKEPT(I).LE.MLAST(I))GO TO 209
262 CONTINUE
   IF(MLAST(I).GT.MSAVE(I))GO TO 422
   GO TO 49
422 COUNT6(I)=1.0
   GO TO 209
49 CONTINUE
   IF(M(I).GT.MLAST(I))GO TO 39
592 CONTINUE
   IF(COUNT3(I).GT.0.1)GO TO 41
212 IF(PSAVE(I).LE.PHICR)GO TO 36
213 GO TO 37
36 IF(M(I).LT.MCR1)GO TO 40
214 PHI(I)=M(I)/EIO1
   PATH(I)=6.
   GO TO 24
40 IF(M(I).LT.MY1)GO TO 404
2100 CONTINUE
   PHI(I)=PHICR1+((M(I)-MCR1)/EIG1)
   PATH(I)=7.
   GO TO 24
404 CONTINUE
   IF(M(I).LT.MFY1)GO TO 803
804 PHI(I)=PHIY1+((M(I)-MY1)/ESH1)
   PATH(I)=19.
   GO TO 24
803 IF(M(I).LT.MWY1)GO TO 805
   PHI(I)=PHIFY1+((M(I)-MFY1)/EFY1)
   PATH(I)=22.
   GO TO 24
805 IF(M(I).LT.MULT1)GO TO 881
   PHI(I)=PHIY1+((M(I)-MWY1)/EWY1)
   PATH(I)=23.
   GO TO 24
881 PHI(I)=PHIUL1+((M(I)-MULT1)/ESSH1)
   PATH(I)=25.
   GO TO 24
37 IF(COUNT7(I).LT.0.9)GO TO 236
   GO TO 632
236 MSAVE1(I)=MCR1
   PSAVE1(I)=PHICR1
632 IF(M(I).LT.MSAVE1(I))GO TO 36
237 EINOW1=MSAVE1(I)/(PSAVE1(I)-PLASTO(I))
   PHI(I)=PLASTO(I)+(M(I)/EINOW1)
   PATH(I)=8.
   GO TO 24
39 COUNT1(I)=COUNT1(I)+1.0
   IF(COUNT1(I).GT.1.1)GO TO 41
215 PSAVE1(I)=PLAST(I)
   MSAVE1(I)=MLAST(I)
   COUNT3(I)=1.0

```



```

41 IF(PSAVE1(I).GE.PHICR1)GO TO 42
216 IF(PSAVE1(I).GE.PHIY1)GO TO 43
217 EIT1X=EIT1
    PHI(I)=PSAVE1(I)-((MSAVE1(I)-M(I))/EIT1X)
    PLASTO(I)=PSAVE1(I)-(MSAVE1(I)/EIT1X)
    IF(COUNT5(I).GT.0.1)GO TO 47
493 CONTINUE
    PATH(I)=9.
    GO TO 24
42 CONTINUE
    PHI(I)=M(I)/EI01
    PLASTO(I)=0.0
    IF(COUNT5(I).GT.0.1)GO TO 47
494 CONTINUE
    PATH(I)=14.
    GO TO 24
43 EITY1=(MCR-MSAVE1(I))/(PHICR-PSAVE1(I))
    PHI(I)=PSAVE1(I)-((MSAVE1(I)-M(I))/EITY1)
    PLASTO(I)=PSAVE1(I)-(MSAVE1(I)/EITY1)
    IF(COUNT5(I).GT.0.1)GO TO 47
495 CONTINUE
    PATH(I)=10.
24 CONTINUE
    IF(M(I).GE.0.0)GO TO 261
    IF(CHECK.GT.0.2)GO TO 303
304 CONTINUE
    MKEPT(I)=MLAST(I)
303 CONTINUE
    MLAST(I)=M(I)
    PLAST(I)=PHI(I)
    COUNT7(I)=1.0
    GO TO 44
32 IF(MLAST(I))45,44,96
45 EIT3=(MCR-MSAVE1(I))/(PHICR-PSAVE1(I))
    IF(MSAVE1(I).LE.MY1)EIT3=EIT1
    PLASTO(I)=PSAVE1(I)-(MSAVE1(I)/EIT3)
    IF(MSAVE1(I).GE.MCR1)PLASTO(I)=0.0
    PHI(I)=PLASTO(I)
    PATH(I)=12.
    IF(CHECK.GT.0.1)GO TO 322
326 CONTINUE
    MKEPT(I)=MLAST(I)
322 CONTINUE
    MLAST(I)=M(I)
    GO TO 44
96 EIT2=(MSAVE(I)-MCR1)/(PSAVE(I)-PHICR1)
    IF(MSAVE(I).GE.MY)EIT2=EIT
    PLASTO(I)=PSAVE(I)-(MSAVE(I)/EIT2)
    IF(MSAVE(I).LE.MCR)PLASTO(I)=0.0
    PHI(I)=PLASTO(I)
    IF(CHECK.GT.0.1)GO TO 324
328 CONTINUE
    MKEPT(I)=MLAST(I)
324 CONTINUE
    MLAST(I)=M(I)
    PATH(I)=13.
44 CONTINUE
    WRITE(6,150)I,PATH(I),M(I),PHI(I),PLASTO(I),PSAVE(I),MSAVE(I),PSAV
1E1(I),MSAVE1(I)
63 CONTINUE

```



```

C
C CURVATURE INTEGRATIONS
C
      SS(NNODES)=HEIGHT
      DO 1501 I=1,NDIV
      SS(I)=S(I)
      S(I)=HEIGHT-S(I+1)
1501 CONTINUE
      DO 1507 NODE=1,NDIV
      HIGH=SS(NODE+1)
      DO 1503 K=1,NDIV
      S(K)=HIGH-SS(K+1)
      I=K
      IF(S(K))91,1505,1505
1505 CONTINUE
      IF((PHI(I)+PHI(I+1)).EQ.0.0)GO TO 91
755 CONTINUE
      IF(PHI(I+1)*PHI(I))180,181,181
180 DZERO=ABS(PHI(I+1))/(ABS(PHI(I+1))+ABS(PHI(I)))*H(I)
      DLEFT=H(I)-DZERO
      AREAM1=PHI(I+1)*DZERO/2.*(DZERO/3.+S(I))
      AREAM2=PHI(I)*DLEFT/2.*(2.*DLEFT/3.+DZERO+S(I))
      AREAM(I)=AREAM1+AREAM2
      GO TO 183
181 CONTINUE
      CTROID(I)=(PHI(I+1)+(2.*PHI(I)))/(3.*(PHI(I)+PHI(I+1)))*H(I)
      SPC(I)=S(I)+CTROID(I)
      AREAM(I)=((PHI(I)+PHI(I+1))/2.)*SPC(I)*H(I)
      GO TO 80
91 AREAM(I)=0.0
183 CONTINUE
80 CONTINUE
1503 CONTINUE
      DO 1502 I=1,NDIV
1502 S(I)=SS(I)
      DF(NNODES)=0.0
      DO 2101 K=1,NDIV
      DF(NNODES)=DF(NNODES)+AREAM(K)
2101 CONTINUE
      AVGRAT(NODE+1)=DF(NNODES)
1507 CONTINUE
      AVGRAT(1)=0.0
      DO 1508 I=1,NNODES
1508 DF(I)=AVGRAT(I)
      DO 710 I=1,NNODES
710 DT(I)=DF(I)+DV(I)
      WRITE(6,908)
      COUNTG=0.0
919 CONTINUE
      DO 711 I=1,NNODES
711 WRITE(6,910)I,M(I),DL(I),DT(I),DF(I),DV(I)
911 CONTINUE
      DO 1510 I=1,NNODES
1510 IF(YYY.LT.0.8)MORIG(I)=M(I)
      IF(DT(14)*M(14))451,450,450
451 SAX=AXIAL
      AXIAL=0.0
      COUNTG=1.0
450 CONTINUE
      DO 411 I=1,NNODES

```





```

      M(I)=MORIG(I)+(AXIAL*(DT(NNODES)-DT(I)))
      YYY=YYY+1.
411  CONTINUE
      IF(COUNTG.GT.0.1)AXIAL=SAX
      IF(COUNTF.GT.0.1)GO TO 717
721  IF(ABS(DT(NNODES)-DL(NNODES)).LT.0.01)GO TO 717
      DO 722 I=1,NNODES
722  DL(I)=DT(I)
      CHECK=1.0
      GO TO 718
100  FORMAT(I5,F10.5,I5)
128  FORMAT(/'DISTANCES FROM BASE TO NODE',10X,'NUMBER OF DIVISIONS=',
      1I4/)
130  FORMAT(20(1X,F5.1))
132  FORMAT(/'HEIGHTS OF DIVISIONS'/)
134  FORMAT(25(1X,F4.1))
150  FORMAT(I3,2X,'PATH',F5.1,7E12.3)
160  FORMAT(18X,'M',13X,'PHI',5X,'PLASTO',8X,'PSAVE',8X,'MSAVE',5X,
      1'PSAVE1',5X,'MSAVE1'/)
313  FORMAT(/'OUTPUT MOMENT AND DEFLECTION VALUES'/)
501  FORMAT(20A4)
901  FORMAT(8F10.5)
902  FORMAT(/2X,'MOD. RATIO',7X,'DEPTH',7X,'THICK',5X,'STIRRUP',2X,'CON
      1C.SHEAR',6X,'ESTEEL',6X,'COUNT9')
904  FORMAT(8(2X,F10.2))
905  FORMAT(18X,'INCHES',6X,'INCHES',2X,'PERCENTAGE',8X,'KIPS',8X,'KSI'
      1/)
907  FORMAT(/12X,'V(I)',7X,'GAMMA(I)',4X,'M(NOW-2)',3X,'M(NOW-1)',5X,'M
      1(NOW)')
908  FORMAT(12X,'M(I)',7X,'DLAST',5X,'D TOTAL',5X,'D FLEX',7X,'D SHEAR'
      *)
909  FORMAT(I4,2X,F10.2,2X,E10.2,3(2X,F10.2))
910  FORMAT(I4,6(2X,F10.2))
926  FORMAT('MCR   =',F15.2,'PHI CR   =',E12.4)
927  FORMAT('MY    =',F15.2,'PHI FY   =',E12.4)
928  FORMAT('MFY   =',F15.2,'PHI FY   =',E12.4)
929  FORMAT('MWY   =',F15.2,'PHI WY   =',E12.4)
930  FORMAT('MULT  =',F15.2,'PHI ULT  =',E12.4)
931  FORMAT('MCR1  =',F15.2,'PHI CR1  =',E12.4)
932  FORMAT('MY1   =',F15.2,'PHI Y1   =',E12.4)
933  FORMAT('MFY1  =',F15.2,'PHI FY1  =',E12.4)
934  FORMAT('MWY1  =',F15.2,'PHI WY1  =',E12.4)
935  FORMAT('MULT1 =',F15.2,'PHI ULT1 =',E12.4)
940  FORMAT('MSSH  =',F15.2,'PHI SSH  =',E12.4)
941  FORMAT('MSSH1 =',F15.2,'PHI SSH1 =',E12.4)
316  FORMAT(/6(2X,E20.9))
937  FORMAT(/'THE M-P-PHI CURVE FOR MEMBER ',I5,' AXIAL LOAD =',F8.1/
      */)
938  FORMAT('XNI =',F15.2,'XNS =',F10.2,'HEIGHT =',F10.2,'FSUBC =',F10.
      *2)
939  FORMAT('*****
      *****')
950  FORMAT(/'INCREMENT NUMBER =',I3,' SHEAR ON COLUMN =',F7.2)
      STOP
      END

```

FILE



















**B30108**